

AD-A163 877

EXPERIMENTAL STUDY OF APEX FENCES FOR LIFT ENHANCEMENT  
ON A HIGHLY SWEPT. (U) AIR FORCE INST OF TECH  
WRIGHT-PATTERSON AFB OH SCHOOL OF ENGI.. M STUART

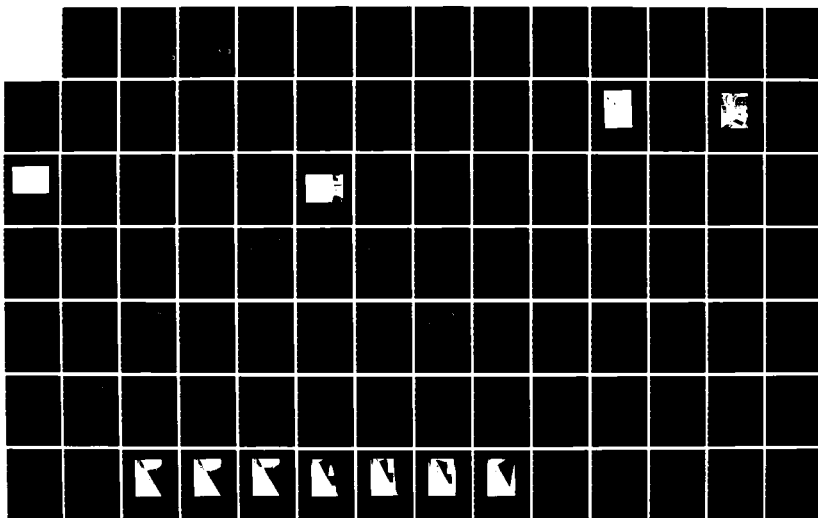
1/3

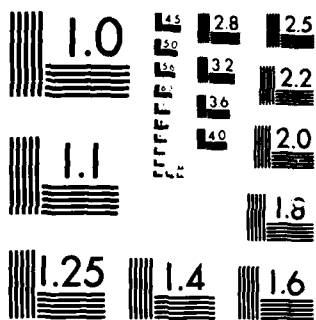
UNCLASSIFIED

DEC 85 AFIT/GRE/AA/85D-14

F/G 12/1

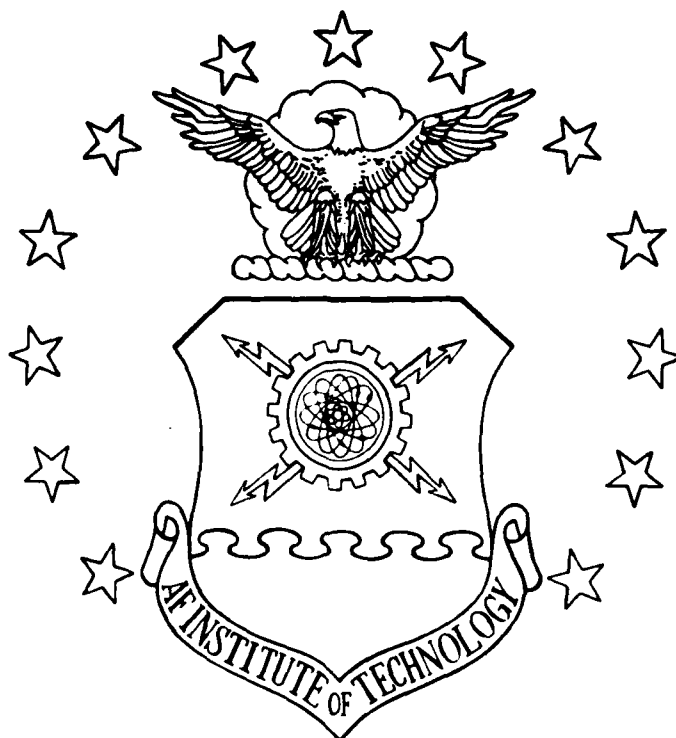
NL





MICROCOPY RESOLUTION TEST CHART  
NATIONAL BUREAU OF STANDARDS-1963-A

AD-A163 877



FOR LIFT ENHANCEMENT ON A HIGHLY  
SWEEP DELTA WING CONFIGURATION

THESIS

Michael Stuart  
Second Lieutenant, USAF

AFIT/GAE/AA/85D-14

DISTRIBUTION STATEMENT A

Approved for public release  
Distribution Unlimited

DEPARTMENT OF THE AIR FORCE  
AIR UNIVERSITY

**AIR FORCE INSTITUTE OF TECHNOLOGY**

Wright-Patterson Air Force Base, Ohio

DTIC  
ELECTE  
FEB 12 1986

B

FILE COPY

AFIT/GAE/AA/85D-14

EXPERIMENTAL STUDY OF APEX FENCES  
FOR LIFT ENHANCEMENT ON A HIGHLY  
SWEPT DELTA WING CONFIGURATION

THESIS

Michael Stuart  
Second Lieutenant, USAF

AFIT/GAE/AA/85D-14

DTIC  
ELECTE  
FEB 12 1986  
S D

B

Approved for public release; distribution unlimited

AFIT/GAE/AA/85D-14

EXPERIMENTAL STUDY OF APEX FENCES FOR LIFT ENHANCEMENT  
ON A HIGHLY SWEPT DELTA WING CONFIGURATION

THESIS

Presented to the Faculty of the School of Engineering  
of the Air Force Institute of Technology

Air University

In Partial Fulfillment of the  
Requirements for the Degree of  
Master of Science in Aeronautical Engineering

Michael Stuart, B.S.

Second Lieutenant, USAF

December 1985

Approved for public release; distribution unlimited

## PREFACE

The purpose of this investigation was to study the aerodynamics of "apex fences" deployed on a conventional delta wing/body model and to measure the resulting forces and moments which the model experienced when they were used. The proposed adaptability of apex fences for STOL operations and the high angle of attack pitch-restoring characteristics motivated the research effort.

The data presented herein represents a general view of the longitudinal stability behavior of a "typical" delta wing aircraft with apex fences. So far, the aerodynamic results look promising. However, lateral stability behavior should and must be examined to complete the overall picture and further the growth of this technology.

It should be noted that previous research on apex fences is scarce and inconclusive. It is limited to pressure measurements of the upper wing surface of a fence-equipped delta wing/body model. Thus, only predictions on aerodynamic performance are possible. This study, however, is the first to deal specifically with force/moment analysis.

Some limitations experienced during testing were the model's size and weight. Aeroelastic effects and the position of the model on the sting/balance system were major factors which contributed to endless hours of modifications and problems with data collection. As such, the model was

affectionately dubbed "Delta BOHICA".

In retrospect, the project was definitely successful and satisfying for me. However, it would have been all for naught without the expert aid of the tunnel operator, Mr. Andy Reimenschneider, to whom I owe a great deal of appreciation. I would also like to thank my advisor, Capt Wesley Cox, for his experimental insight, and John Brohaus and Jack Tiffany of the AFIT Fabrication Shop for their patience and skill in making and re-making the model. Also, I owe thanks to Lt Mark Frassinelli of AFWAL and Jim Grove of the Flight Dynamics Lab for his sometimes whimsical but helpful suggestions on instrumentation setups and programming. Indeed, we all will be known as the "last of the Bohicans."



Accession For	
NTIS GRAM	<input checked="checked" type="checkbox"/>
DATE TCR	<input type="checkbox"/>
Revised	<input type="checkbox"/>
Accession	
Distribution/	
Availability Codes	
Dist	Avail and/or Special
A-1	

## TABLE OF CONTENTS

	Page
Preface.....	ii
List of Symbols.....	vi
List of Figures.....	vii
Abstract.....	xi
I. Introduction.....	1
II. Theory.....	3
III. Experimental Apparatus.....	8
Description of Experimental Setup.....	8
Description of Wind Tunnel.....	11
Description of Individual Components.....	11
IV. Experimental Procedure.....	21
V. Results.....	27
Baseline Characteristics.....	27
Baseline without Flap Setting.....	28
Baseline with Flap Settings.....	30
Basic Fence Effects.....	31
Parametric Investigations.....	42
Shape.....	42
Length-to-Height.....	43
Cant.....	48
Surface Area.....	54
Movement.....	59
Flap Effects on Fence Aerodynamics.....	63
Asymmetric Fence Deployment.....	63



Flow Visualization.....	69
Baseline.....	69
Fence 12.....	70
Fence 2 Inboard.....	70
VI. Conclusions and Recommendations.....	79
Appendix A: Model Dimensions.....	A1
Appendix B: Additional Flow Visualization .....	B1
Appendix C: Reduced Aerodynamic Plots.....	C1
Bibliography.....	BIB1
Vita.....	V1

# LIST OF SYMBOLS

$\alpha$	angle of attack (degrees)
$\beta$	sideslip angle (degrees)
$\delta$	inboard t.e. flap angle (degrees)
$\sigma$	cant angle of fence (degrees)
l.e.	"leading edge"
t.e.	"trailing edge"
$C_L$	lift coefficient
$C_D$	drag coefficient
$C_M$	pitching moment coefficient
$C_y$	side force coefficient
$C_l$	rolling moment coefficient
$C_n$	yawing moment coefficient
$C_{Lmax}$	maximum lift coefficient
L/D	lift-to-drag ratio
F1 - F12	fences 1 through 12
c	root chord (inches)
q	dynamic pressure (psf)
Re	Reynold's number
M	mach number

## LIST OF FIGURES

Figures in Text	Page
1. Schematic of Leading Edge Vortex Formation on a Delta Planform.....	4
2. Experimental Setup used for Data Collection.....	9
3. Sting/Mounting Plate Structure.....	10
4. Controller's/Operator's Station.....	12
5. Delta Wing/Body Model (with Fence 6 deployed).....	14
6. Fence Dimensions.....	15
7. Fence Planforms (Fences 1-6).....	16
8. Fence Planforms (Fences 7-12).....	17
9. Data Collection Station.....	19
10. Baseline Runs used to Determine Repeatability of Data.....	23
11. Baseline with Inboard Trailing Edge Flap Deflections.....	32
12. Baseline with Twin (Inboard and Outboard) Trailing Edge Flap Deflections.....	34
13. Baseline Case vs. F1 Gothic Fence Case.....	38
14. Effects of Fence Shape.....	44
15. Effects of Different Double Gothic Fence Shapes.....	46
16. Effects of Fence Length-to-Height Ratio.....	49
17. Schematic of Model with Fences Deployed at a Negative Cant Angle.....	51
18. Effects of Fence Cant.....	52
19. Effects of Fence Surface Area using the Gothic Shape.....	55
20. Effects of Fence Surface Area using the Delta Shape.....	57
21. Effects of Fence Movement.....	61

22.	Asymmetric Deployment of F5 Double Gothic Fence on Left Wing.....	65
23.	Oil Flow Visualization for the Baseline Case at 9.5 degrees.....	72
24.	Oil Flow Visualization for the Baseline Case at 20 degrees.....	73
25.	Oil Flow Visualization for the Baseline Case at 30 degrees.....	74
26.	Oil Flow Visualization for the F12 Double Gothic II Fence Case at 9.5 degrees.....	75
27.	Oil Flow Visualization for the F12 Double Gothic II Fence Case at 20 degrees.....	76
28.	Oil Flow Visualization for the F12 Double Gothic II Fence Case at 30 degrees.....	77
29.	Oil Flow Visualization for the F2 Delta Fence Inboard 1.0 inches.....	78

Note: For all graphical data, plots are identified by the following sub-headings:

- (a.) Lift Coefficient vs. Drag Coefficient
- (b.) Lift Coefficient vs. Angle of Attack
- (c.) Pitching Moment Coefficient vs. Angle of Attack
- (d.) Drag Coefficient vs. Angle of Attack
- (e.) Rolling Moment Coefficient vs. Angle of Attack
- (f.) Side Force Coefficient vs. Angle of Attack
- (g.) Lift/Drag vs. Lift Coefficient
- (h.) Yawing Moment Coefficient vs. Angle of Attack

#### Figures in Appendices

A-1.	Model Dimensions (Top View).....	A2
A-2.	Model Dimensions (Side View).....	A3
A-3.	Model Dimensions (Front View).....	A4
B-1.	Oil Flow Visualization for the F7 Modified Gothic II Fence Case at 9.5 degrees.....	B2

B-2.	Oil Flow Visualization for the F7 Modified Gothic II Fence Case at 20 degrees.....	B3
B-3.	Oil Flow Visualization for the F7 Modified Gothic II Fence Case at 30 degrees.....	B4
C-1.	Baseline.....	C2
C-2.	Baseline with -10 degrees Flap.....	C4
C-3.	Baseline with 10 degrees Flap.....	C6
C-4.	Baseline with 20 degrees Flap.....	C8
C-5.	Baseline with 30 degrees Flap.....	C10
C-6.	Baseline with -10 degrees Twin Flap.....	C12
C-7.	Baseline with 10 degrees Twin Flap.....	C14
C-8.	Baseline with 20 degrees Twin Flap.....	C16
C-9.	F1 (Gothic) Fence.....	C18
C-10.	F2 (Delta) Fence.....	C20
C-11.	F3 (Cropped) Fence.....	C22
C-12.	F4 (Mini Cropped) Fence.....	C24
C-13.	F5 (Double Gothic) Fence.....	C26
C-14.	F6 (Modified Gothic) Fence.....	C28
C-15.	F7 (Modified Gothic II) Fence.....	C30
C-16.	F8 (Short Delta) Fence.....	C32
C-17.	F9 (Short Cropped) Fence.....	C34
C-18.	F10 (Mini Delta) Fence.....	C36
C-19.	F11 (Chopped Cropped) Fence.....	C38
C-20.	F12 (Double Gothic II) Fence.....	C40
C-21.	F1 (Gothic) with 10 degrees Flap.....	C42
C-22.	F1 (Gothic) with 20 degrees Flap.....	C44
C-23.	F1 (Gothic) with 30 degrees Flap.....	C46

C-24.	F1 (Gothic) with 10 degrees Twin Flap.....	C48
C-25.	F1 (Gothic) with 20 degrees Twin Flap.....	C50
C-26.	F2 (Delta) with 10 degrees Flap.....	C52
C-27.	F2 (Delta) with 20 degrees Flap.....	C54
C-28.	F7 (Modified Gothic II) with 10 degrees Flap.....	C56
C-29.	F1 (Gothic) with -15 degrees Cant.....	C58
C-30.	F2 (Delta) with -15 degrees Cant.....	C60
C-31.	F5 (Double Gothic) with -15 degrees Cant.....	C62
C-32.	F5 (Double Gothic) with -7.5 degrees Cant.....	C64
C-33.	F5 (Double Gothic) with 7.5 degrees Cant.....	C66
C-34.	F1 (Gothic) at 1.5 inches Inboard.....	C68
C-35.	F2 (Delta) at 0.5 inches Inboard.....	C70
C-36.	F2 (Delta) at 1.0 inches Inboard.....	C72
C-37.	F2 (Delta) at 1.5 inches Inboard.....	C74
C-38.	F3 (Cropped) at 0.5 inches Inboard.....	C76
C-39.	F3 (Cropped) at 1.0 inches Inboard.....	C78
C-40.	F5 (Double Gothic) at 1.0 inches Inboard.....	C80
C-41.	F6 (Modified Gothic) at 1.0 inches Inboard.....	C82
C-42.	F2 (Delta) on Left Wing.....	C84
C-43.	F5 (Double Gothic) on Left Wing.....	C86
C-44.	F7 (Modified Gothic II) on Left Wing.....	C88
C-45.	F2 (Delta) on Left Wing at 0.5 inches Inboard.....	C90

## ABSTRACT

The longitudinal stability characteristics of a 60 degree delta wing/body model equipped with various types of apex fences were studied experimentally. The experimental effort utilized force balance instrumentation and oil flow visualization, and produced conclusive results. The locations of the fence generated vortices and leading edge vortices associated with high lift swept wings were also determined. Five major fence parameters (shape, surface area, cant, length-to-height, movement) were studied and the results are given in a qualitative analysis.

The results indicate a favorable application of apex fences for STOL operations. The fences increase lift and positive pitching moment which dictates the use of trailing edge flaps, further increasing the available maximum lift for takeoff and landing. Accompanying this is a large increase in drag at low angles of attack and a marginal increase at moderate to high angles. The relative strength of nose-down pitching moments at high (above 35°) angles of attack produced by apex fences is slight.

The assessment is made that apex fences are a technology whose time may have come. Further research of the lateral behavior of a "fenced" aircraft appears warranted.

## INTRODUCTION

Current trends in tactical fighter technology have focused on many diverse aerodynamic qualities. Receiving particular attention is the ability of an aircraft to out-maneuver, or "out-fly", opposing aircraft in tactical theater operations, as well as flexibility of takeoff and landing operations. In terms of the latter, emphasis is towards producing fighter aircraft with Vertical Takeoff and Landing (VTOL) and Short Takeoff and Landing (STOL) capabilities, or a combination of these (V/STOL).

Conventional delta wing aircraft face an acute problem in terms of their adaptability to STOL conditions. Namely, they are quite limited in their subsonic maneuvering ability due to marginal dynamic stability at angles of attack above  $20^\circ$ . Thus, delta wing aircraft require long runways because takeoff and approach airspeeds are relatively high (again, due to the limits on angle of attack).

The purpose of this study was to determine the effectiveness of "apex fences" deployed on the upper wing surface of a  $60^\circ$  swept delta wing/body model in improving the high angle of attack characteristics of lift and pitching. Specifically, the emphasis was on confirming and quantifying the role of apex fences with respect to lift augmentation and longitudinal stability characteristics. The evaluation criteria used compared families of fences based on: 1)



Improved STOL abilities; and 2) High angle of attack pitch restoring stability, with a reduced pitch-stiffness at angles of attack greater than about  $30^\circ$ . This was realized by performing a trend analysis on fence designs and associated parameters so that their effects could be determined qualitatively. The overall assessment was based on comparison of the apex fence configured model with the baseline (unconfigured) model within a subsonic flight regime.

## THEORY

To understand and analyze the effects of apex fences, one needs to be familiar with the spanwise development of the flow over a delta wing. For a planar wing with no centerbody and sharp leading edges, this field is characterized by flow detachment from the leading edges. This results in the formation of leading edge "free" vortices which produce a substantial normal force on the wing (Fig 1). The core of these vortices grows linearly downstream along the axis, moving along a ray upward and outward from the wing's centerline axis. This path, of course, depends on the attitude of the wing (angle of attack). The vortices are not axisymmetric. Sforza and Smorto (ref 1) noted that due to viscous effects the core expands, resulting in subsequent vortex breakdown. The complications associated with this vortex-generated flow are a high drag penalty and instability of the vortex "system" at angles of attack above 30 degrees (especially when combined with yaw).

Delta wings are designed for use primarily in the supersonic and transonic regimes. Thus, they have sharp leading edges and tend to perform poorly at subsonic speeds. In terms of delta wing fighter aircraft, high angles of attack are needed to produce the required lift during takeoff, landing, initial climb and maneuvering. Consequently, the aircraft must momentarily operate in a

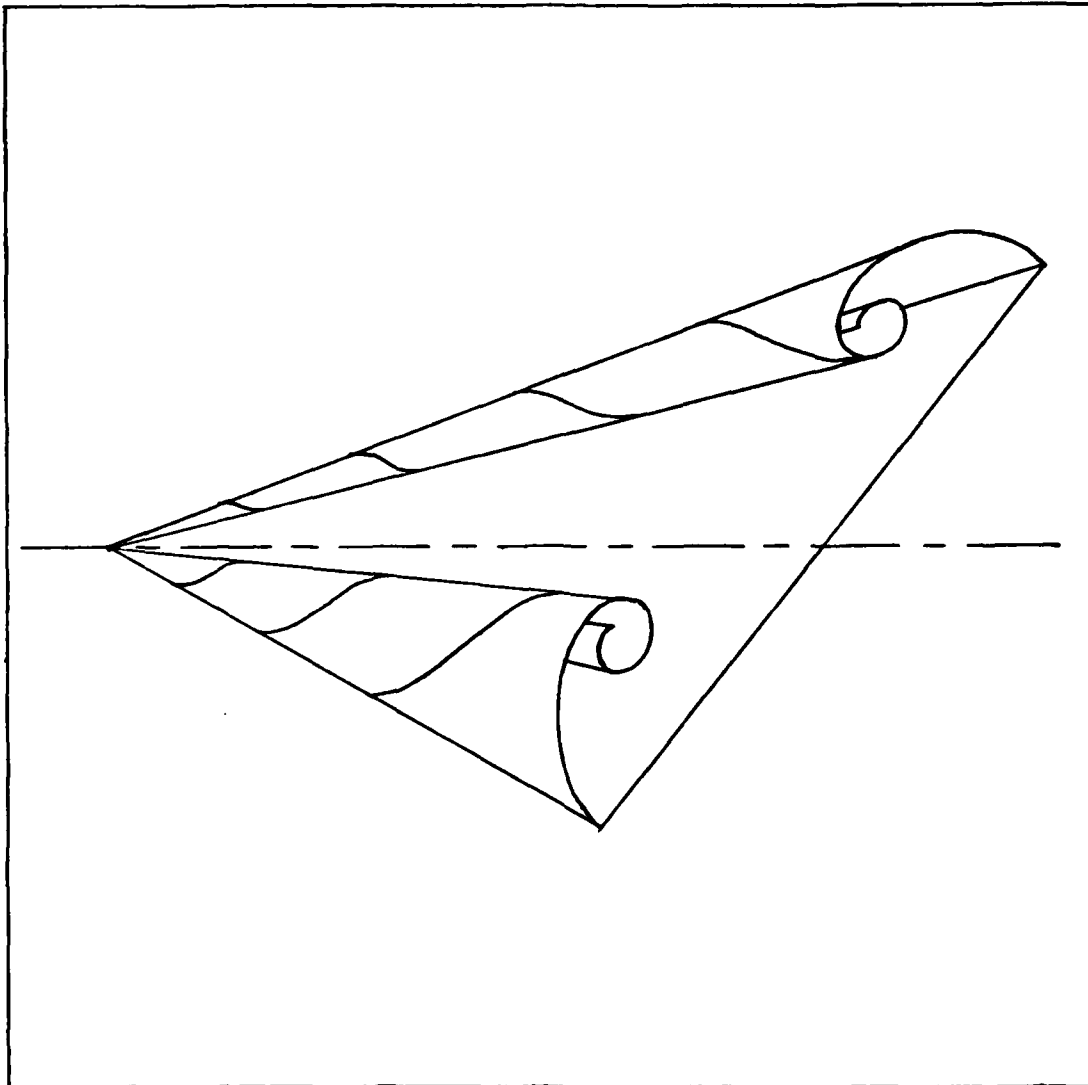


Fig. 1. Schematic of Leading Edge Vortex Formation  
on a Delta Planform

regime where high drag and yawing/high alpha flow instability (i.e. asymmetric "bursting" of vortices) are of particular concern.

Proposals to counter these adverse effects have centered on: 1) Altering the vortex generation by means of Leading Edge Vortex Flaps (LEVFs) in an attempt to reduce drag and increase stability (ref 2, 3, 5) and 2) Increasing the lift-to-drag ratio (L/D) by deployment of vertical flaps (ref 10). LEVFs effectively add camber to the wing. As a result, a portion of the normal force vector is tilted forward, reducing the drag somewhat. A drawback, however, is that a small portion of lift is lost and thus it can only be recouped by increasing the airspeed (or angle of attack), thereby adding complications to the problem of landing and takeoff. Wing stall occurs at a much lower angle of attack, it is much more pronounced, and  $C_{Lmax}$  is reduced by about 16% (ref 2). A nose-up pitching moment is evident with LEVF deployment, and helps in alleviating the decrease in lift since trailing edge flaps can be used to trim the aircraft (ref 4). However, no advantage is realized in improving the lift characteristics over that of the unconfigured wing. Consequently, LEVFs were discovered to be best suited for subsonic cruise and "loitering" operations since their main advantage is increasing the aerodynamic efficiency (L/D) of the aircraft. Thus, LEVFs do not effectively solve the takeoff and landing problems.

The vertical flap application deals with positioning the flap on the wing's upper surface along a ray from the apex of the delta wing. The results of this type of arrangement demonstrate a large increase (up to 33%) in the aerodynamic efficiency of a typical 60° swept, sharp-edged delta wing. This indicates that vertical flaps are applicable to improved cruise and loiter performance, as are LEVF, but they do not alter the lift and pitching characteristics.

In order to counter the performance limitations inherent with delta wing aircraft at high angles of attack, the concept of using Vortex Fences to modify the classic wing vortex system was first presented formally by Rao (ref 7) in 1984. Basically, vortex fences are flap-like devices which are hinged along the leading edge and (usually) deployed normal to the wing upper surface. They are used to generate an additional pair of vortices on the wing's upper surface (near the apex region). These vortices (of the same sense as the leading edge vortices) are freely convected downstream between the leading edge vortices, augmenting the lift distribution in the poorly loaded inboard section of the wing. At higher angles of attack, the idea is to redistribute the aerodynamic loading so as to delay vortex breakdown (stall) and obtain stabilizing pitching moment characteristics. At low to moderate angles of attack, the fences are expected to provide a positive lift increment and move the center of pressure forward to produce positive

pitching moments. These fences, positioned at the apex region (i.e. "apex fences") would be deployed at high angles of attack for subsonic pitch maneuvering, and at moderate angles of attack to enhance the trim and control characteristics for takeoff and landing.

Recent studies dealing with apex fences (ref 6, 7) have focused on: 1) Qualitatively describing the aerodynamic flow field on a  $74^\circ$  delta planform using helium bubble and oil flow visualization and 2) Quantifying upper-surface pressure distributions using pressure taps. Results of these efforts have shown that the apex fence designs tested (fences F1, F2, F3, F4, and F5) increase inboard suction approximately 10% for  $0 \leq \alpha \leq 20$  and that an increased nose-up pitching moment is produced over that of the planar wing case. Data above  $\alpha = 30$  was not taken, and the lower surface aerodynamics were not investigated. Hence, actual aerodynamic loads could not be calculated.

## EXPERIMENTAL APPARATUS

### Description of Experimental Setup

The AFIT 5-foot subsonic wind tunnel was used for the investigation. The experimental setup (Fig. 2) consisted of a delta wing/body model which slid onto a six-component cylindrically-shaped strain gauge balance. The balance was attached to a modified supporting sting/mounting plate (Fig. 3), which was then supported on a hyperbolic-shaped yoke which could be pitched from  $-60^\circ$  (minimum) to  $260^\circ$  (maximum). Force/moment instrumentation consisted of the strain gauge balance output connected through an amplifier circuit and then into a data acquisition unit. This data acquisition unit also received output from pressure transducers, voltage excitation sources, and angle of attack meters. The unit's voltmeter readings were selectively passed to both a computer and to two strip chart recorders. The computer then processed and reduced the data into a useable engineering form. The two strip chart recorders were used to monitor individual balance component outputs. In this way, the loads on the balance were constantly checked so as to insure that the load limit for any individual component was never reached.

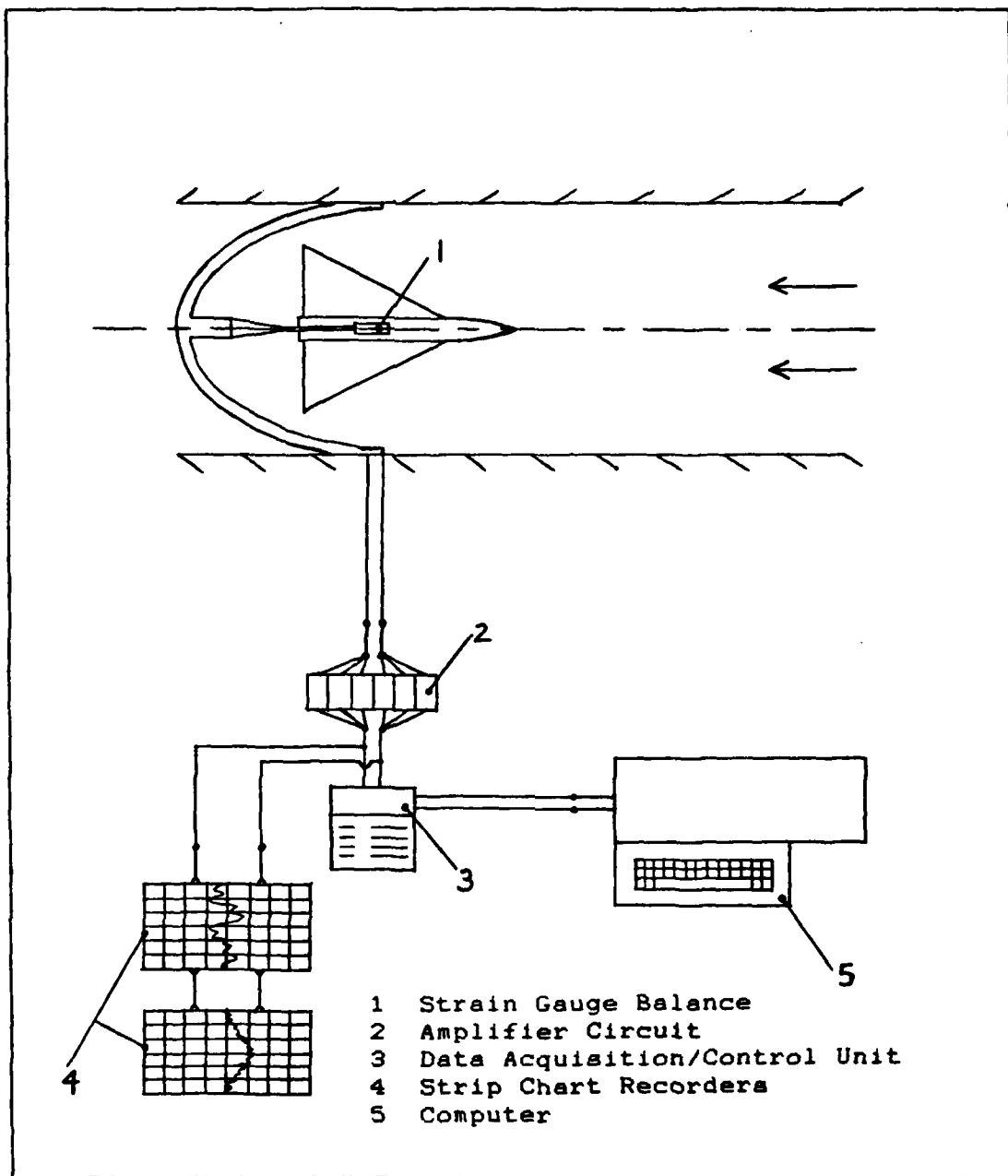


Fig. 2. Experimental Setup used for Data Collection





Fig. 3. Sting/Mounting Plate Structure

## Description of Wind Tunnel

The wind tunnel is an open circuit, continuous flow type with a contraction ratio of 3.7 to 1. It has a closed test section which is five feet in diameter and 18 feet in length. The tunnel is in a large building which provides a double return for air. The airflow is induced by two 12 foot counter-rotating fans and can reach a maximum velocity of 300 fps. Total pressure is atmospheric. Static pressure is measured by eight sets of static ports located 30 inches upstream from the test section. Digital voltmeters display tunnel dynamic pressure (approximately 20 psf for this test), angle of attack, and yaw angle. A control panel is used to govern each parameter (Fig. 4). The turbulence factor is about 1.5, there is a  $0.3^\circ$  downwash, and a slight sidewash.

## Description of Individual Components

The following is a list of the experimental components and instrumentation used:

- Delta wing/body model
- Task MK I 0.75 inch 80-40-40 strain gauge balance
- Hewlet-Packard 9826 computer with 9872C plotter
- Hewlet-Packard 3497A Data Acquisition/Control Unit
- Two strip chart recorders
- Twelve pairs of apex fences; each different

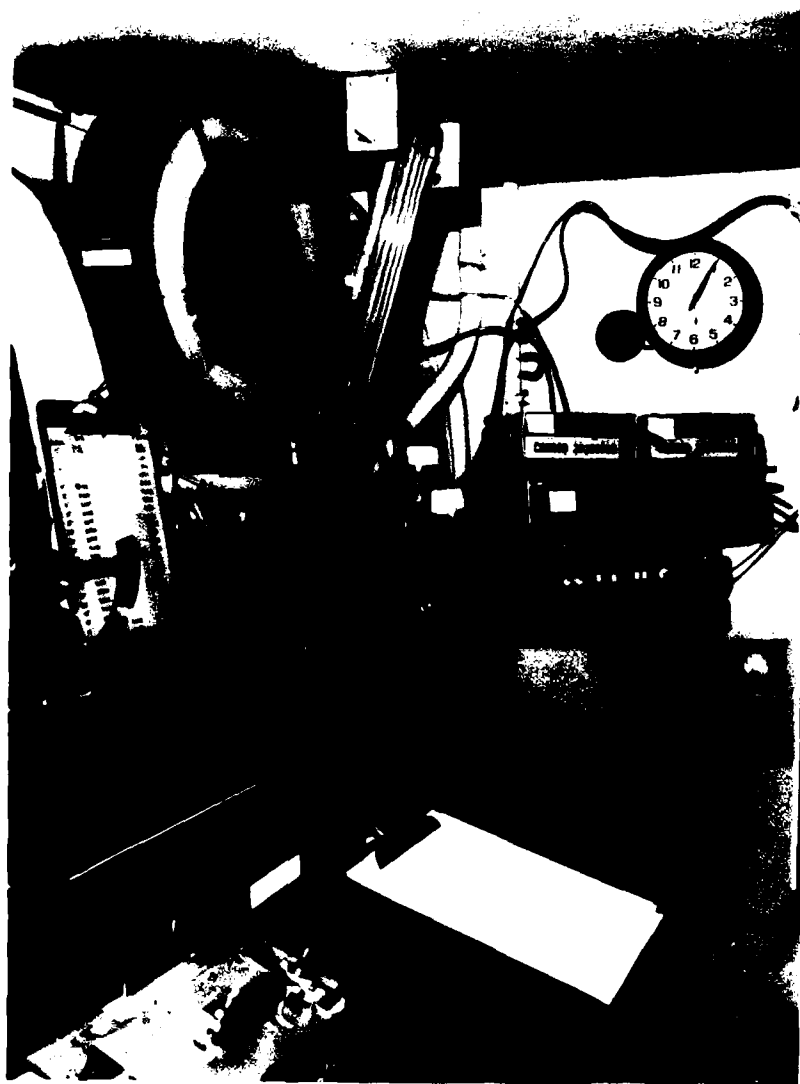


Fig. 4. Controller's/Operator's Station

## Model

The model chosen was a conventional delta wing/body configuration (Fig. 5). The wings, tail, and main fuselage were aluminum, while the nose was wooden and the trailing edge flaps were epoxy. A rubber band was positioned on the nose 3.5 inches from the tip in order to prevent asymmetric shedding of forebody vortices which destabilize the model and interfere with aerodynamic study of the fences. The maximum tunnel blockage was 7.4% at  $\alpha = 44$ . Minimum blockage was 0.05% at  $\alpha = 0$ . Fences were attached with screws (maximum of four each) to the wing's upper surface. Detailed model specifications are given in Appendix A.

## Fences

The fences were constructed from thin galvanized sheet metal which provided adequate strength and minimum "bulk" or thickness. Countersunk screw holes were drilled to minimize aerodynamic interference from the screw heads, and tape was applied along the fence/leading edge junction to give a smooth joining between the fence and wing, sealing the small gap. Fence dimensions and shapes are given in Figs. 6-8.

## Balance

The Task MK I 0.75 inch strain gauge balance is specifically designed for use in force/moment testing of wind

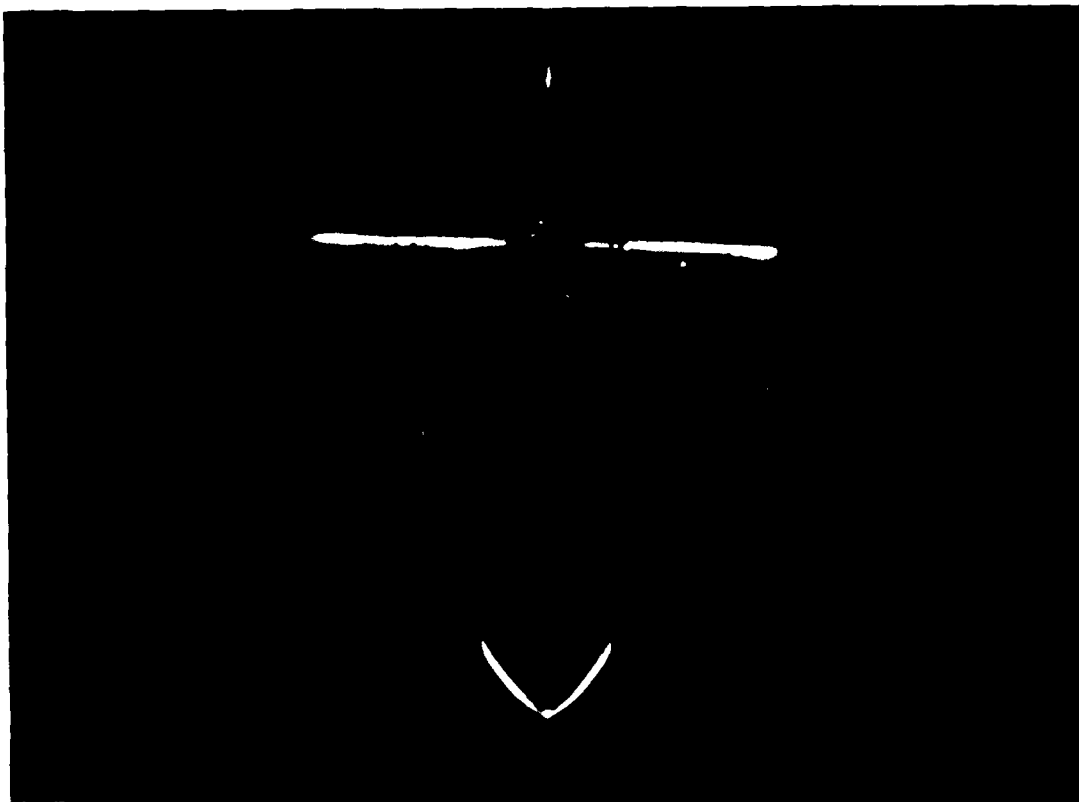


Fig. 5. Delta Wing/Body Model  
(with Fence 6 deployed)

FENCE/SHAPE	(in.)	(in.)	L/H RATIO	% WING AREA
	LENGTH	HEIGHT		
F1 Gothic	13.75	2.50	5.500	22.8
F2 Delta	13.75	2.50	5.500	14.2
F3 Cropped	10.25	1.50	6.833	11.3
F4 Mini Cropped	5.25	1.50	3.500	5.1
F5 Double Gothic	12.00	1.75	6.857	10.8
F6 Modified Gothic	13.25	2.25	5.889	18.3
F7 Mod. Gothic II	9.25	1.94	4.774	11.1
F8 Short Delta	9.75	1.81	5.500	7.3
F9 Short Cropped	7.69	1.50	5.125	8.2
F10 Mini Delta	7.19	1.32	5.500	4.0
F11 Chopped Cropped	7.69	0.88	8.786	5.1
F12 Dble Gothic II	10.69	1.56	6.853	9.2

Figure 6: Fence Dimensions

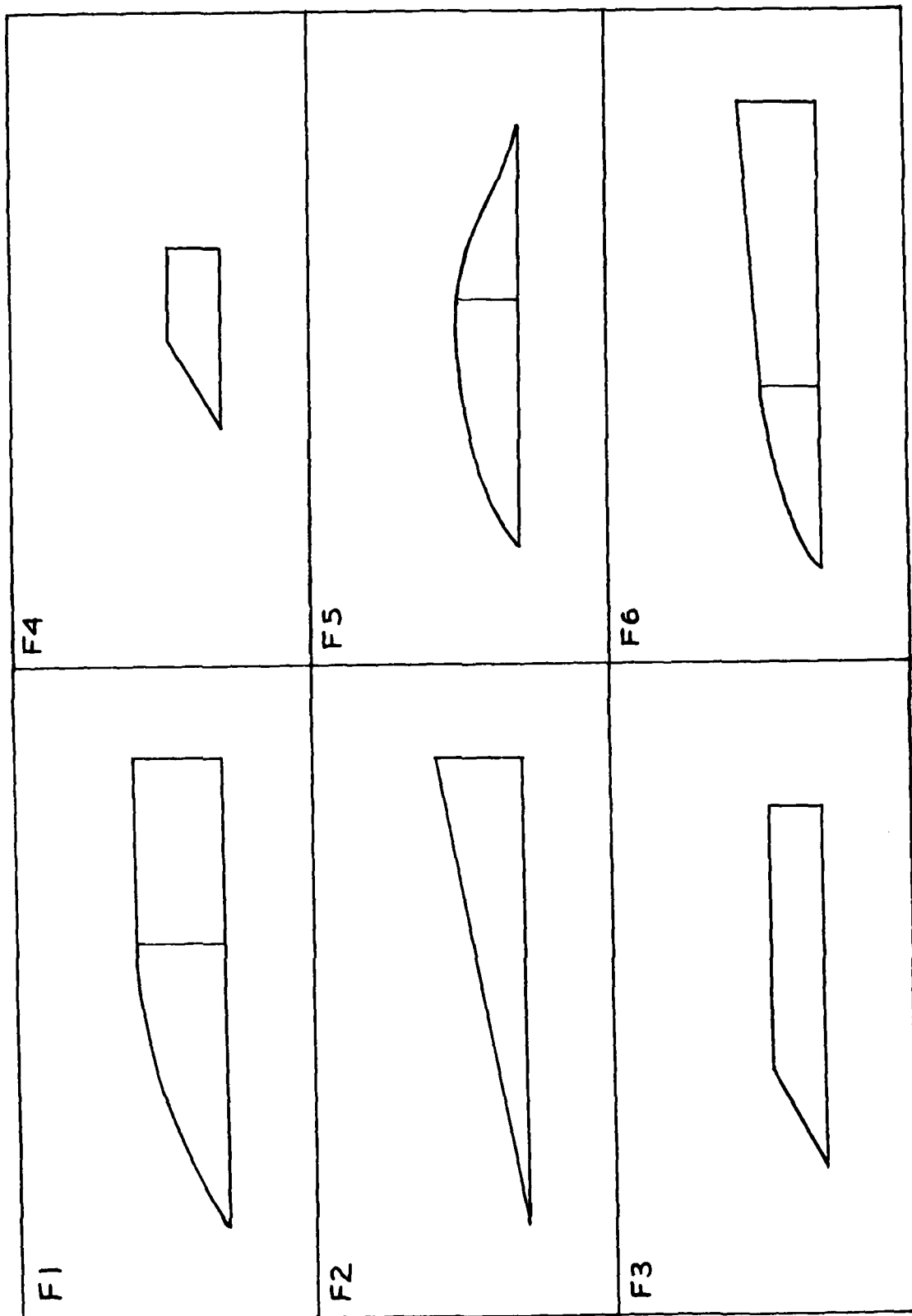


Fig. 7. Fence Planforms (Fences 1- 6)

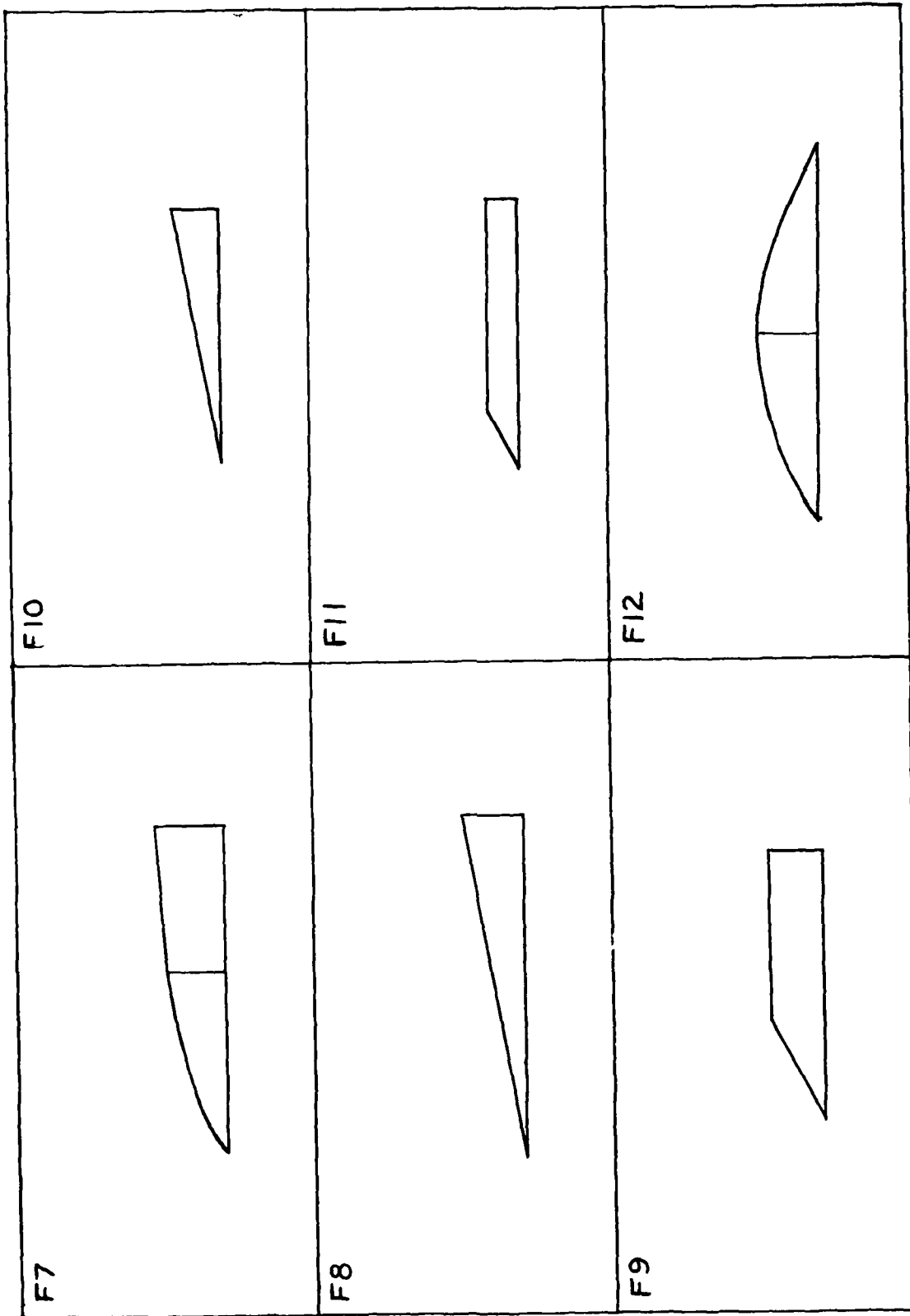


Fig. 8. Fence Planforms (Fences 7-12)



tunnel models and provides output precision of fractions of millivolts for full scale readings of up to 6 volts. It has a range of 80 lbs normal force, 40 lbs axial force, and 40 lbs side force. The maximum forces obtained during testing were monitored so that the balance was not over-stressed. The balance has six strain gauges; one pair labelled "forward" and "aft" for each of the three force components (normal axial, and side). The gauges are positioned equidistant from a common midpoint on the balance. The balance was mounted on the sting/yoke system so that the center of rotation (of the yoke) coincided with the midpoint of the balance (the center of rotation became the force/moment resolving point). Additionally, the model was placed on the balance so that the approximate aerodynamic center (@ 2/3 centerline chord for delta wings) was coincident with the balance midpoint and thus the center of rotation. In this way, the model was neutrally stable, thereby allowing greater ease in analysing the pitching characteristics when fences or trailing edge flaps were deployed. (Note: The model's weight was removed from the balance readings by the use of tare output values subtracted from the true outputs.)

#### Computer

The HP 9826 computer, along with the HP 3497A data acquisition/control unit, were the principal instruments used

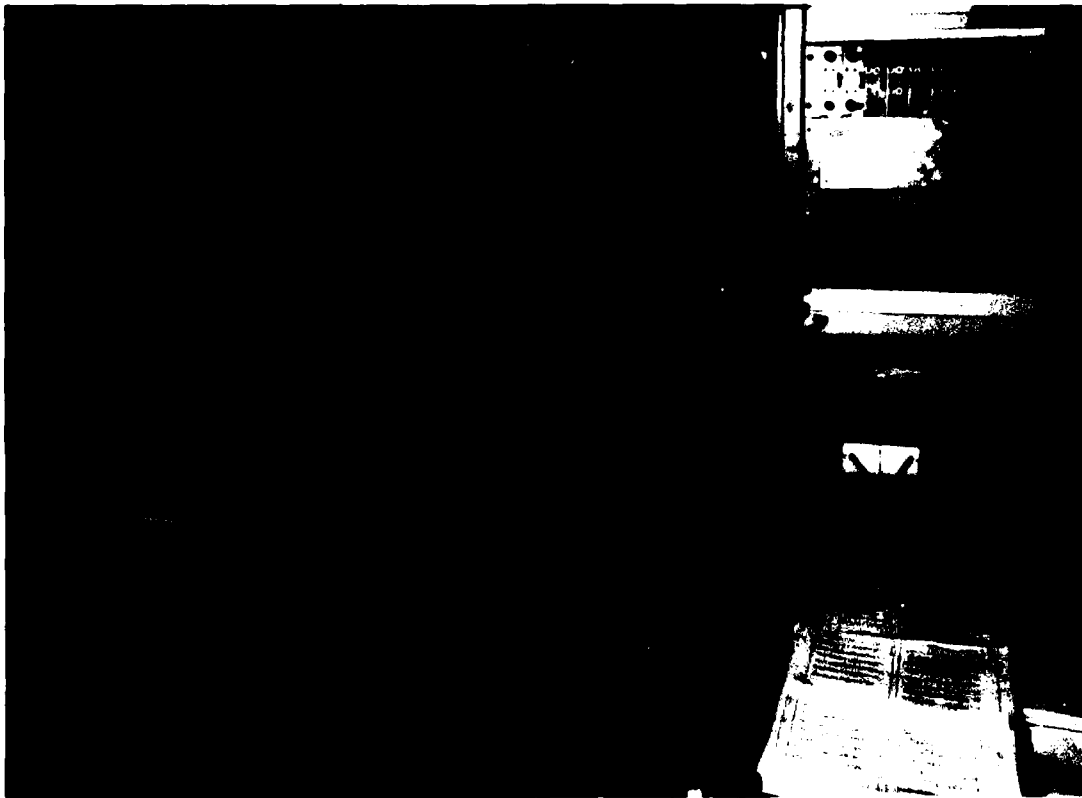


Fig. 9. Data Collection Station

in sampling and reducing data (Fig. 9). The output from the balance and other devices (angle of attack voltmeter, tunnel dynamic pressure) was sampled at 200 samples/sec for each channel (from the control unit) and repeated six times for each data point taken. The data for each channel was then averaged and subsequently stored on computer discs. The only problem encountered was measuring side forces at high angles of attack (above  $35^\circ$ ). This was due to lateral instability at this flight condition. A reduction program, which had been used in two previous force studies (ref 8, 9) was used to output data in standard aerodynamic coefficient form as well as true force/moment units. A graphics plotter was then used to produce aerodynamic plots (i.e.  $C_L - \alpha$ ). Output plots are given in Appendix C.

#### Strip Chart Recorders

Two strip chart recorders were used to monitor side force and normal force gauges to insure against overstressing their limits. By using these two recorders, strip chart "data" was taken that revealed a natural frequency of about 7.5 Hz for the model/support system. This frequency did not hamper or interfere with collecting true force/moment data during testing. Other than this, the recorders were not used in conjunction with the computer to sample or record data.

## EXPERIMENTAL PROCEDURE

Testing was broken down into roughly two major phases: baseline characteristics and parametric studies. Baseline testing was needed to provide a reference for comparison. This involved the investigation of the model's characteristics for yaw, trailing edge flap deflection, and of the random error in the instruments. Parametric studies were made to determine the influence of five fence variables (size, shape, length-to-height ratio, cant angle, and position). The results of these studies were used to choose a "best overall fence" (i.e. based on the trends observed in each case). The testing was conducted at a dynamic pressure of roughly 20 psf, with  $M = 0.12$  and a mean Reynold's number of  $9 \times 10^5/\text{ft}$ .

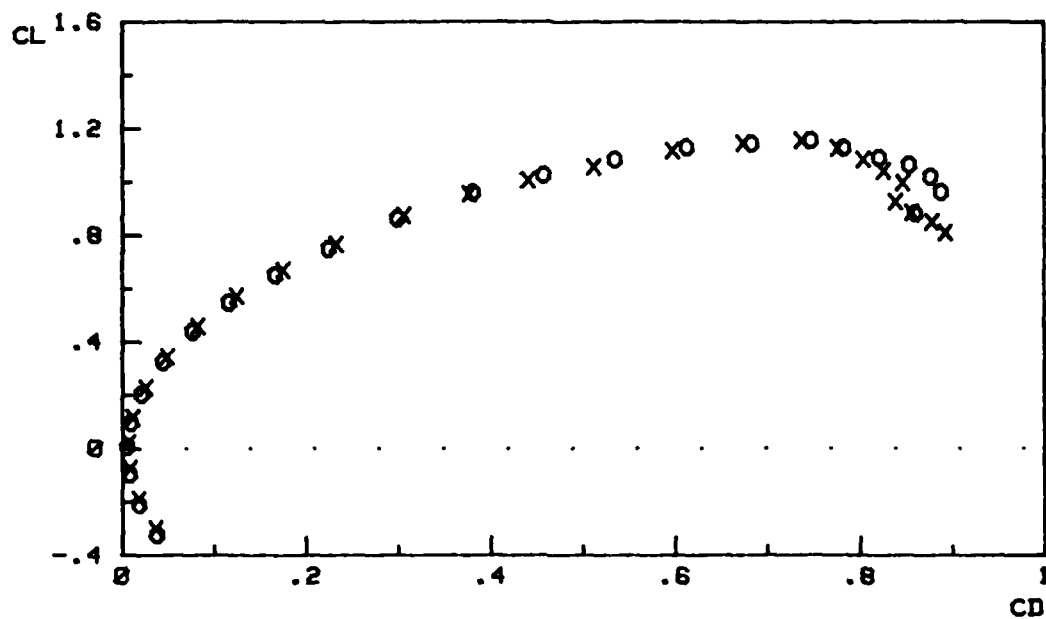
Following the force balance testing, flow visualization was conducted using oil droplets applied to the upper surface of the wing. This revealed the position of the vortices on the wing and thus the basic flow structure involved.

In all, a methodical approach was taken in each study to determine the qualitative effects of each variable. As a result, certain fences were bypassed in certain studies in order to concentrate on a particular fence (or class of fences) which demonstrated a higher sensitivity to the variable in question.

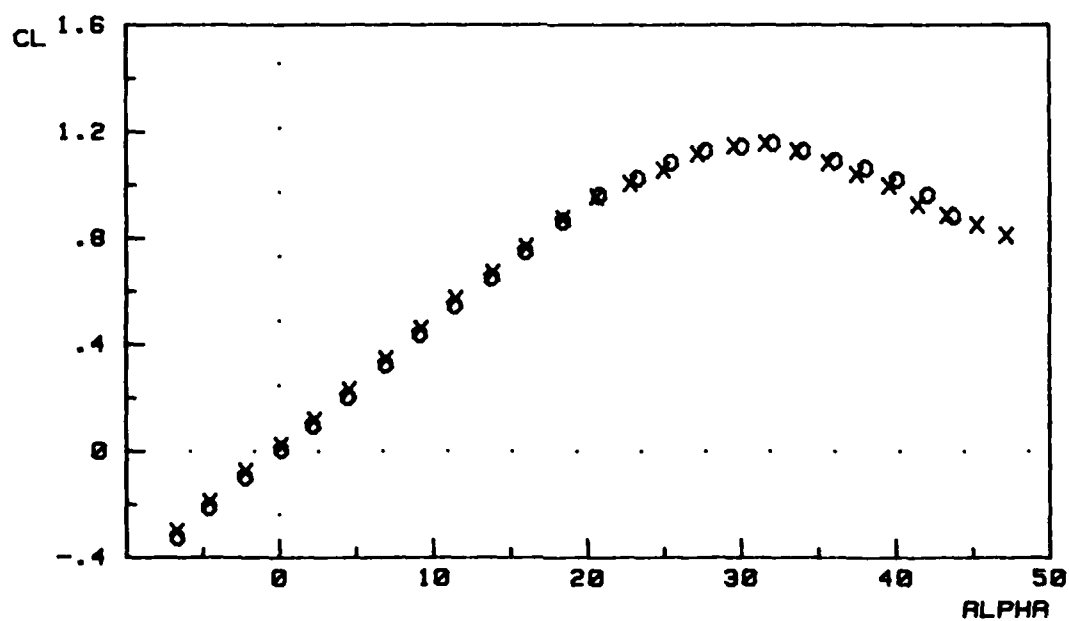
No rigorous error analysis was conducted during the

test. The output of the strain gauge balance and the control unit allowed an output sensitivity in the fraction of a millivolt range, however, data was rounded to the third significant digit (millivolts) on all readings. Using a check-loading rig on the balance, the maximum error was consistently between 0.5% and 1% of full scale. This was considered sufficient for the purposes of the entire test.

Two baseline runs were made to determine output repeatability (Fig. 10). As can be seen, deviations occur only around high  $\alpha$  and are within acceptable limits for trend analyses. Side force data was of no concern and the anomalies present are indicative of lateral instabilities at high  $\alpha$ . In addition, repeat data points were taken on all runs to insure acceptable repeatability.



a.



b.

Fig. 10. Baseline Runs used to Determine Repeatability of Data

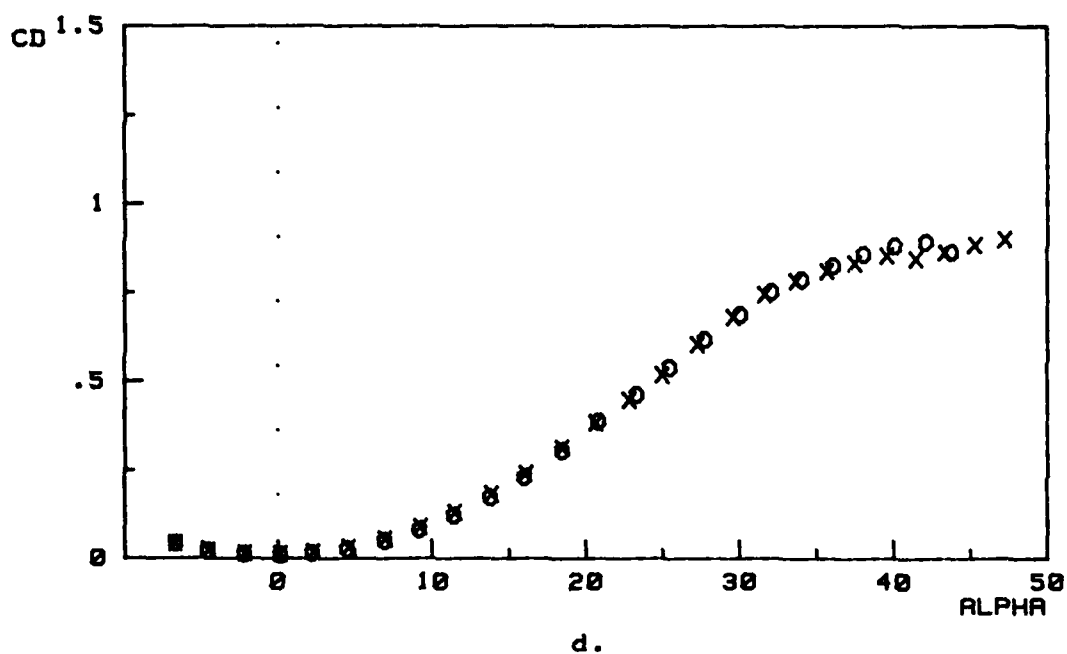
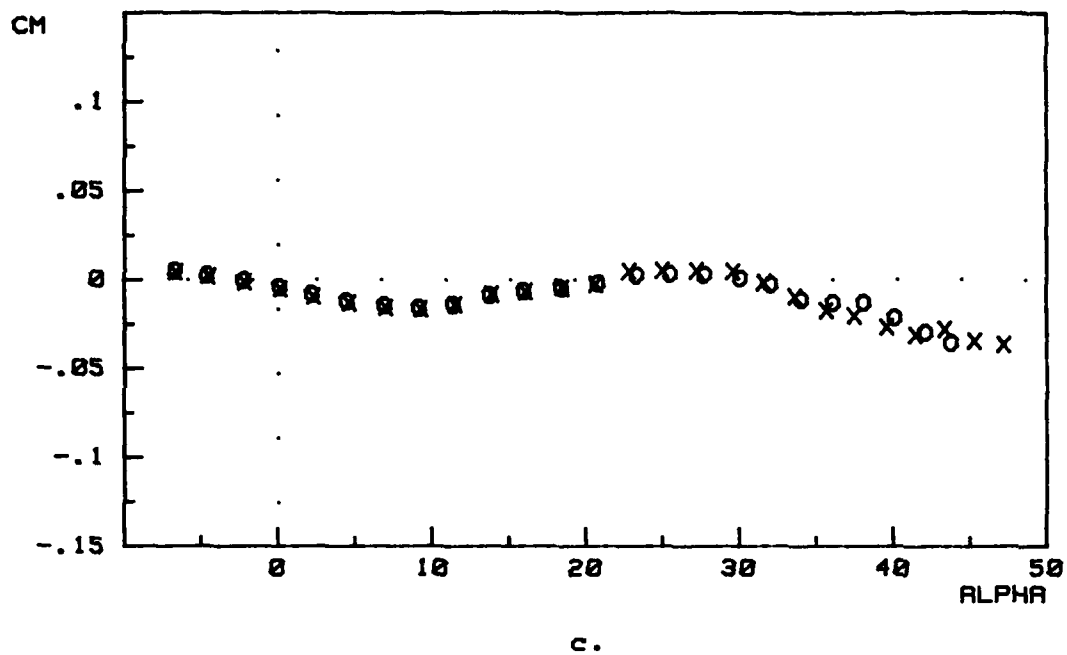
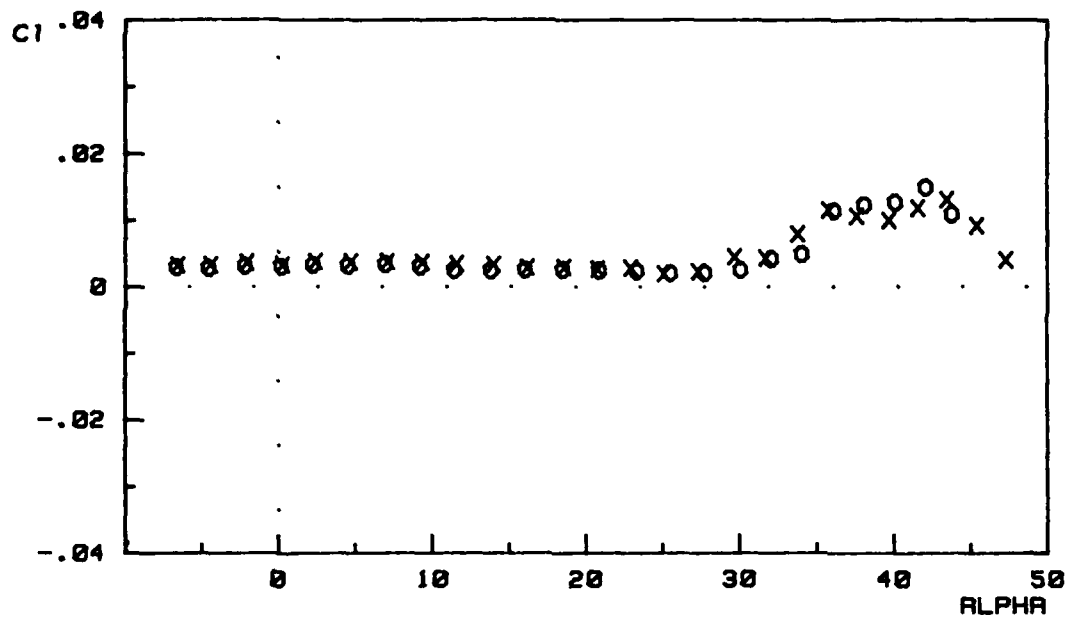
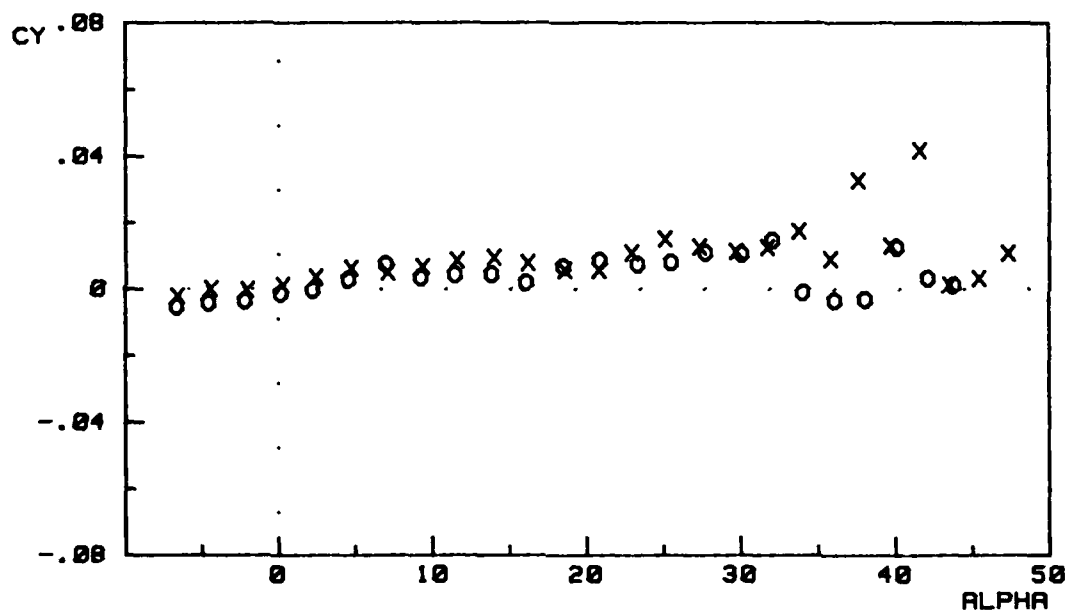


Fig. 10. (continued)



e.



f.

Fig. 10. (continued)



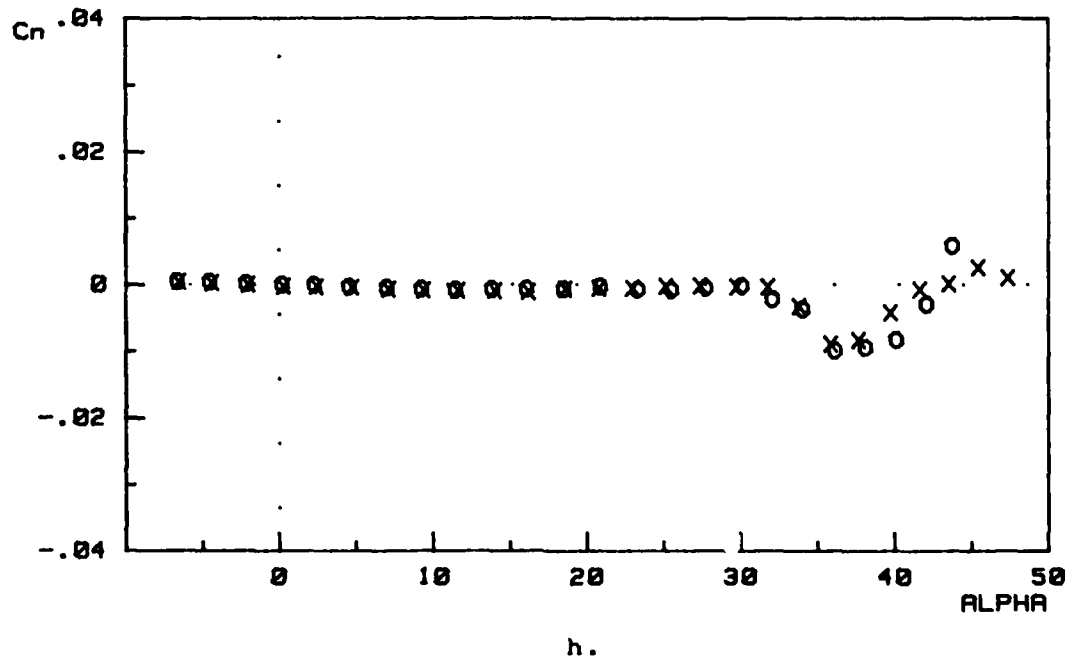
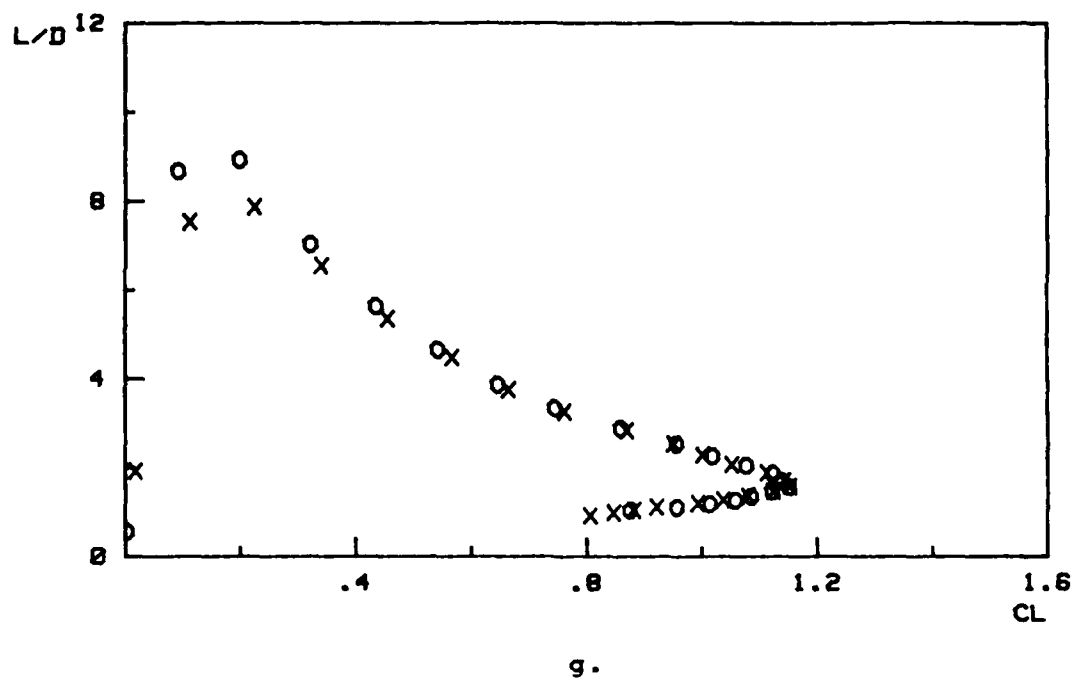


Fig. 10. (continued)

## RESULTS

This study examined the aerodynamic effects produced with 1) deployment of different fences, and 2) their placement at various positions and angles on the wing. The amount of data taken was quite large. As such, it was inconceivable and far too cumbersome to present every combination. The purpose of this section is to relate only those observable trends which have an impact on the overall goal of the investigation. Namely, to determine the potential of apex fences for V/STOL application and high  $\alpha$  pitching qualities for high-power maneuver recovery. These qualities can be realized if the lift and pitching moment coefficients are increased at the "expense" of increased drag. Lateral handling qualities must not be degraded, and no sudden deviations from baseline characteristics can be allowed. Because of this, "favorable" trends are ones which exhibit any or all of the above mentioned items. Likewise, "unfavorable" means the reverse is true.

### Baseline Characteristics

The delta wing/body model was shown in Fig. 5. The aerodynamic data (Fig. 10) agrees quite well with the results given by Marchman and Hollins (ref 5) and is summarized as follows:

## Baseline Without Flap Setting

### $C_L$ vs. $C_D$

This curve is indicative of the rate-of-increase in lift per unit drag.

### $C_L$ vs. $\alpha$

Typical of basic lift curves, the slope is constant (approximately 2.36/radian) up to  $\alpha = 24$ , at which point the wing begins to stall and the lift curve slope decreases in a moderate and smooth fashion. Wing stall for delta wings is known as vortex breakdown or "bursting". There is no lift generated for  $\alpha = 0$ , as expected.

### $C_M$ vs. $\alpha$

Because the model is pivoted around its predicted neutral point, the pitching moment should be zero initially. There are slight changes in the pitching moment slope through  $\alpha = 35$ , at which point a negative  $C_M$  is evident. This is an indication of a rearward movement of the center of pressure. It should be noted that stable (straight and level) flight can be maintained only when  $C_M = 0$  and the slope is negative.

#### $C_D$ vs. $\alpha$

Drag parabolic characteristics are evident in the model, as expected, except at high  $\alpha$  (where the small angle approximations in wing theory are not valid).

#### $C_l$ vs. $\alpha$

The rolling moment should theoretically be zero for no sideslip. However, vortex bursting occurs at high  $\alpha$  and creates asymmetric lifting forces on the wings which induces rolling. Additionally, model asymmetries are a contributing factor. Although not investigated, rolling moment behavior is radically changed for the asymmetric fence deployment cases.

#### $C_y$ vs. $\alpha$

Theoretically, no net side force should be present. However, given the lateral instability, model asymmetries, and probably some tunnel sidewash, the deviations are evident at high  $\alpha$ . (Side force was not considered of experimental interest and is presented only for the complete "picture".)

#### L/D vs. $\alpha$

This represents the typical aerodynamic efficiency

(L/D) of the model. The maximum point represents the "minimum drag at trim" condition. For an actual aircraft, this would be the minimum power required for straight and level flight. L/D is also an important design parameter for cruise, loiter, climb, and turning, since engine power is a critical factor.

#### $C_n$ vs. $\alpha$

Yawing moment follows directly from side force characteristics, and the same argument applies.

#### Baseline With Flap Settings

##### (Effects With Inboard Flap Settings Only)

Fig. 11 gives the lift, drag, and pitching behavior of the model with inboard flaps deflected to -10, 0, 10, 20, and 30 degrees. Of interest is the usual step increase in  $C_L$  and  $C_M$  for a given flap deflection. The incremental amount decreases as angle of attack is increased. Also, for  $\alpha = 30$  there appears to be a tendency to produce nose-down (negative) pitching moments (i.e. slope is negative) relative to each case. This indicates that the rearward portion of the wing begins to contribute [relatively] more normal force overall,

and the model is in a pitch stable attitude. The drag characteristics are considered "normal" in the sense that positive  $\delta$  shifts the curve to the left and up.

#### (Effects With Inboard and Outboard Flap Settings)

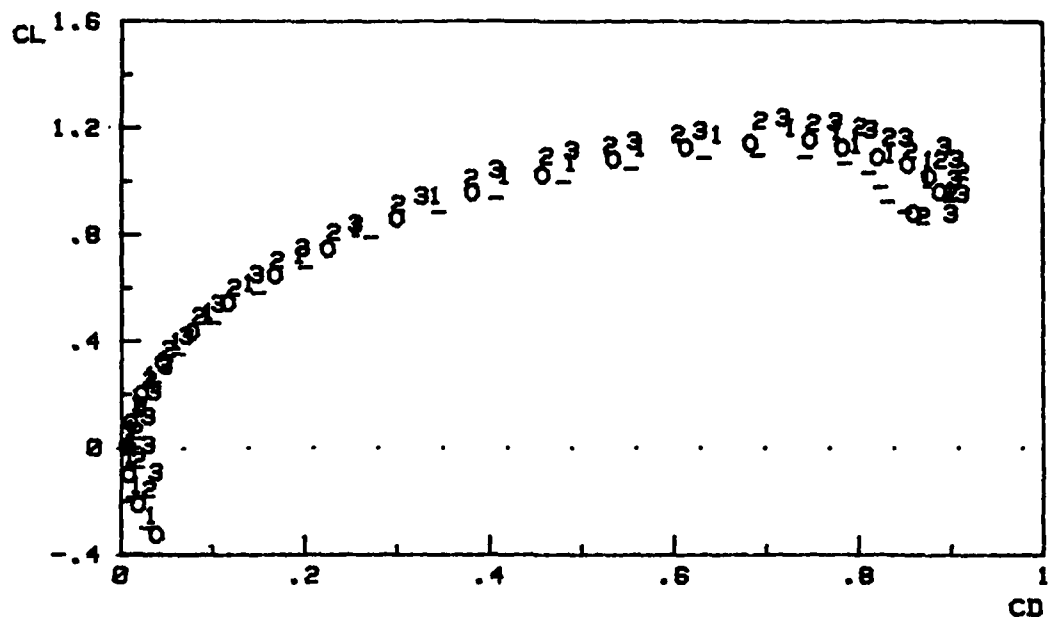
Fig. 12 shows the effects of both sets of flaps deflected to -10, 0, 10, and 20 degrees. The basic characteristics of twin deployment mirror those of the previous case except that the effects are more pronounced.

#### Basic Fence Effects

In order to gain an understanding of the aerodynamic qualities or effects which apex fences produce, a discussion of the F1 configuration is now presented. This fence illustrates the general aerodynamic effects common to all apex fences tested and exhibits these effects more clearly than other configurations.

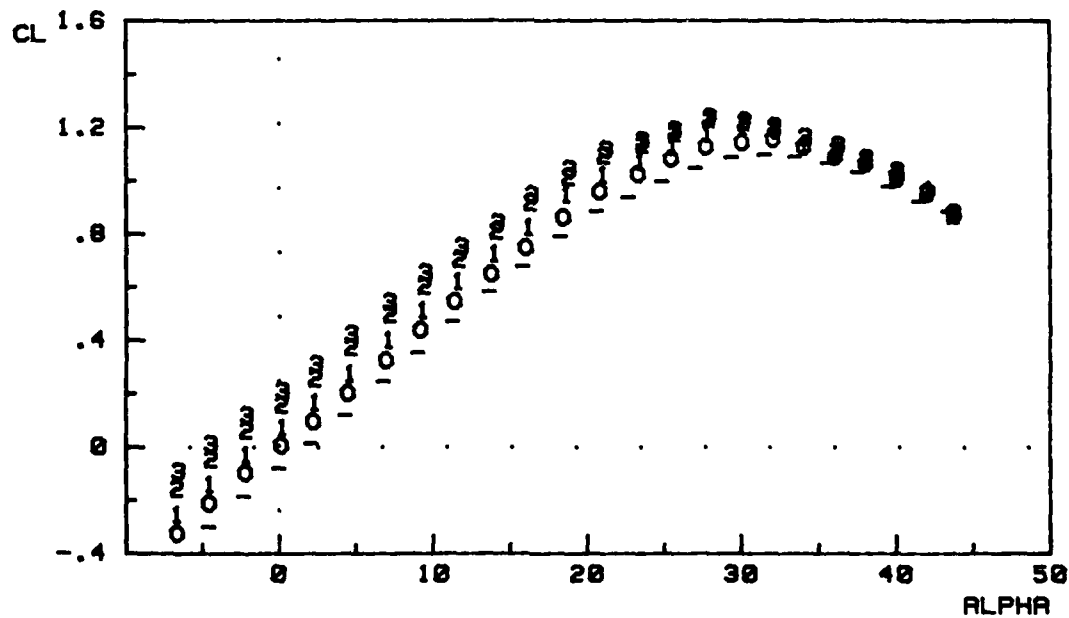
The F1 (Gothic) vs. baseline results given in Fig. 13 demonstrate that apex fences deployed normal to the wing's surface plane:

A. produce a shift in the zero lift line; creating an increase in  $C_L$  at lower  $\alpha$  but no change in  $C_{Lmax}$ . In other words, the lift curve is roughly shifted to the left, with a



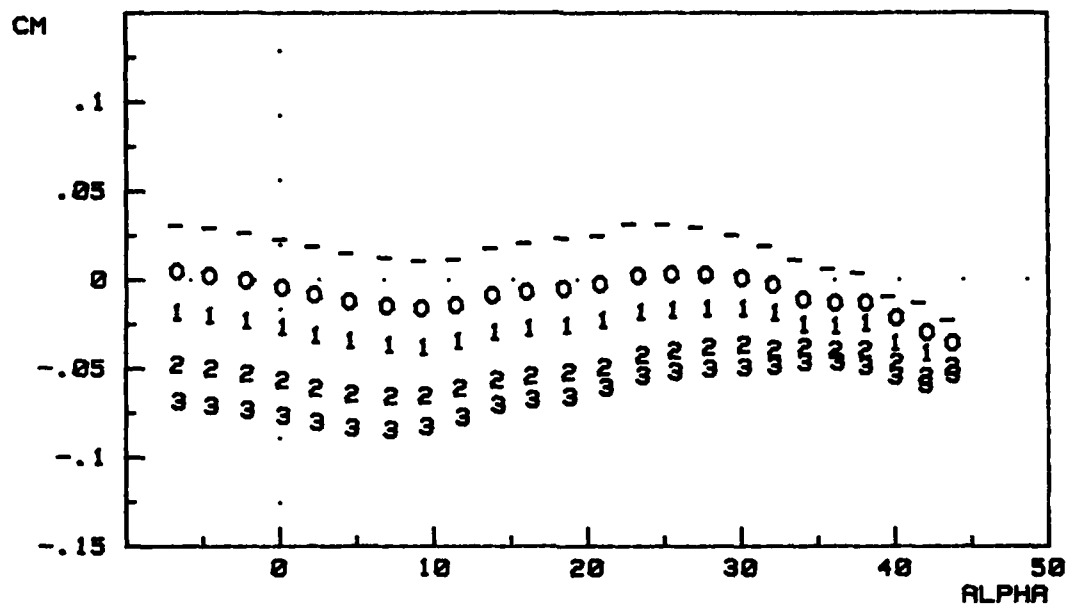
a.

-	-10°	inboard flap
0	0°	inboard flap
1	10°	inboard flap
2	20°	inboard flap
3	30°	inboard flap



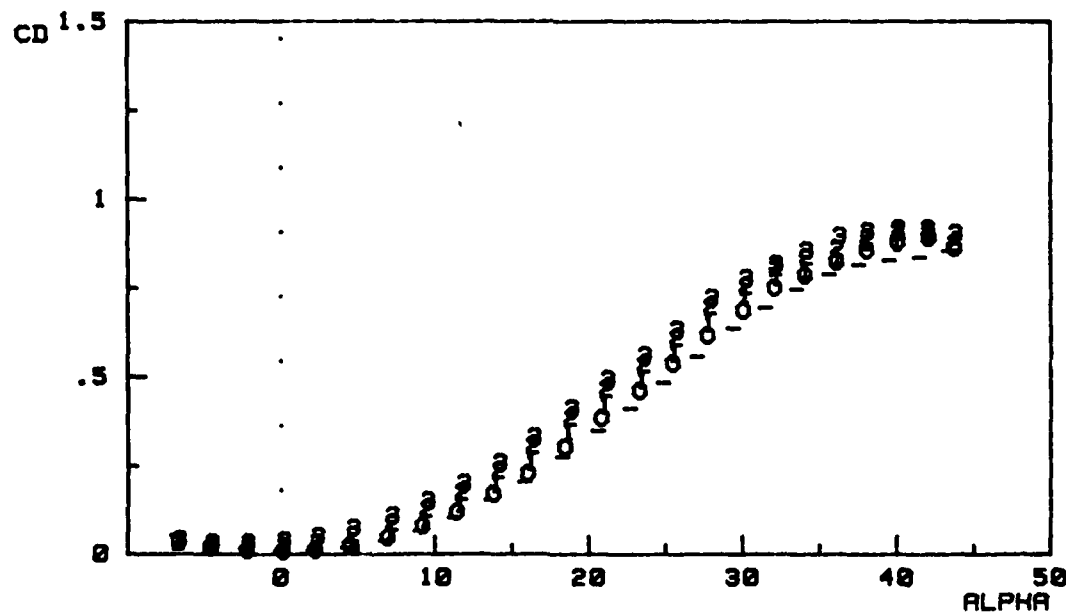
b.

Fig. 11. Baseline with Inboard Trailing Edge Flap Deflections



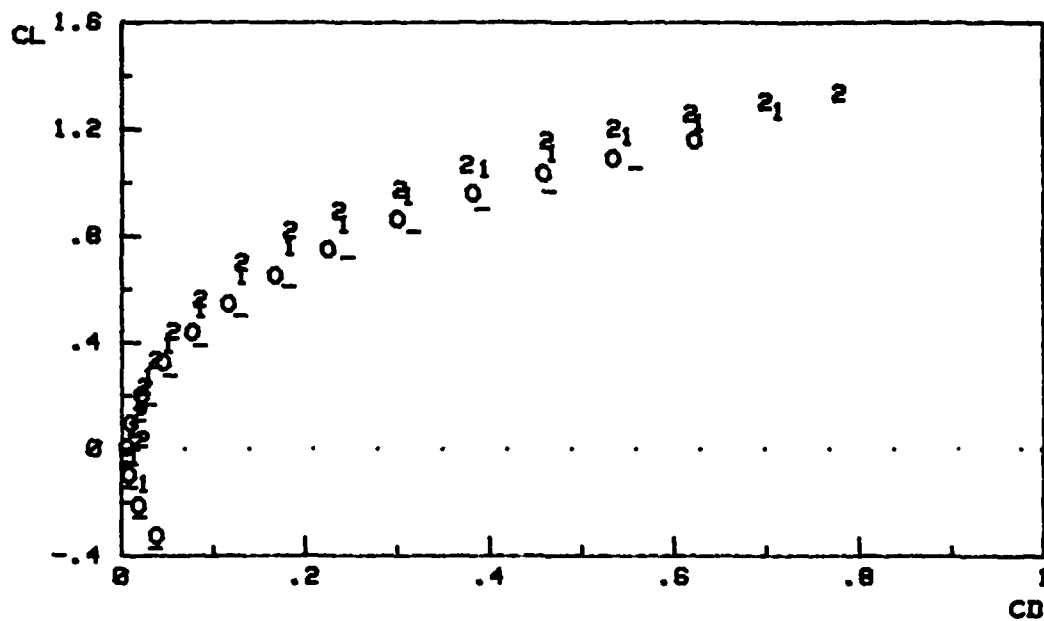
c.

-	-10°	inboard flap
0	0°	inboard flap
1	10°	inboard flap
2	20°	inboard flap
3	30°	inboard flap



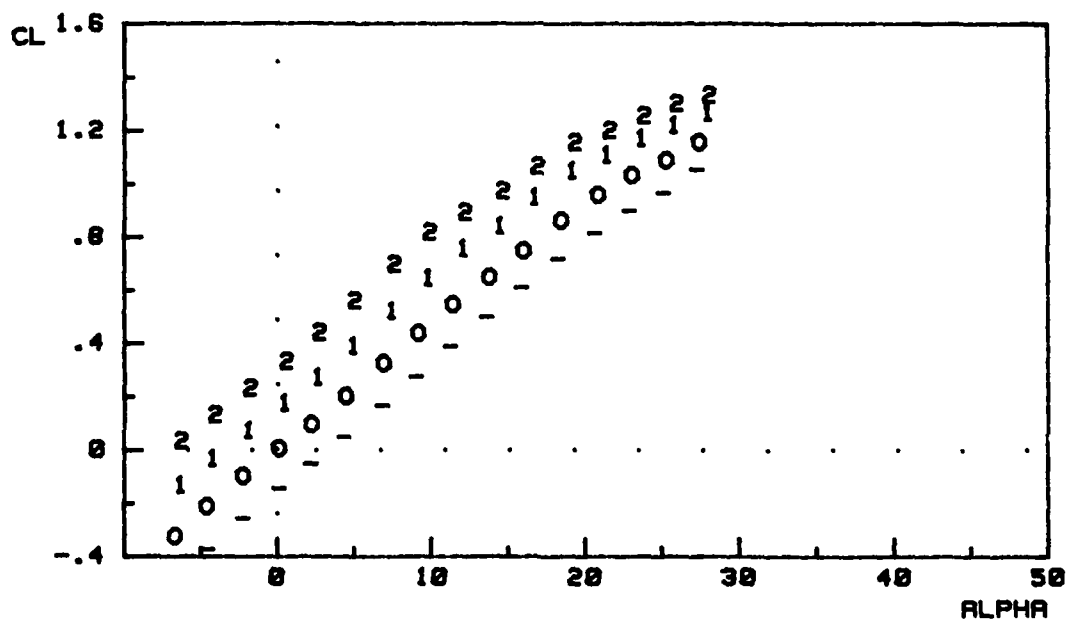
d.  
Fig. 11. (continued)





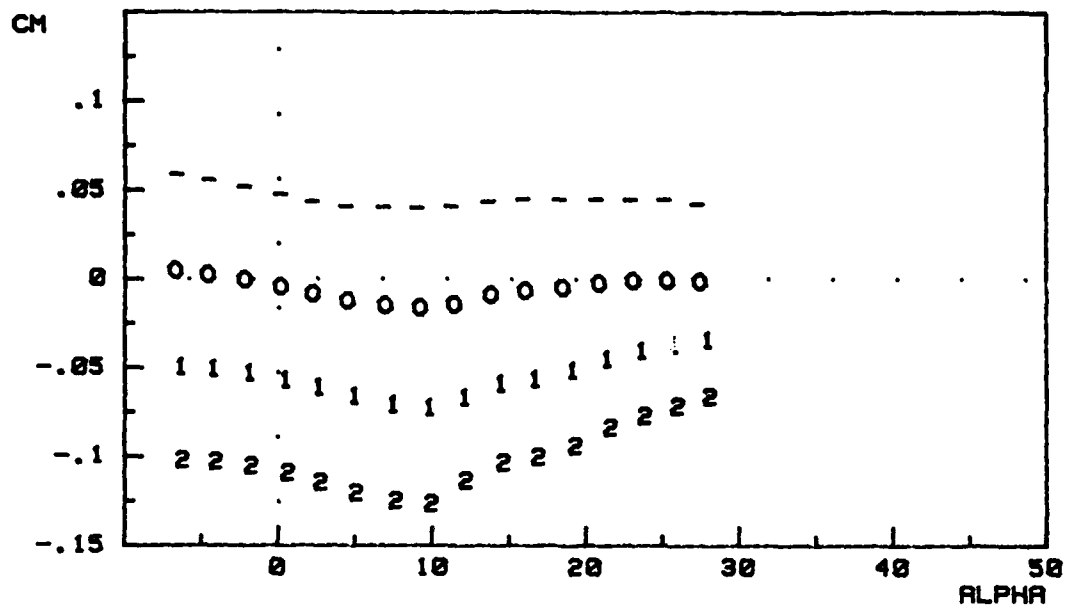
a.

-	-10°	twin flap
0	0°	twin flap
1	10°	twin flap
2	20°	twin flap



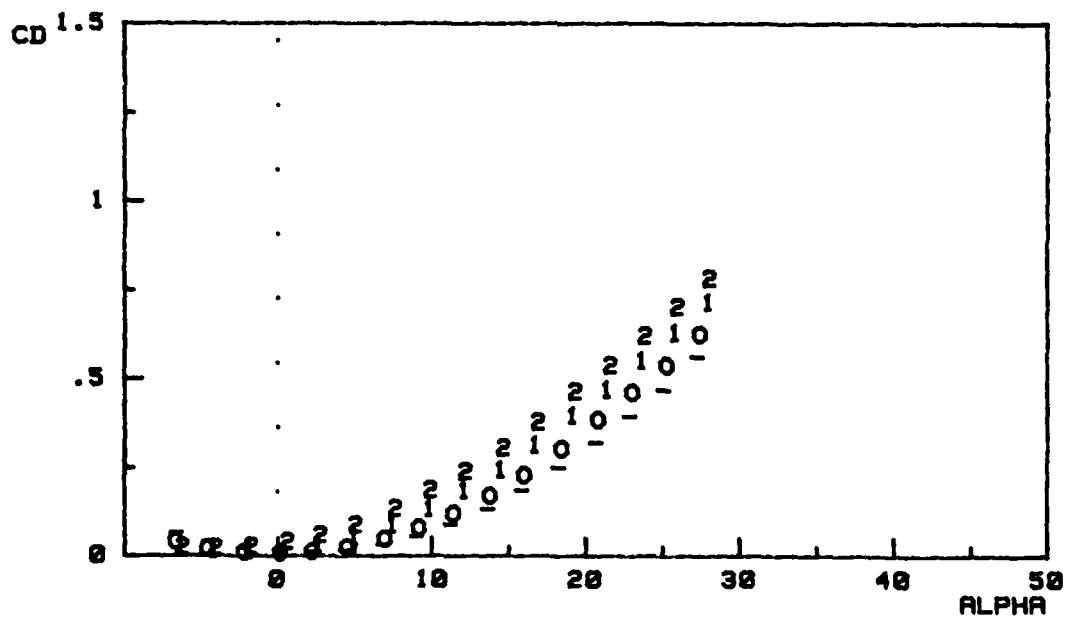
b.

Fig. 12. Baseline with Twin (Inboard and Outboard) Trailing Edge Flap Deflections



c.

-	-10°	twin flap
0	0°	twin flap
1	10°	twin flap
2	20°	twin flap



d.  
Fig. 12. (continued)

relative decrease of  $C_L$  around  $\alpha = 30$ . This was predicted by Rao (ref 7), who showed that an increase in the normal force coefficient (based on upper surface pressure data) was evident with Gothic fence deployment.

B. increase the drag. However, beyond a certain angle (around  $\alpha = 30$ ) the drag is lower than the baseline case.

C. generate less normal force relative to the baseline case for  $\alpha > 30$ . This is suggested by the results given in A. & B. above, but was not investigated in previous studies. Aerodynamically, the vortex structures generated by the fences are weaker at this attitude. This can be understood from the fact that, beyond  $\alpha = 30$ , the fence plays a lesser role in apex vortex generation since it is tilted "back" from the oncoming freestream. Additionally, the minute reduction in the lift curve slope suggests that this is the case.

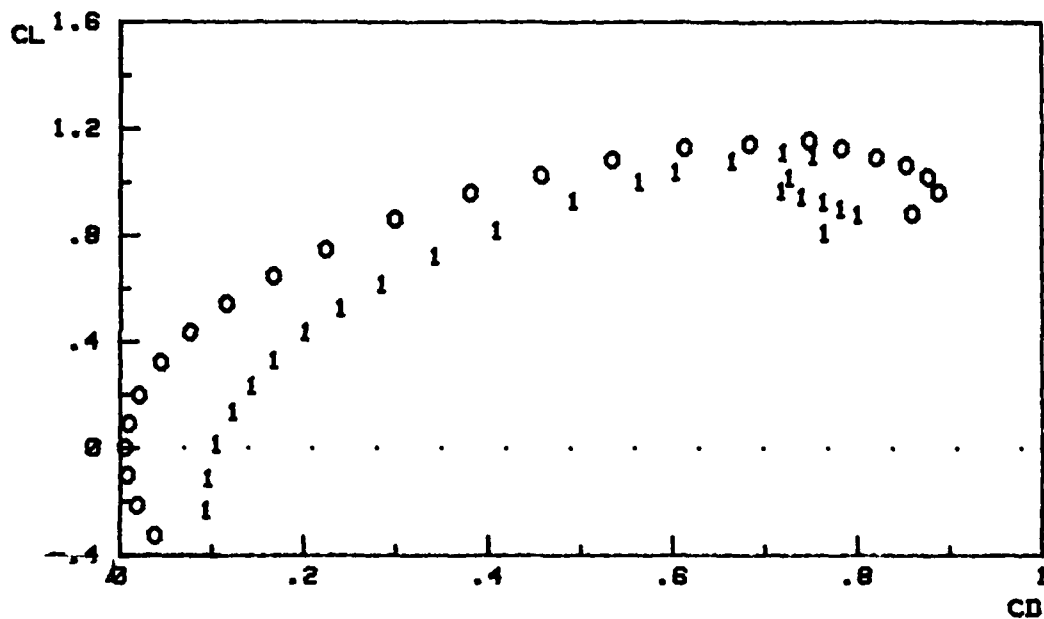
D. produce positive pitching moments up to about  $\alpha = 32$ . This result stems from the enhanced lift generated by the fences due to the increased loading at the wing apex region. The result agrees with the pressure data given in references 6 and 7 for the apex region. This is essentially the effect of camber near the leading edge, because the fence simulates thickness and camber over its span.

E. produce somewhat larger nose-down (restoring) moments beyond  $\alpha = 32$  or 35. From C. it is seen that, in general, apex fences reduce the normal force generation over the entire wing above  $\alpha = 30$  but even more so at the apex

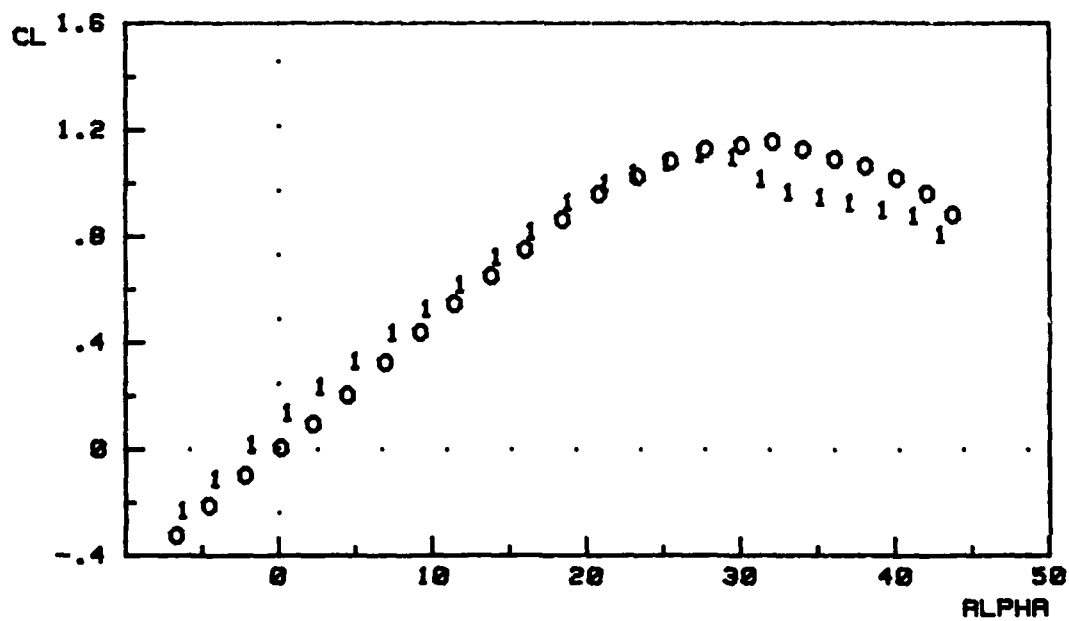
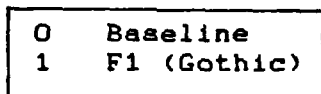
region for  $\alpha > 35$ . In all, this is no great mystery: As angle of attack increases, the baseline wing's leading edge trips the formation of vortices much more strongly, whereas the fence trips the formation of apex vortices most strongly at  $\alpha = 0$ . (I.e. the projected frontal area decreases with increasing  $\alpha$ . Imagine the vortex generation at  $\alpha = 0$  and  $\alpha = 90$  to get a clear picture.) The rearward portion of the wing also acts in producing nose-down moments as  $\alpha$  increases for both the baseline and configured cases.

F. when deployed symmetrically, generate no rolling moment, yawing moment, or side force. Additionally, they do not appreciably effect the lateral stiffness characteristics. (See side force data for  $\alpha > 20$ .)

G. substantially reduce the aerodynamic efficiency (L/D) by 25% to 50%. This is largely due to the increased form drag or "pressure drag" caused by the bluntness of the fences. This parameter is primarily of concern for cruise flying, shallow climbs and turning, where efficiency of useable engine power is crucial; regimes not intended for apex fence deployment. Hence, it has little relevance in the context of STOL operations.



a.



b.

Fig. 13. Baseline Case vs. F1 Gothic Fence Case

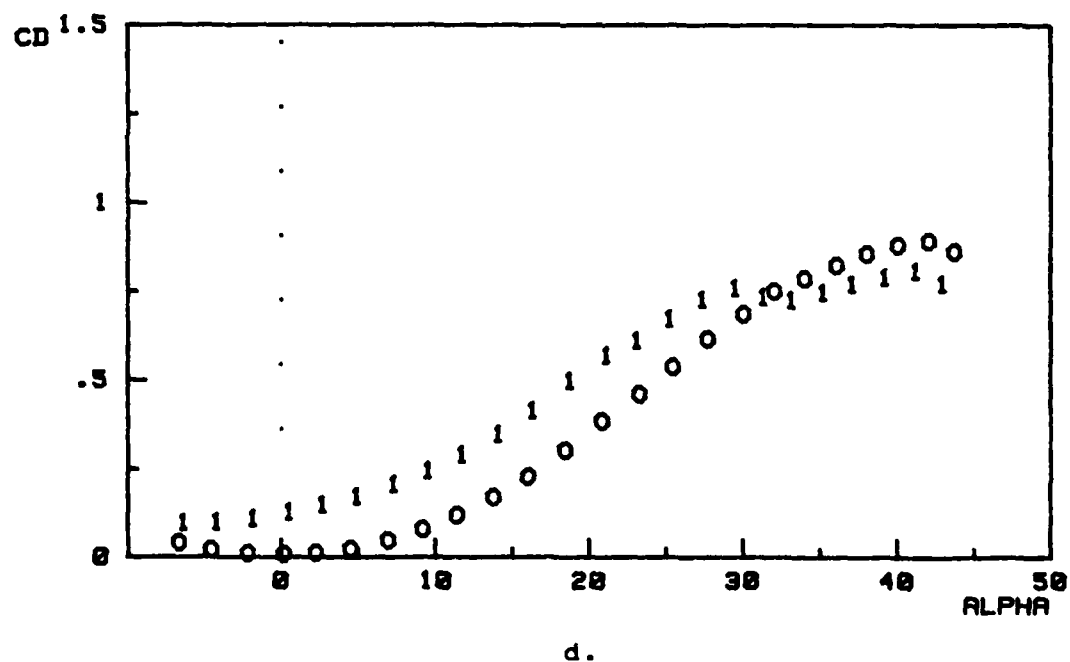
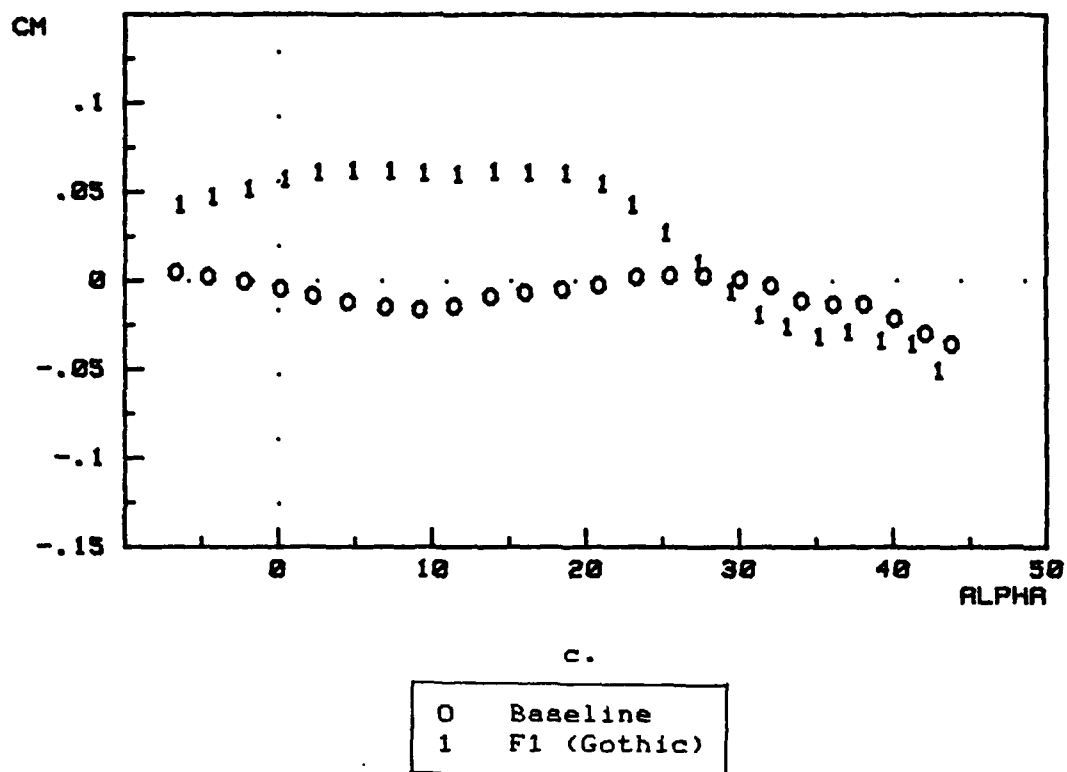
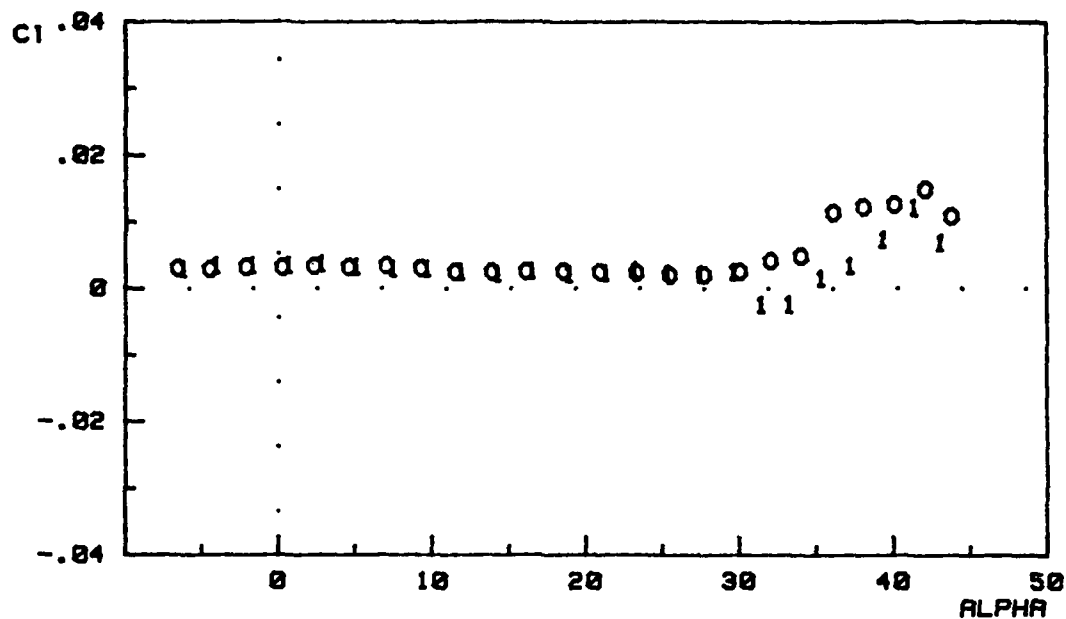
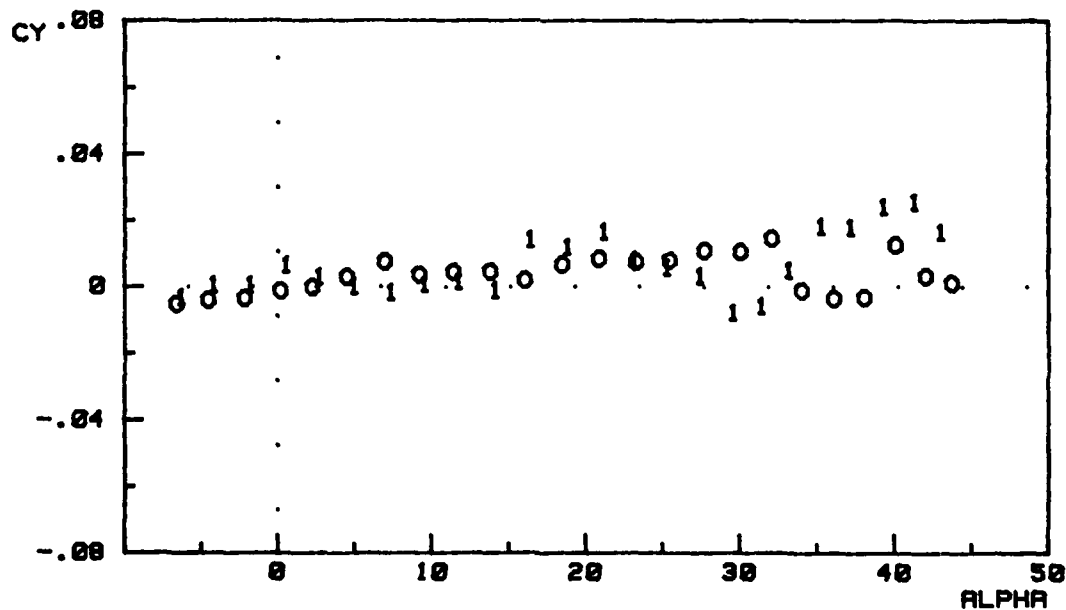


Fig. 13. (continued)



e.

0	Baseline
1	F1 (Gothic)



f.

Fig. 13. (continued)

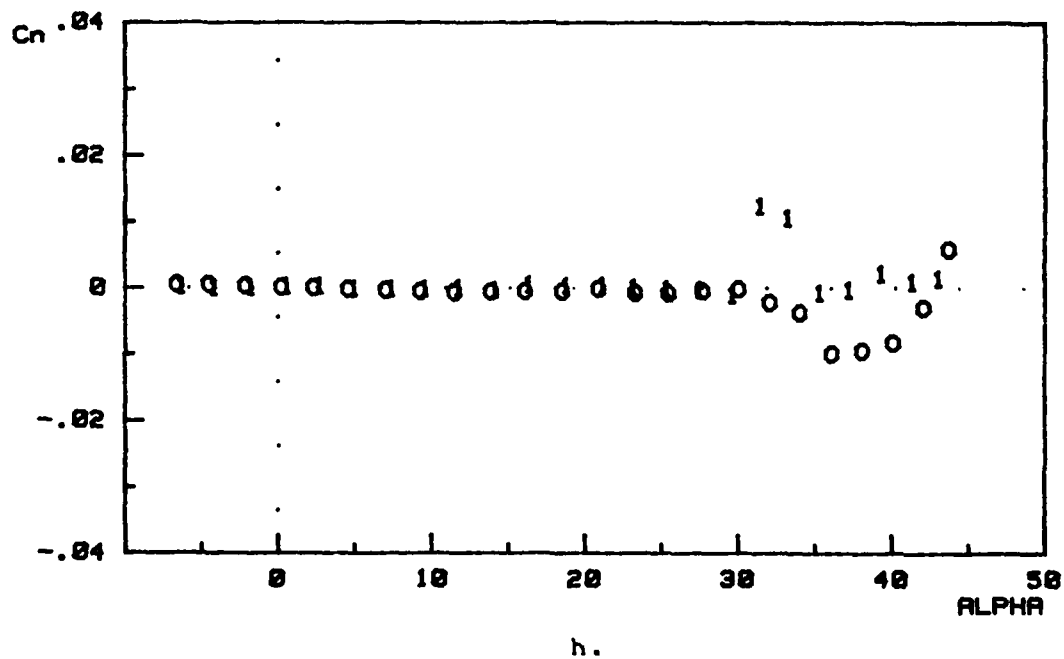
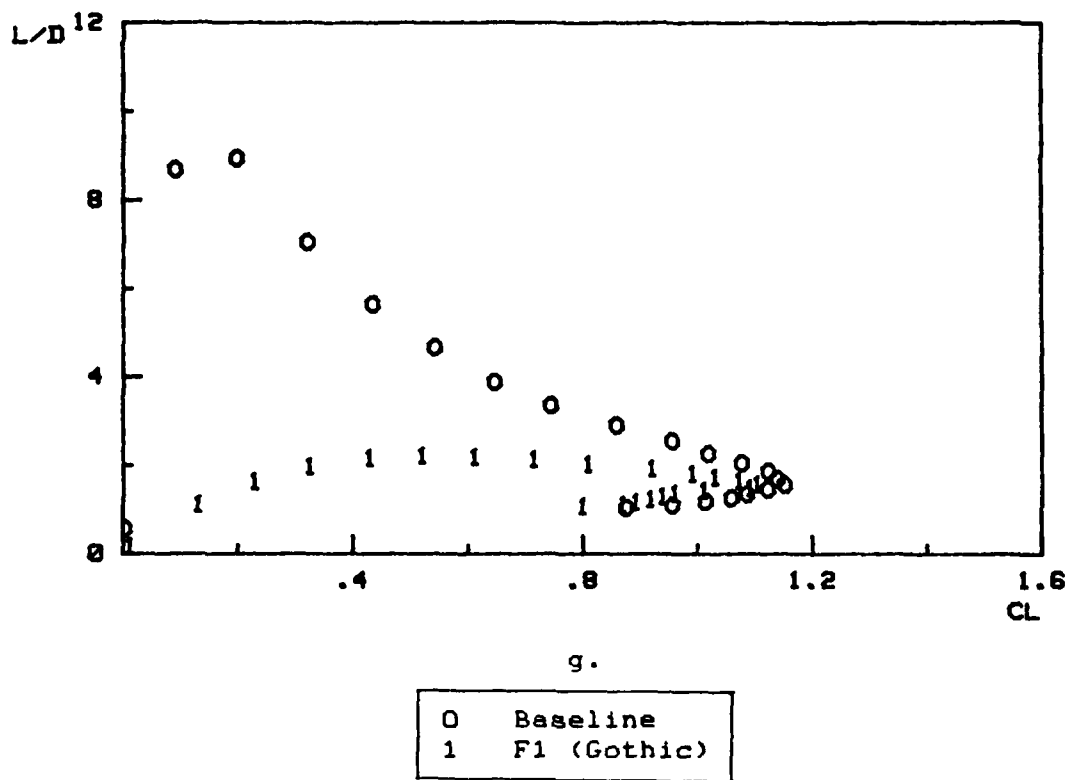


Fig. 13. (continued)



## Parametric Investigations

Five fence parameters were varied and examined separately to determine the qualitative effects they have on "overall fence performance". As such, comparisons are made between selected fences in order to observe any trend. Finally, all optimal parameter values were combined in such a way as to produce the most favorable or "best" fence design in light of the proposed applications to STOL and high angle of attack pitching. This is discussed in a following section.

The five parameters that will be defined and reported here are, in order:

- I. Shape
- II. Length-to-Height
- III. Cant
- IV. Surface Area
- V. Movement

Note: Unless otherwise indicated, all fences are at the apex, on the leading edge, and perpendicular to the symmetry plane of the wing. Shape, Length-to-Height ratio, and Surface Area values for each fence were given in Figs. 6 - 8.

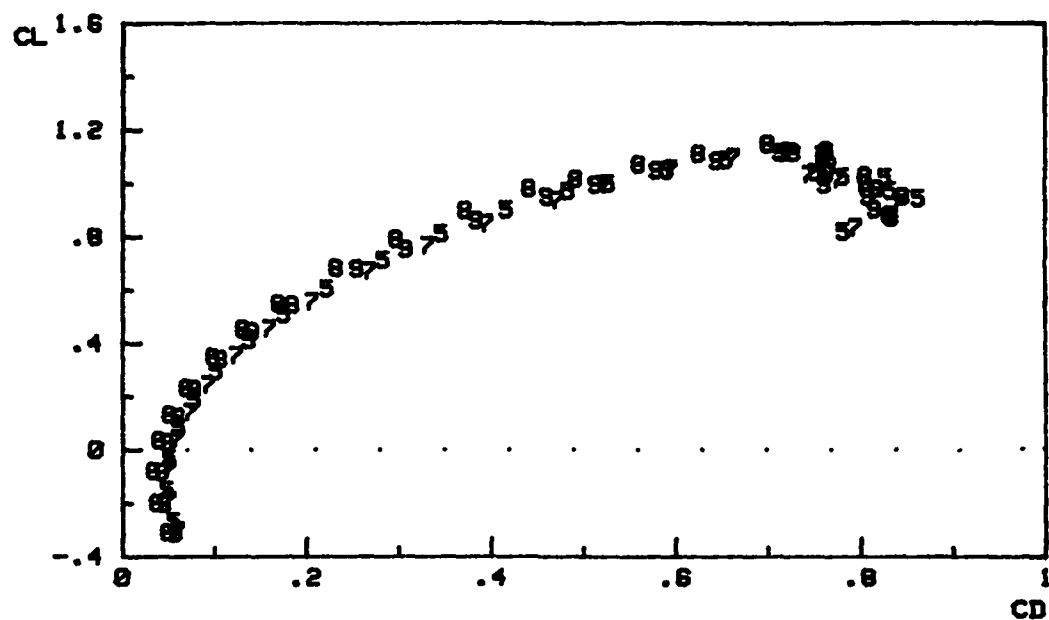
### I. Shape

The four basic fence shapes used, based on previous testing and experience (ref 7), are the Double Gothic type, Modified Gothic type, Delta type, and Cropped type. They are

represented by the four fences F5, F7, F8, and F9, respectively. These fences were chosen because the remaining parameters were, for the most part, equal among them. Fig. 14 demonstrates the effect of shape on the aerodynamics. As can be seen, F5 (Double Gothic) stands out among the other fences in terms of improved  $C_L$  and higher  $C_M$  whereas the other fences are marginal at best. F5 does produce a slightly higher drag coefficient, but overall, this is of no consequence for STOL requirements. It would seem that F5 does suffer somewhat at high  $\alpha$  in pitching, but its curve is better behaved than F8 (Delta), which produces more restoring moment but in an inconsistent manner. In all, F5 is the better choice for shape. This implies that the smooth trailing taper of the fence is preferable to a sudden break. (Compare especially F5 and F7 shapes.) An additional case was needed to determine if this holds for the "middle ground" case of F12 (Double Gothic). This fence has a tapered geometry, but it is more drastic than F5. The results (Fig. 15) show a degrading trend. Hence, a Double Gothic shape with a gently tapered rear edge is preferable.

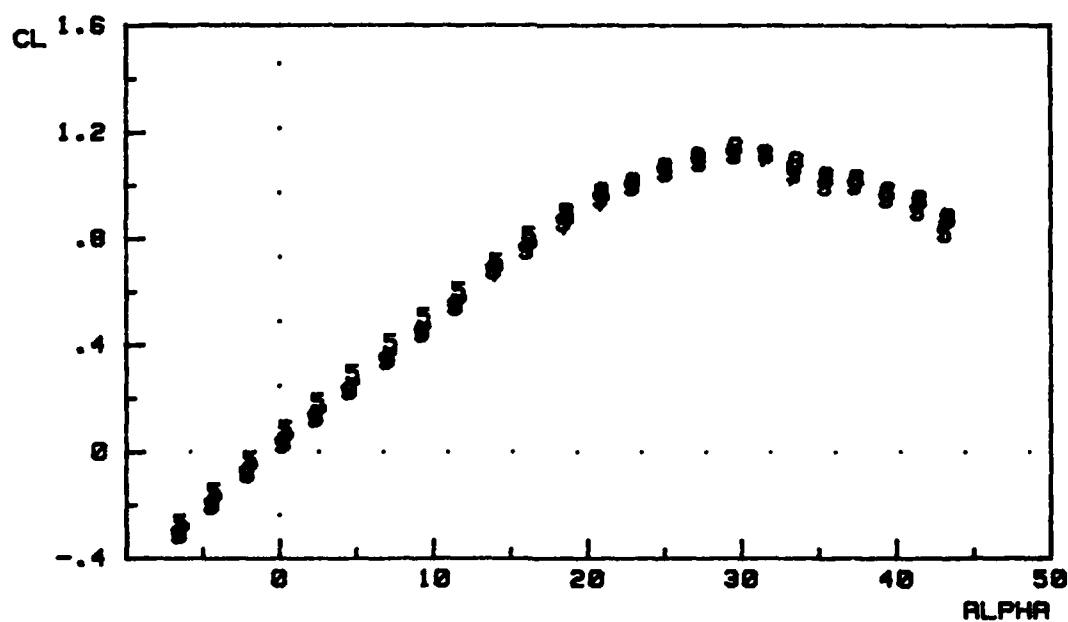
## II. Length-to-Height

This parameter is based on the ratio between the overall fence length to its maximum height. In order to make clear distinctions on the effect of this parameter, the Cropped type fences were utilized. These are fences F3, F4, F9, and



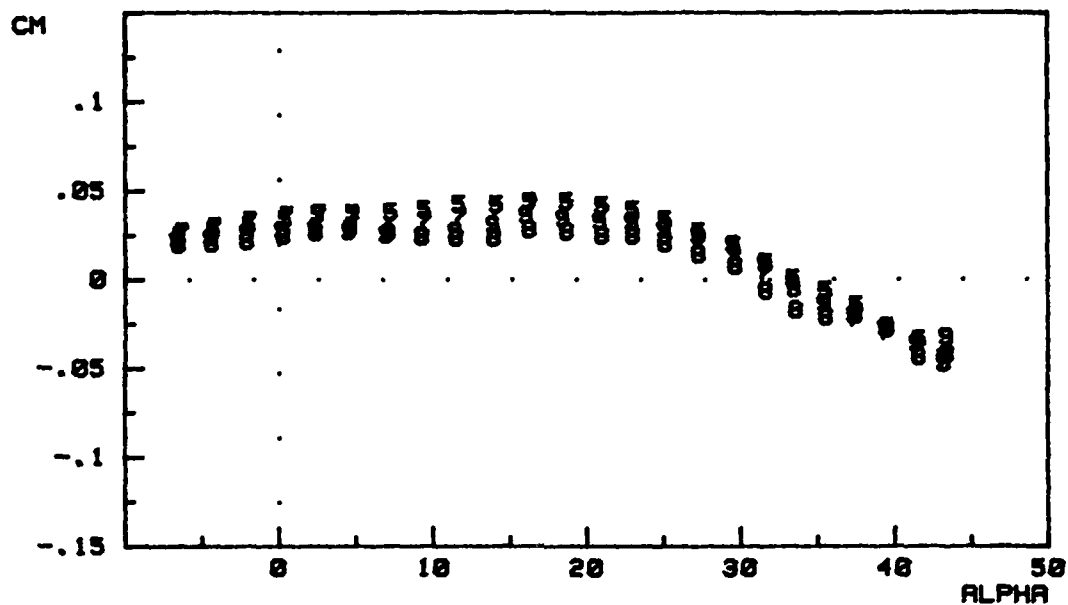
a.

5	F5 (Double Gothic)
7	F7 (Modified Gothic II)
8	F8 (Short Delta)
9	F9 (Short Cropped)



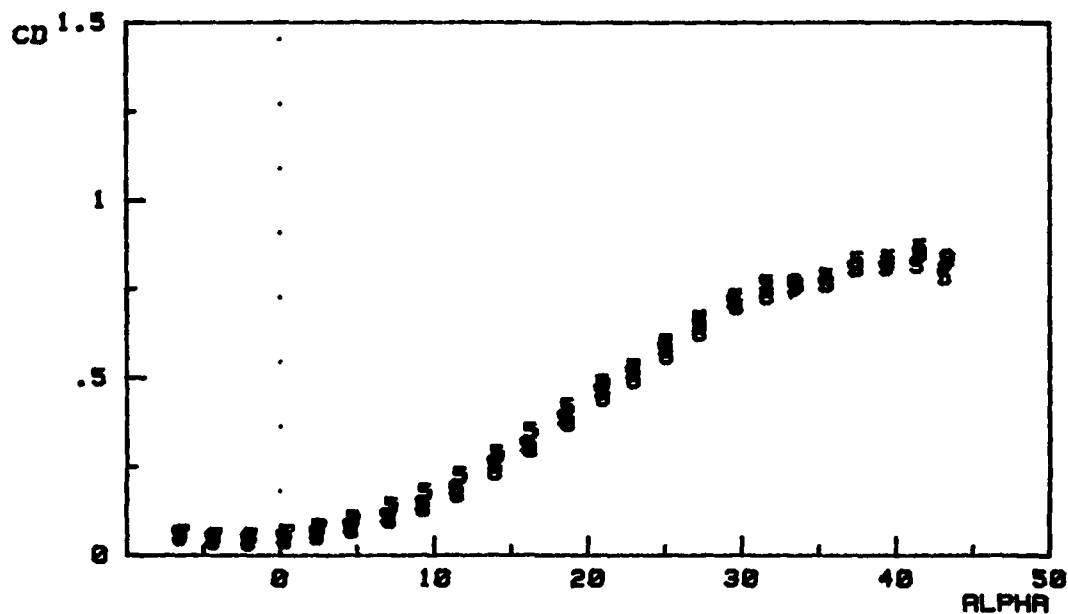
b.

Fig. 14. Effects of Fence Shape

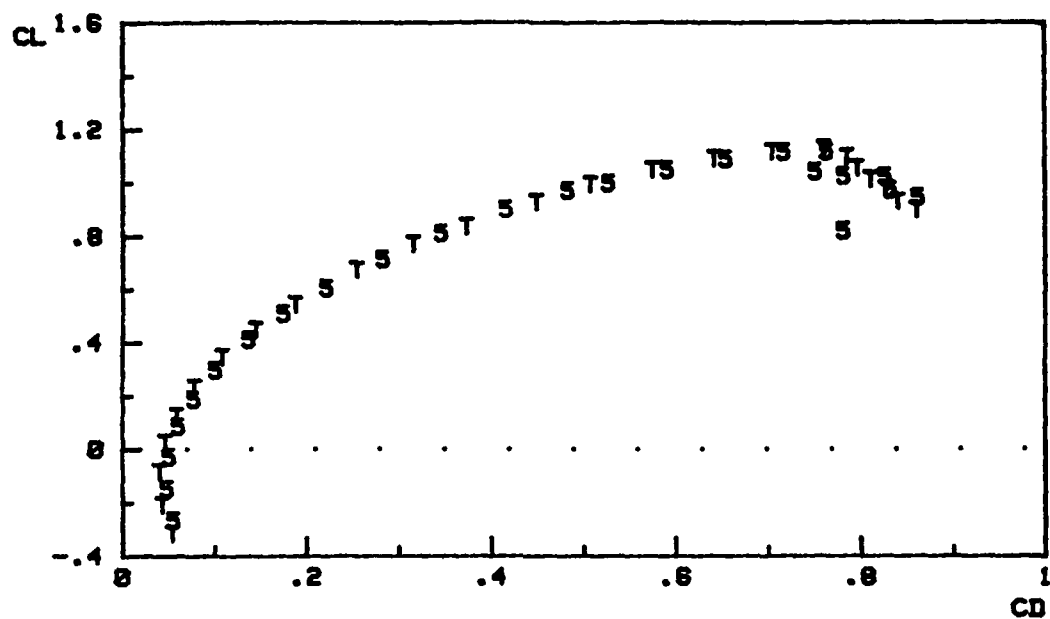


c.

5	F5 (Double Gothic)
7	F7 (Modified Gothic II)
8	F8 (Short Delta)
9	F9 (Short Cropped)

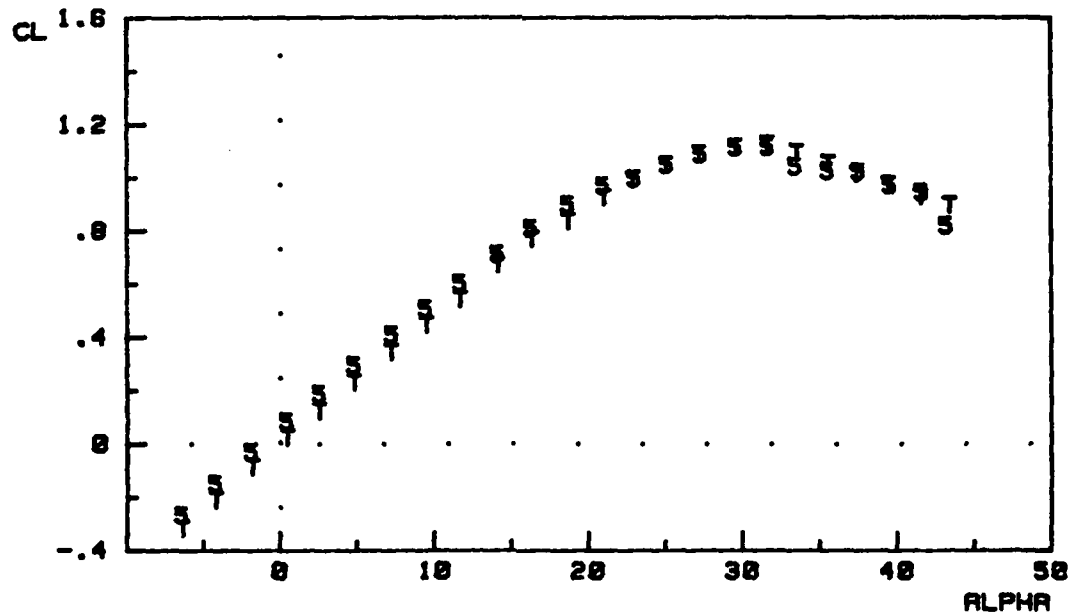


d.  
Fig. 14. (continued)



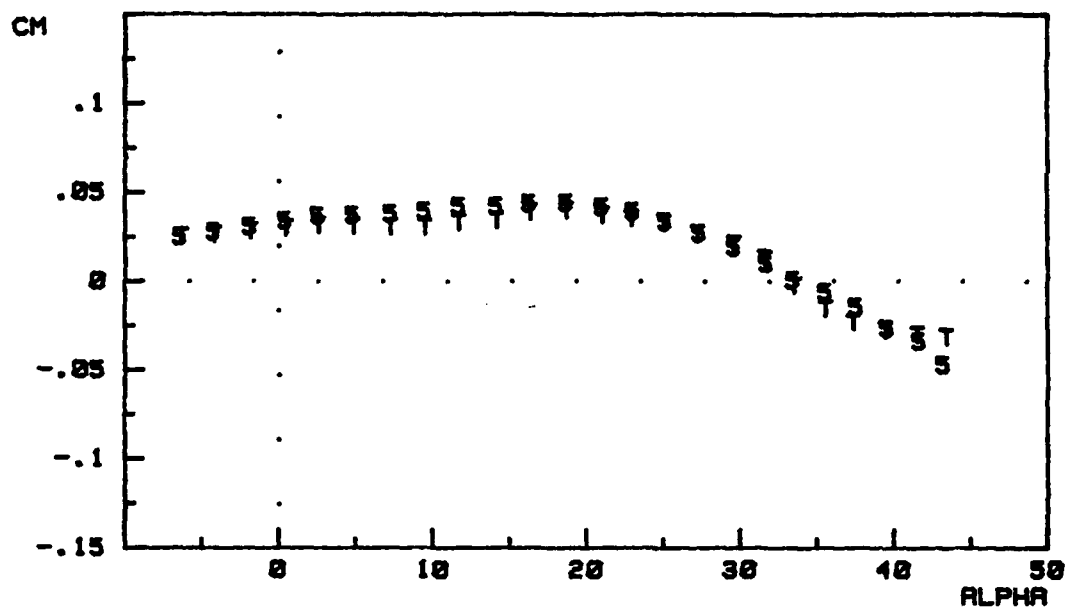
a.

S	F5 (Double Gothic)
T	F12 (Double Gothic II)



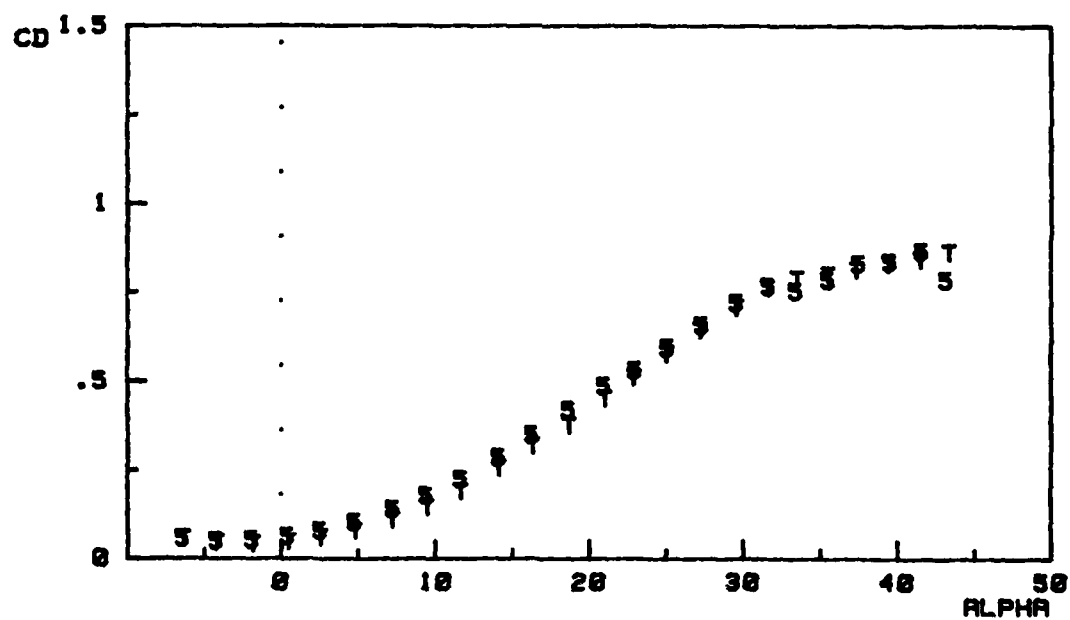
b.

Fig. 15. Effects of Different Double Gothic Fence Shapes



c.

S	F5 (Double Gothic)
T	F12 (Double Gothic II)



d.

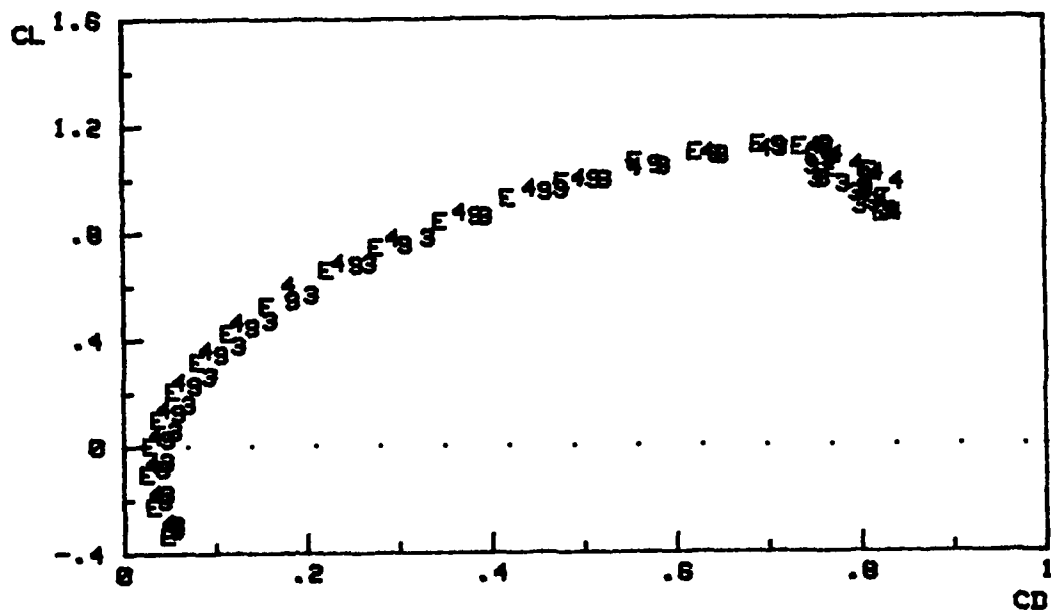
Fig. 15. (continued)

F11. The fences are common in terms of shape and cant, however, the surface areas are different with the exception that F4 and F11 have equal area. In view of this, the differences observed between F4 and F11 take on more meaning than those of the other two fences. Logically, since F3 is much larger than F4, one expects the aerodynamic effects caused by each fence to be a function of length-to-height as well as surface area. With this in mind, Fig. 16 gives the parametric results. From this information it is seen that this parameter becomes important as it grows. (I.e. note that the ratio is 8.786 for F11 compared to 3.5 for F4.) Thus, slender fences cause enhanced loading in the apex region at low-to-medium  $\alpha$  while retarding it more at high  $\alpha$ . (Note the  $C_M$  curve). In addition, this parameter has very little influence on the lift of the model through the entire range of angle of attack.

### III. Cant

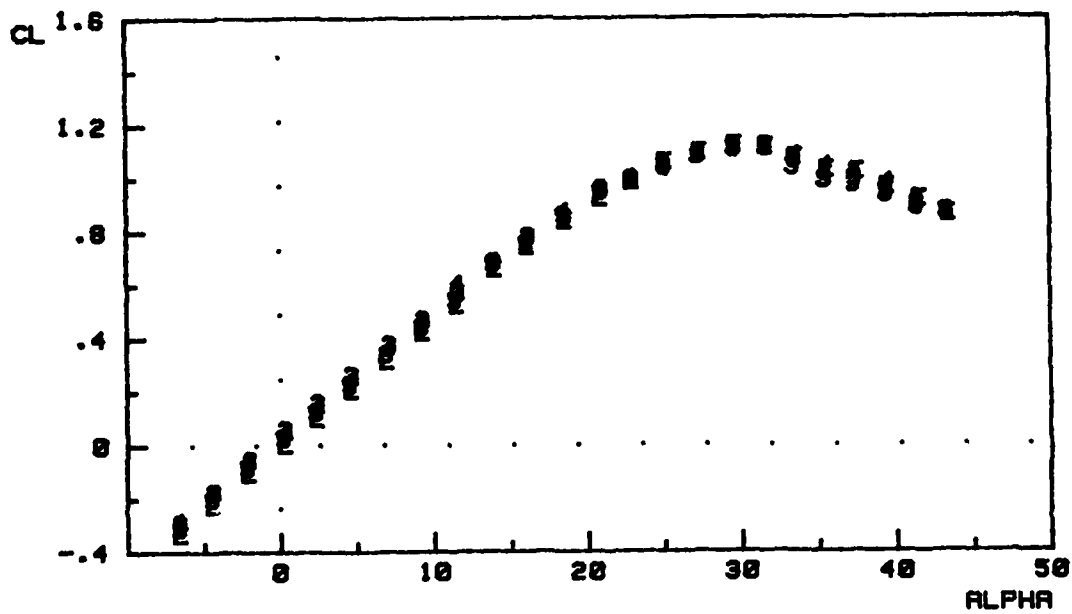
Cant is defined as the angle between the fence plane and the vector normal to the wing plane (Fig. 17). It effectively alters the projected frontal area of a fence by (roughly) the cosine of  $(\alpha - \sigma)$ . Fences used in this study were F1, F2, and F5. The trends observed in each case were similar, and so the results are given here using F5 as an example (Fig. 18).

Cant angles of  $\sigma = 7.5, 0, -7.5$ , and  $-15$  were used. The



a.

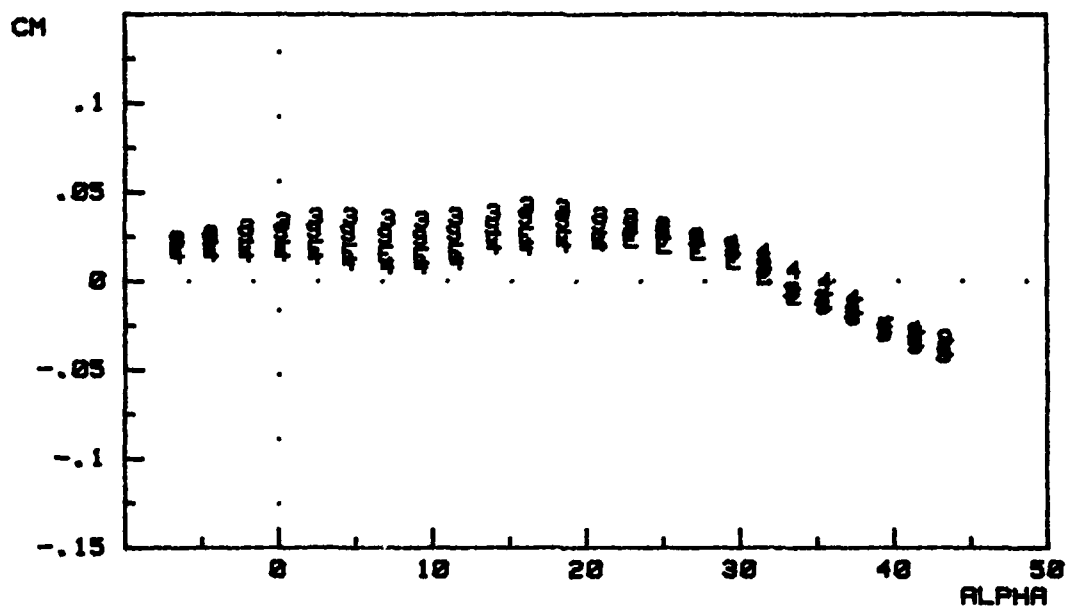
3	F3 (Cropped)
4	F4 (Mini Cropped)
9	F9 (Short Cropped)
E	F11 (Chopped Cropped)



b.

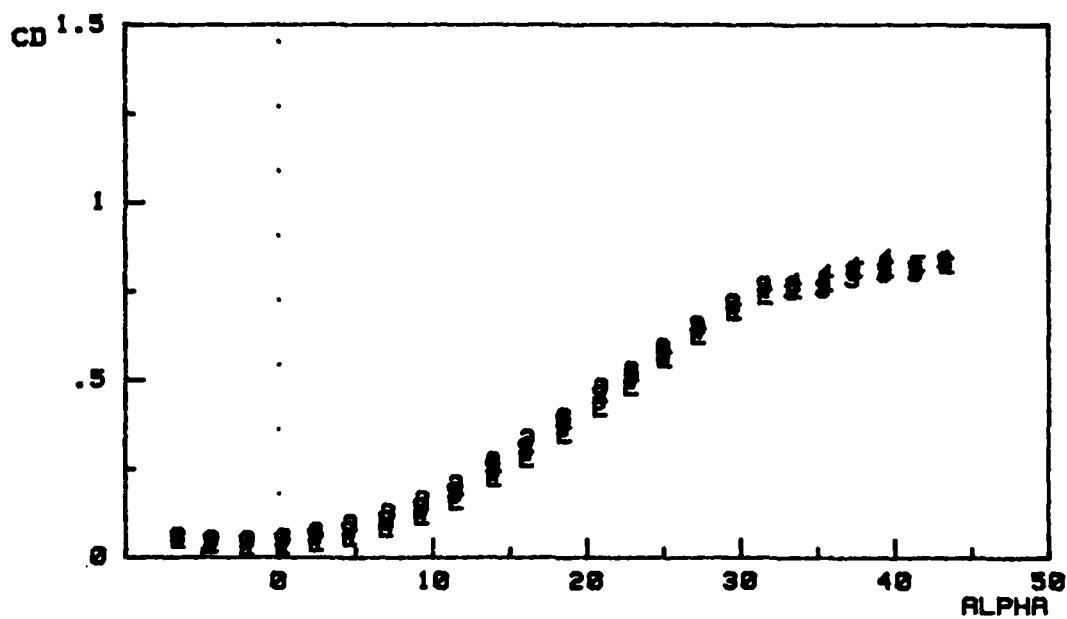
Fig. 16. Effects of Fence Length-to-Height Ratio





c.

3	F3 (Cropped)
4	F4 (Mini Cropped)
9	F9 (Short Cropped)
E	F11 (Chopped Cropped)



d.  
Fig. 16. (continued)

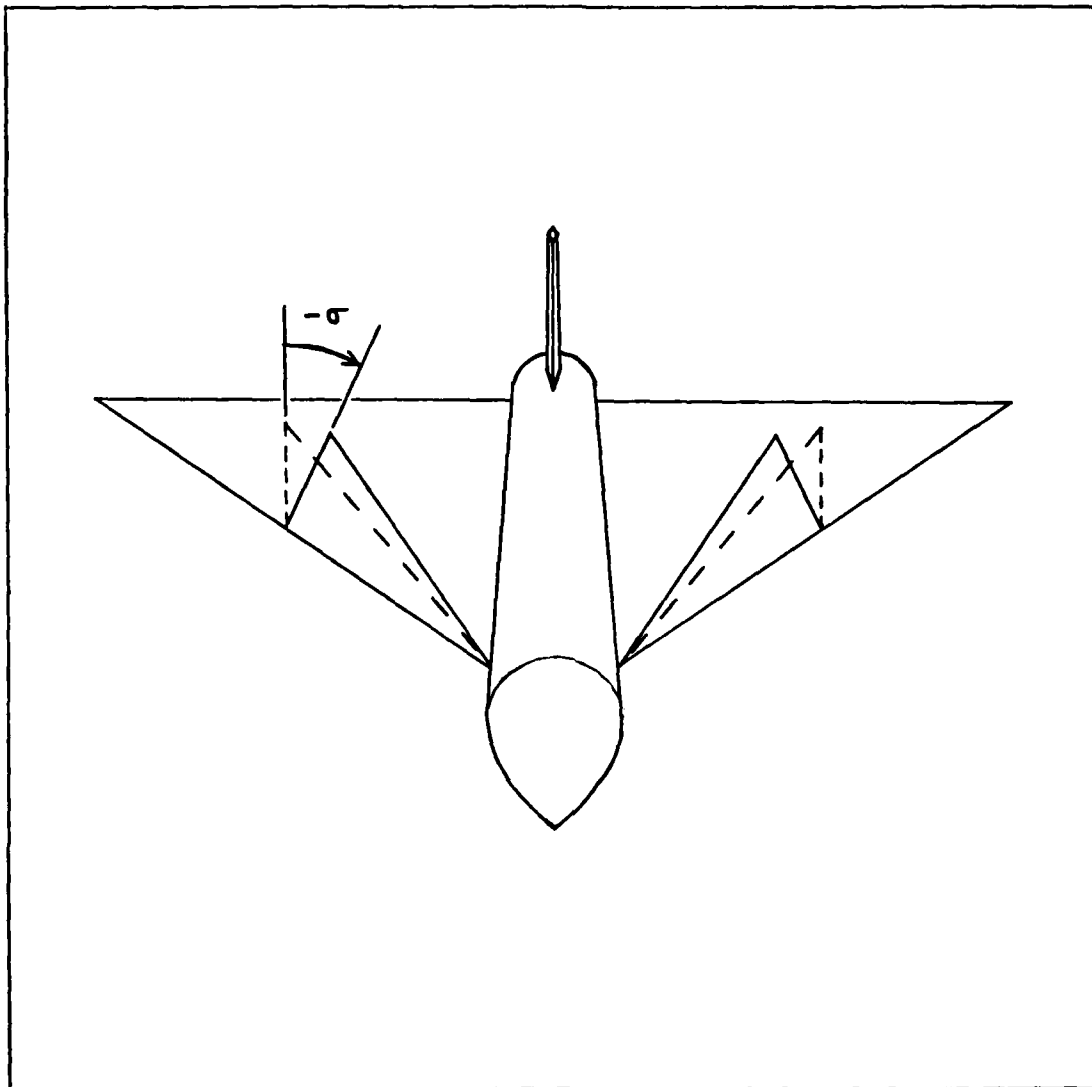
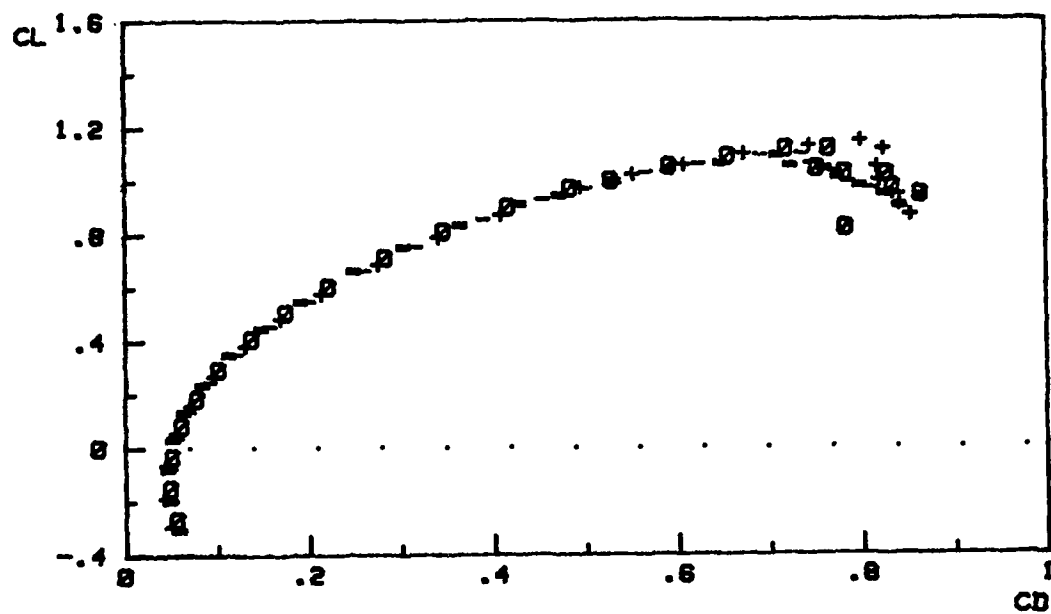
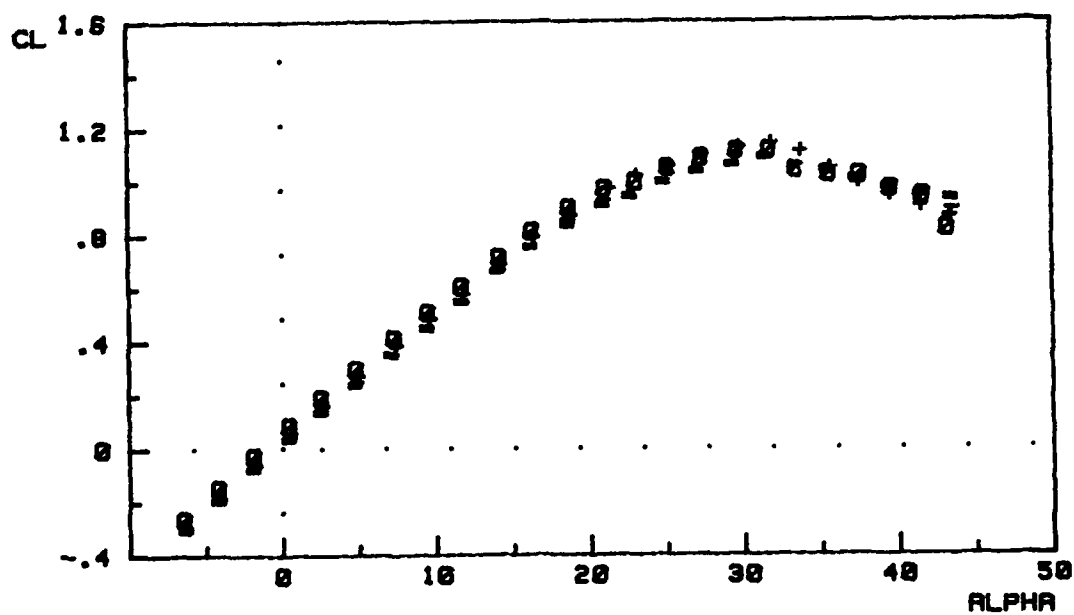


Fig. 17. Schematic of Model with Fences Deployed at a Negative Cant Angle



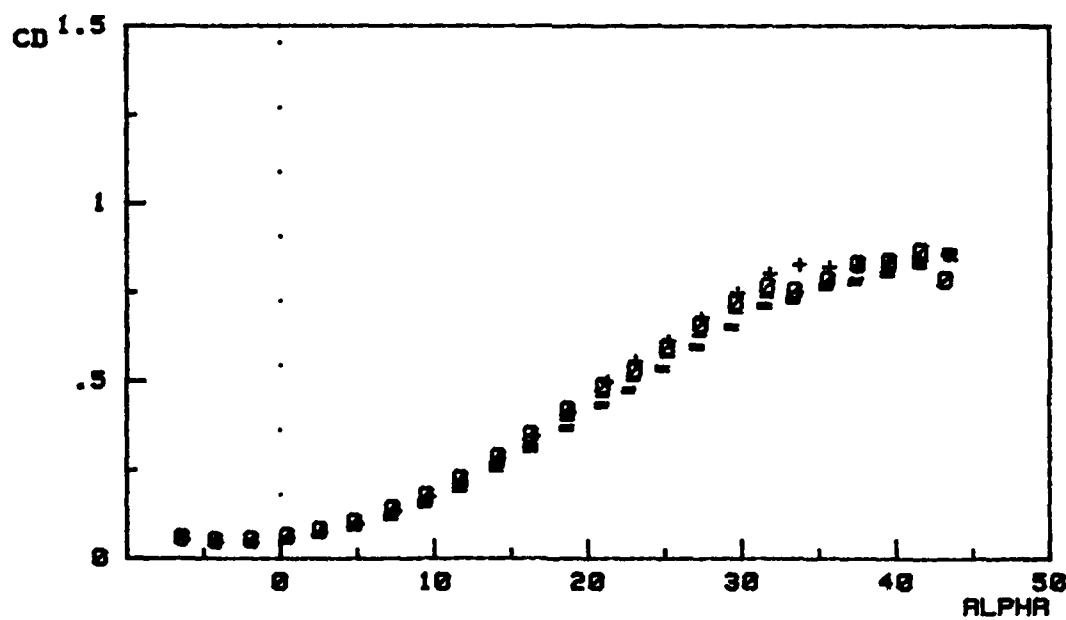
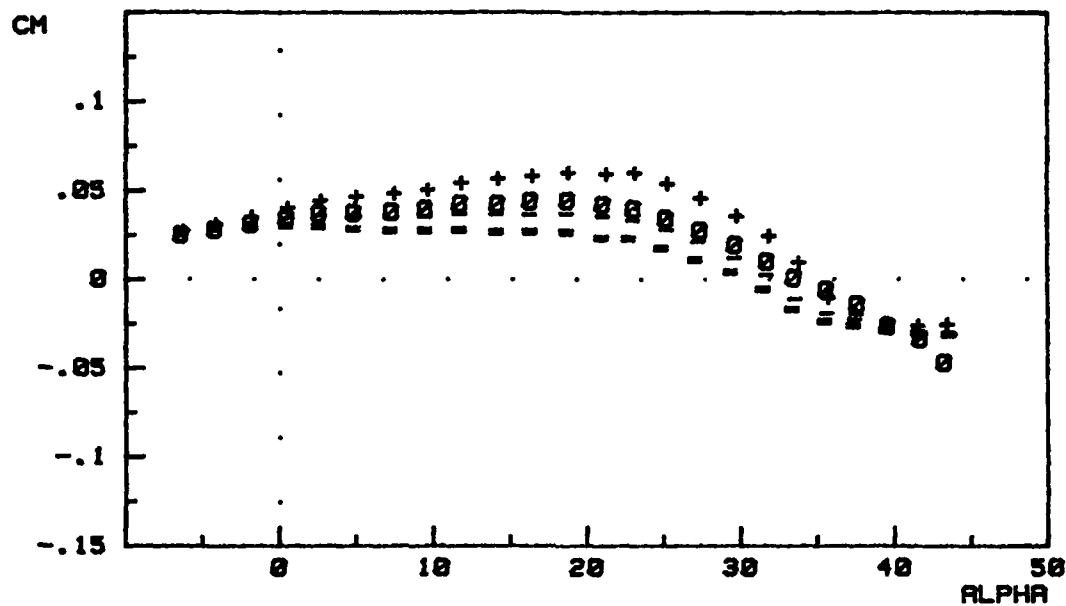
a.

+	7.50 cant
0	0° cant
-	-7.50 cant
=	-15° cant



b.

Fig. 18. Effects of Fence Cant



d.  
Fig. 18. (continued)

effects can be summarized as follows:

A. Positive or negative cant results in a reduction of  $C_L$  by about 0.03 at low  $\alpha$ , and about 0.05 at moderate to high  $\alpha$ . A small reduction in  $C_D$  is evident for all  $\alpha < 30$ . Note the shift in the equilibrium point on the  $C_M$  curve.

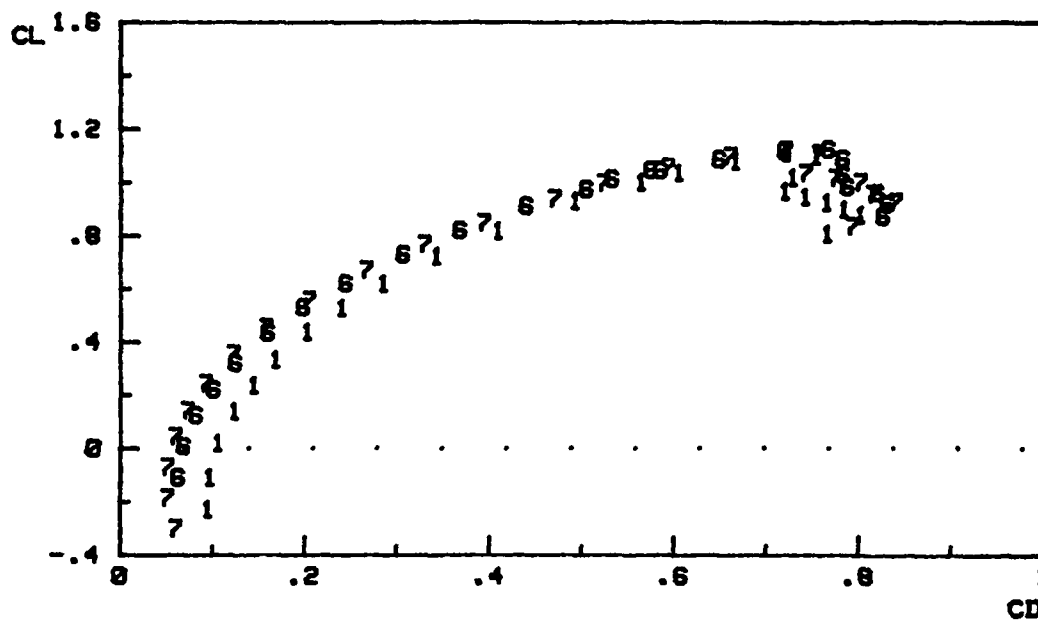
B. Positive cant gives positive pitching (relative to  $\sigma = 0$ ) from the point where  $\alpha \geq \sigma$ . Also, a slight increase in drag is evident at high  $\alpha$ .

C. Negative cant reduces  $C_M$  (relative to the  $\sigma = 0$  case) starting from the point where  $\alpha = -5$  or so. Drag is slightly reduced through the entire  $\alpha$  range.

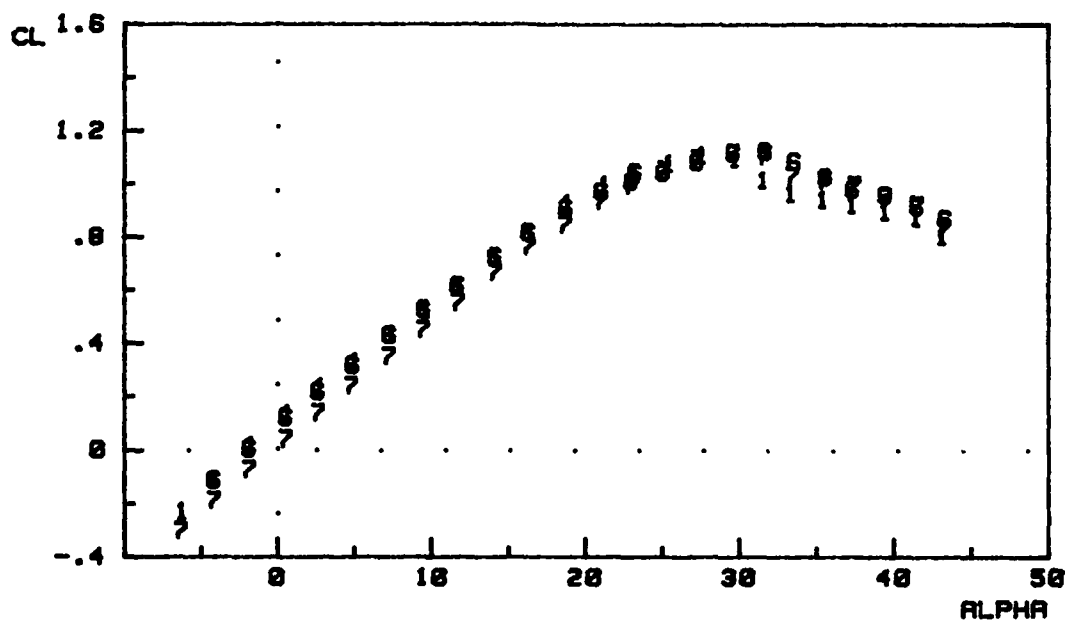
Thus, it would appear that a positive cant is preferable for STOL operations, but no gain is realized for nose-down pitching at very high  $\alpha$ .

#### IV. Surface Area

Variation of this parameter relates the effects of overall fence size on the aerodynamic behavior of the model. Two fence classes were used in this study: Gothic type (F1, F6, F7) and Delta type (F2, F8, F10). Both sets of data (Figs. 19 and 20) agree quite well with each other. The Delta fences have a common area reduction of 54% between F2 and F8, F8 and F10, whereas the Gothic fences have an area

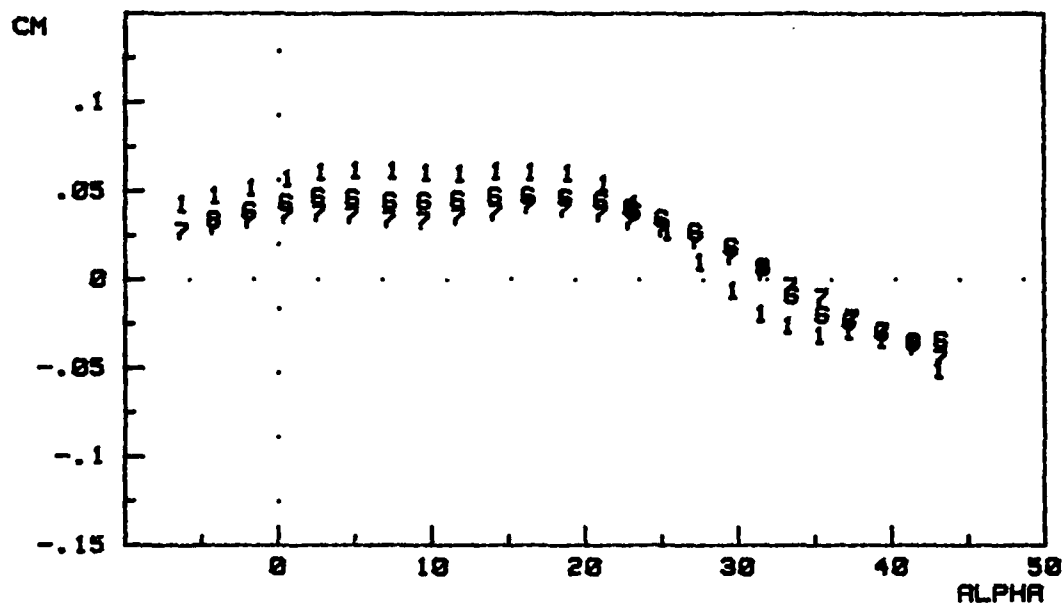


- a.
- |   |                         |
|---|-------------------------|
| 1 | F1 (Gothic)             |
| 6 | F6 (Modified Gothic)    |
| 7 | F7 (Modified Gothic II) |



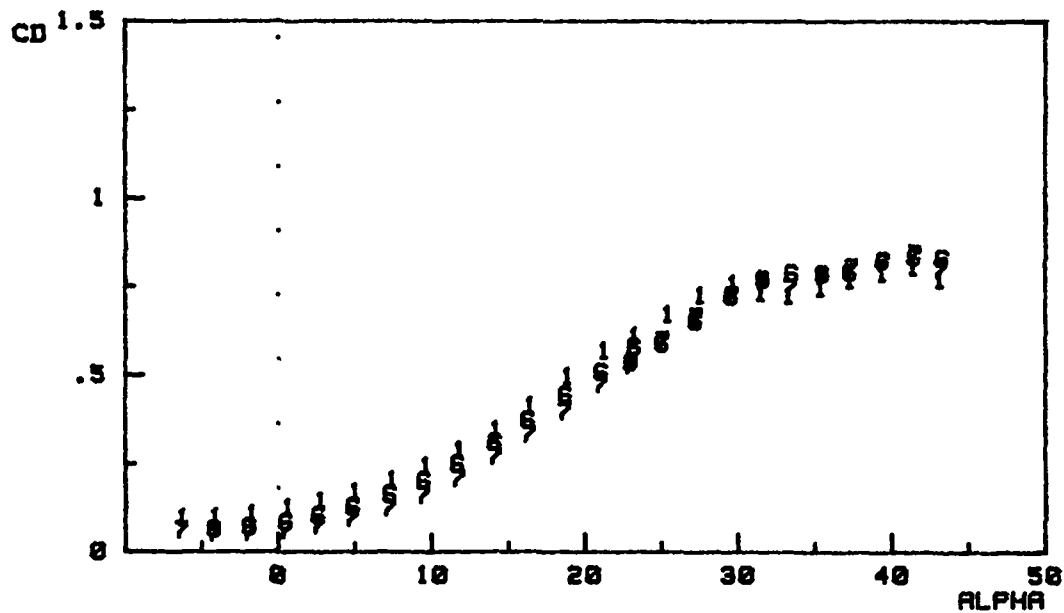
b.

Fig. 19. Effects of Fence Surface Area using the Gothic Shape

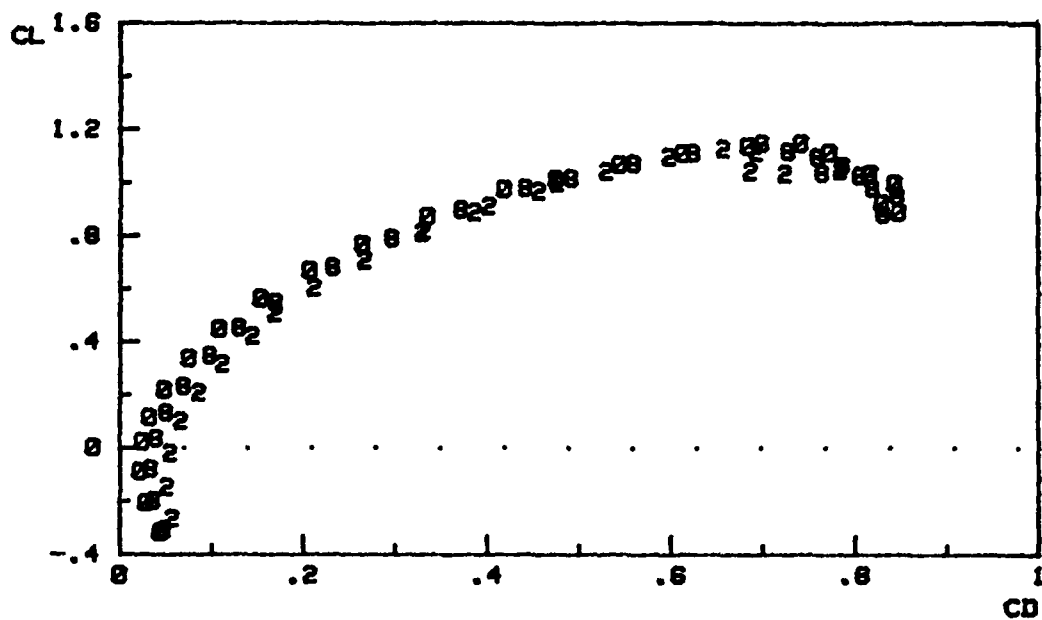


c.

1	F1 (Gothic)
6	F6 (Modified Gothic)
7	F7 (Modified Gothic II)

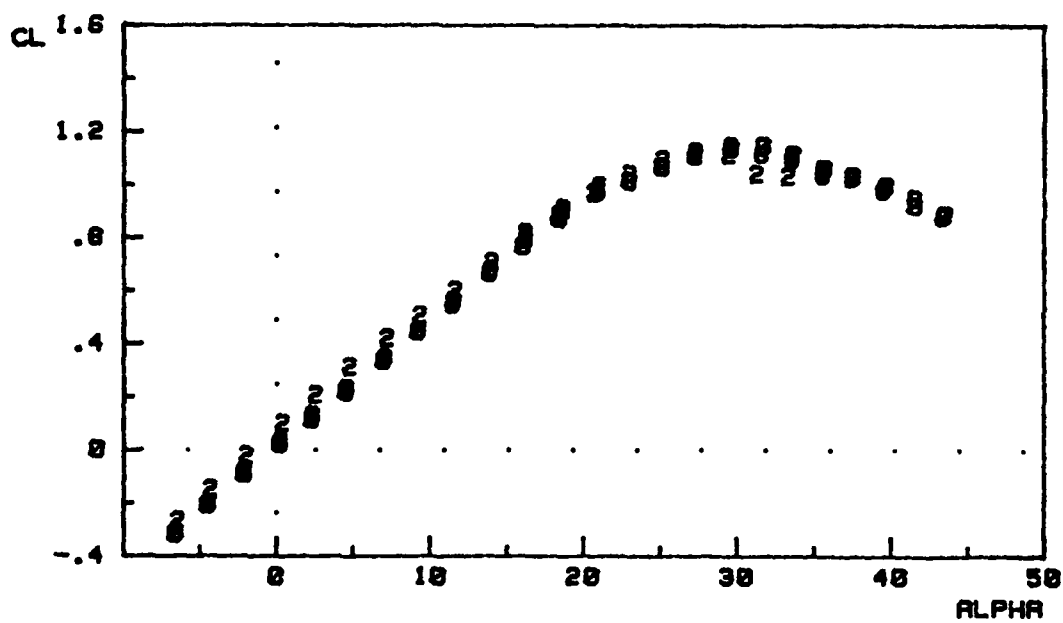


d.  
Fig. 19. (continued)



a.

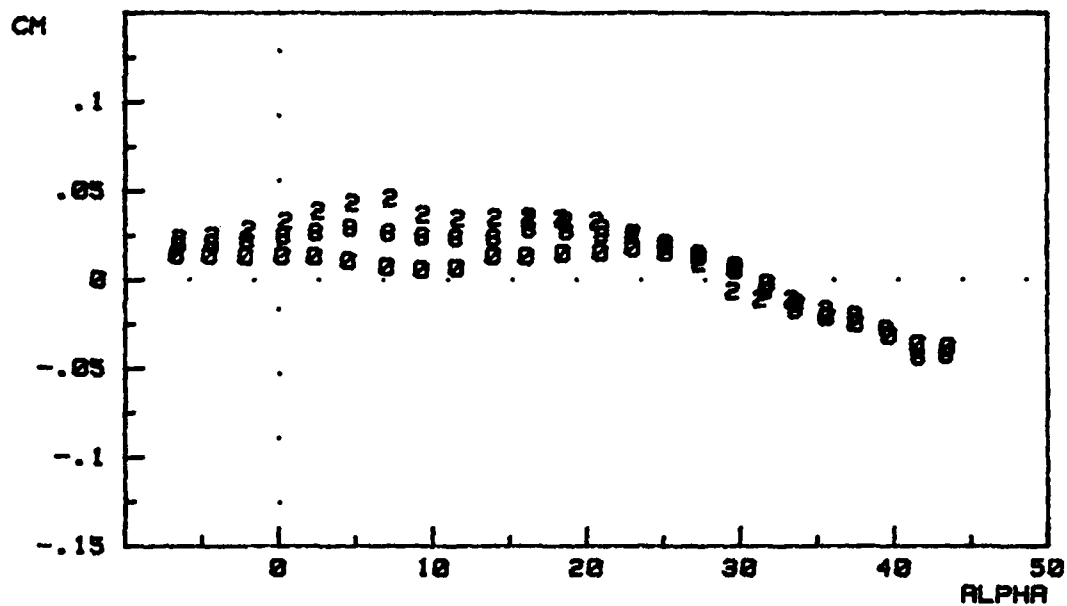
2	F2 (Delta)
8	F8 (Short Delta)
O	F10 (Mini Delta)



b.

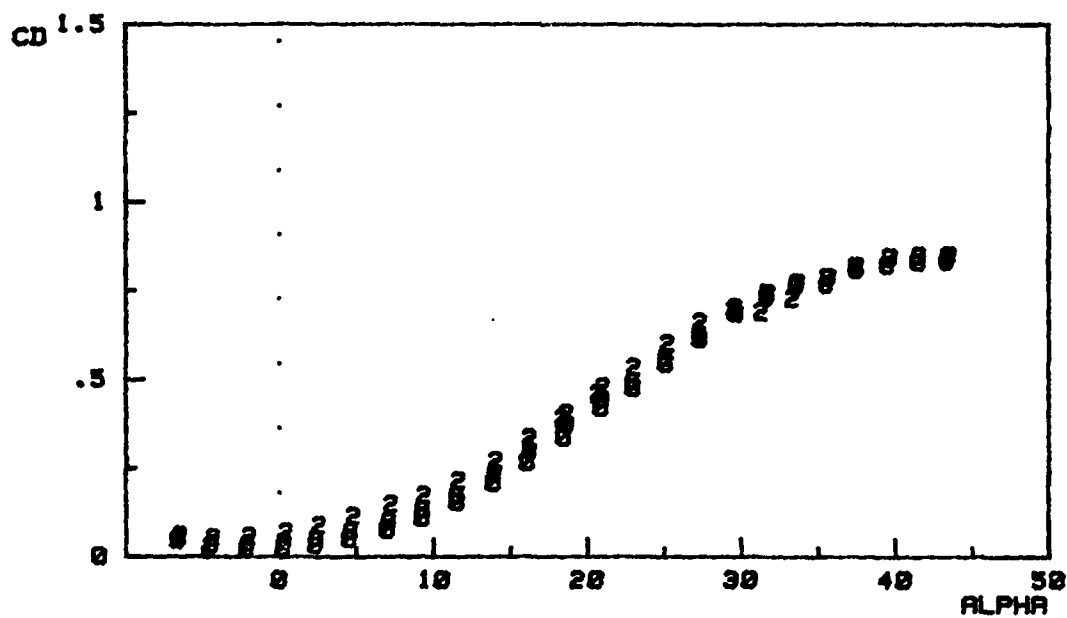
Fig. 20. Effects of Fence Surface Area using the Delta Shape





c.

2	F2 (Delta)
8	F8 (Short Delta)
0	F10 (Mini Delta)



d.  
Fig. 20. (continued)

reduction of 20% between F1 and F6, and 40% between F6 and F7. Surface area reduction has a tendency to reduce both lift, drag, and pitching effectiveness. In short, the smaller the fence, the more each configuration approaches the baseline case. Comparing the trends between F6/F7 and F8/F10, it is seen that the actual size differential is of paramount importance rather than percent changes in area.

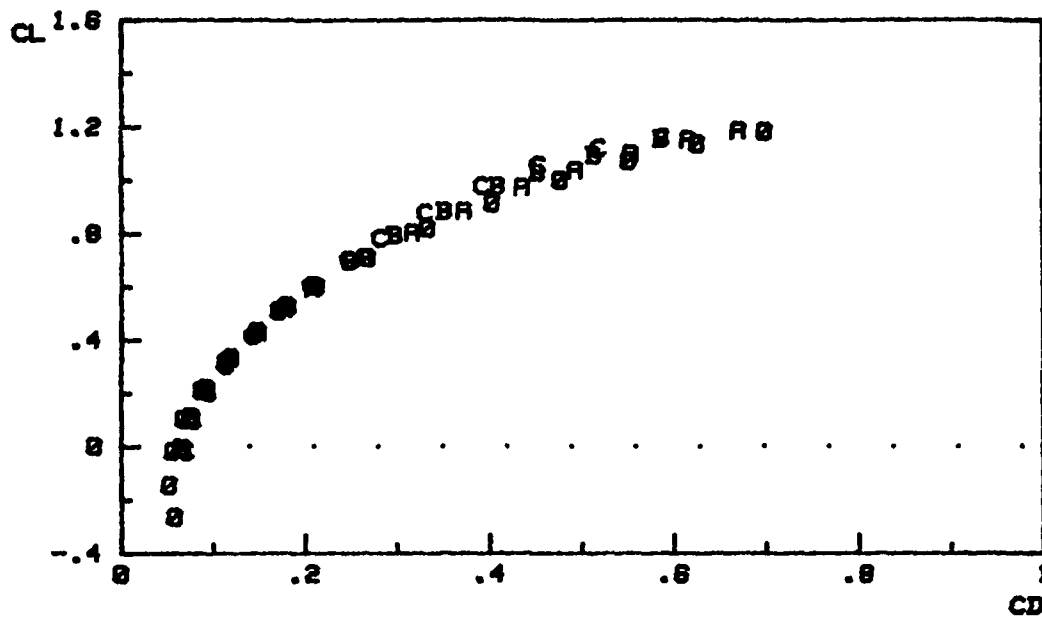
The optimal size would therefore be somewhere in the intermediate range of 14% to 18% of the wing's area. Of course, if it is found that a certain fence shape gives "good" results for a smaller size, so much the better. It is a trade-off between aerodynamic performance and engineering feasibility.

## V. Movement

Movement refers to the parallel displacement of a fence away from the leading edge. Selected fences (F1, F2, F5, F6) were tested at various positions of 0.5 , 1.0, and 1.5 inches inboard. In terms of a dimensionless parameter based on the root chord length (20.08 inches), the displacements would be 2.5%, 5%, and 7.5% of root chord, respectively. Results for F2 mimic those of the other fences and are given in Fig. 21.

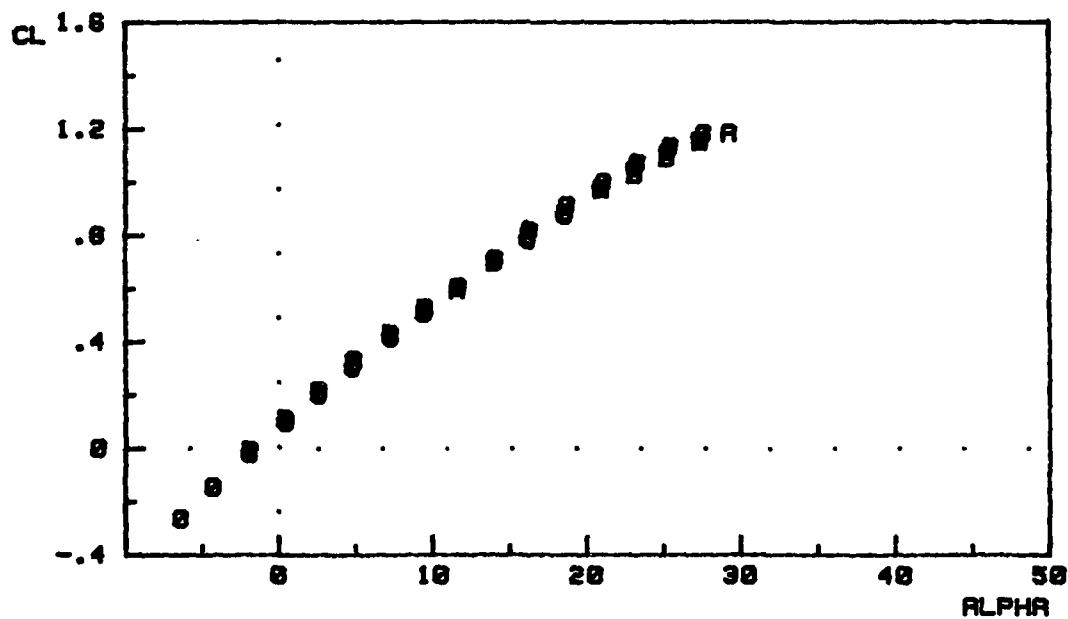
The effects of movement are twofold. First, the parasite drag coefficient is lowered. This "flattens out" the parabolic drag curve. Second,  $C_M$  is reduced substantially for 0.5 inches displacement (0.025c); reducing

further but at a lesser magnitude each time the fence is moved 0.5 inches farther back (this is the camber effect again). No changes in lift are apparent. (Note: Due to time restraints, data points for  $\alpha > 30$  were not taken.)



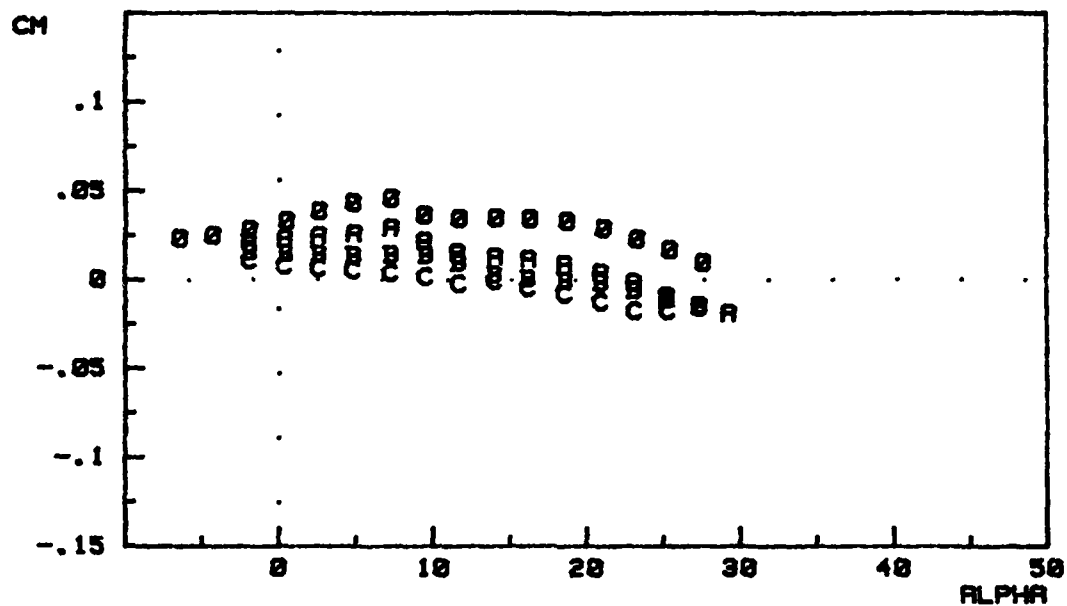
a.

O	F2 (Delta) at the Leading Edge
A	F2 (Delta) Inboard 0.5 inches (0.025c)
B	F2 (Delta) Inboard 1.0 inches (0.05c)
C	F2 (Delta) Inboard 1.5 inches (0.075c)



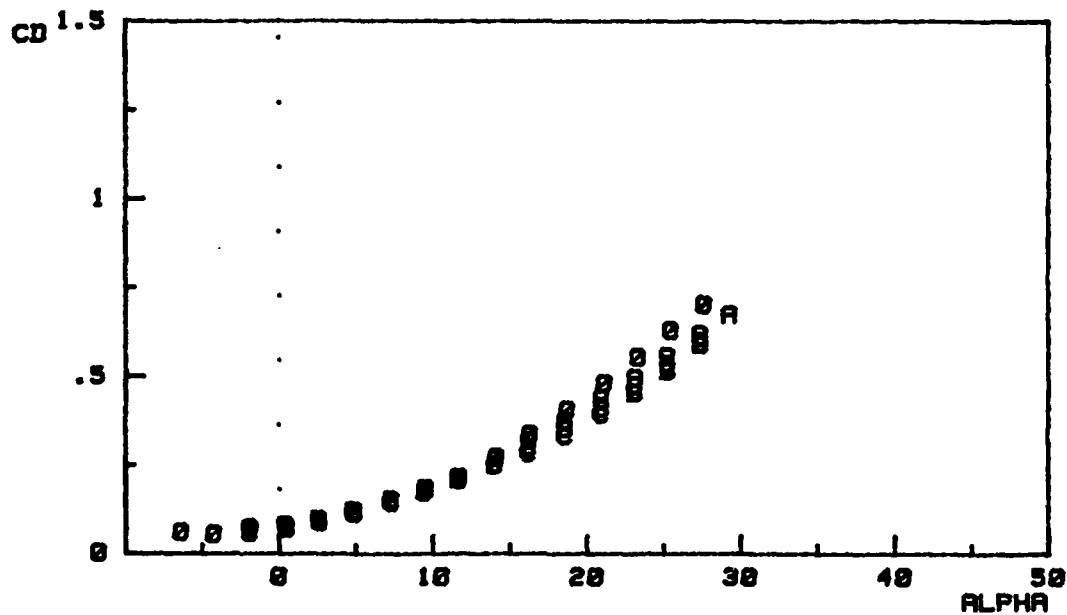
b.

Fig. 21. Effects of Fence Movement



c.

O	F2 (Delta) at the Leading Edge
A	F2 (Delta) Inboard 0.5 inches (0.025c)
B	F2 (Delta) Inboard 1.0 inches (0.05c)
C	F2 (Delta) Inboard 1.5 inches (0.075c)



d.  
Fig. 21. (continued)

## Flap Effects on Fence Aerodynamics

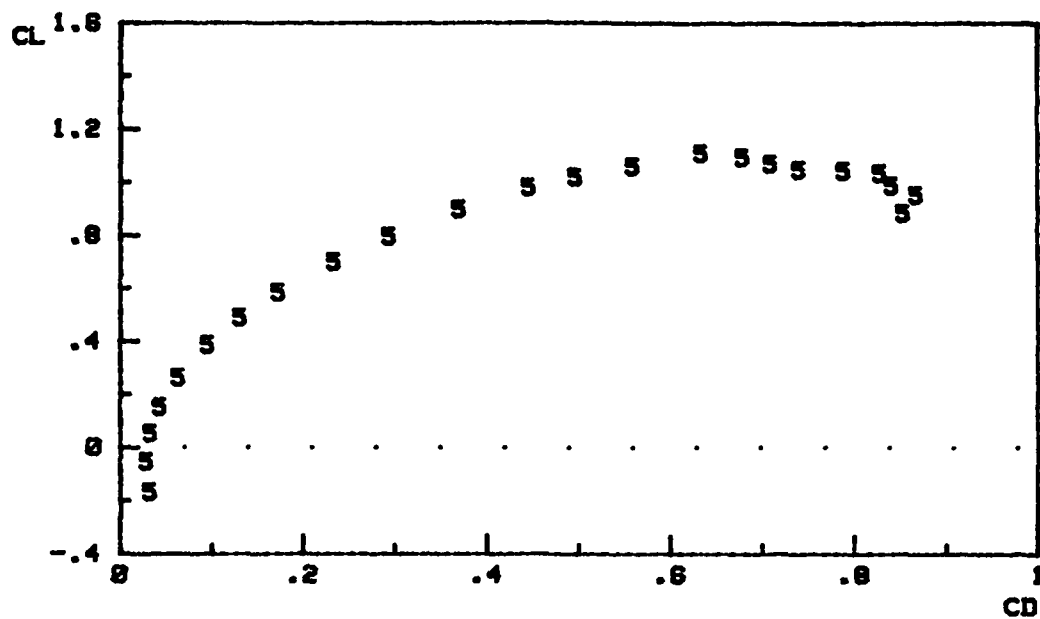
Trailing edge flaps (both inboard and twin deployment) were deflected between -10 degrees and 20 degrees, in 10 degree increments. The results are of the same order as the baseline flap run cases, as expected. That is, flap deflections cause step responses in lift, drag, and pitching. For a given deflection, the step changes are equal for both the fence and baseline cases, which supports the conclusion that t.e. flaps do not alter the fence generated vortex field.

## Asymmetric Fence Deployment

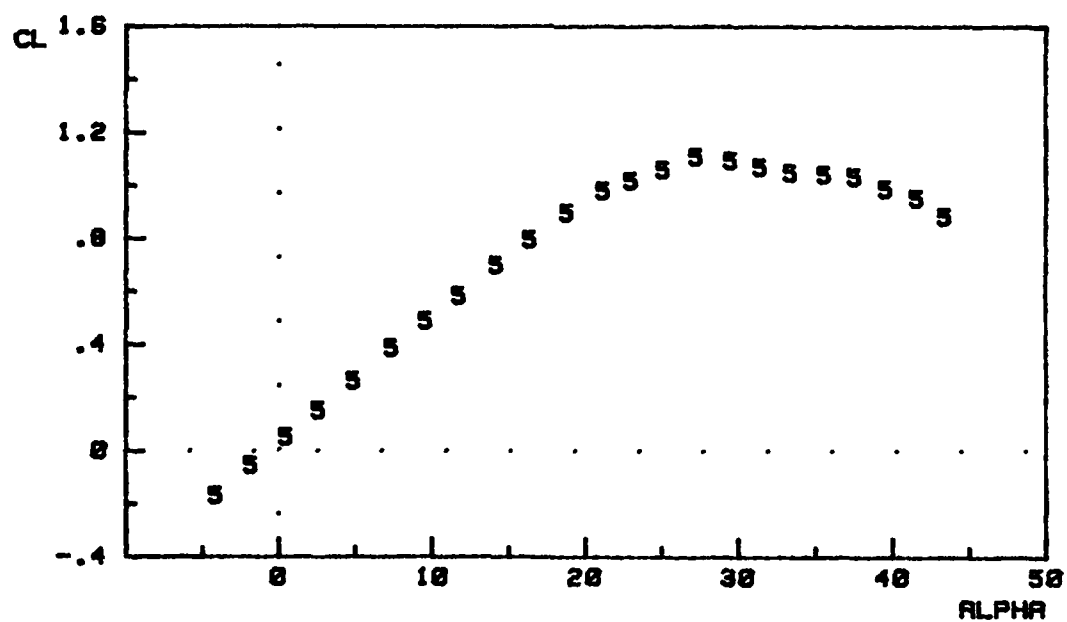
This section, along with the flow visualization data, gives some insight into the actual structure of the flow field induced by apex fences. (Deployment of a single fence on the left wing was the approach taken.) Fences F2, F5, and F7 were tested. Each fence produced a similar behavior pattern, therefore, the trends given here for F5 are applicable to other fences.

Fig. 22 displays the data. The lift, drag, and pitching data follows suit with that observed in the "conventional" F1 configuration given earlier. The plots of side force, rolling and yawing reveal some interesting facts, however. First, since the inboard section of the "fenced" wing is loaded more than the "plain" wing (i.e. the suction peak is further inboard; see ref 7) the model has a tendency to roll

left. Second, there is a very low pressure region at the leeward portion of the fence which accounts for the positive side force (see ref 7). This low pressure area is the highly separated flow/apex fence generated vortex region. It grows in strength as angle of attack increases, until a maximum is reached around  $\alpha = 25$ . Lastly, this side force produces a positive yawing moment which more than counteracts the negative moment produced by the drag on the fence.



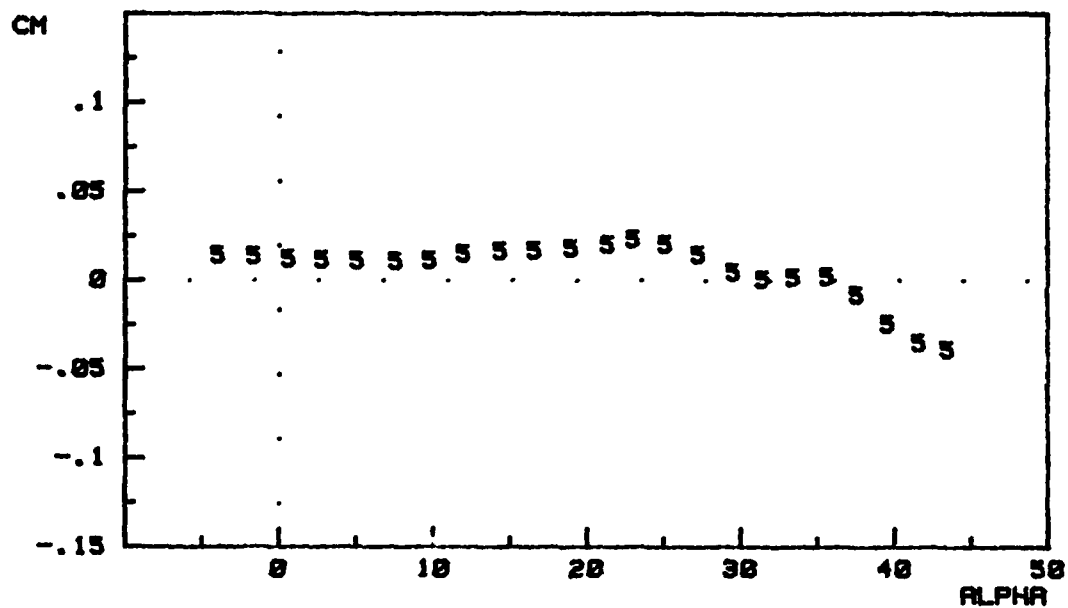
a.



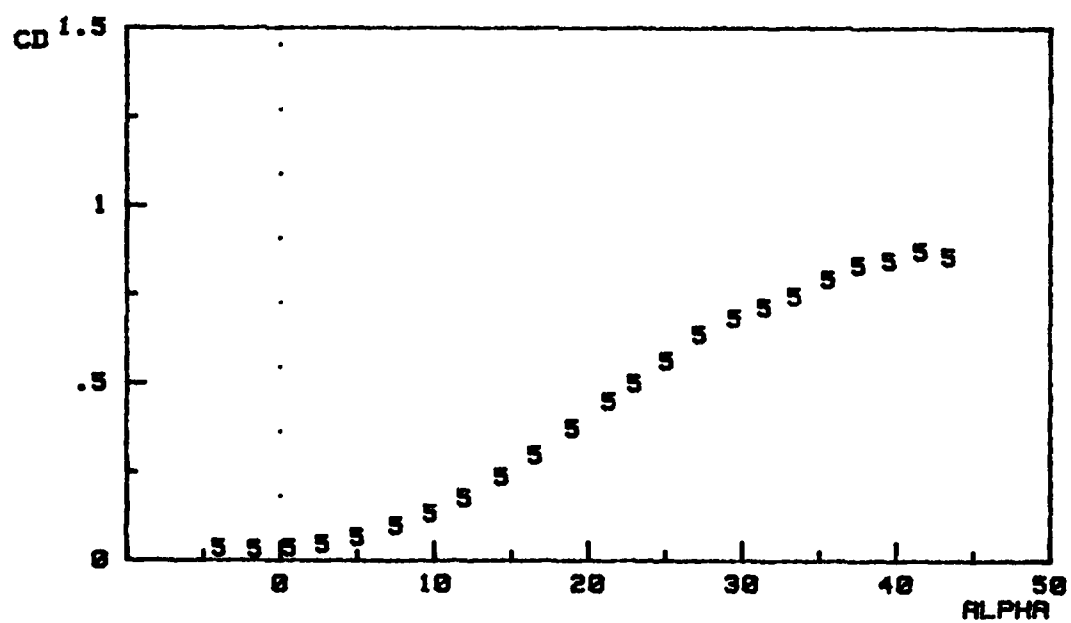
b.

Fig. 22. Asymmetric Deployment of F5 Double Gothic Fence on Left Wing



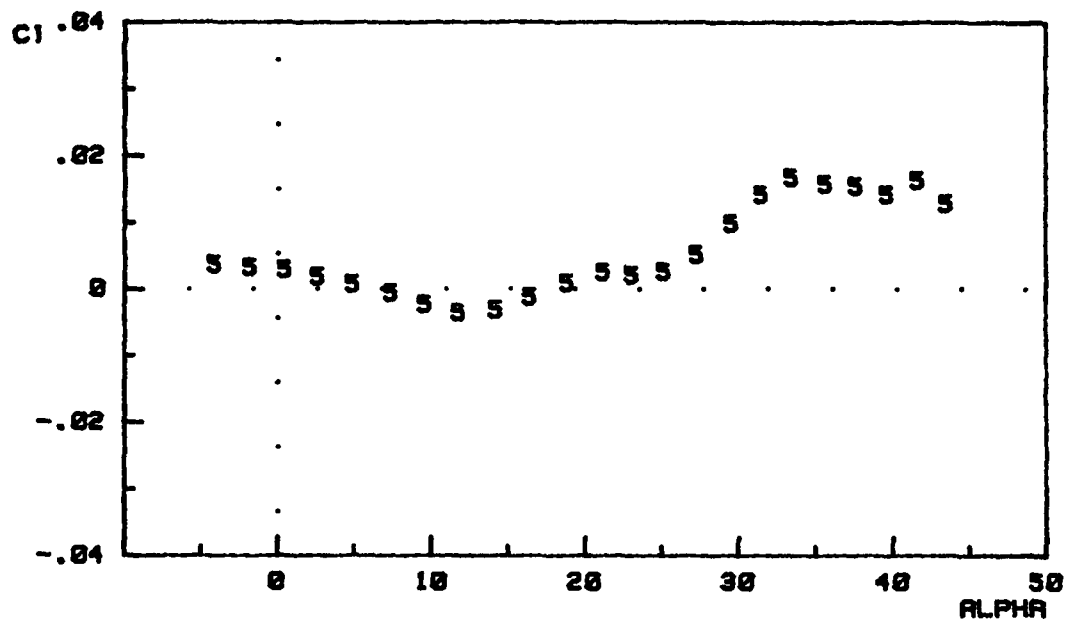


c.

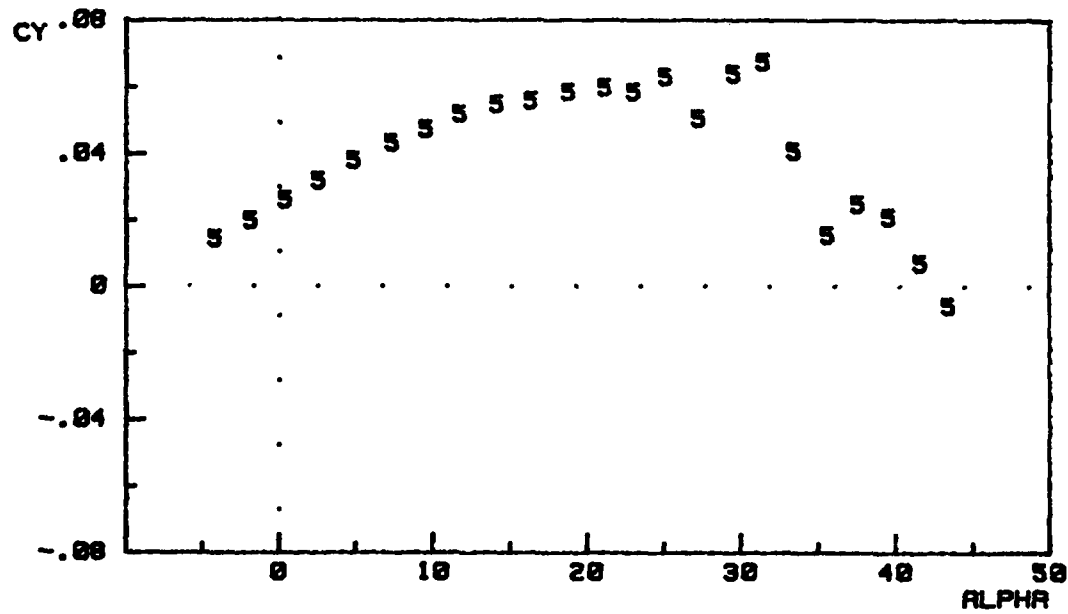


d.

Fig. 22. (continued)

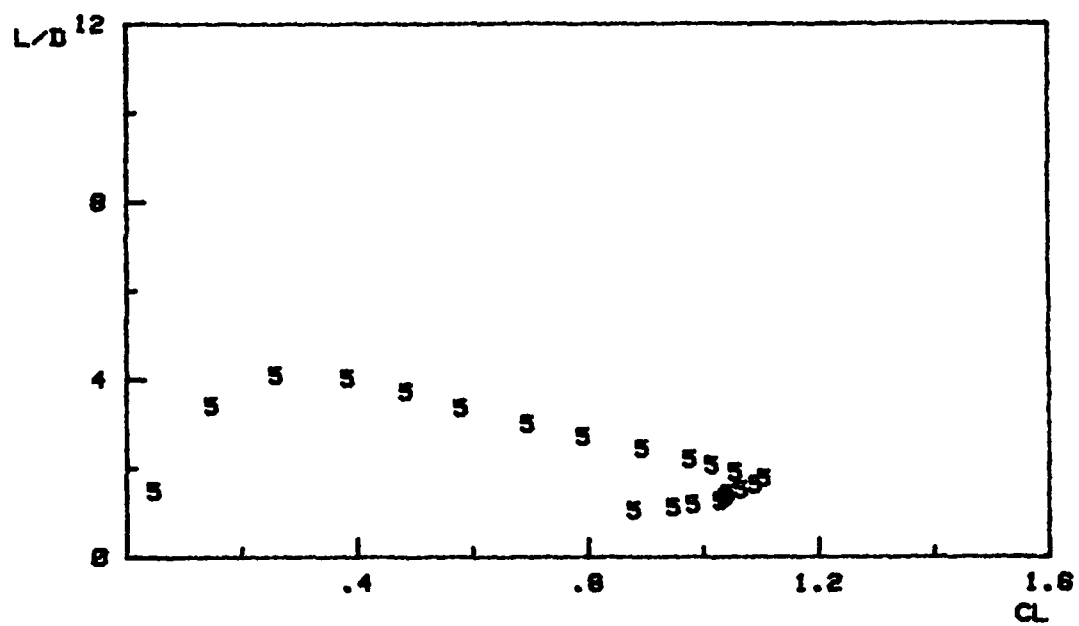


e.

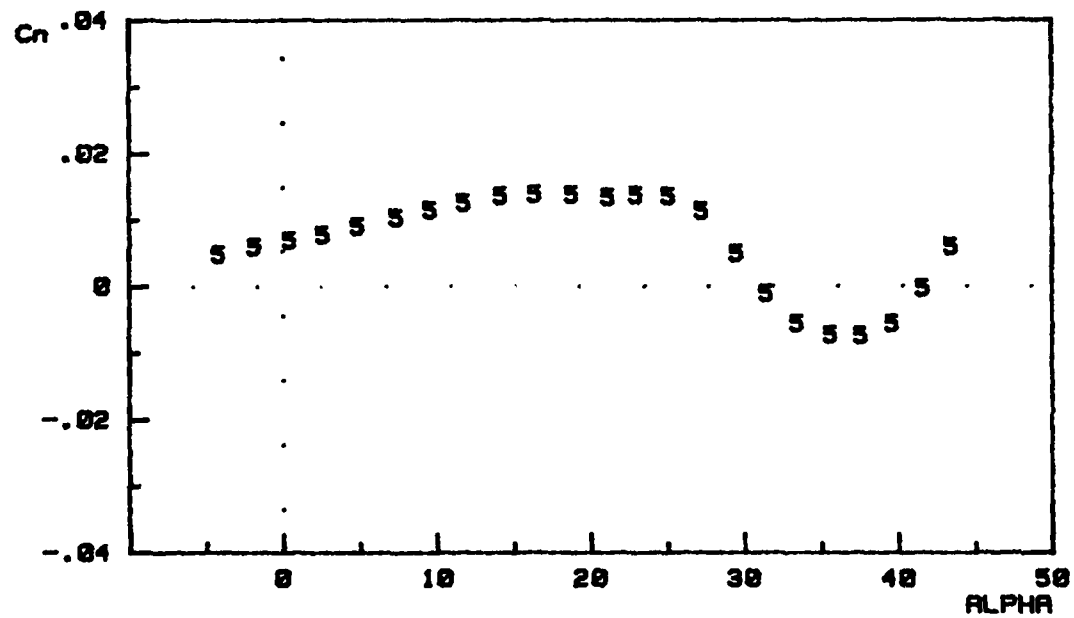


f.

Fig. 22. (continued)



g.



h.

Fig. 22. (continued)

## Flow Visualization

Flow visualization was conducted using oil droplets applied to the upper surface of the wing and allowing the oil to flow smoothly over the wing while the tunnel velocity and angle of attack were held constant. Photographs were taken of the baseline and selected fence configurations at  $\alpha = 9.5$ , 20, and 30. The results indicate clearly the vortex flow field generated by the fences. A general guideline for interpreting the results is that 1) regions of high velocity cause the oil marks to elongate more than regions of low velocity, and 2) the oil droplet size carries no significance. The photos which are given here cover, in order:

Baseline

F12

F2 @ 1.0 inches inboard

Note: The F12 photos present all of the significant characteristics of fence generated vortices and give sufficient information in the absence of other photographs. In all cases, "fence vortex" carries the same meaning as "fence generated vortex". Additional flow visualization photographs are given in Appendix B, and helium bubble photographs are given in references 6 and 7.

Baseline: Figs. 23-25 give evidence of the classical vortex system generated by delta wings. The vortex rotates

in the counterclockwise sense, origin at the apex, with the core traversing the entire length of the wing. The outermost "edge" of the vortex is where the oil streams come together near the leading edge. Note that as  $\alpha$  increases, the vortex grows in size and strength until it covers almost the entire wing.

F12: Figs. 26-28 detail the apex fence vortex. At low  $\alpha$ , it is seen that the vortex system is a combination of the fence vortex and l.e. vortex. In all cases, however, the predominant vortex is the fence vortex. This means that a delta wing equipped with apex fences derives its lift primarily through suction caused by fence vortices and not by the classical l.e. vortex system. The fence vortex is generated at the apex, follows the length of the fence, and then turns back more in the freestream direction (see ref 7). Thus, the inboard section is loaded more (especially at low  $\alpha$ ) which increases the lift. Note that the l.e. vortex disappears in the range  $9.5 < \alpha < 20$ , so that the wing produces lift solely through the presence of the fence vortex. Comparing the baseline and F12 cases for  $\alpha = 30$ , the flow field appears to be the same, which aids in explaining why the lift and pitching behavior at this attitude are roughly the same.

F2 @ 1.0 inches inboard: Fig. 29 was taken at  $\alpha = 20$ . This picture reveals that the fence vortex is moved aft, thus moving the center of pressure on the wing rearward (again,

due to a change in the effective camber). This explains the drop in  $C_M$ . The complex flow pattern ahead of the fence cannot be described accurately. However, note that there are three stagnation points along the leading edge at approximately  $0.2c$ ,  $0.4c$ , and  $0.6c$ .

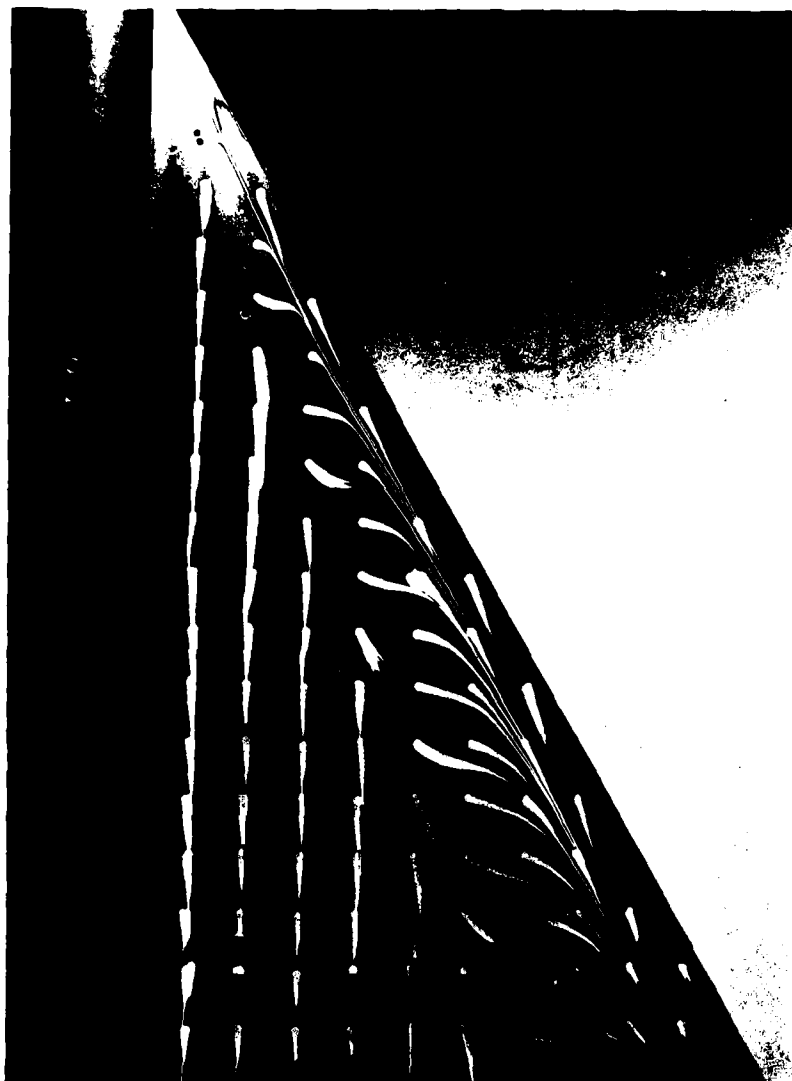


Fig. 23. Oil Flow Visualization for the Baseline Case  
at 9.5 degrees

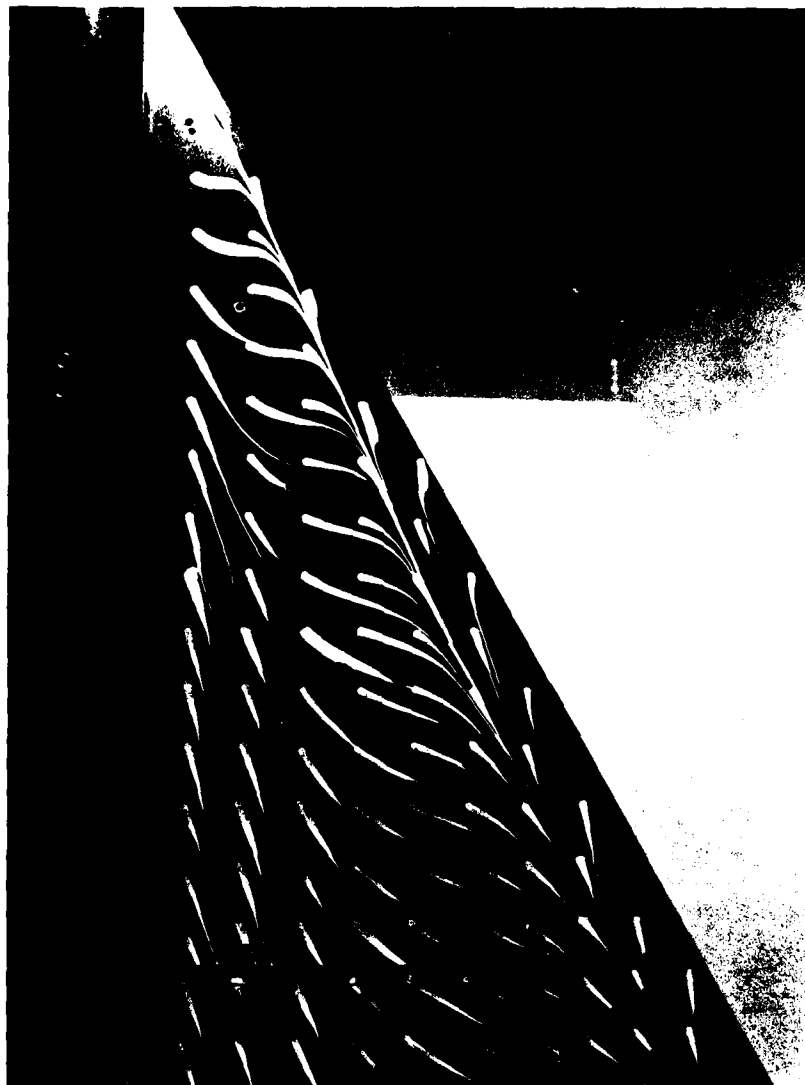


Fig. 24. Oil Flow Visualization for the Baseline Case  
at 20 degrees



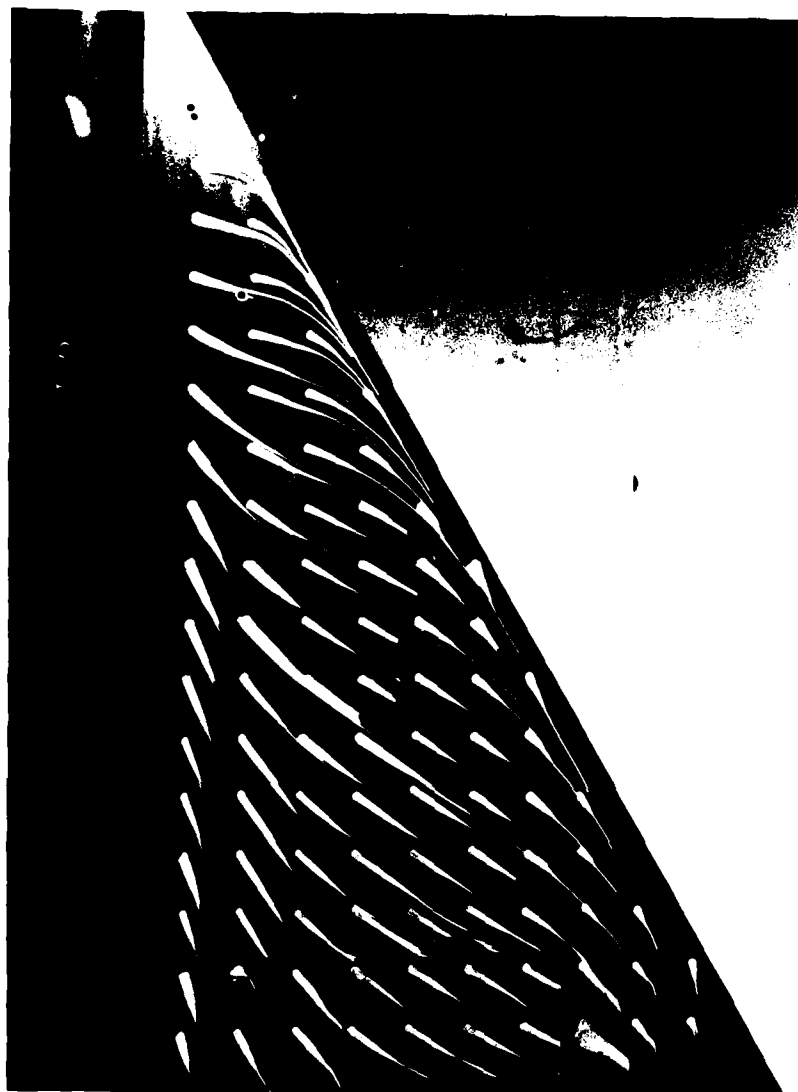


Fig. 25. Oil Flow Visualization for the Baseline Case  
at 30 degrees



Fig. 26. Oil Flow Visualization for the F12 Double Gothic II  
Fence Case at 9.5 degrees

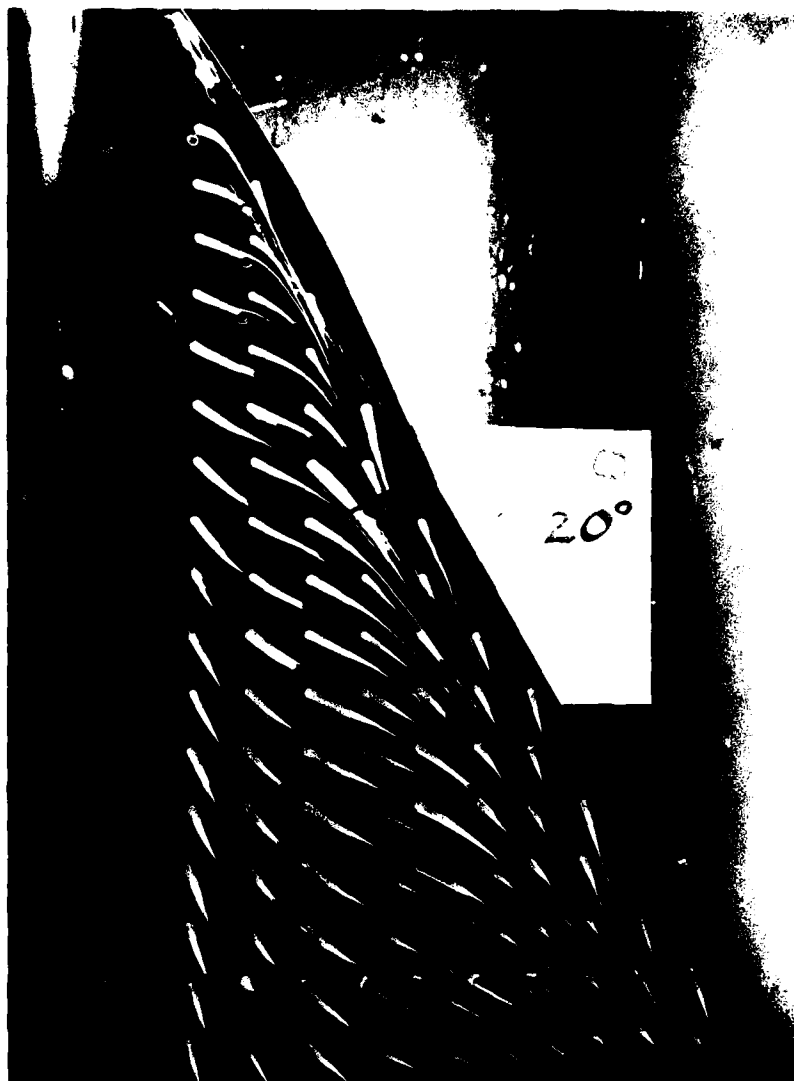


Fig. 27. Oil Flow Visualization for the F12 Double Gothic II  
Fence Case at 20 degrees

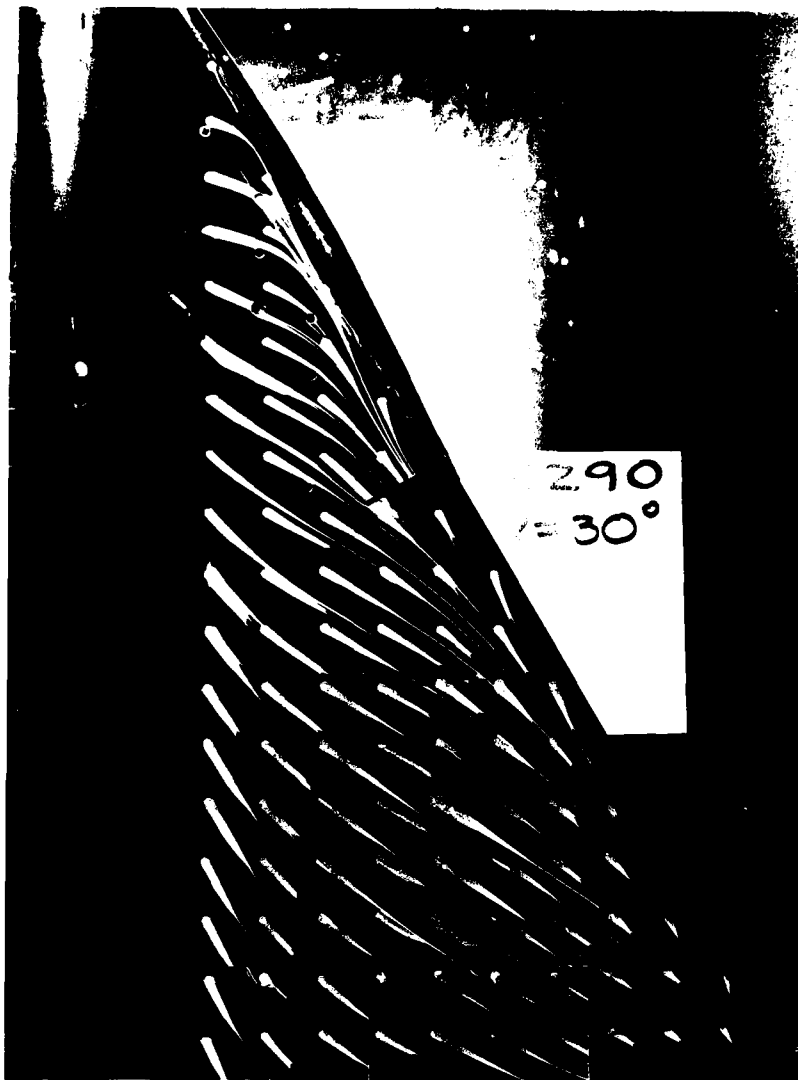


Fig. 28. Oil Flow Visualization for the F12 Double Gothic II  
Fence Case at 30 degrees



Fig. 29. Oil Flow Visualization for the F2 Delta Fence  
Inboard 1.0 inches (0.05c)

## CONCLUSIONS AND RECOMMENDATIONS

Based on the preceding results, deployment of apex fences can improve delta wing aircraft STOL performance at moderate angles of attack (up to about  $\alpha = 30^\circ$ ). The additional lift and large pitching moment they provide allows trailing edge flap deflections, for both trim and providing needed lift for the aircraft during landing or approach. The results indicate an increase of about 0.05 to 0.1 in  $C_L$  at low to moderate  $\alpha$ , with smaller increases as  $\alpha$  grows. Likewise, an increase in  $C_M$  on the order of 0.05 (comparable to  $-20^\circ$  trailing edge flap) at low to moderate  $\alpha$  is given, with the pitching behavior becoming stable and trimmed around  $\alpha = 30^\circ$ . Coupled with this is the increase in drag which aids in speed reduction (for shorter landings) and dictates steeper approaches (with the use of full engine power). A 0.2 increase in  $C_D$  at takeoff attitude (roughly 15 to 25 degrees) is a minor adverse effect. However, given that the takeoff speed is reduced (due to a higher  $C_{Lmax}$ ) the actual drag force might very well be less than that of the unconfigured case.

The high  $\alpha$  behavior of fences is not as promising. Although nose-down pitching is slightly enhanced, there is a lack of sufficient data to predict the dynamic effects. In addition, there is no evidence that vortex breakdown is delayed by the use of fences. In fact, because fences

decrease  $C_L$  at high  $\alpha$ , the problems of vortex breakdown have not been eliminated with this configuration.

The parametric study on fence geometries and placement on the wing's upper surface indicate that:

- A. A Double Gothic fence shape produces enhanced pitching and lift characteristics compared with Gothic, Delta, and Cropped shape..
- B. A fence surface area of 14% to 18% of the wing's area allows adequate lift and pitching moment (characteristic of all fence shapes).
- C. Positive cant gives additional positive pitching moment over the "conventional" zero cant condition, but reduces the lift slightly. Negative cant reduces pitching effectiveness as well as lift.
- D. A length-to-height ratio of about 7 or 8 causes enhanced apex loading (compared with ratios of about 3 or 4), giving greater pitching effectiveness.
- E. Leading edge deployment of fences gives the most favorable pitching behavior. Rearward displacement results in reduced pitching moment but no noticeable change in lift.

In light of this, the "best" fence appears to be F5; a fairly slender, gently sloping Double Gothic shape. The preferred geometries would be a surface area 11% of the wing's area, leading edge placement, length-to-height ratio of about seven, and a positive cant at moderate  $\alpha$ . Note that

this investigation assumes a linear variation of parameters yields predictable, well-behaved changes in aerodynamic characteristics and their associated coefficients. This seems to be a good assumption, but care should be taken when applying these results for special cases (such as movement with cant, etc...).

It is recommended that the lateral/directional behavior of a model with fences be tested to determine stability in yaw, side force generation, and the like. Asymmetric deployment reveals that fences could be used to generate the forces and moments required for stable flight, even with sideslip. Thus, it is possible that apex fences could have dual application: STOL/pitching enhancement and flight path control (maneuver ability enhancement).



APPENDIX A: MODEL DIMENSIONS

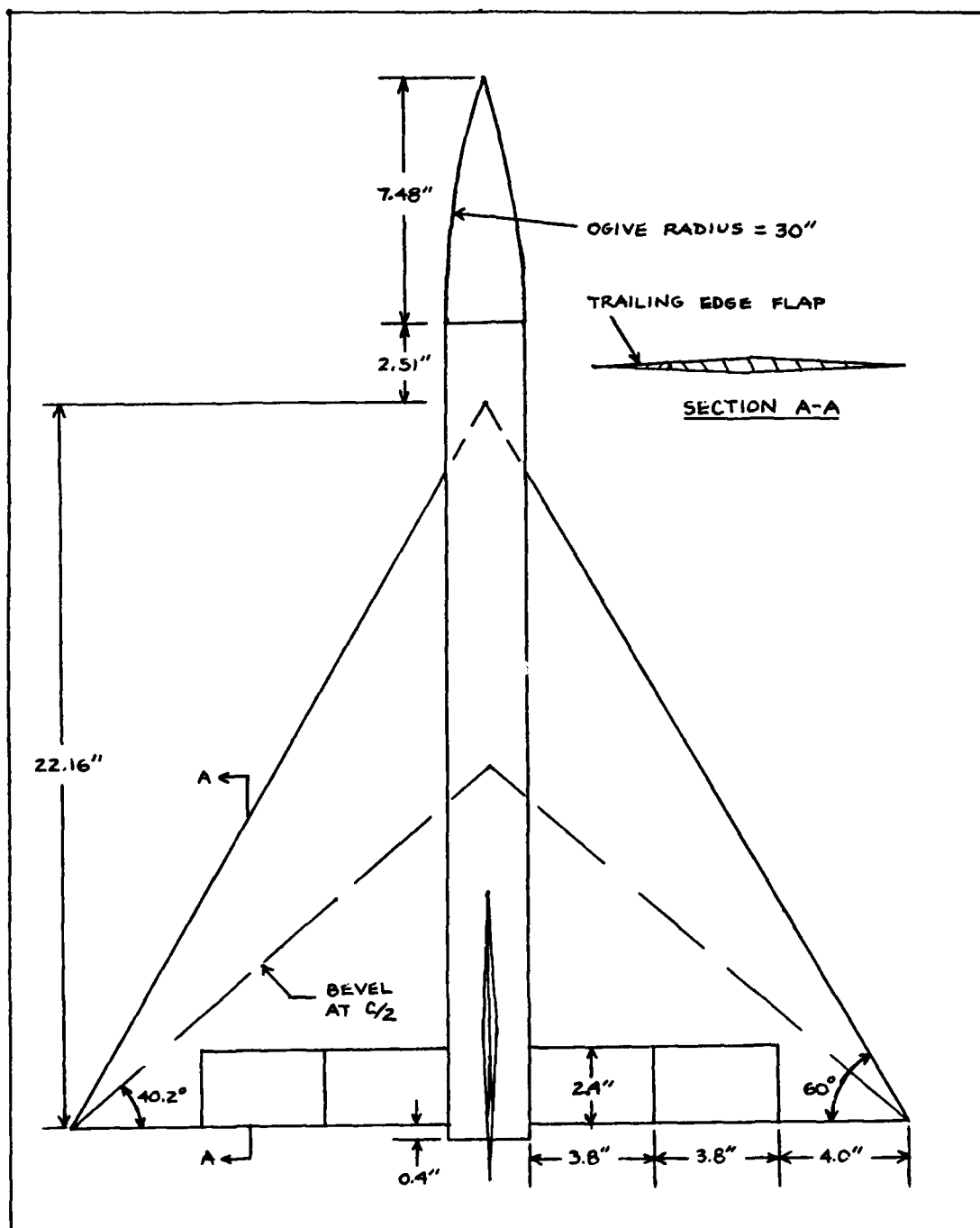


Fig. A-1. Model Dimensions (Top View)

AD-A163 877

EXPERIMENTAL STUDY OF APEX FENCES FOR LIFT ENHANCEMENT

2/3

ON A HIGHLY SWEPT. (U) AIR FORCE INST OF TECH

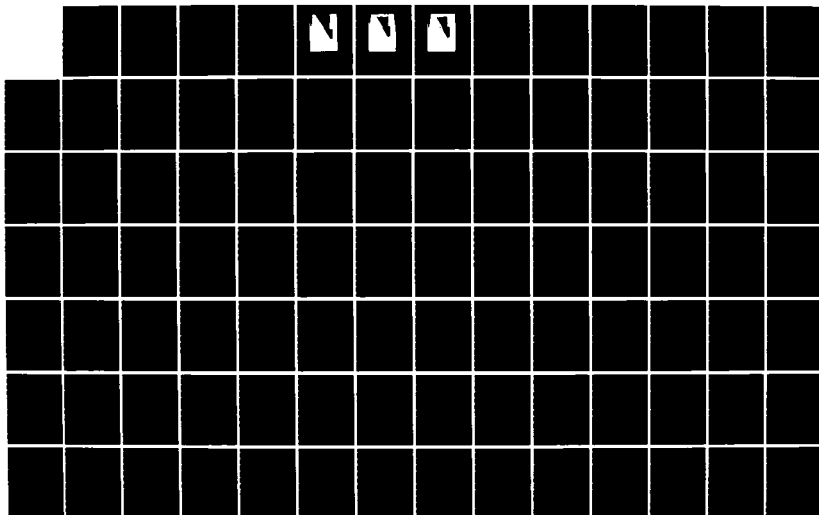
WRIGHT-PATTERSON AFB OH SCHOOL OF ENGI.. N STUART

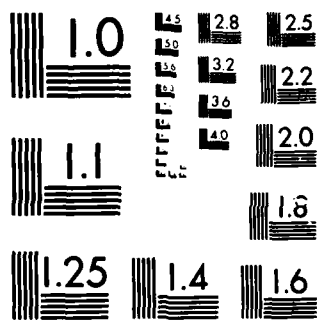
UNCLASSIFIED

DEC 85 AFIT/GAE/AA/85D-14

F/G 12/1

NL





MICROCOPY RESOLUTION TEST CHART  
NATIONAL BUREAU OF STANDARDS 1963-A

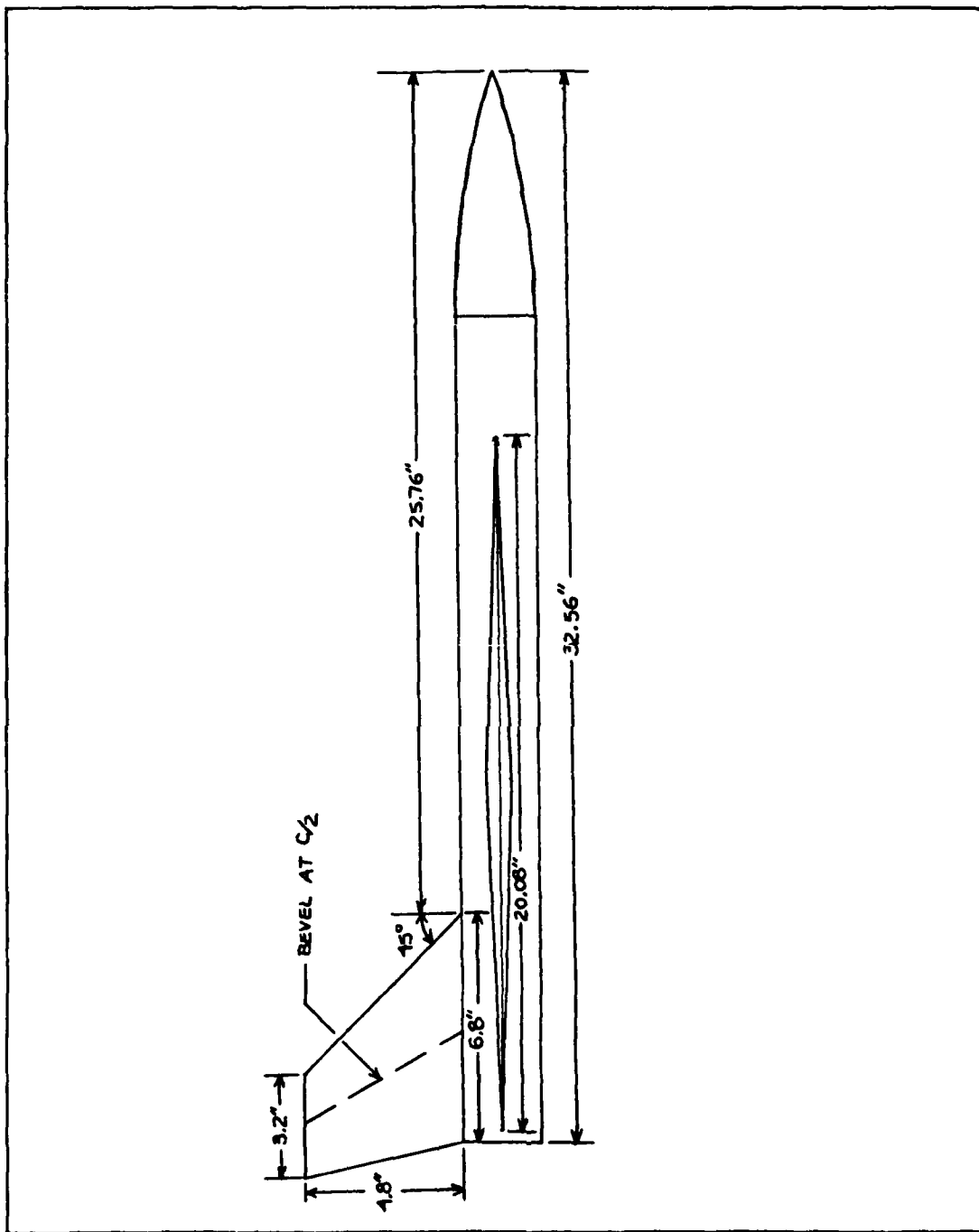


Fig. A-2. Model Dimensions (Side View)

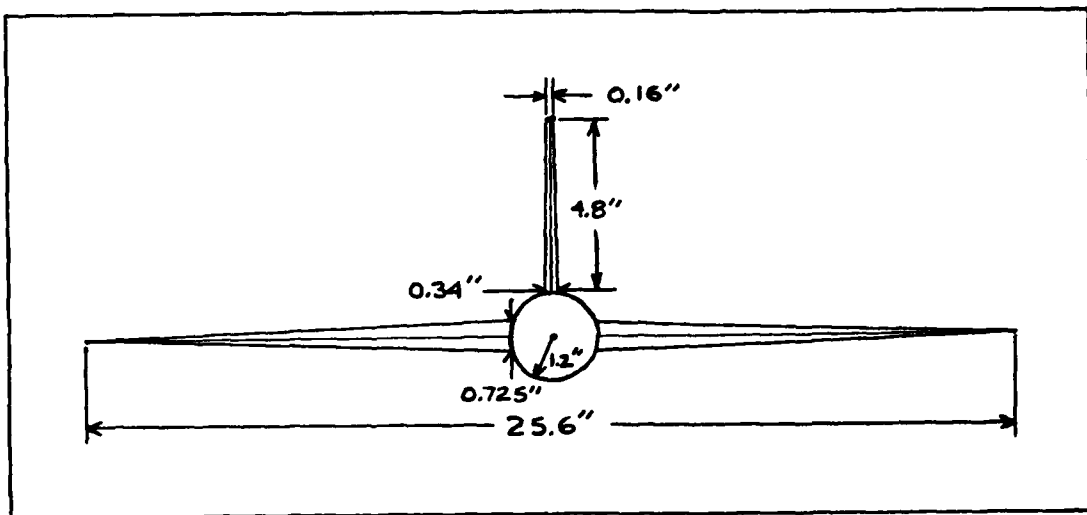


Fig. A-3. Model Dimensions (Front View)

APPENDIX B: ADDITIONAL FLOW VISUALIZATION

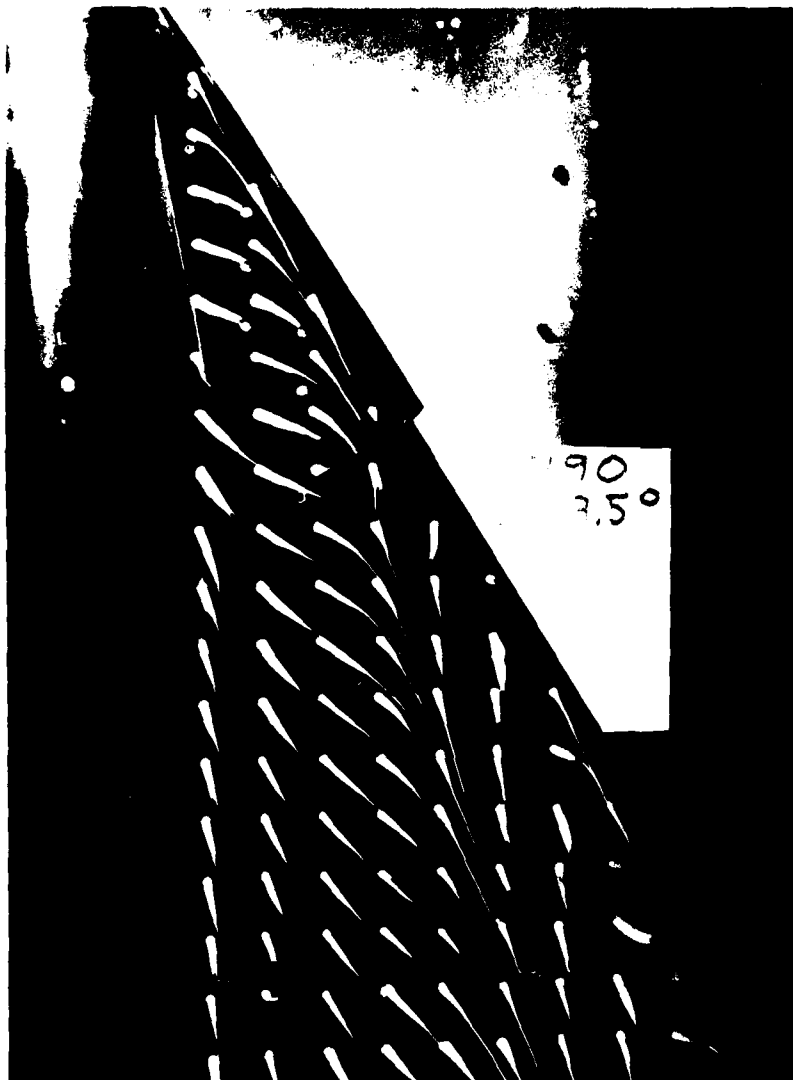


Fig. B-1. Oil Flow Visualization for the F7 Modified Gothic  
II Fence Case at 9.5 degrees



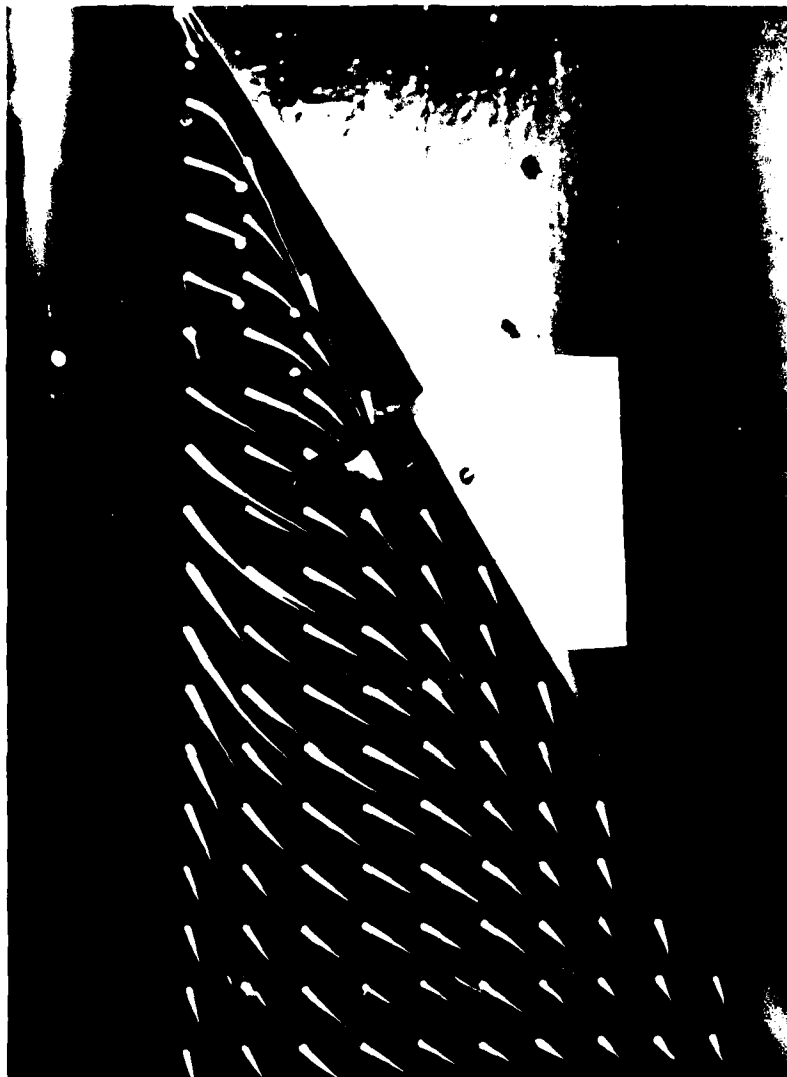


Fig. B-2. Oil Flow Visualization for the F7 Modified Gothic  
II Fence Case at 20 degrees

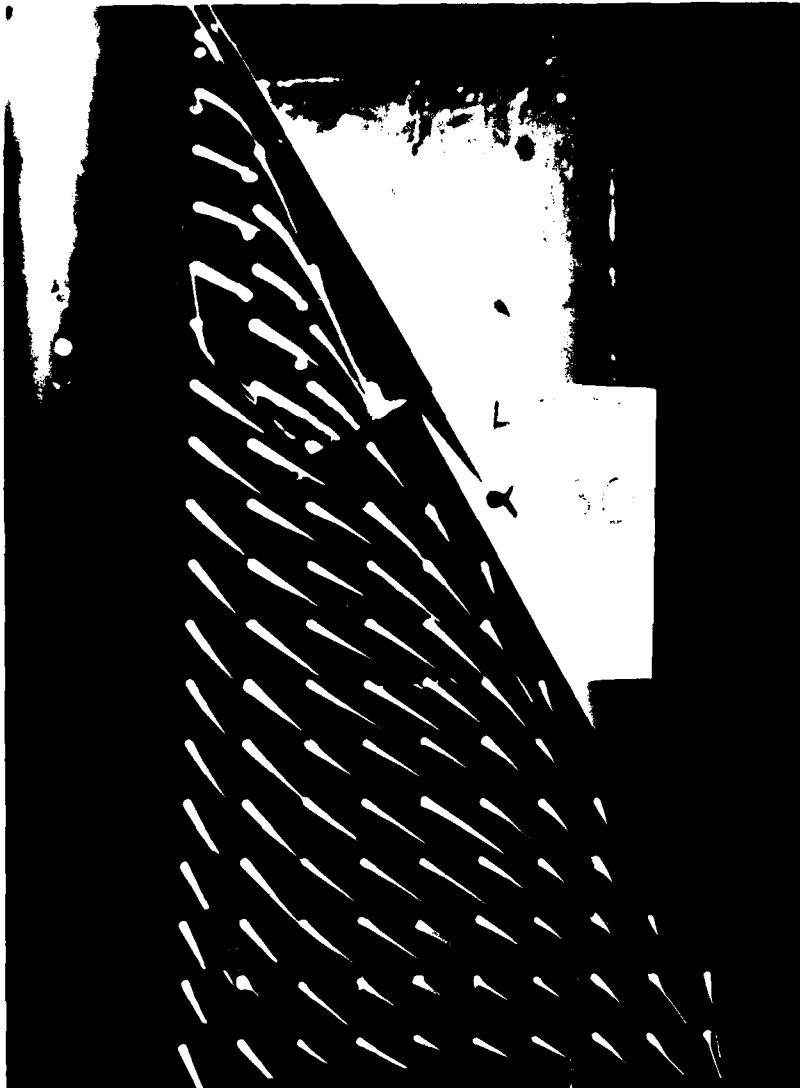


Fig. B-3. Oil Flow Visualization for the F7 Modified Gothic  
II Fence Case at 30 degrees

APPENDIX C: REDUCED AERODYNAMIC PLOTS

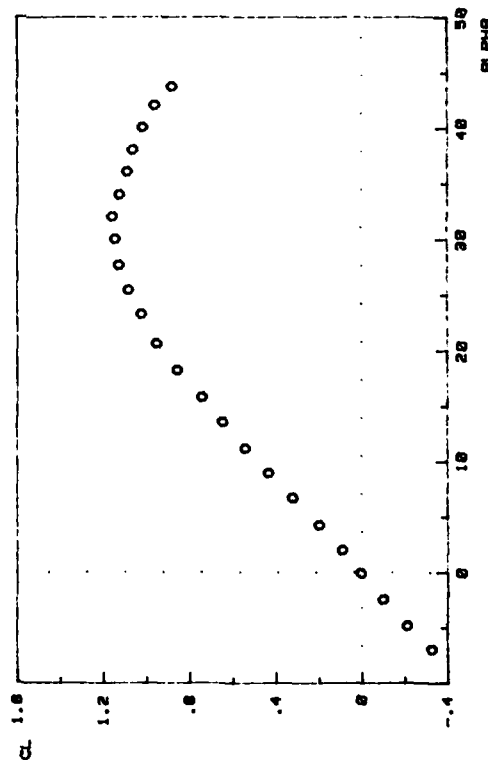
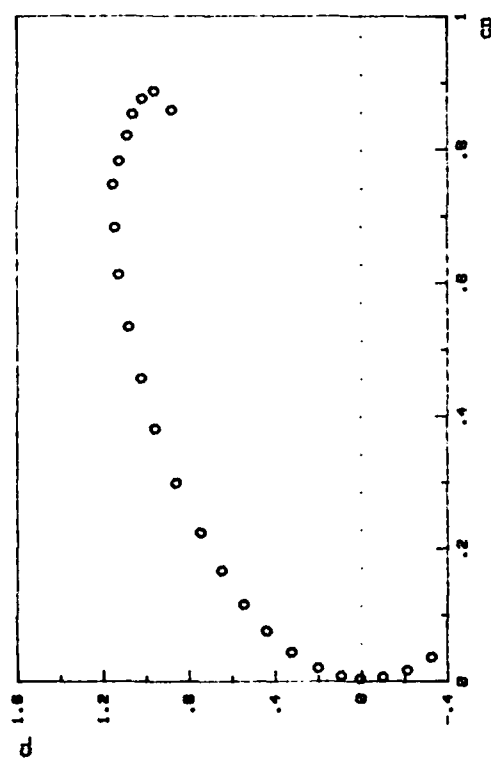
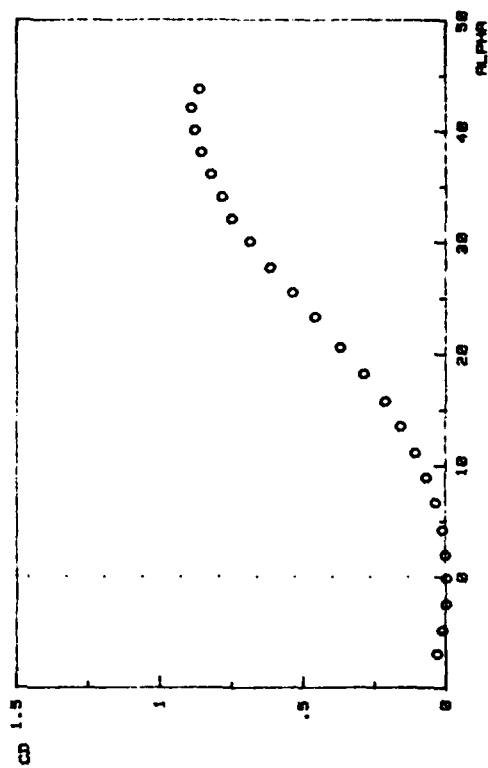
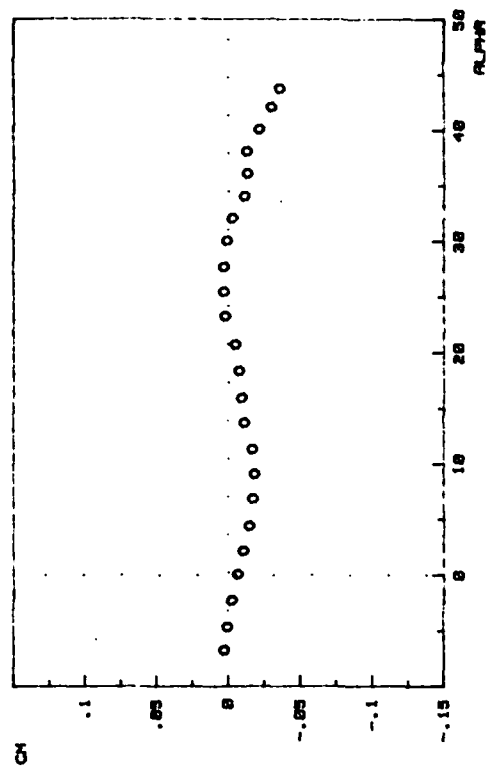


FIG. C-1.  
BASELINE CASE

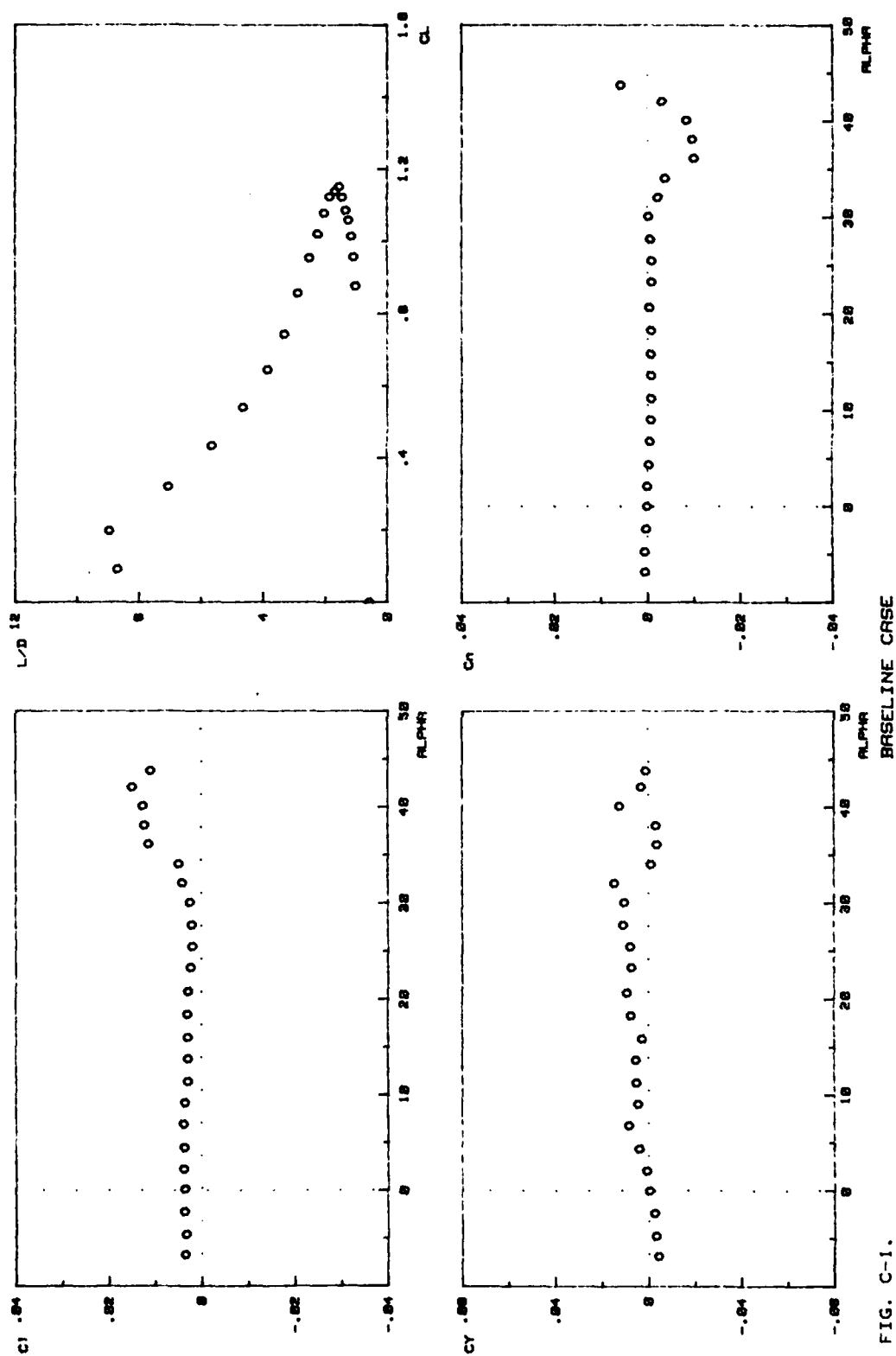


FIG. C-1.

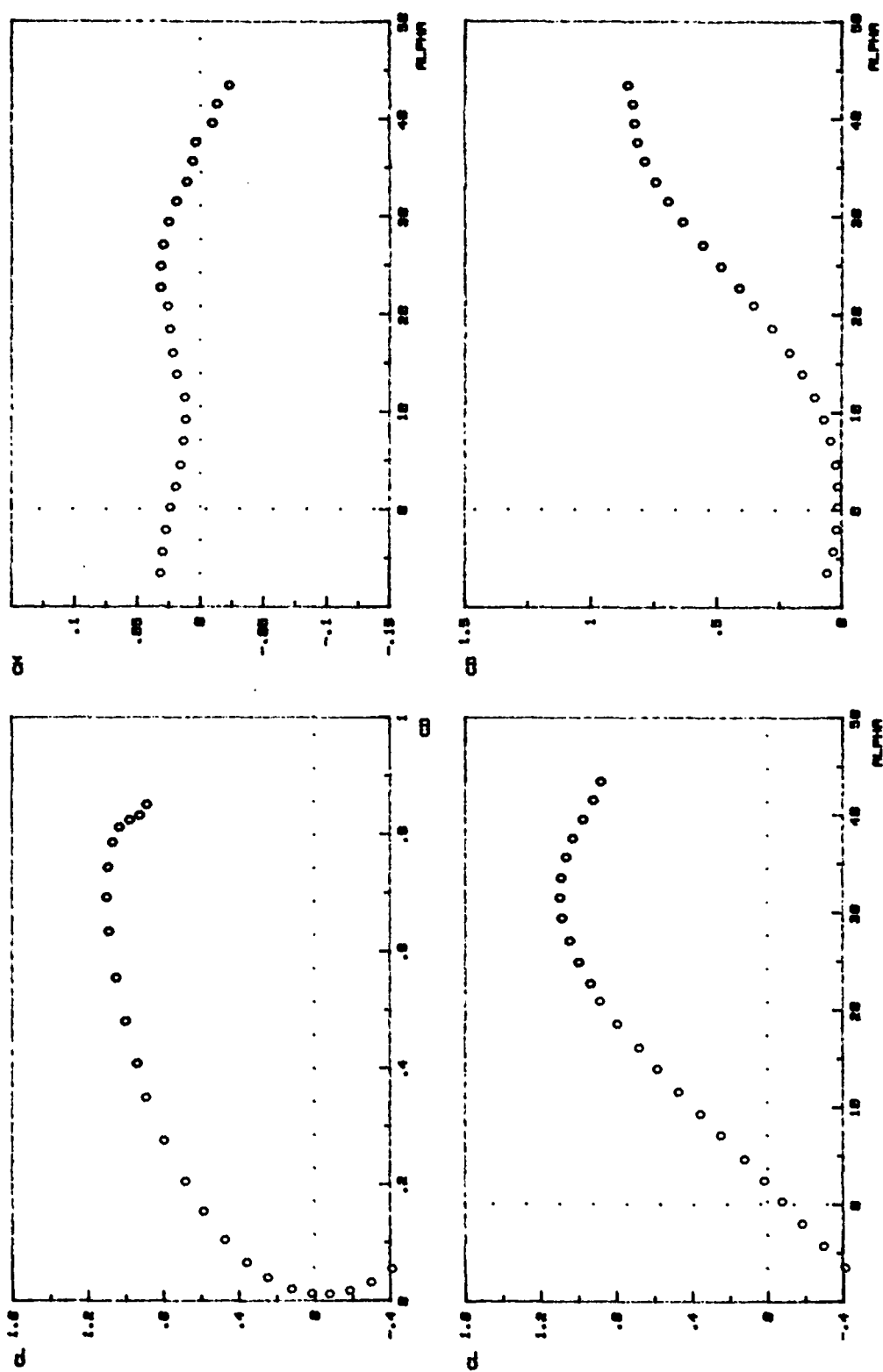
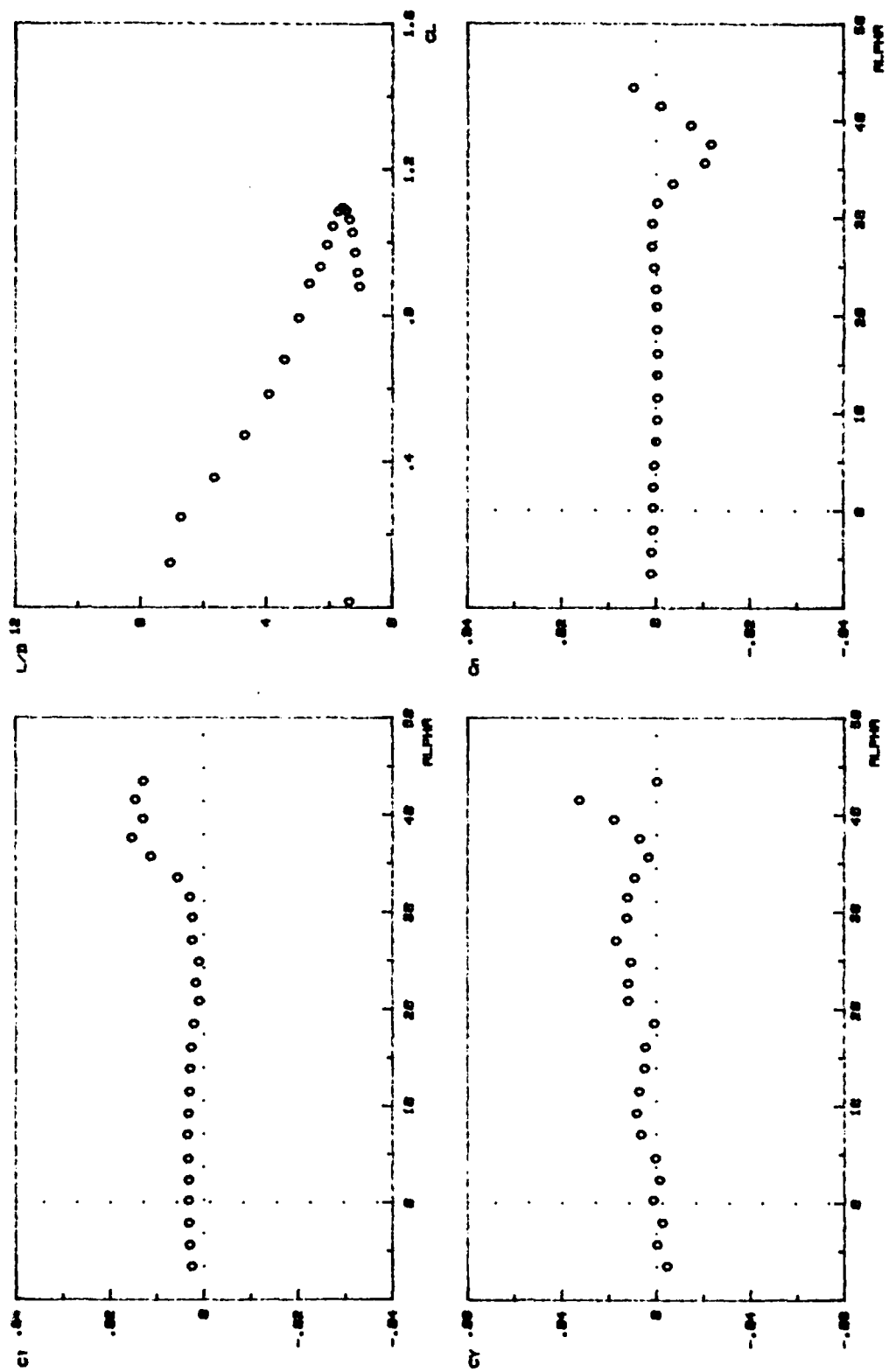


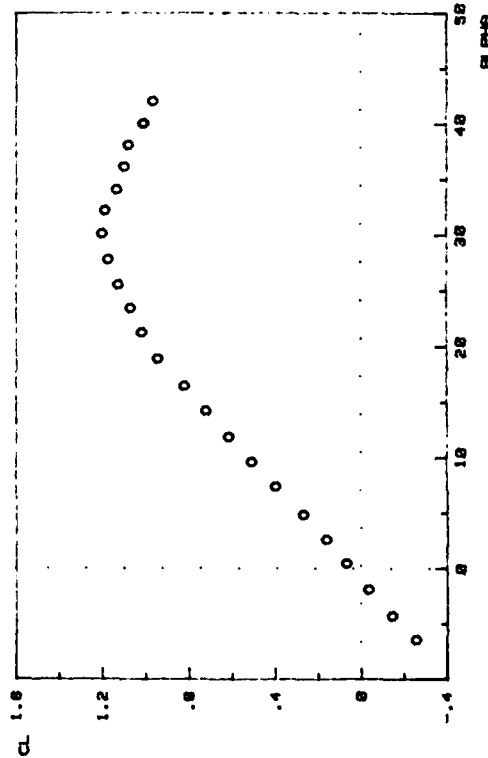
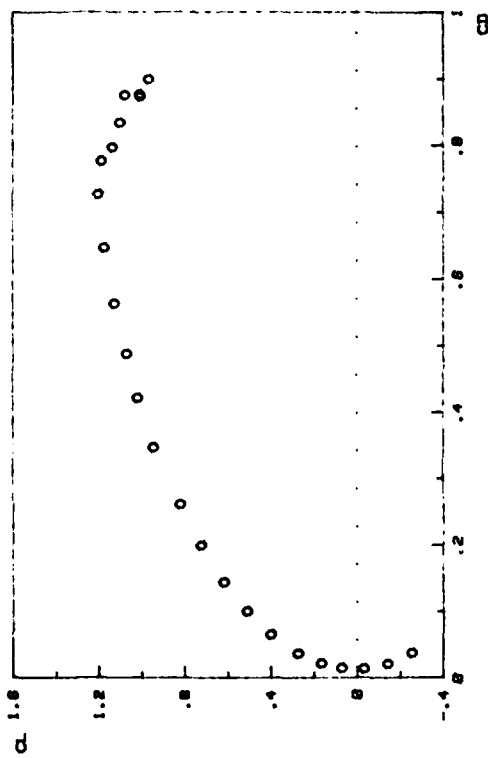
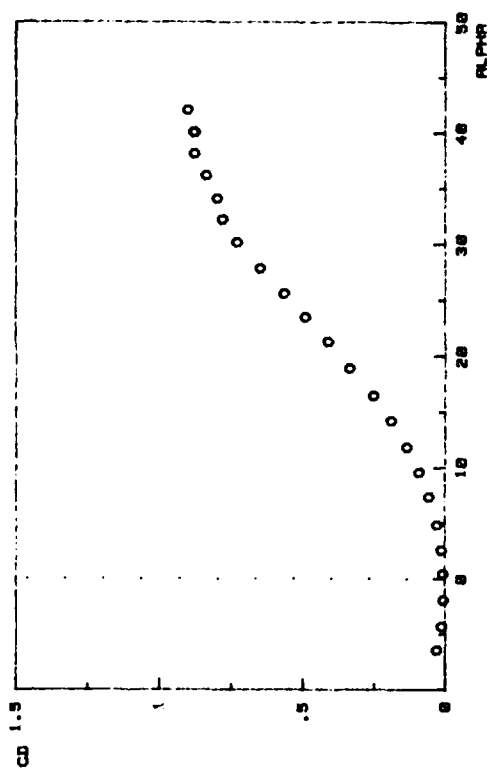
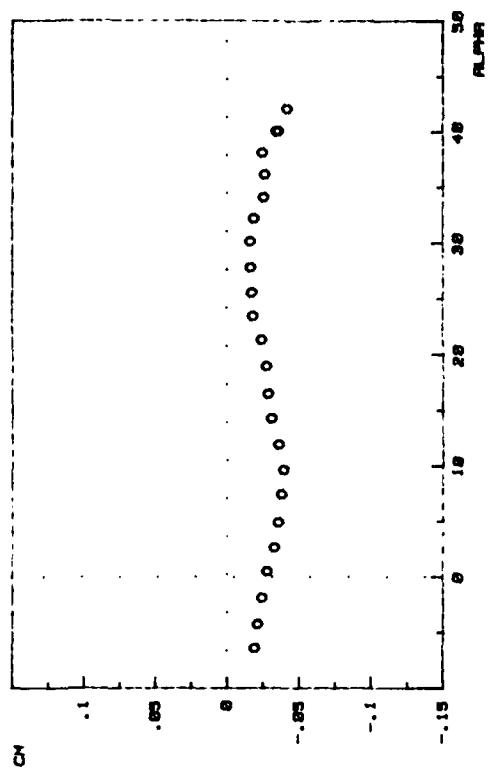
FIG. C-2.

BASLINE CASE  $\bullet$   $-10^\circ$  deg FLAP



BASELINE CASE @ -10 deg FLAP

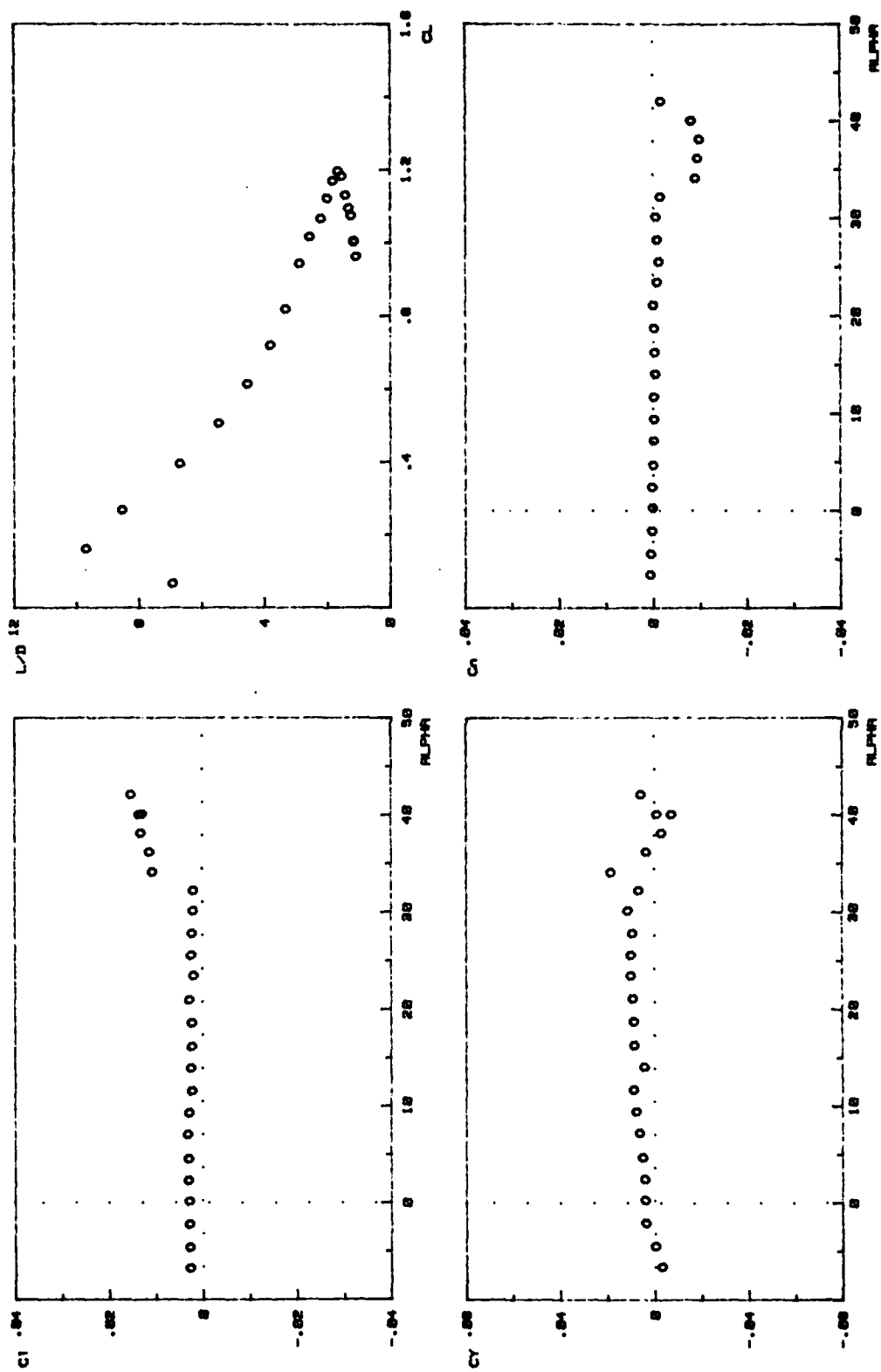
FIG. C-2.



BASELINE CASE @ 10 deg FLAP

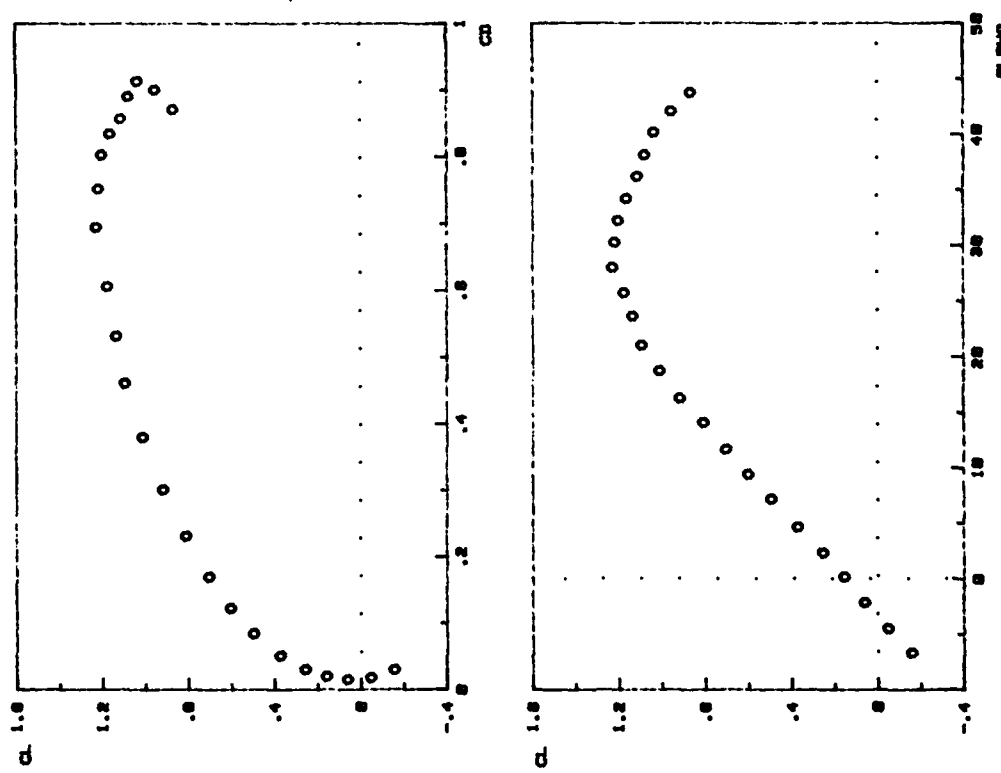
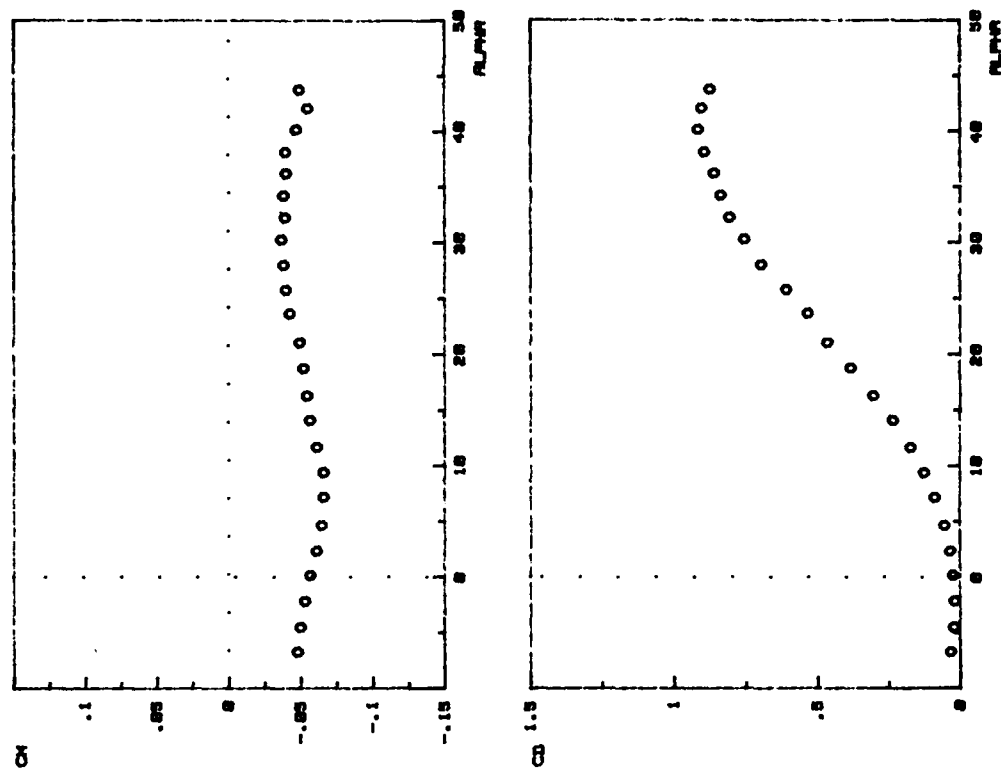
FIG. C-3.





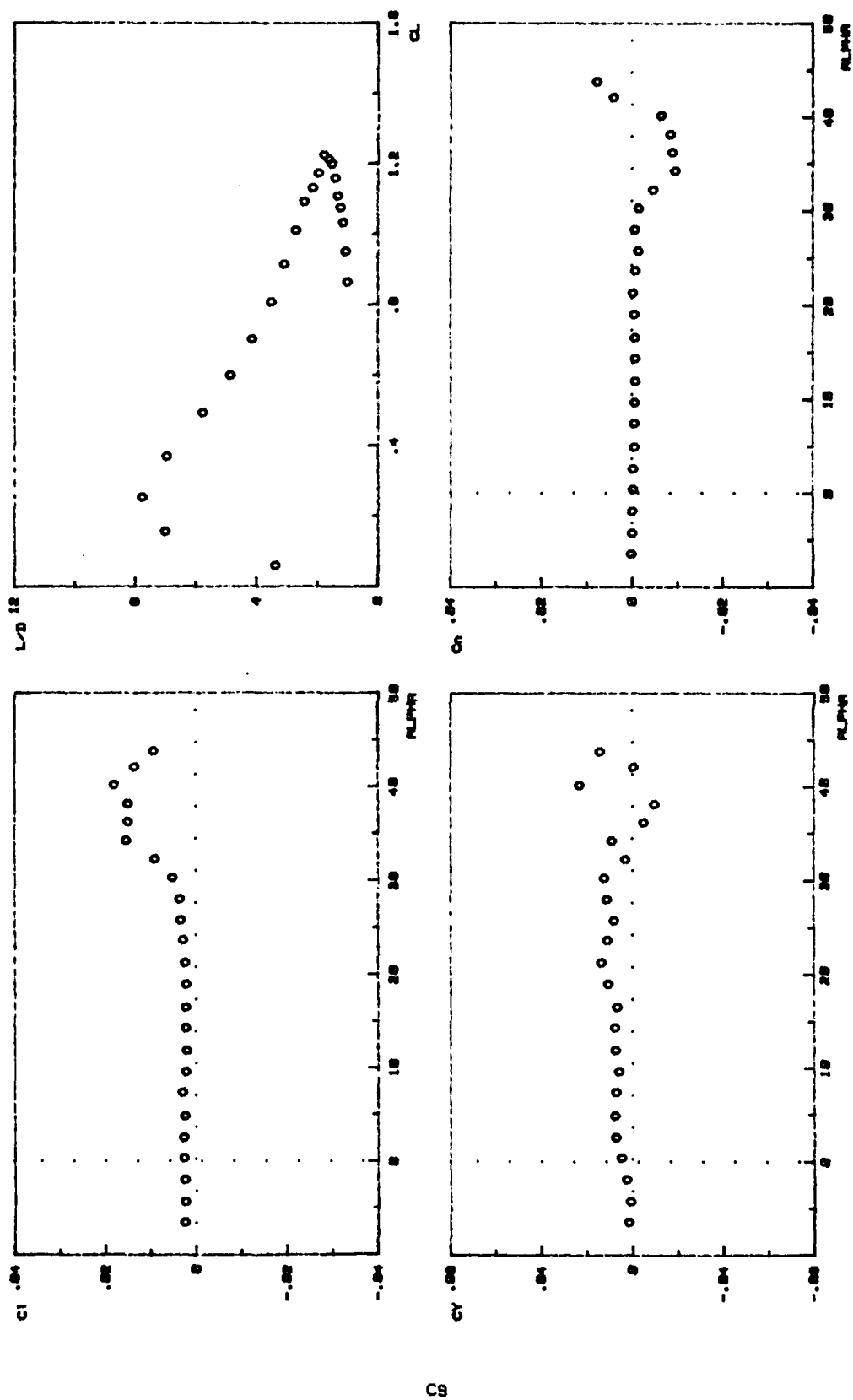
BASELINE CASE @ 10 deg FLAP

FIG. C-3.



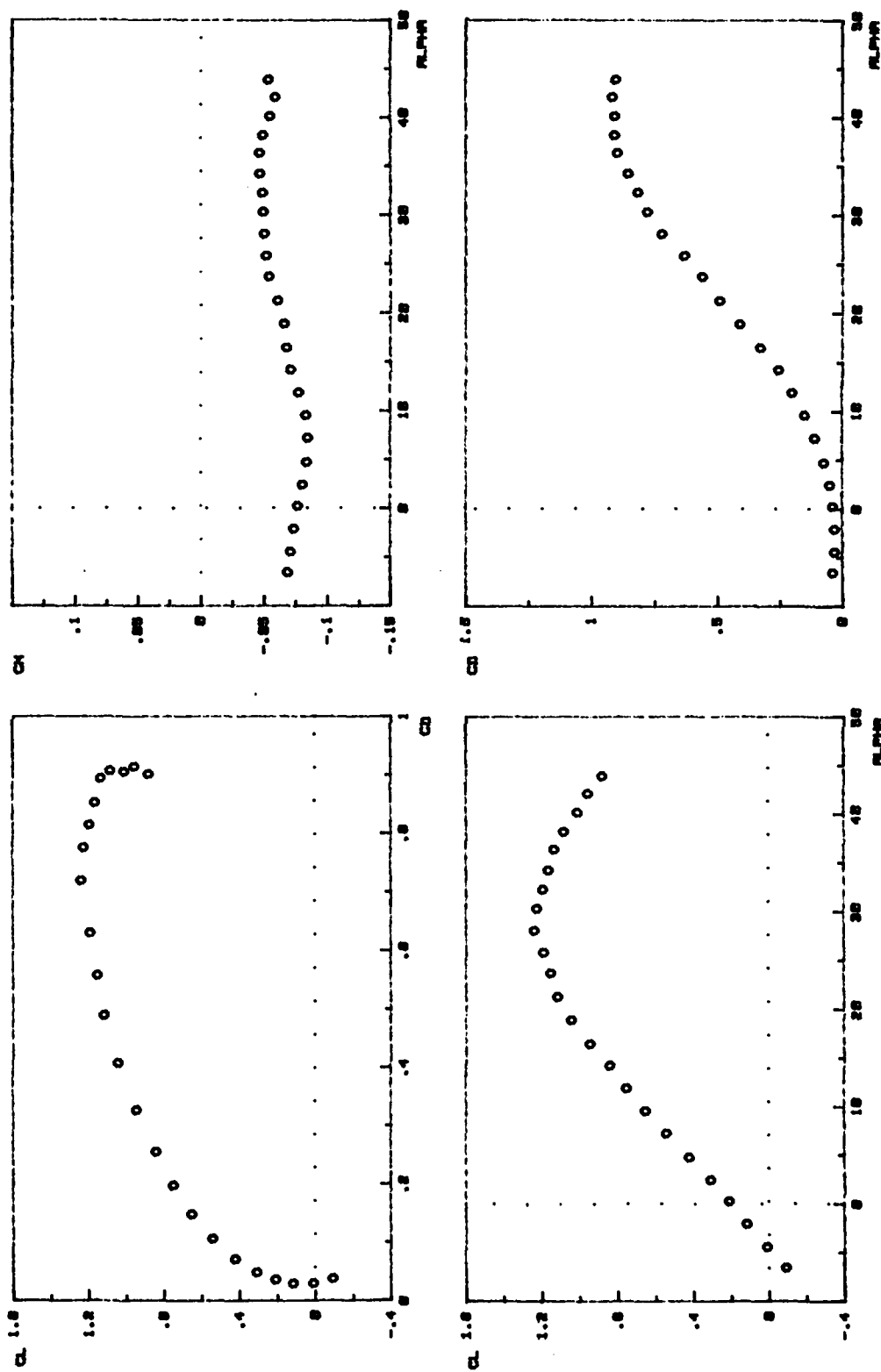
BASELINE CASE @ 20 deg FLAP

FIG. C-4.



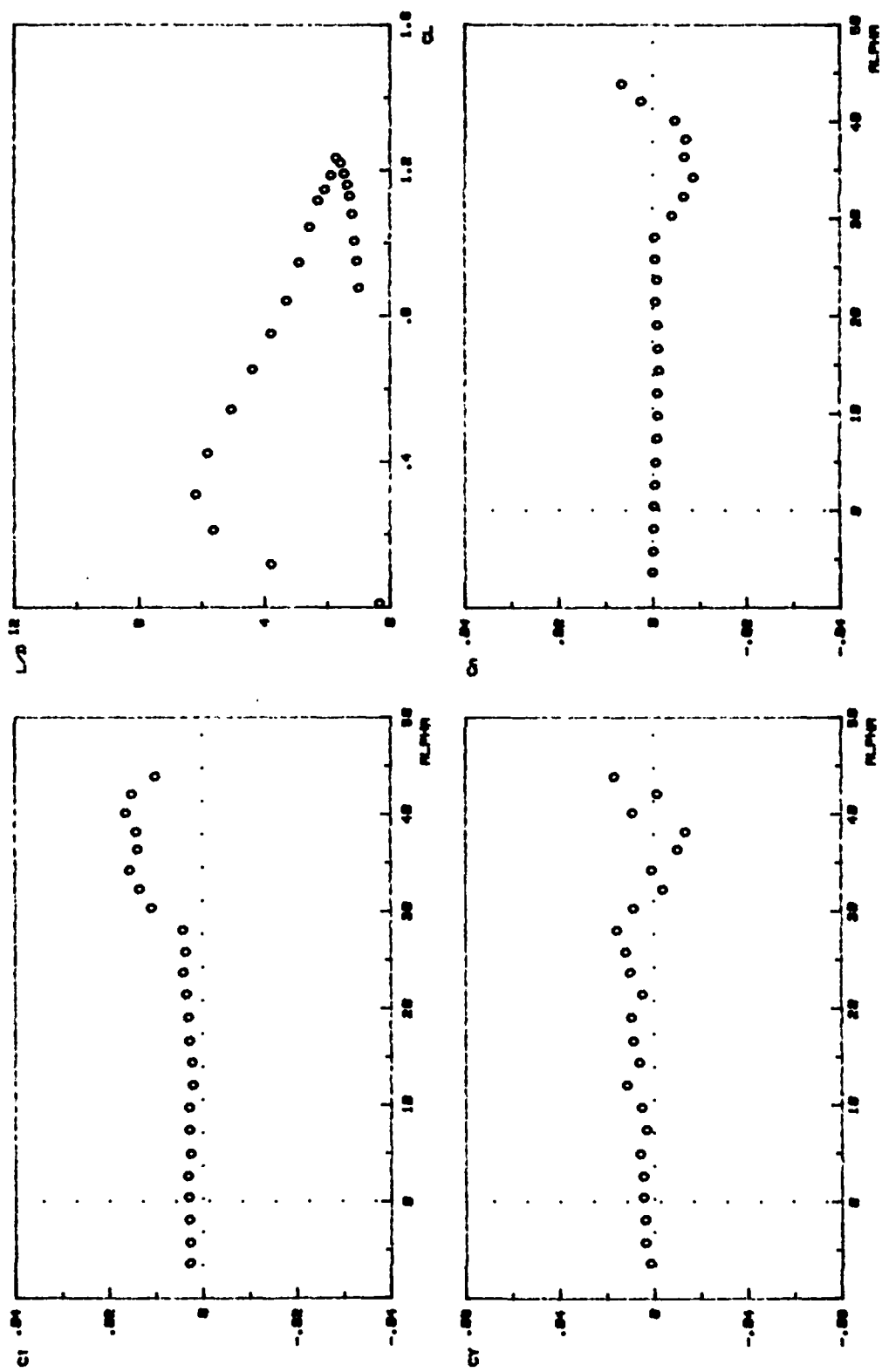
BASELINE CASE @ 20 deg FLAP

FIG. C-4.



BASELINE CASE @ 30 deg FLAP

FIG. C-5.



BASELINE CASE @ 30 deg FLAP

FIG. C-5.

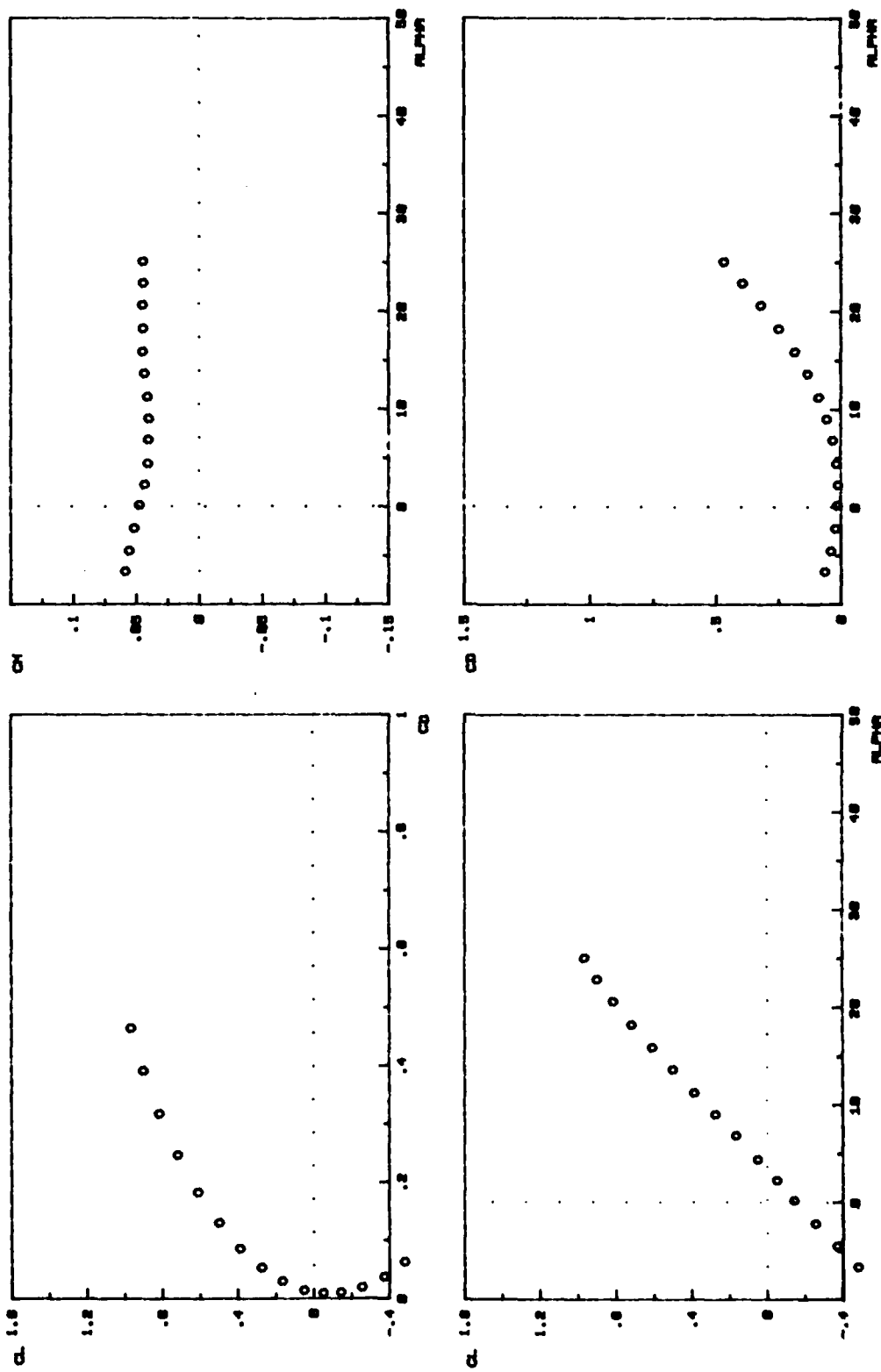
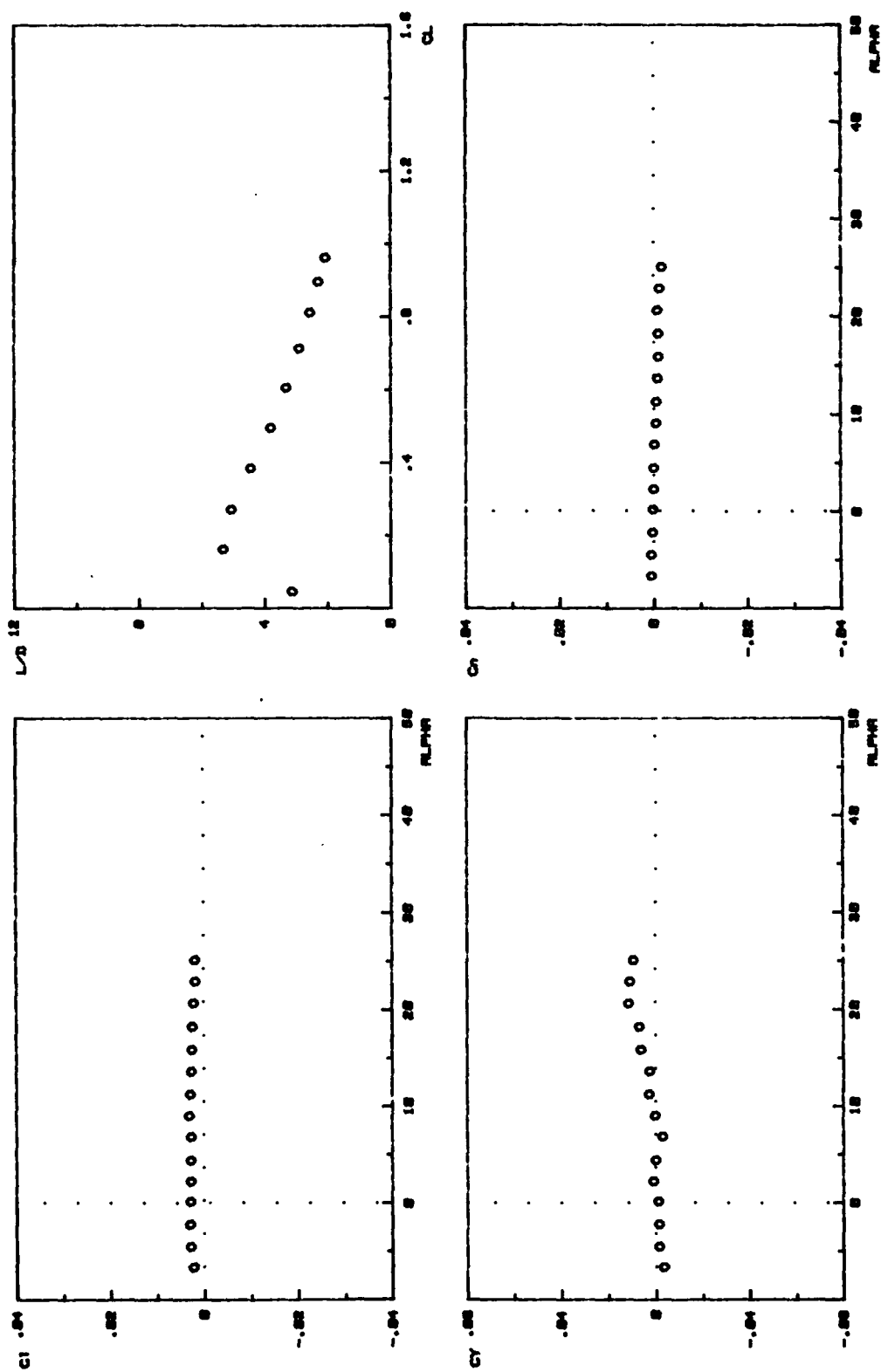
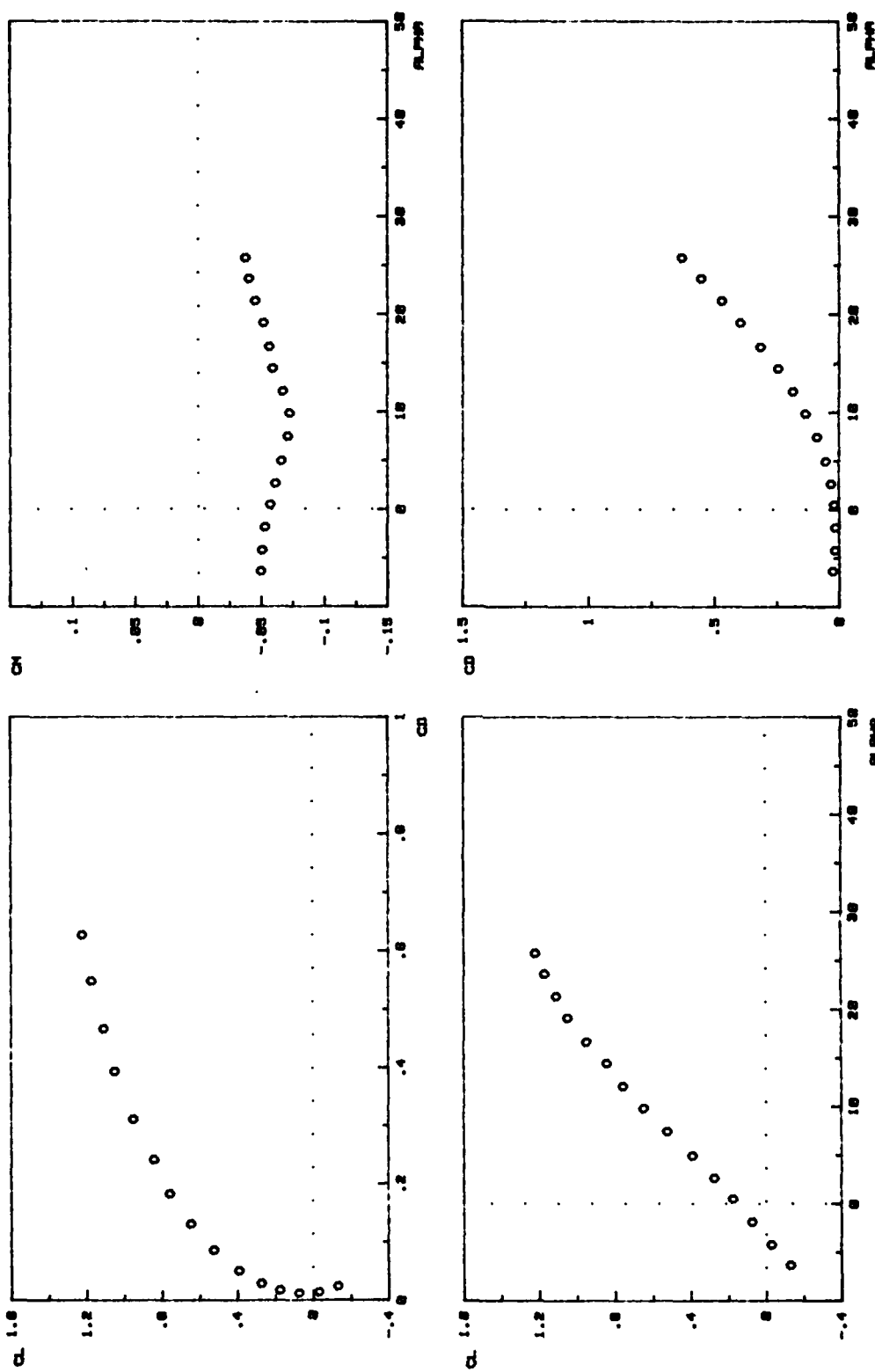


FIG. C-6.



BASELINE CASE @ -10 deg TWIN FLAP

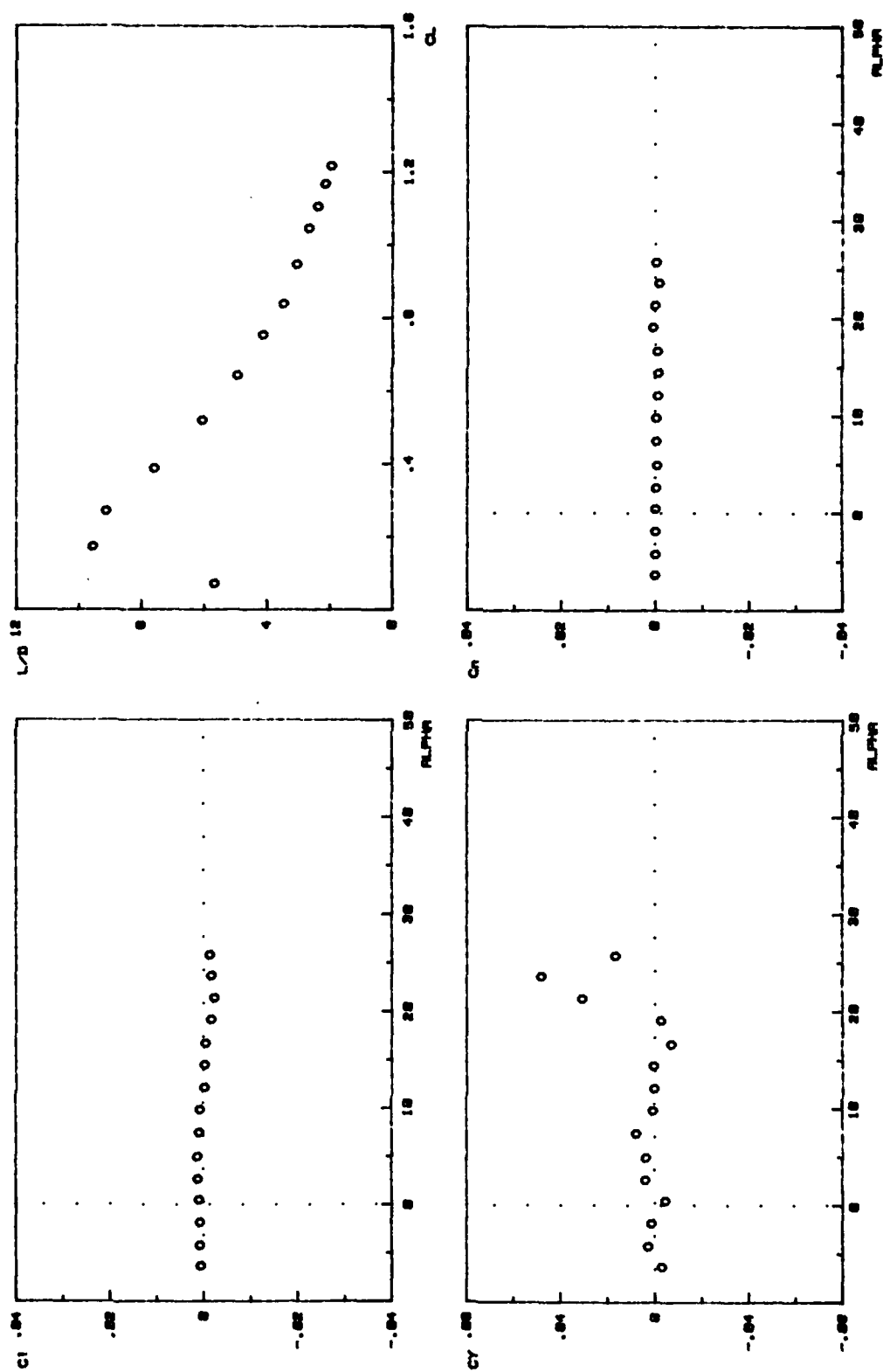
FIG. C-6.



BASELINE CASE @ 10 deg TWIN FLAP

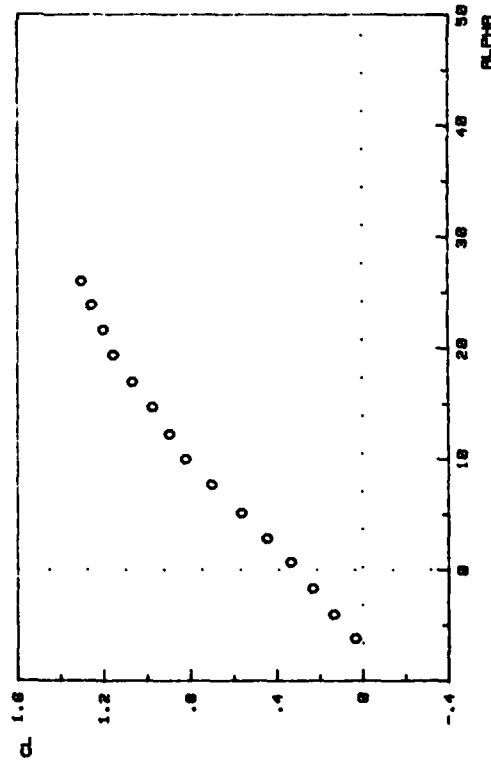
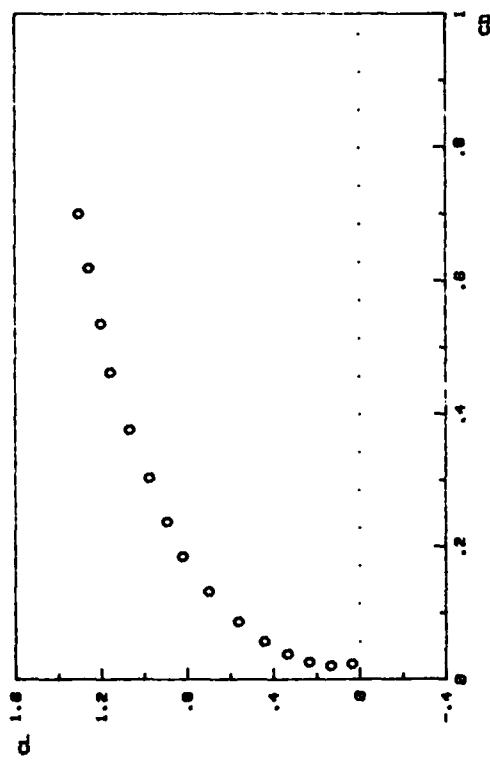
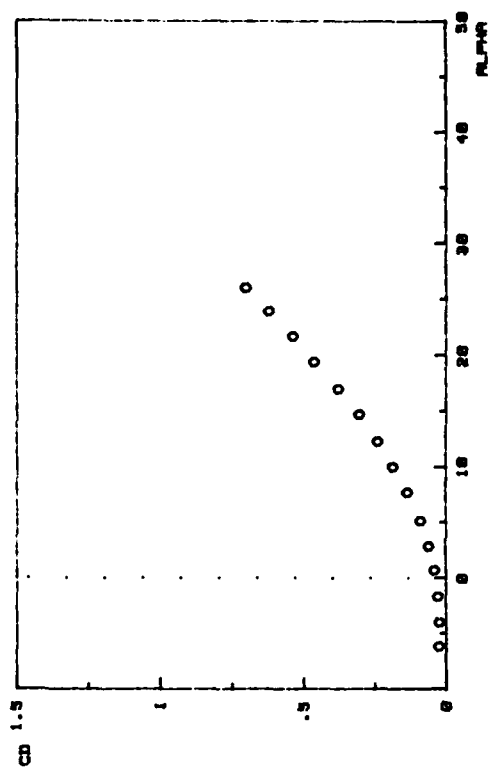
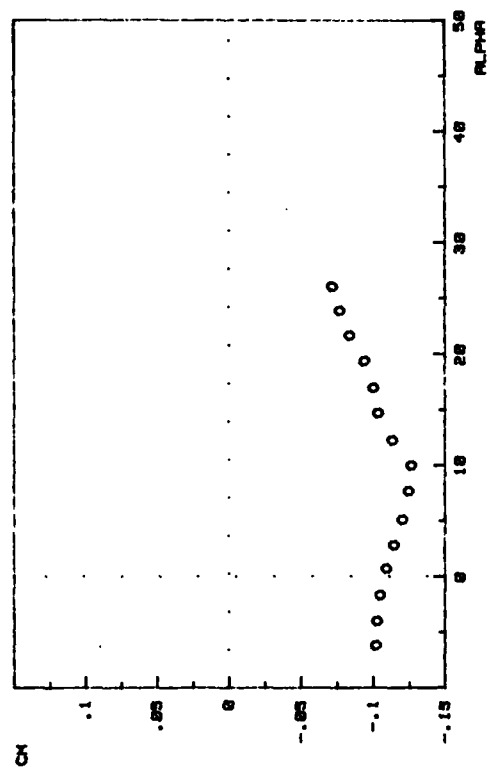
FIG. C-7.





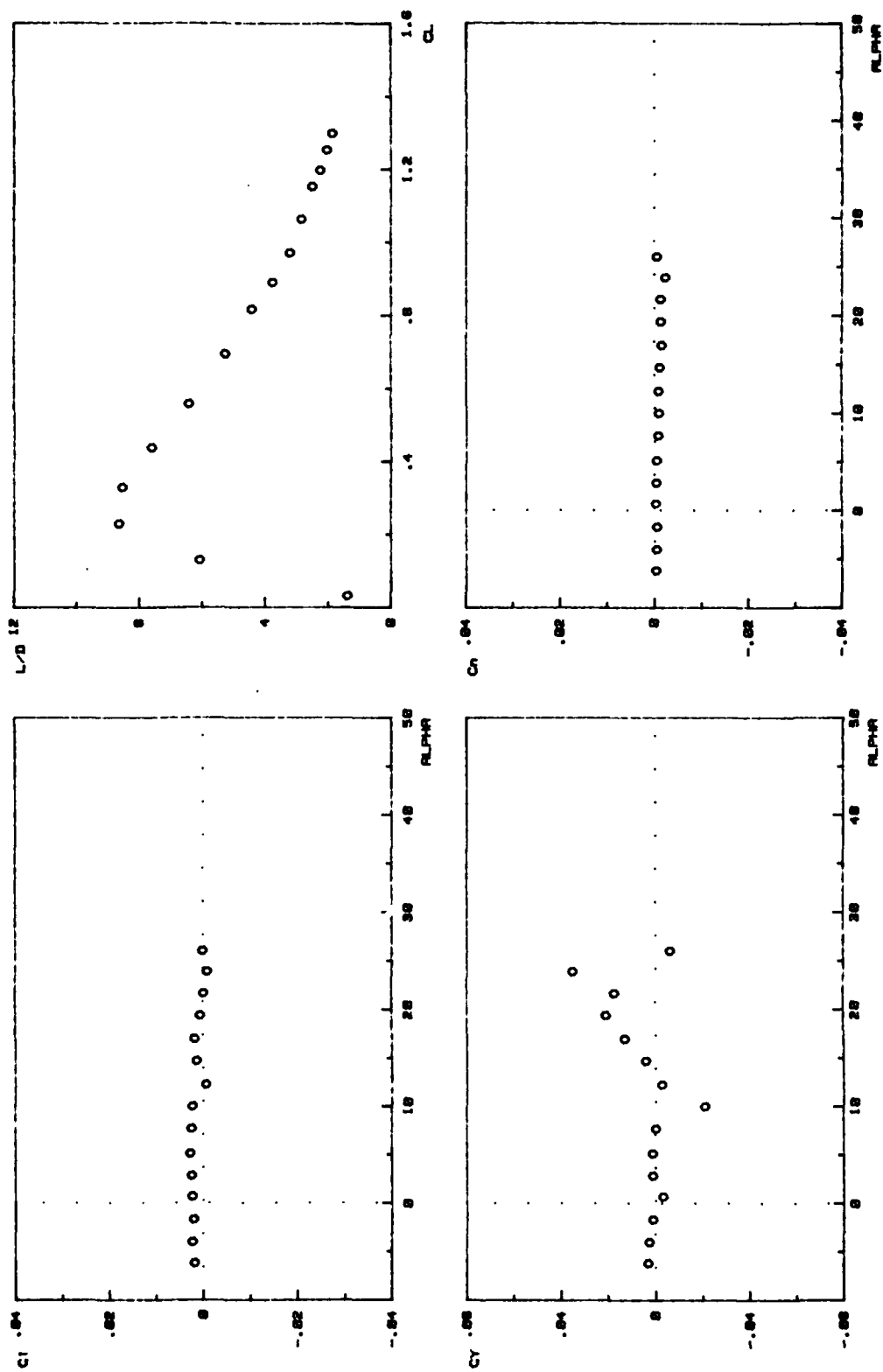
BASELINE CASE @ 10 deg TWIN FLAP

FIG. C-7.



BASELINE CASE @ 20 deg TWIN FLAP

FIG. C-8.



BASELINE CASE @ 20 deg TWIN FLAP

FIG. C-8.

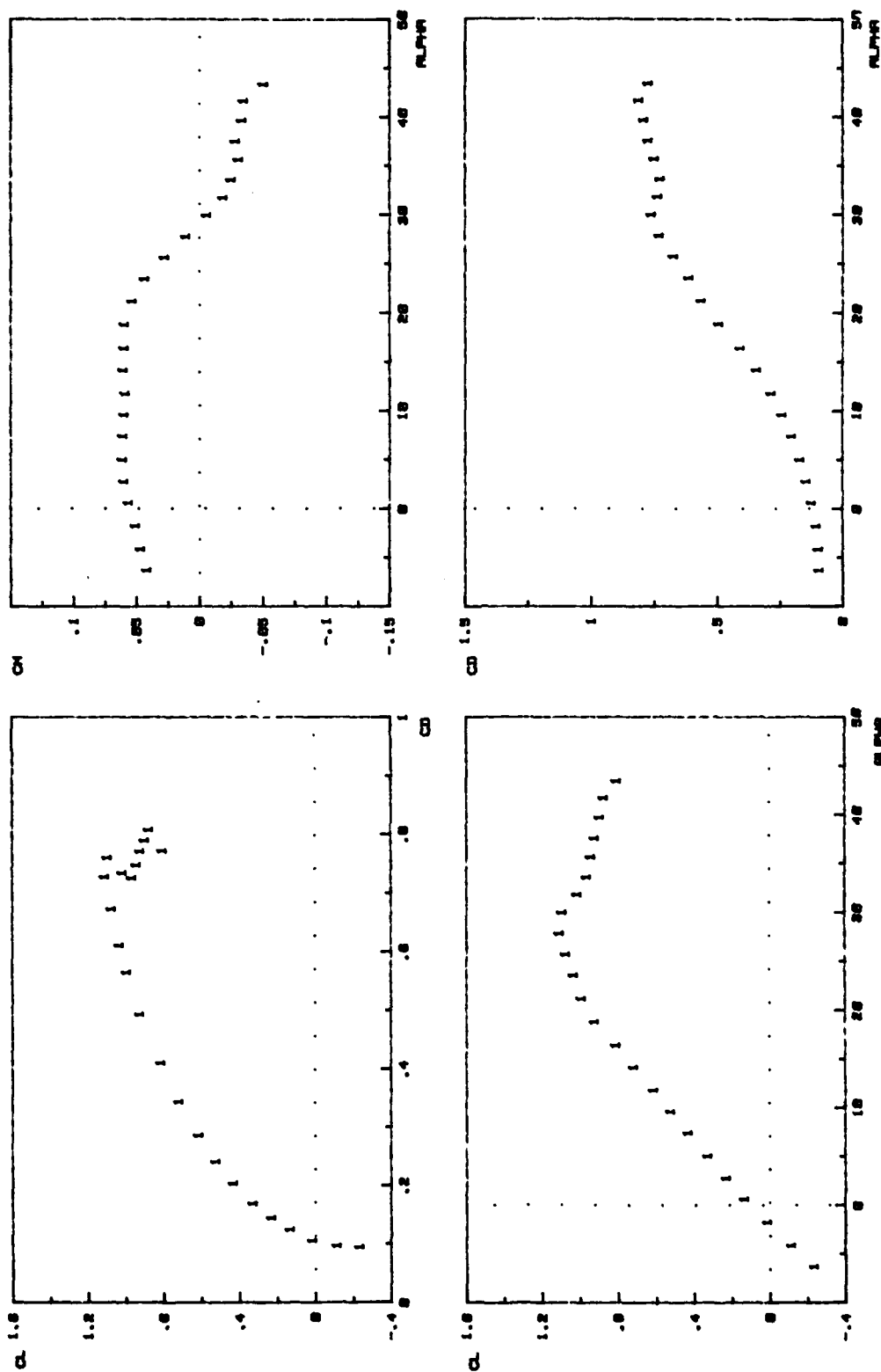


FIG. C-9.

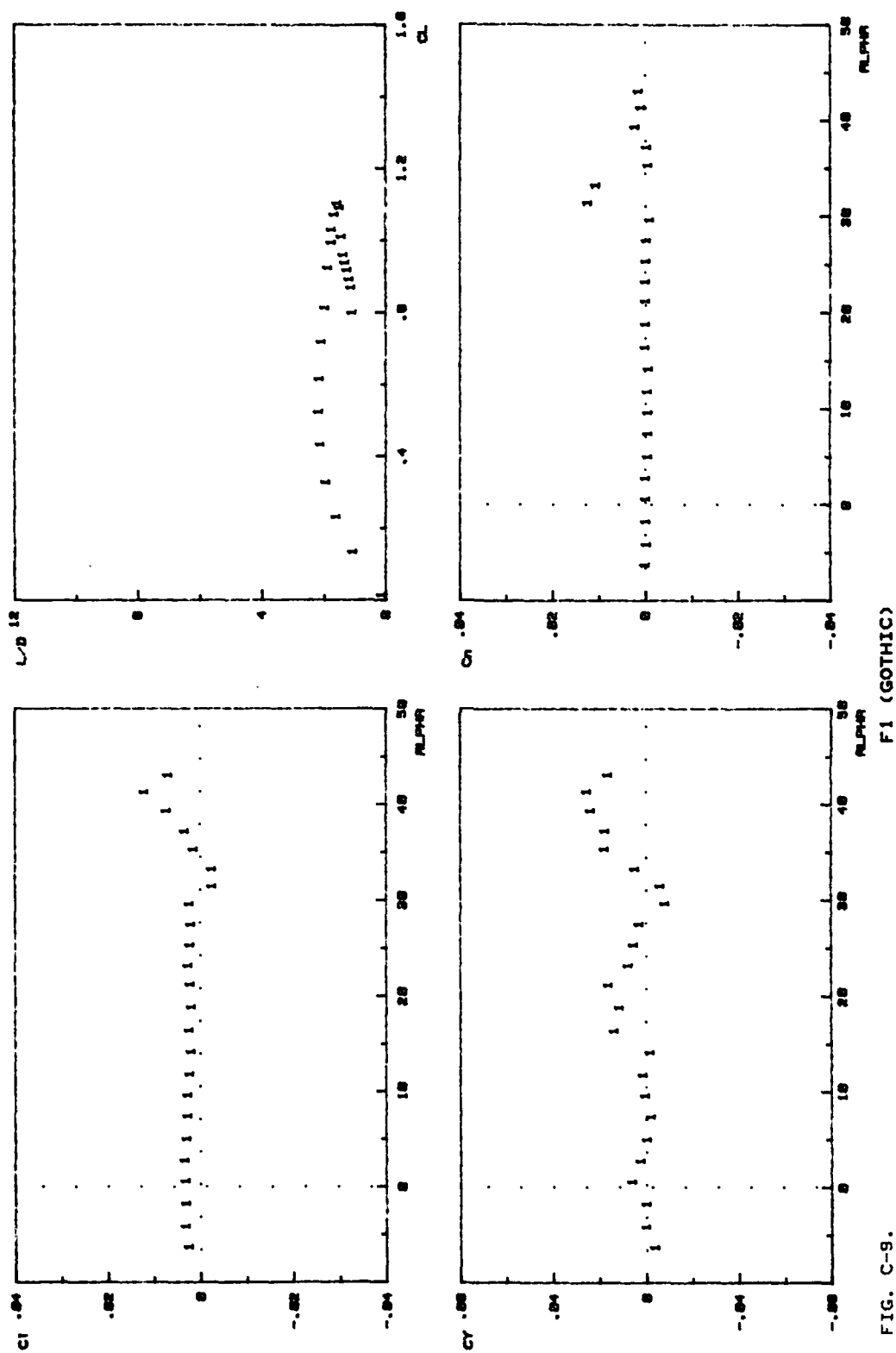


FIG. C-9.

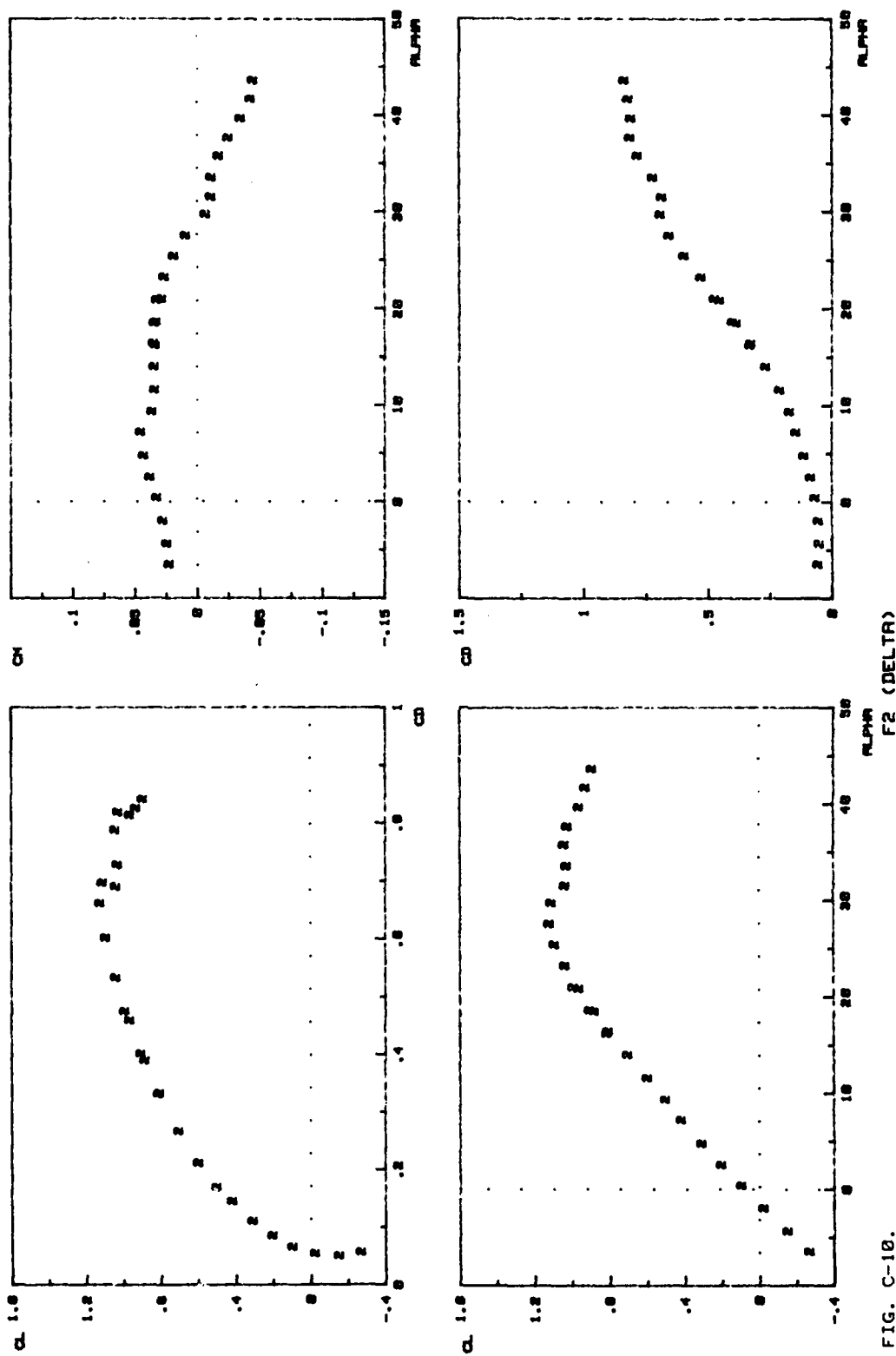


FIG. C-10.

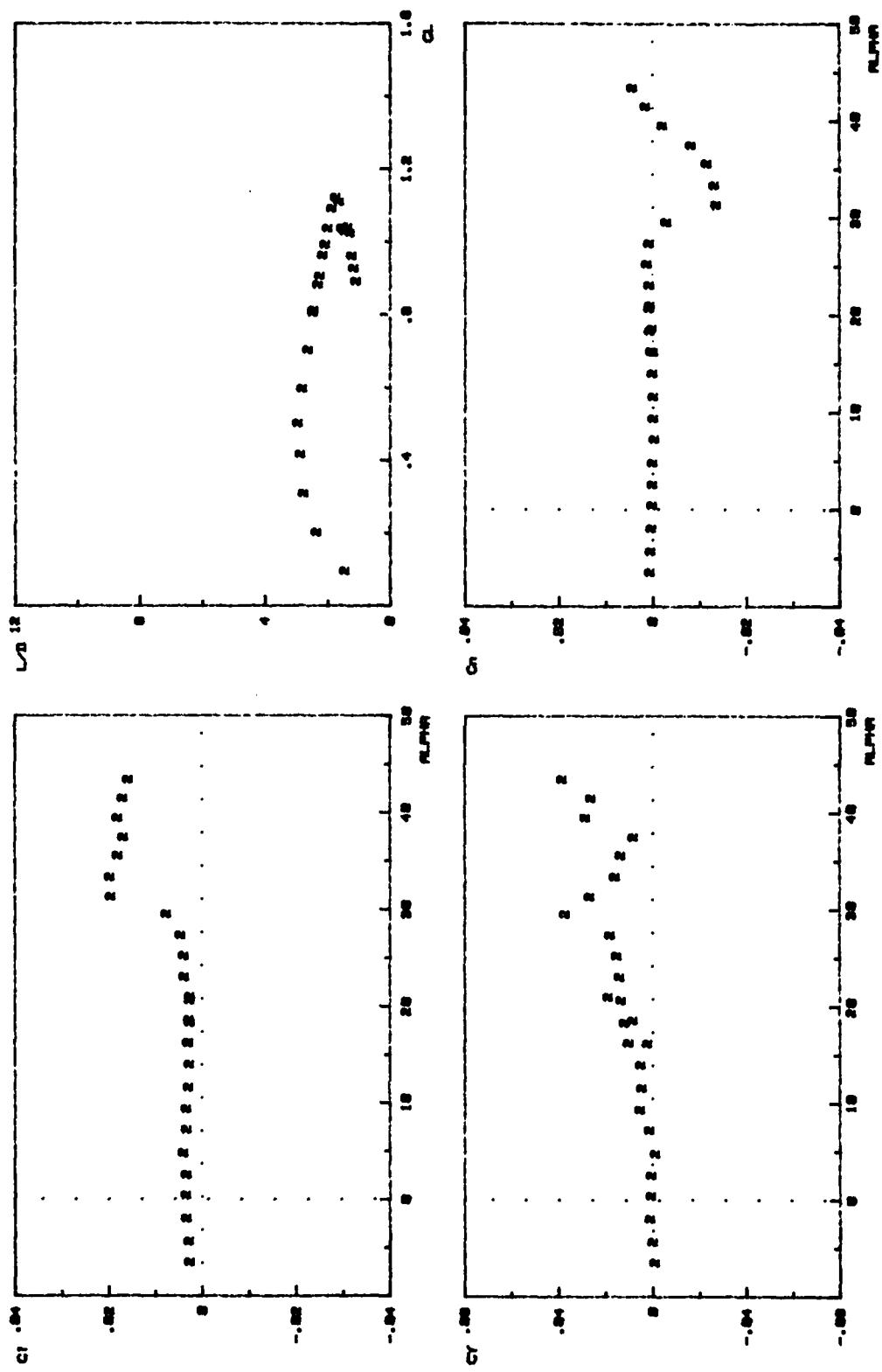


FIG. C-10.

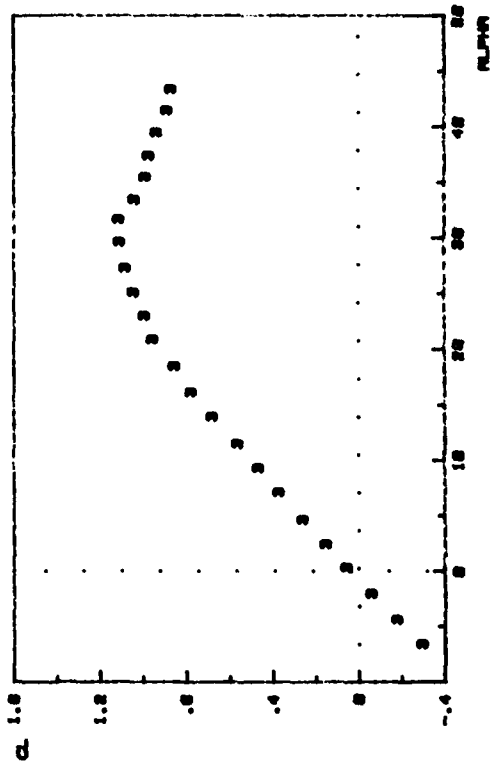
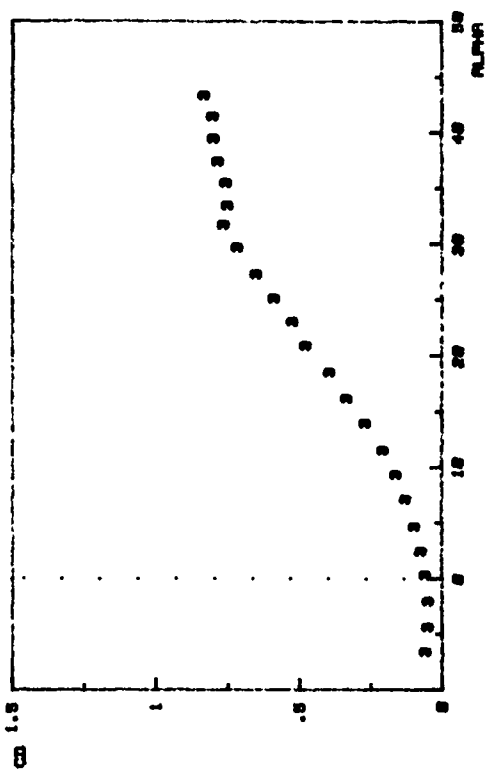
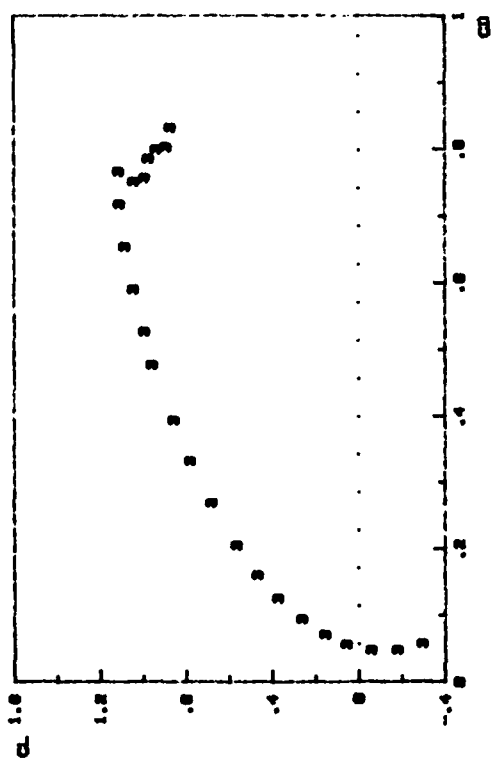
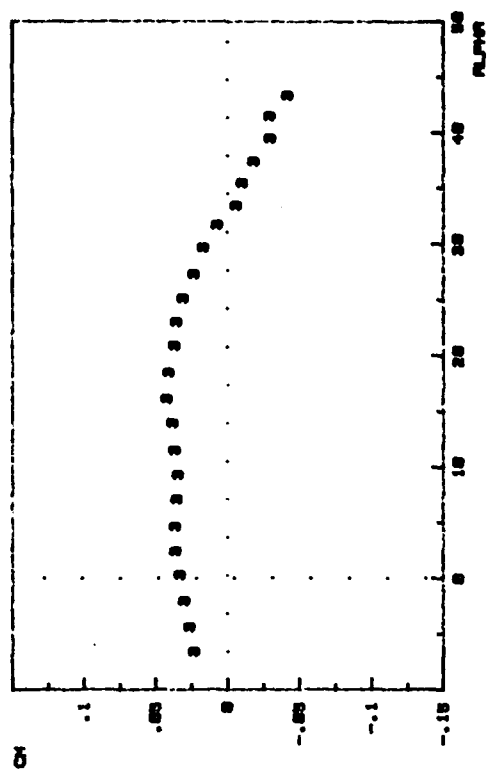


FIG. C-11.



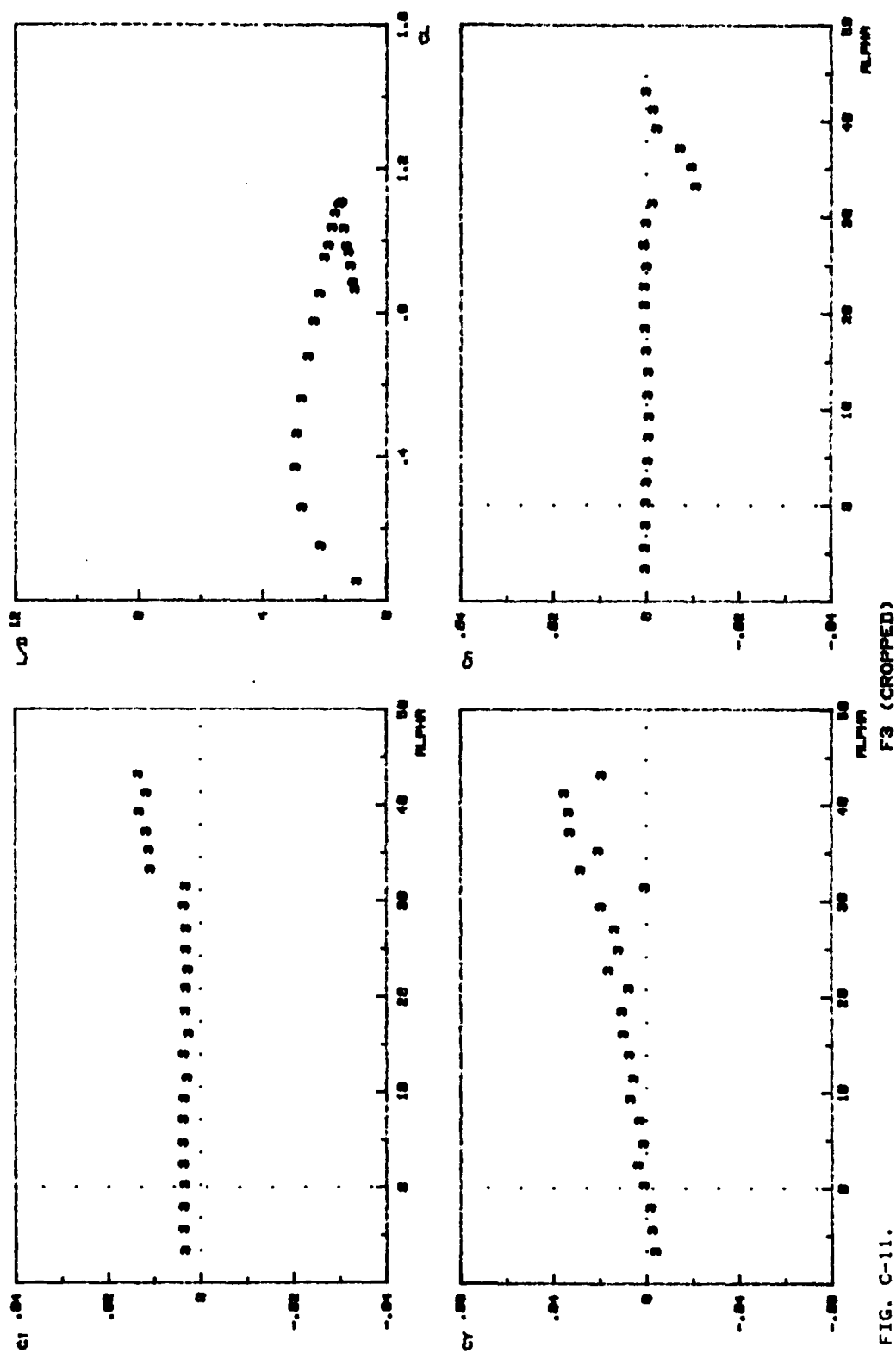


FIG. C-11.

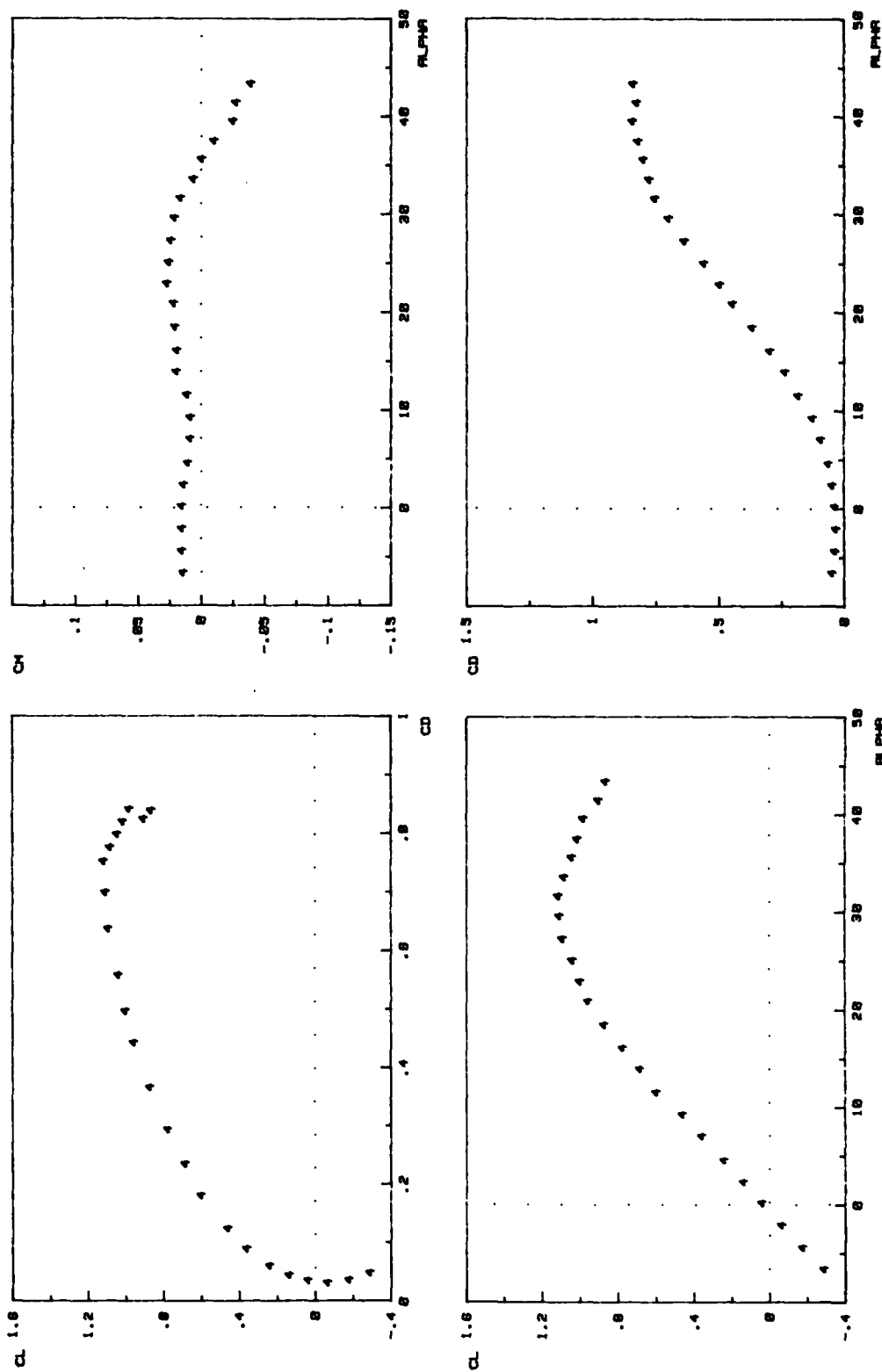
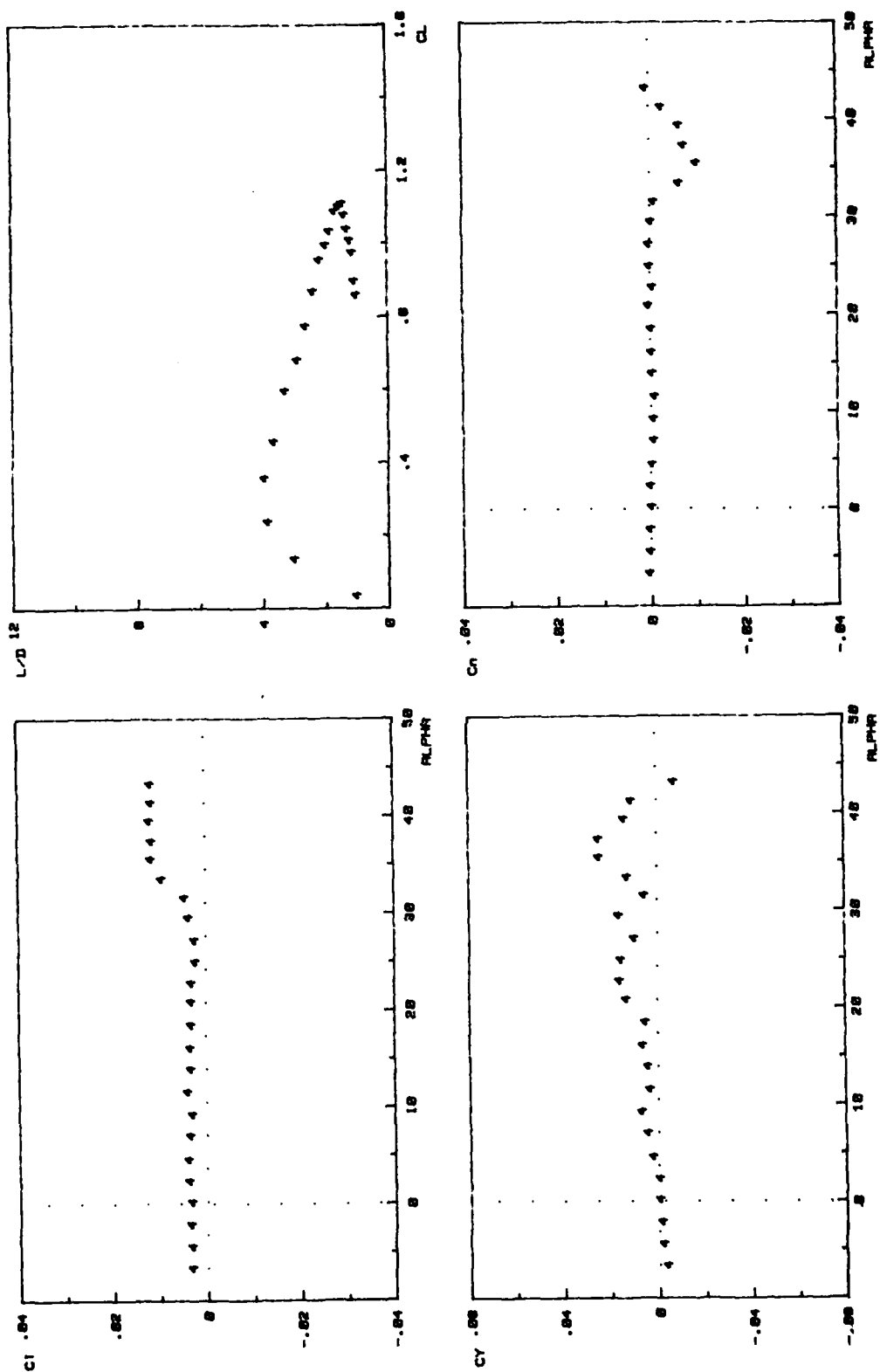


FIG. C-12.



F4 (MINI CROPPED)

FIG. C-12.

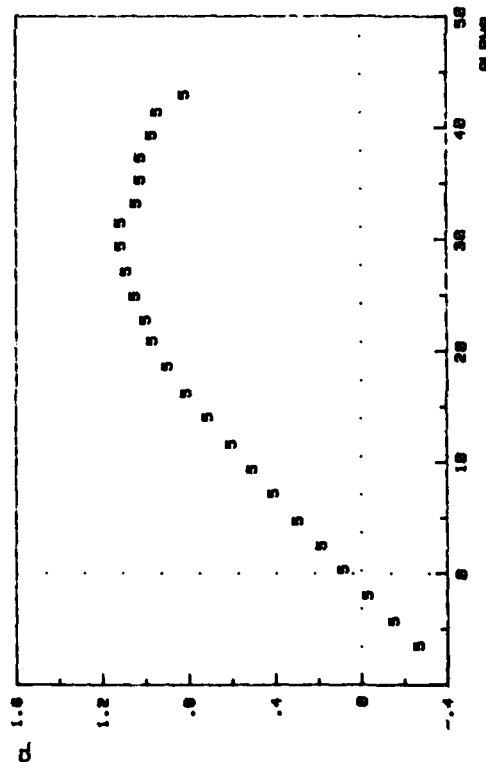
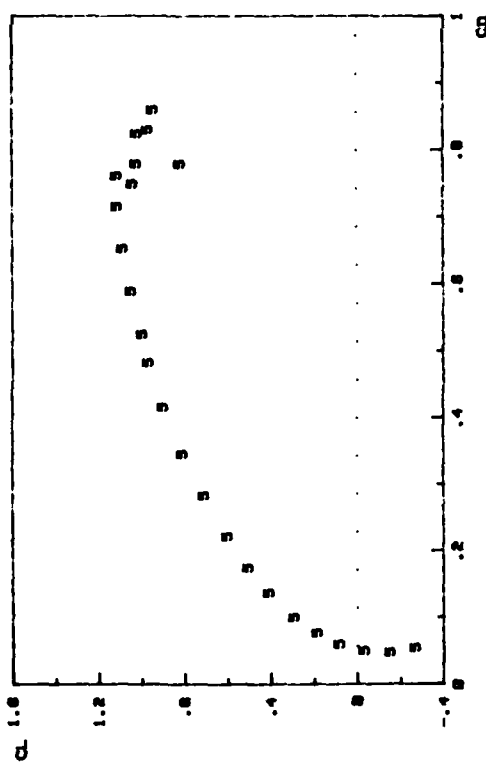
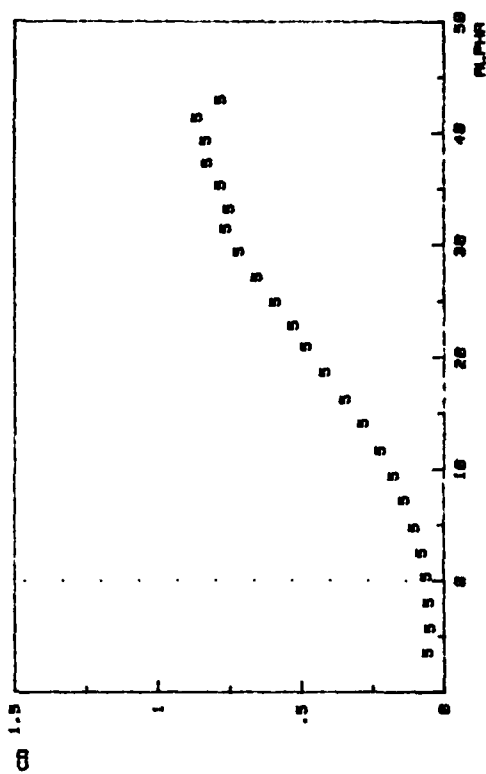
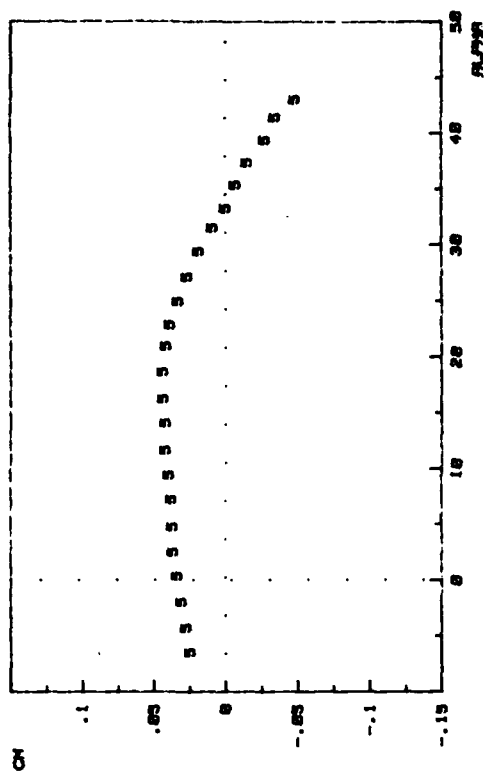


FIG. C-13.

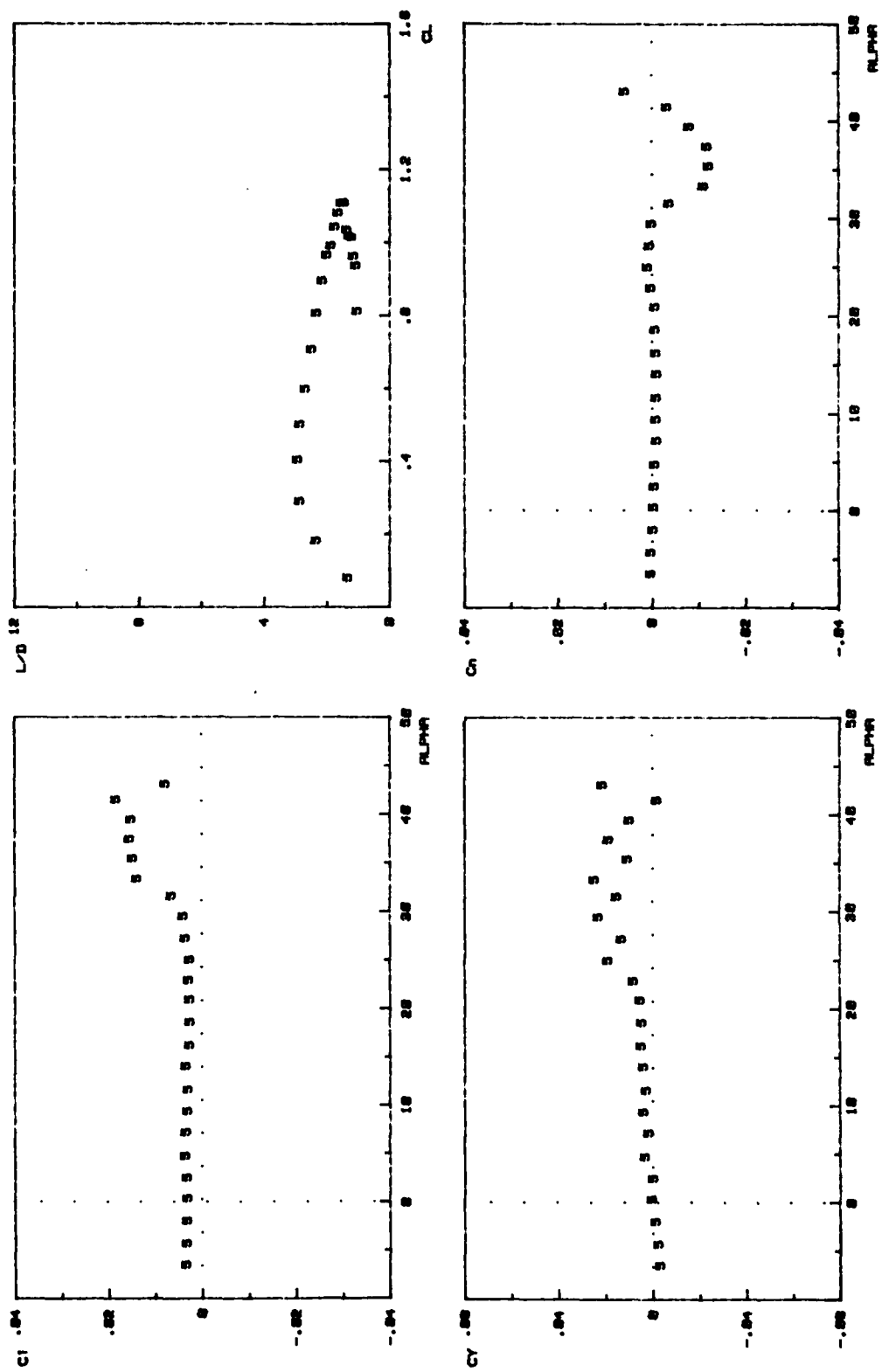


FIG. C-13.

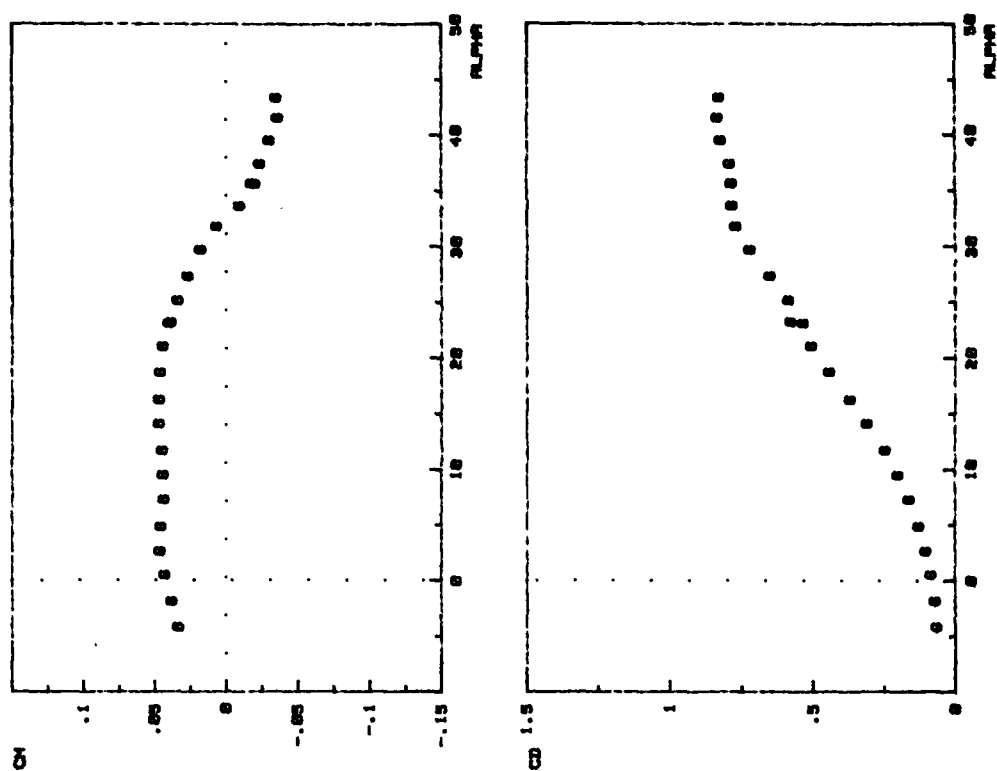
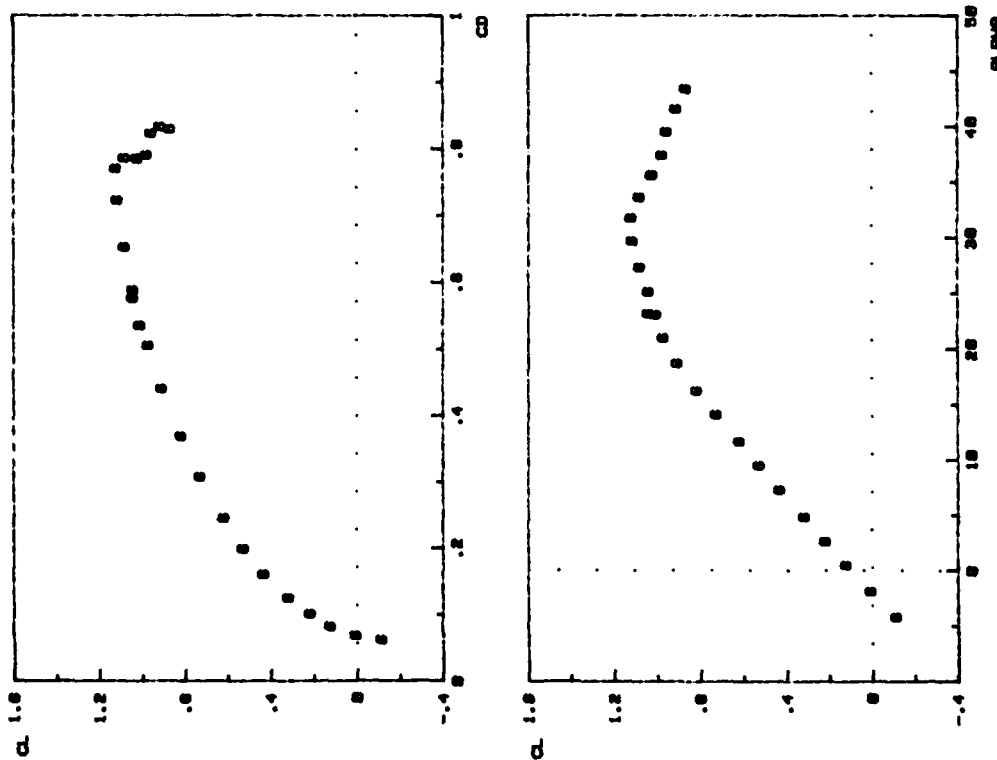


FIG. C-14.



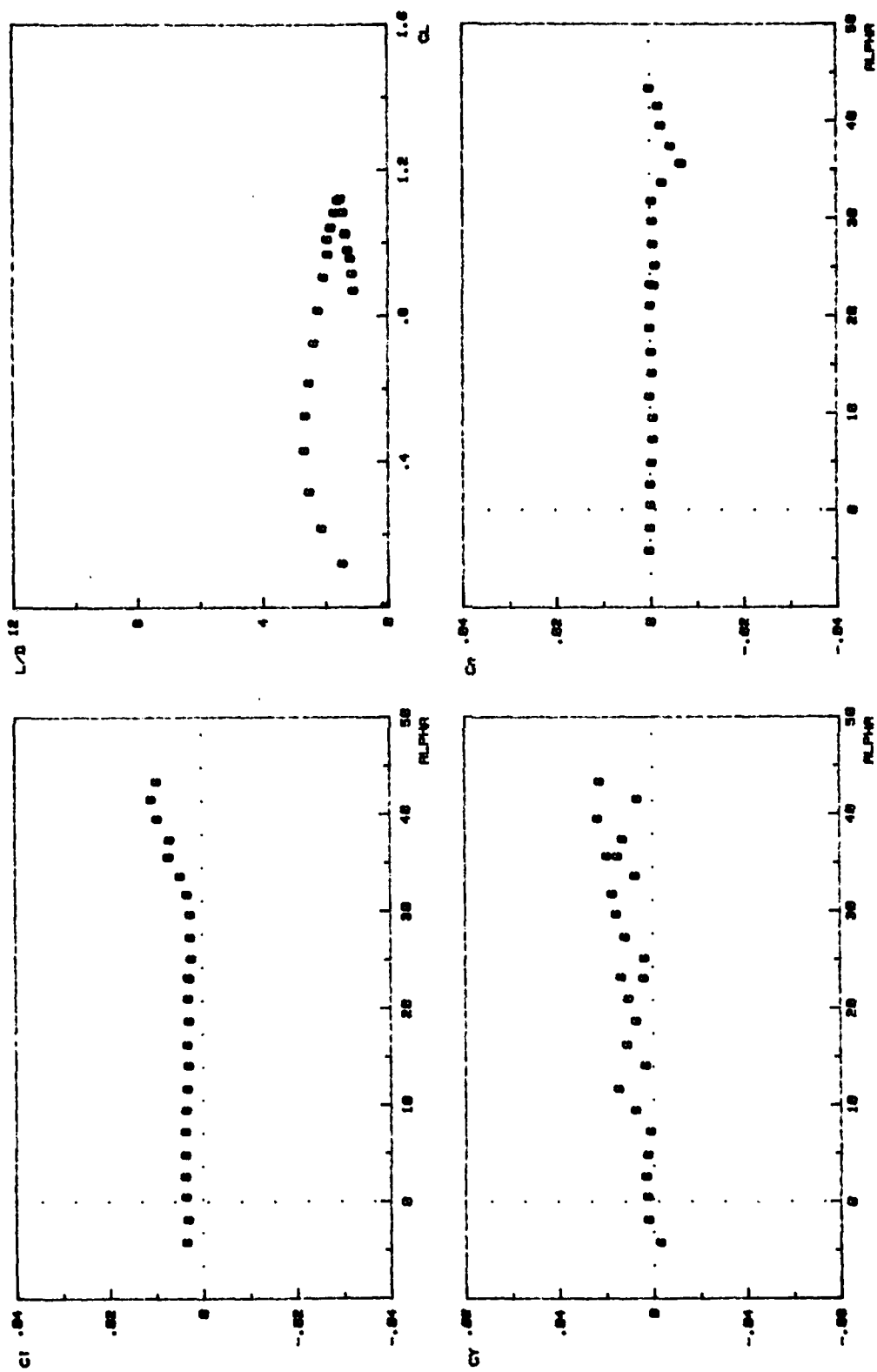


FIG. C-14.

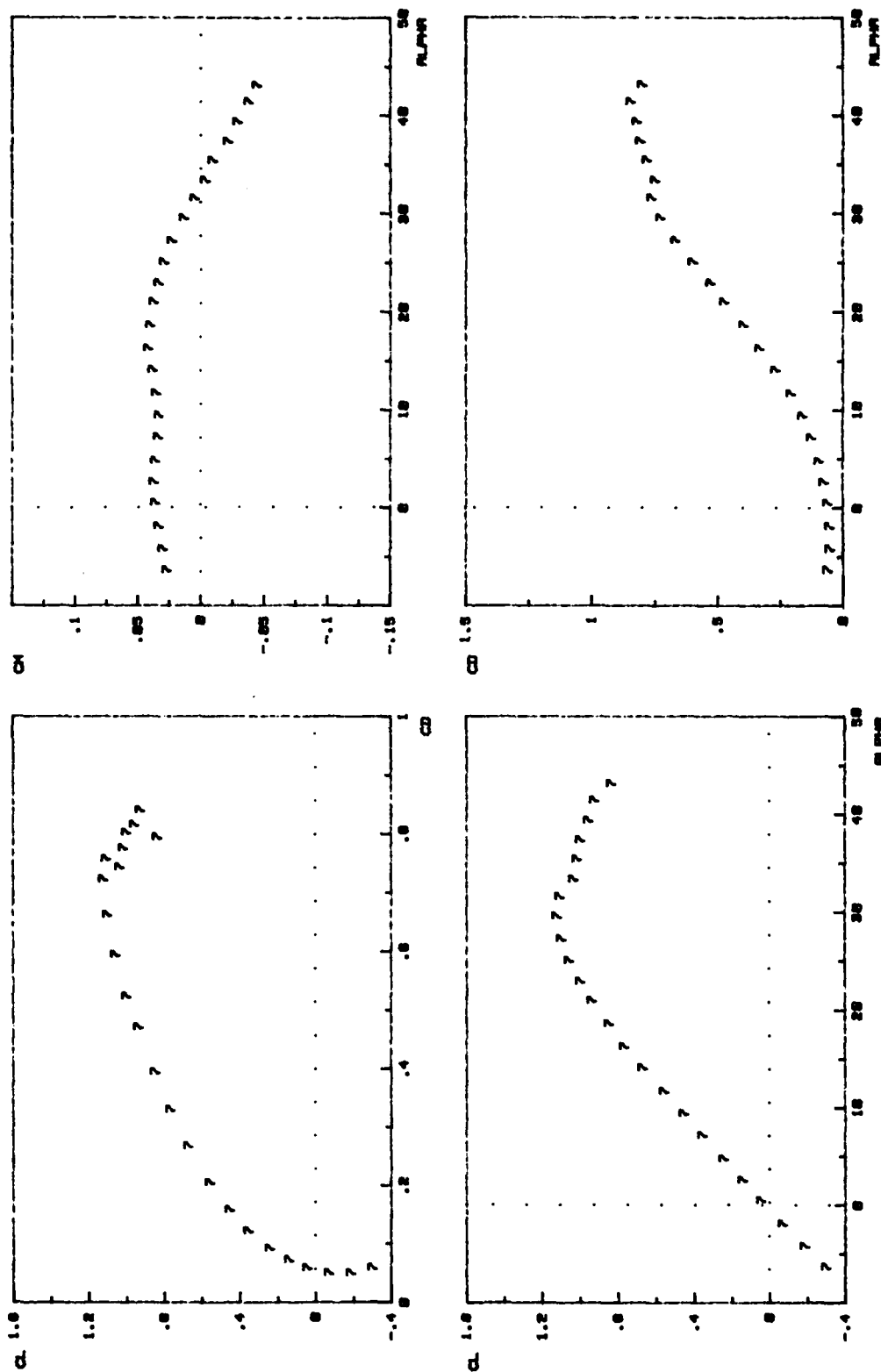
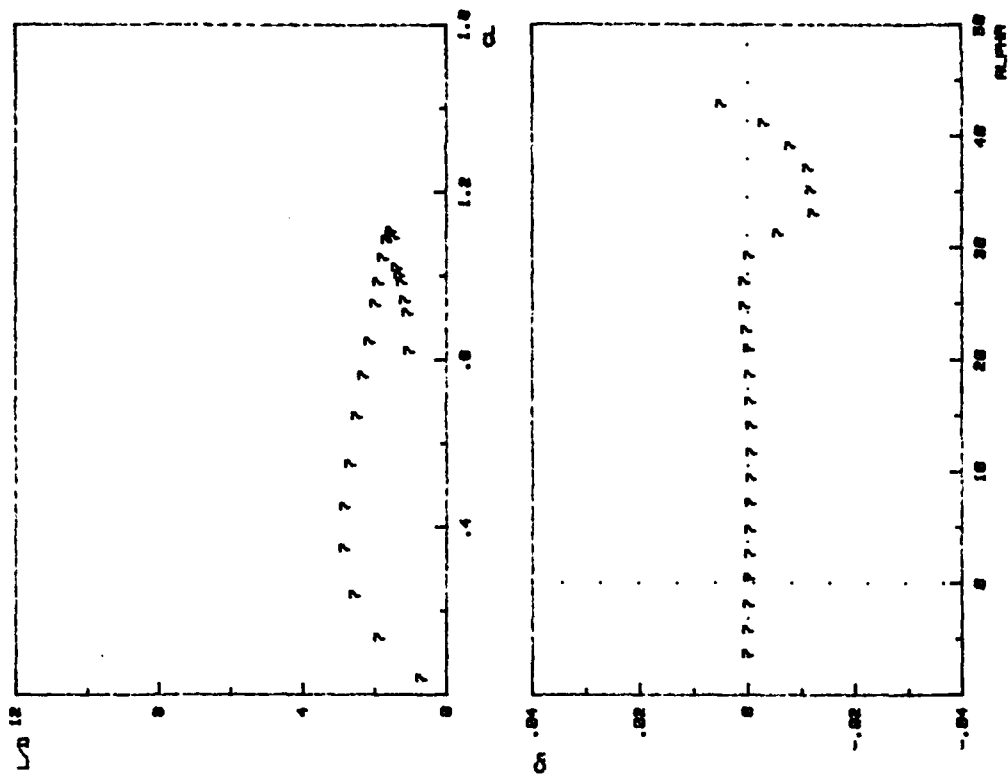


FIG. C-15. F7 (MODIFIED GOTHIC II)





F7 (MODIFIED GOTHIC II)

FIG. C-15.

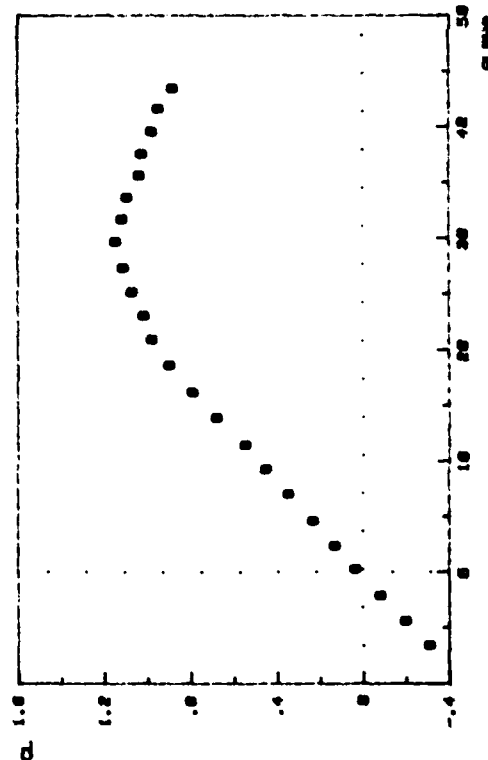
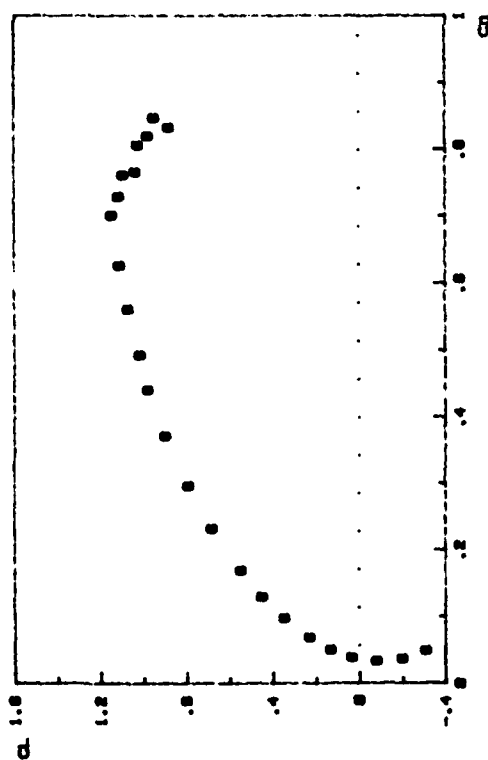
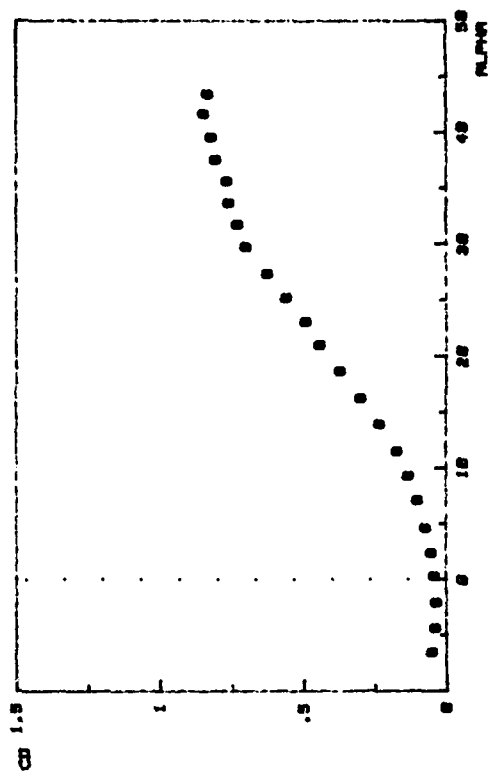
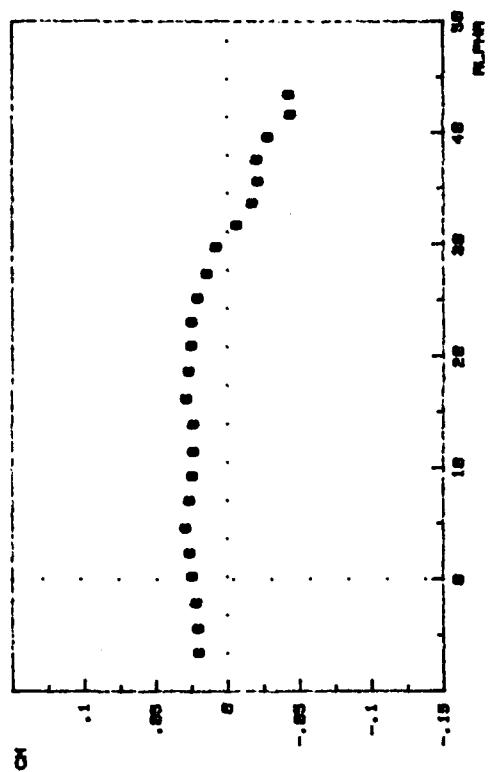


FIG. C-16.

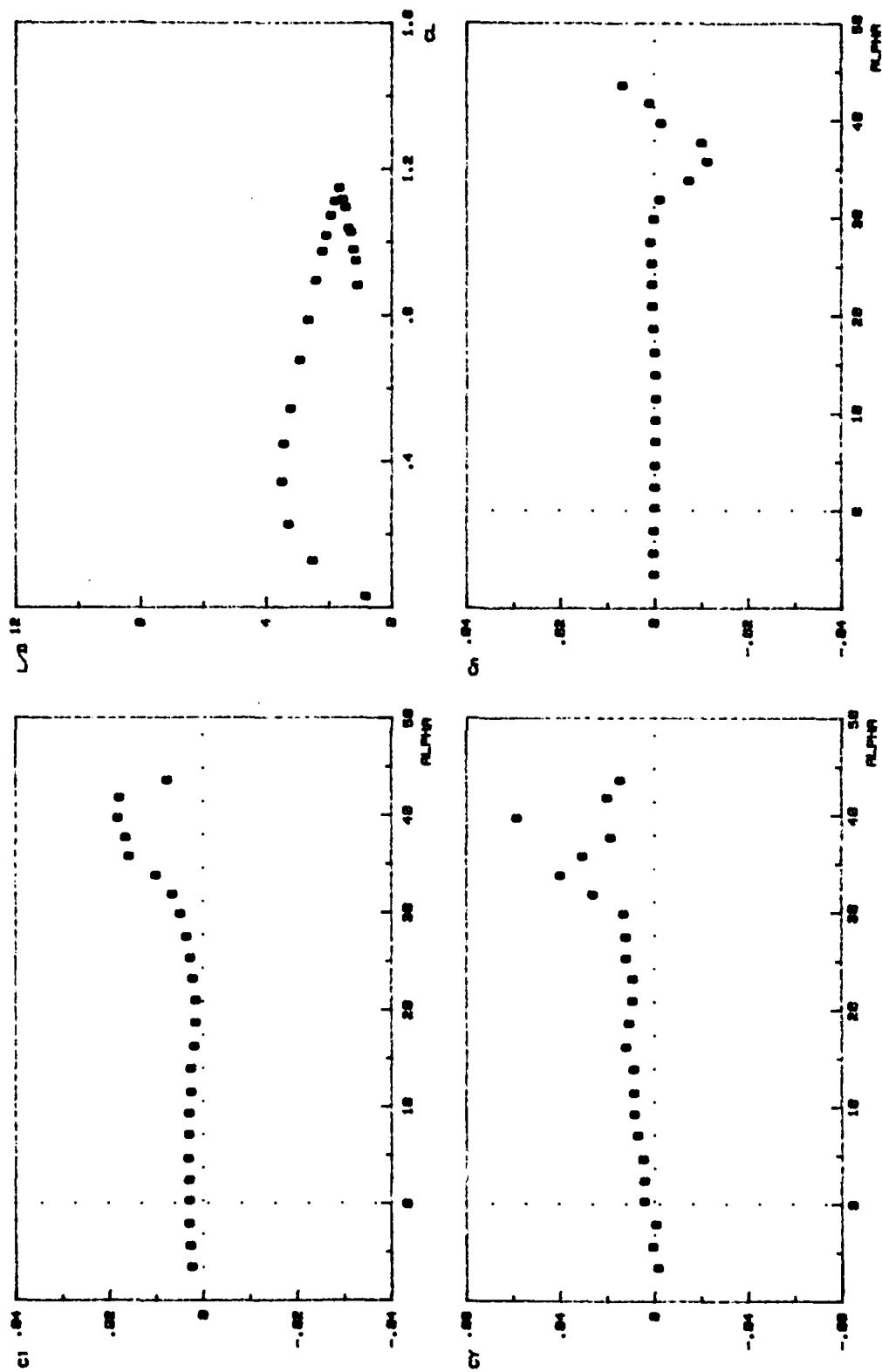


FIG. C-16.

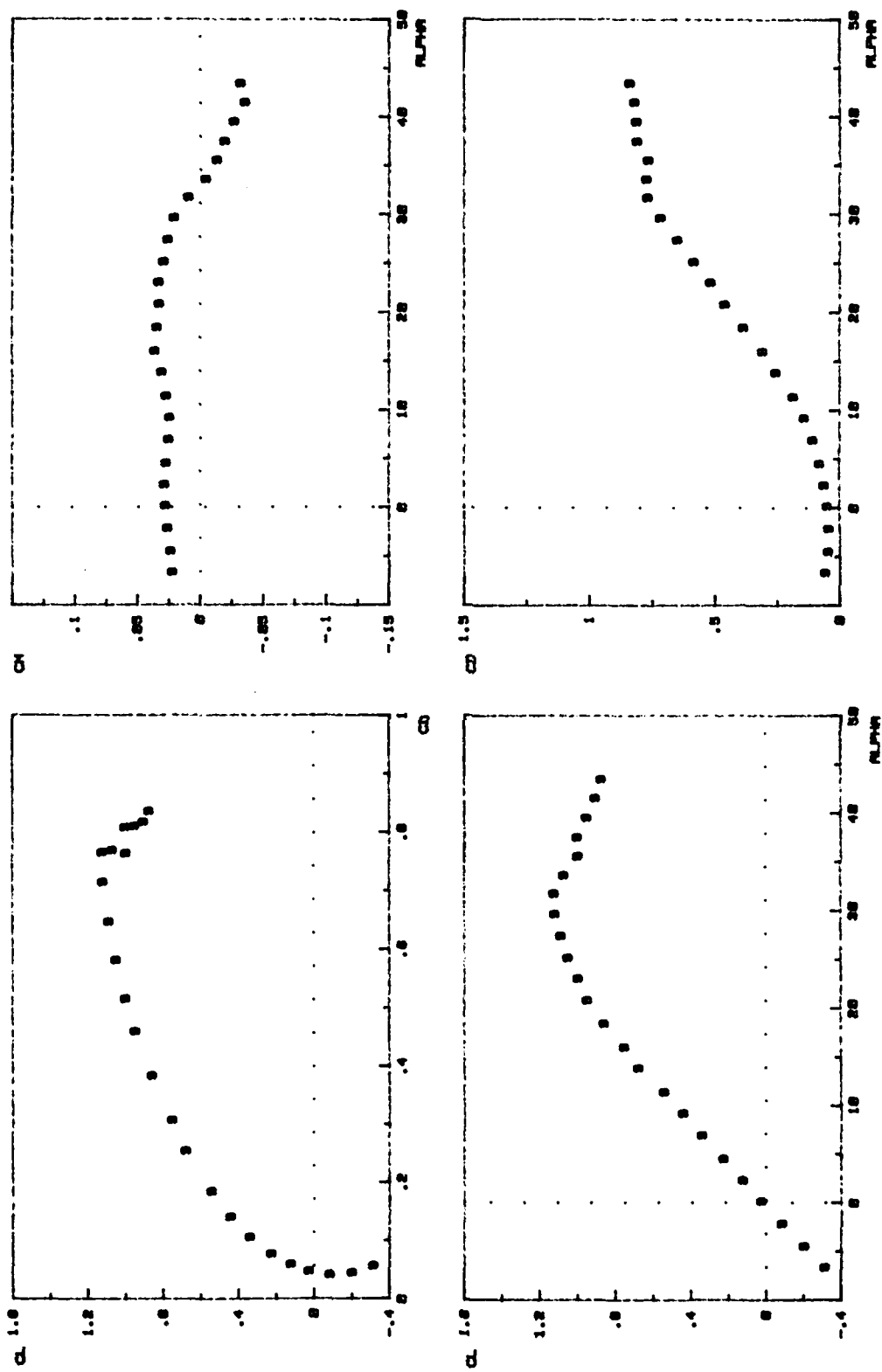


FIG. C-17.

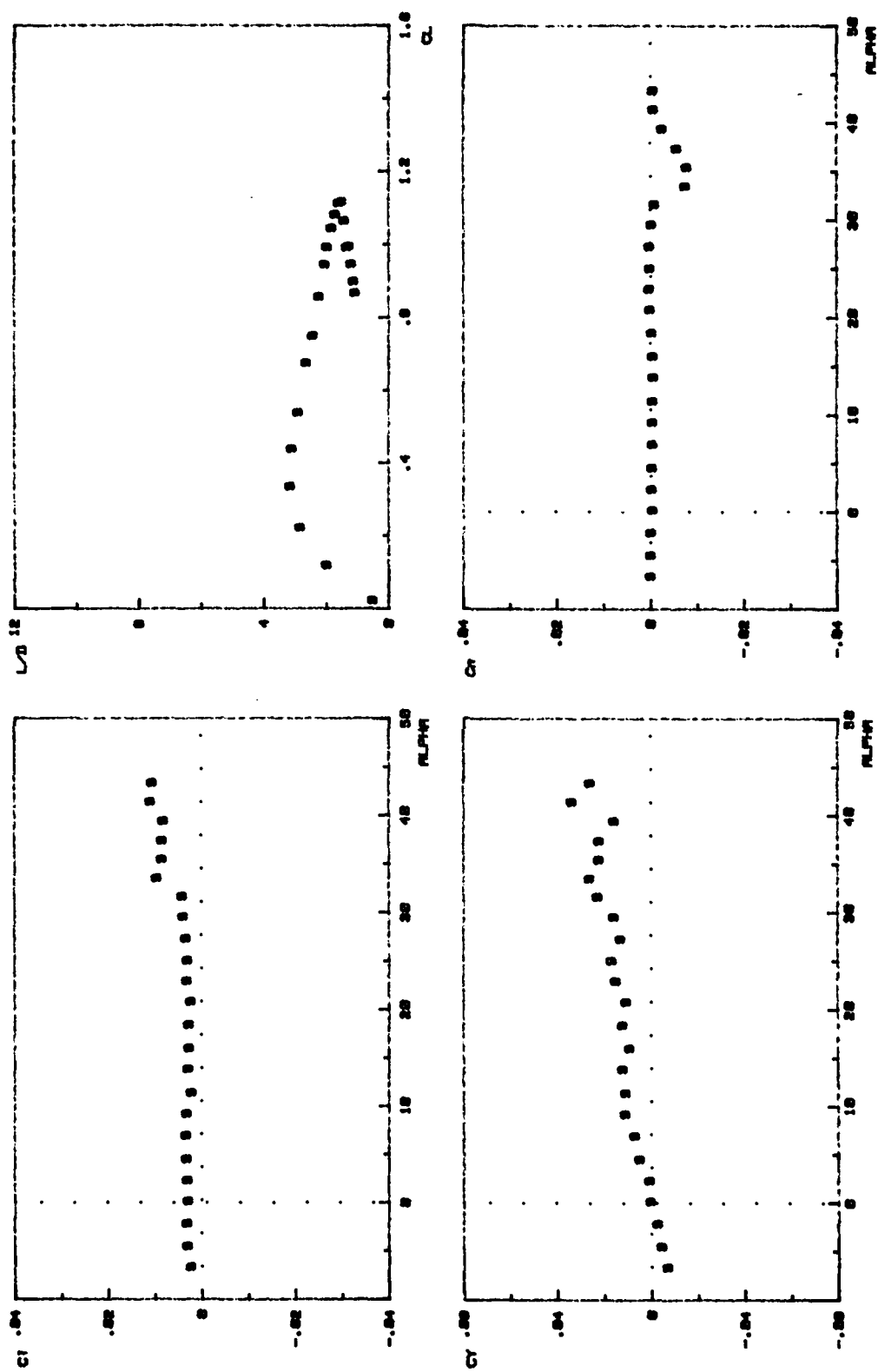


FIG. C-17.

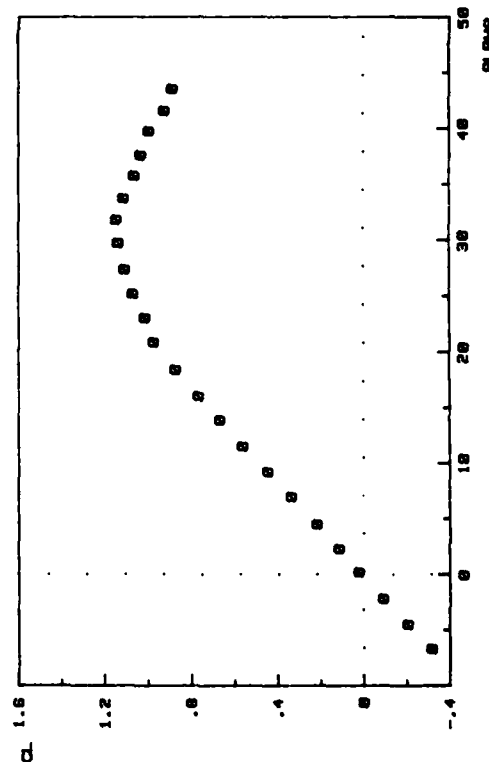
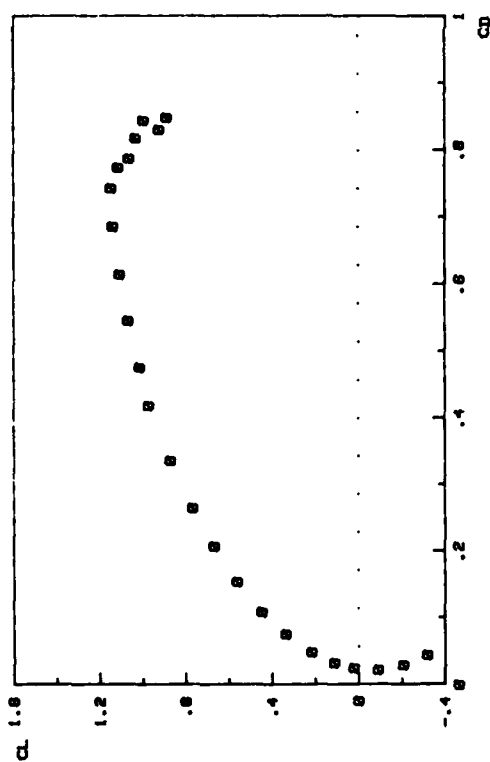
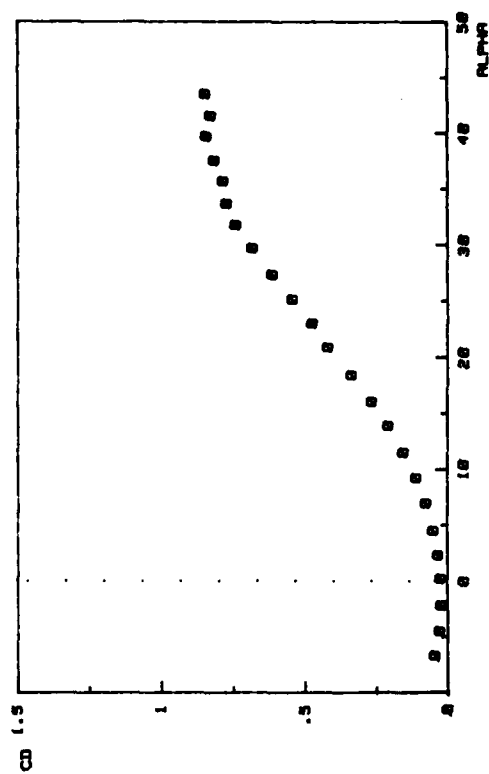
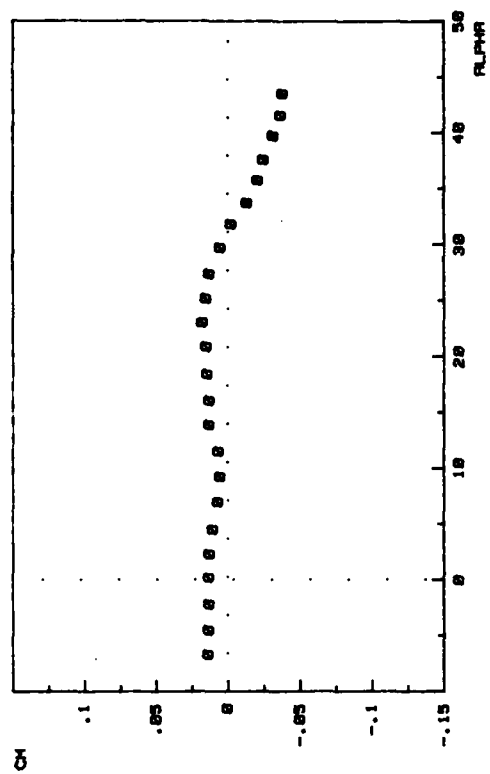


FIG. C-18.

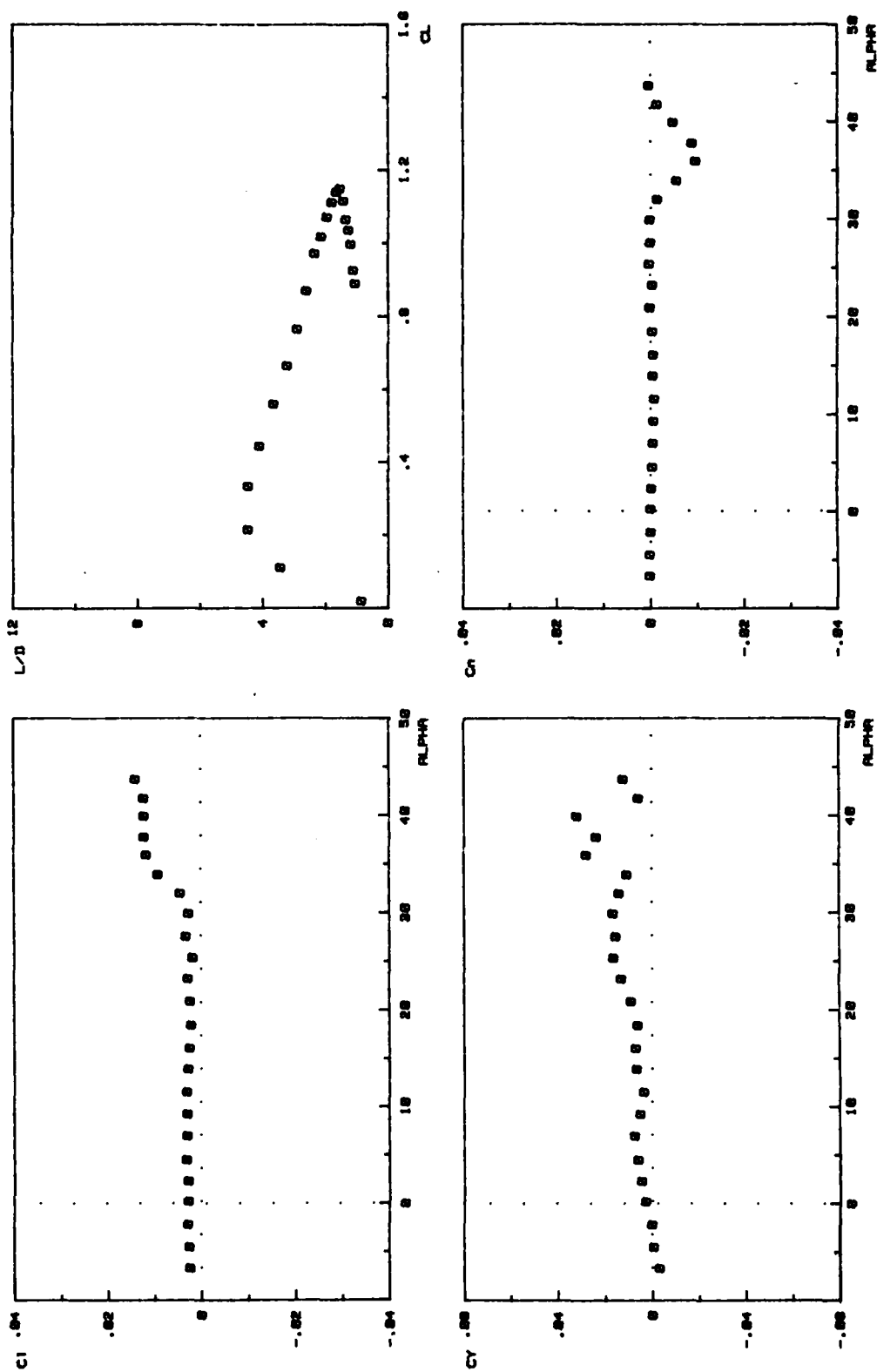


FIG. C-18.

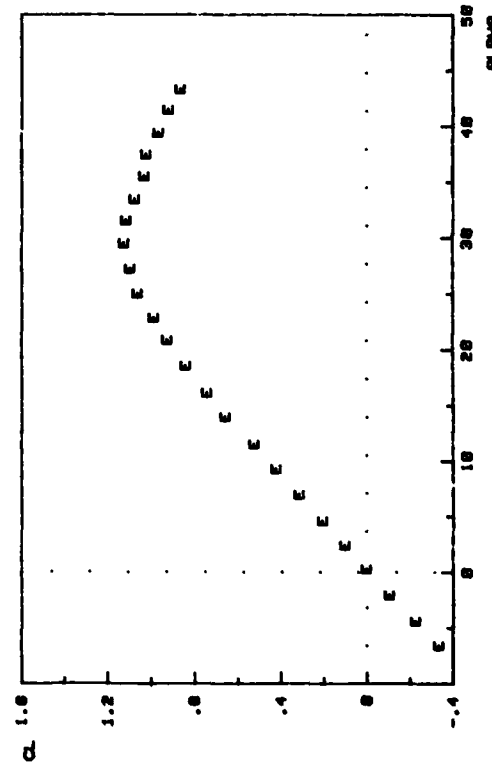
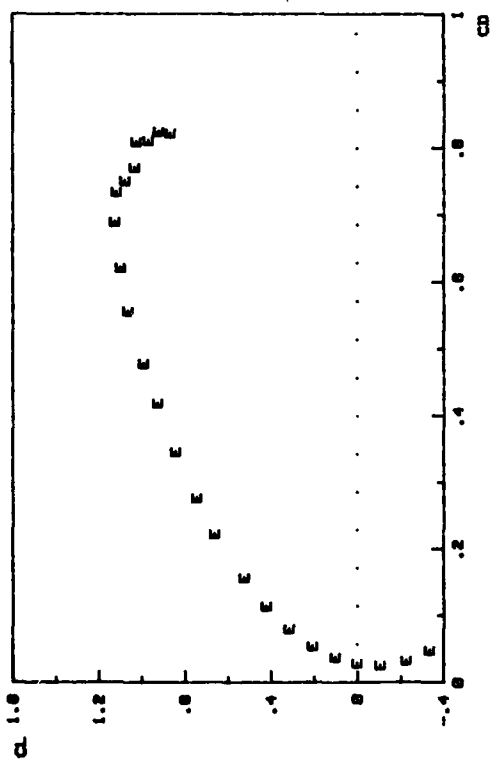
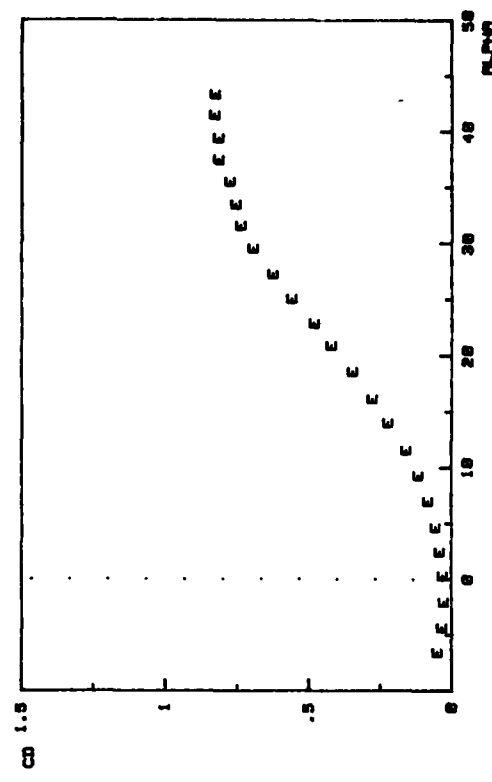
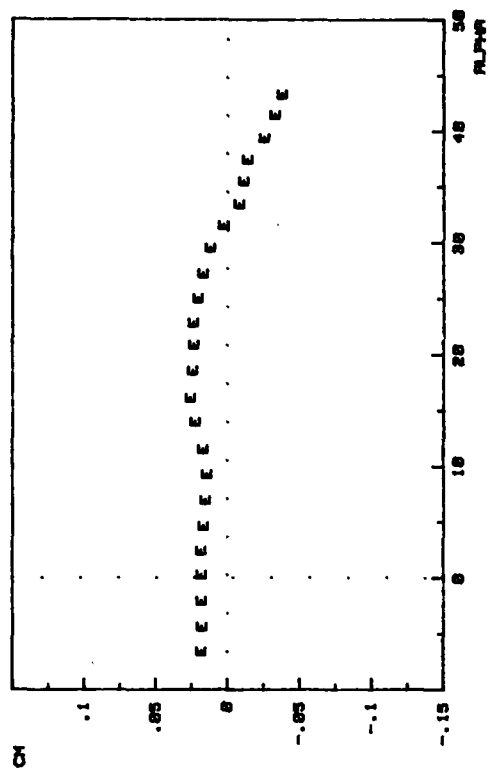


FIG. C-19.



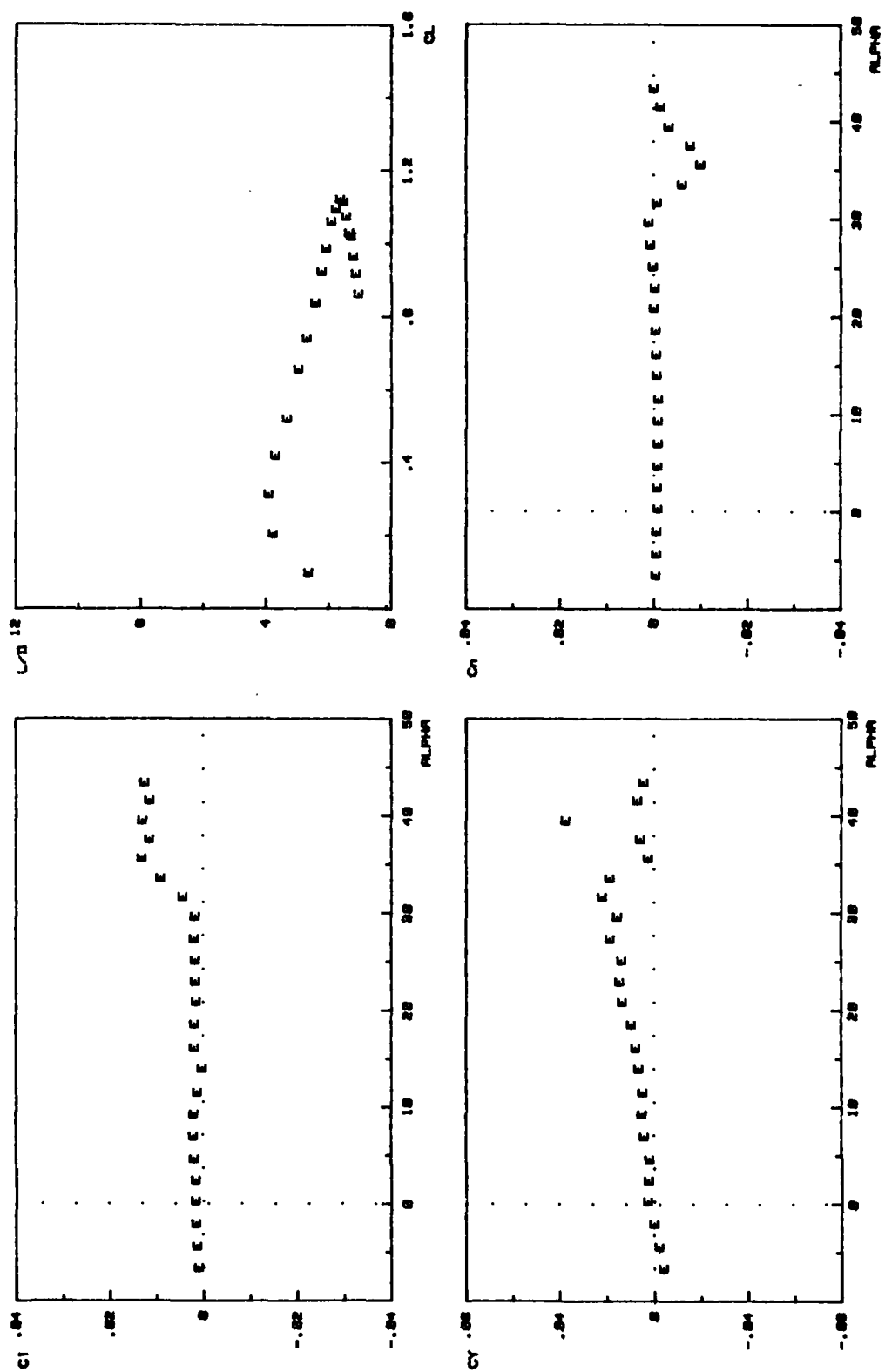


FIG. C-19.

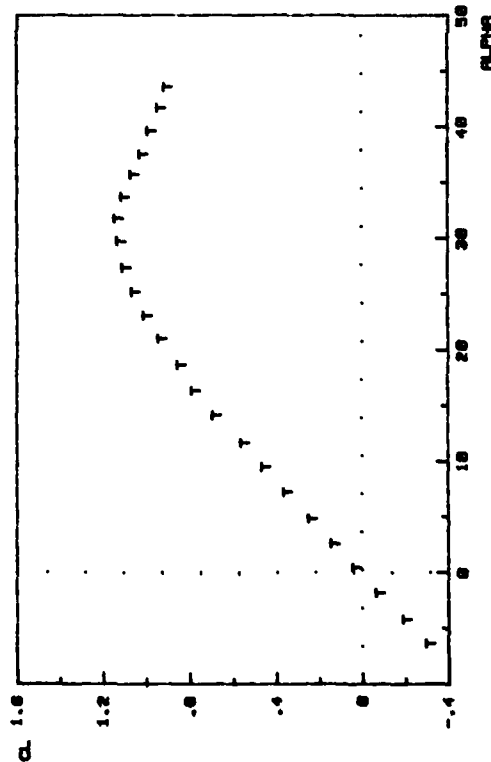
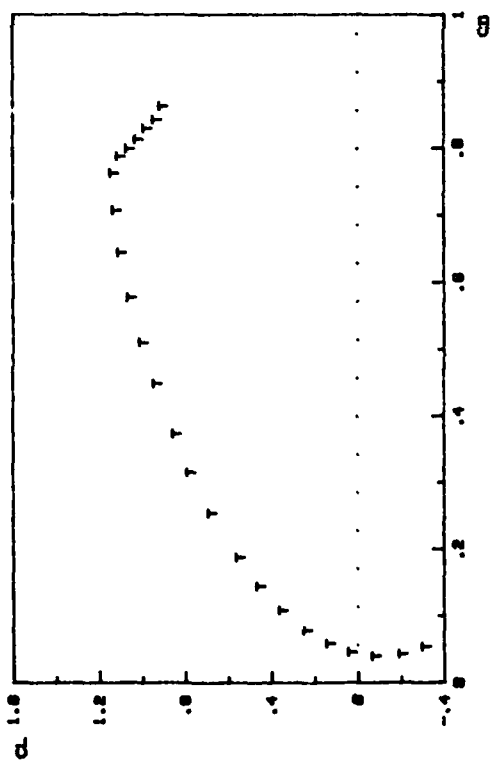
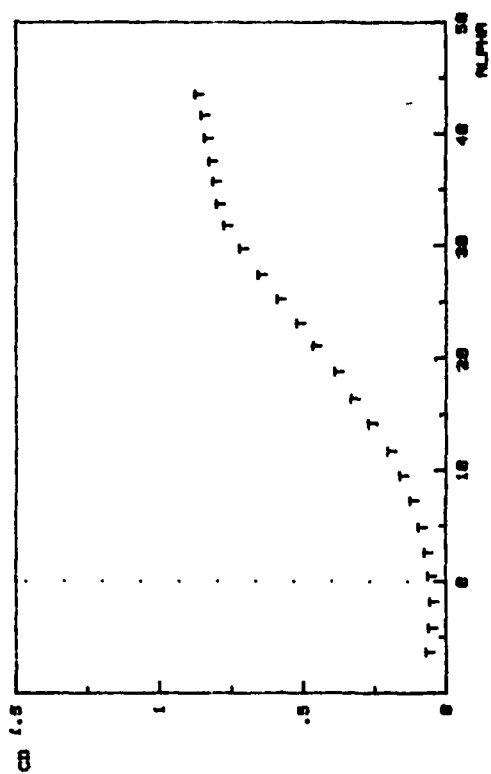
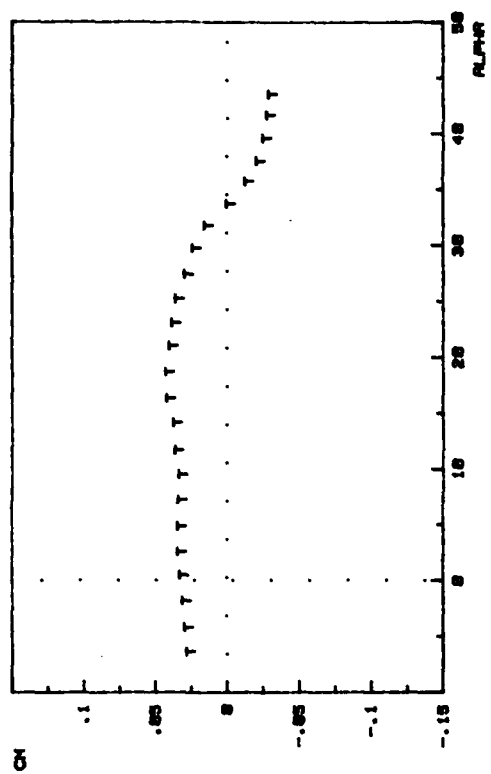


FIG. C-28.

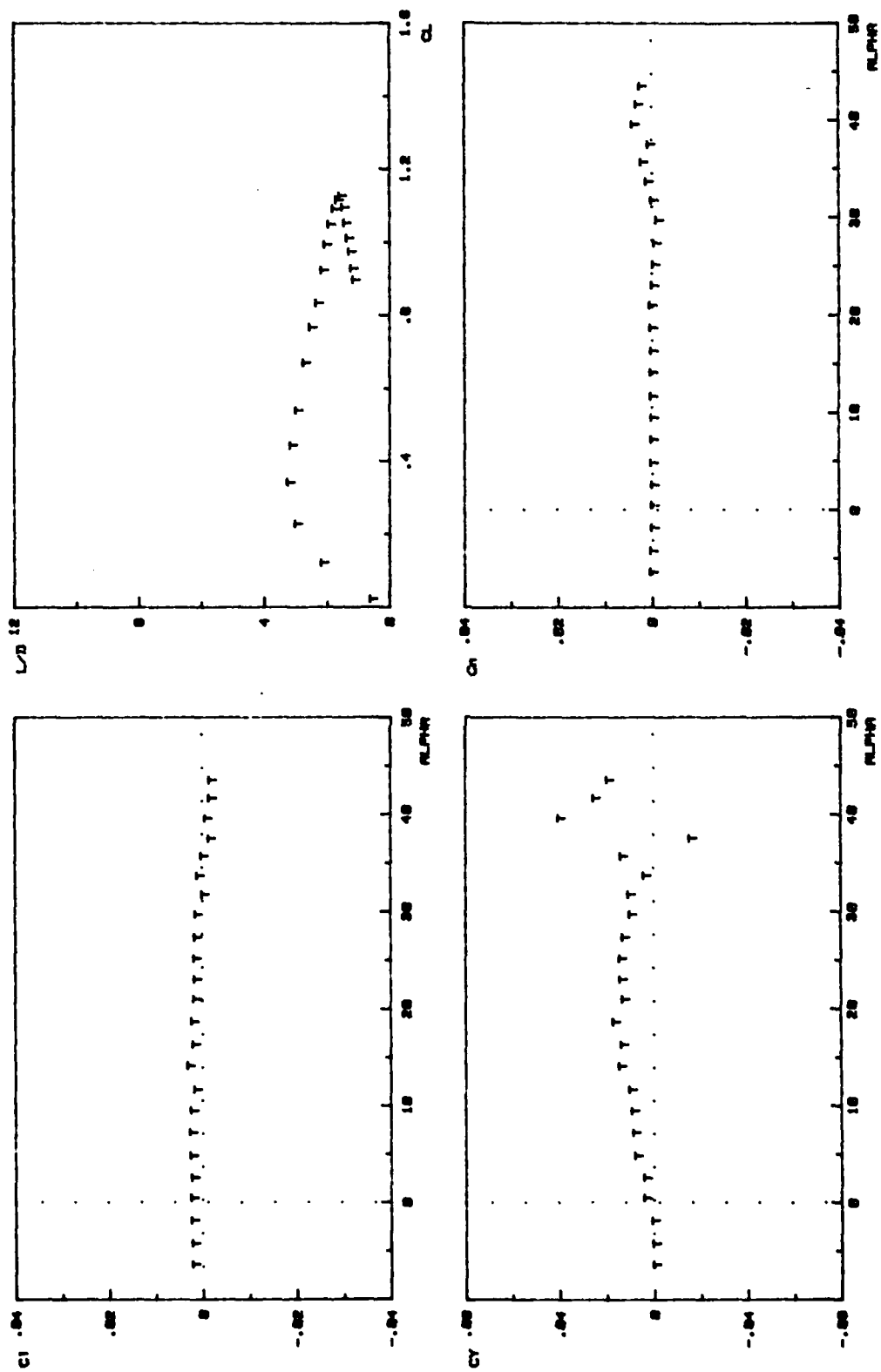
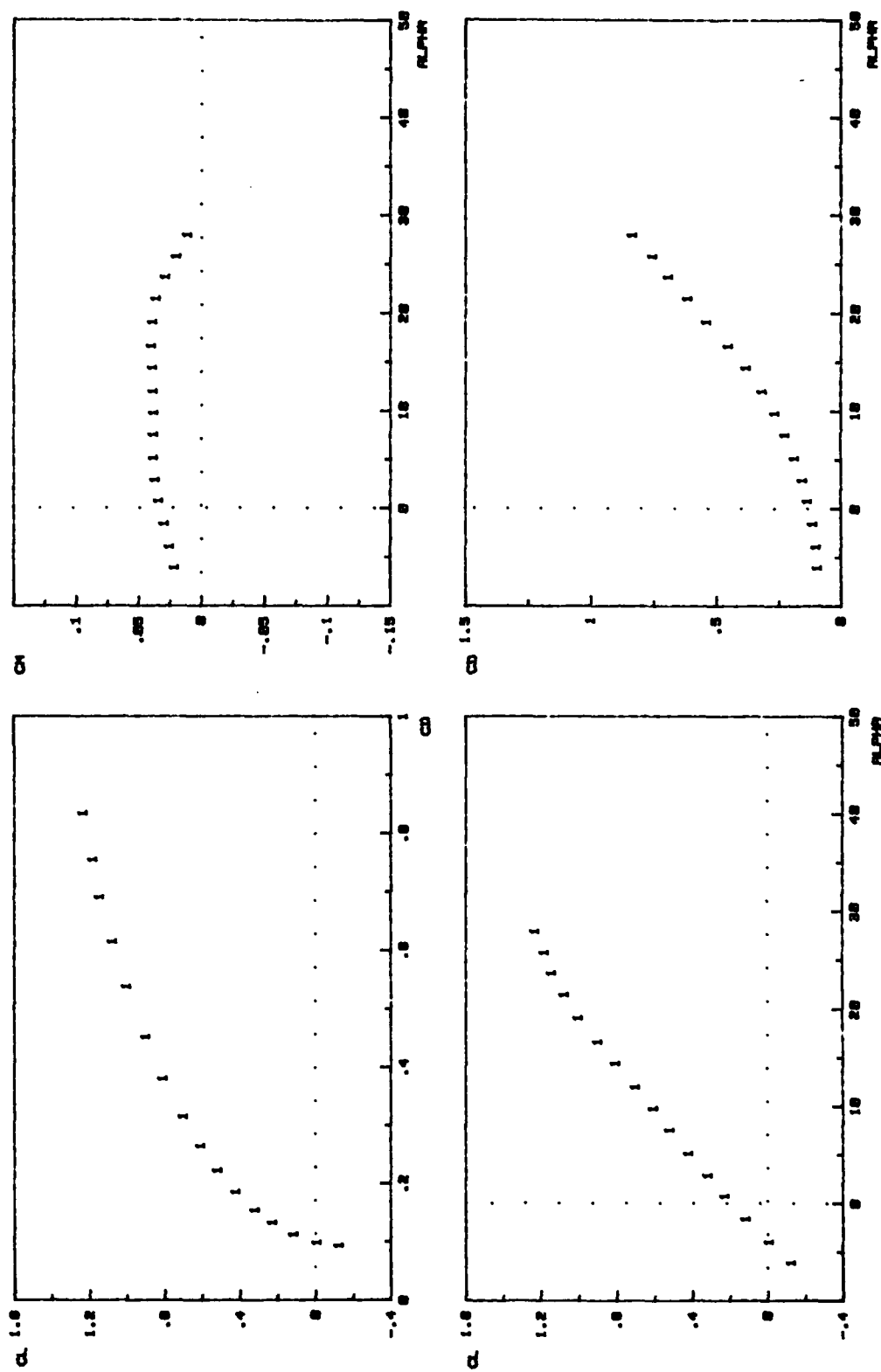


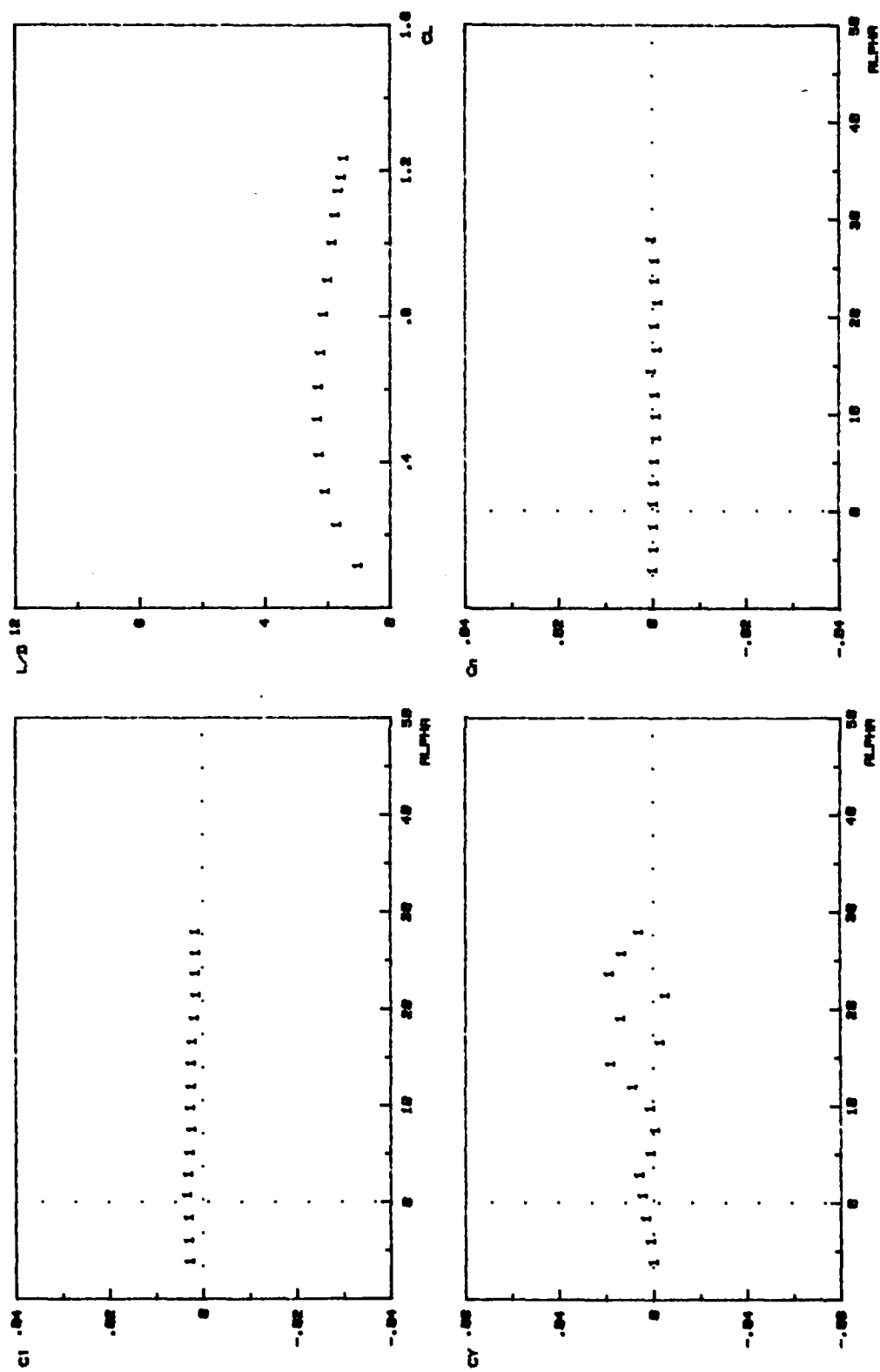
FIG. C-28.

FIG. 12 (DOUBLE GOTHIC II)



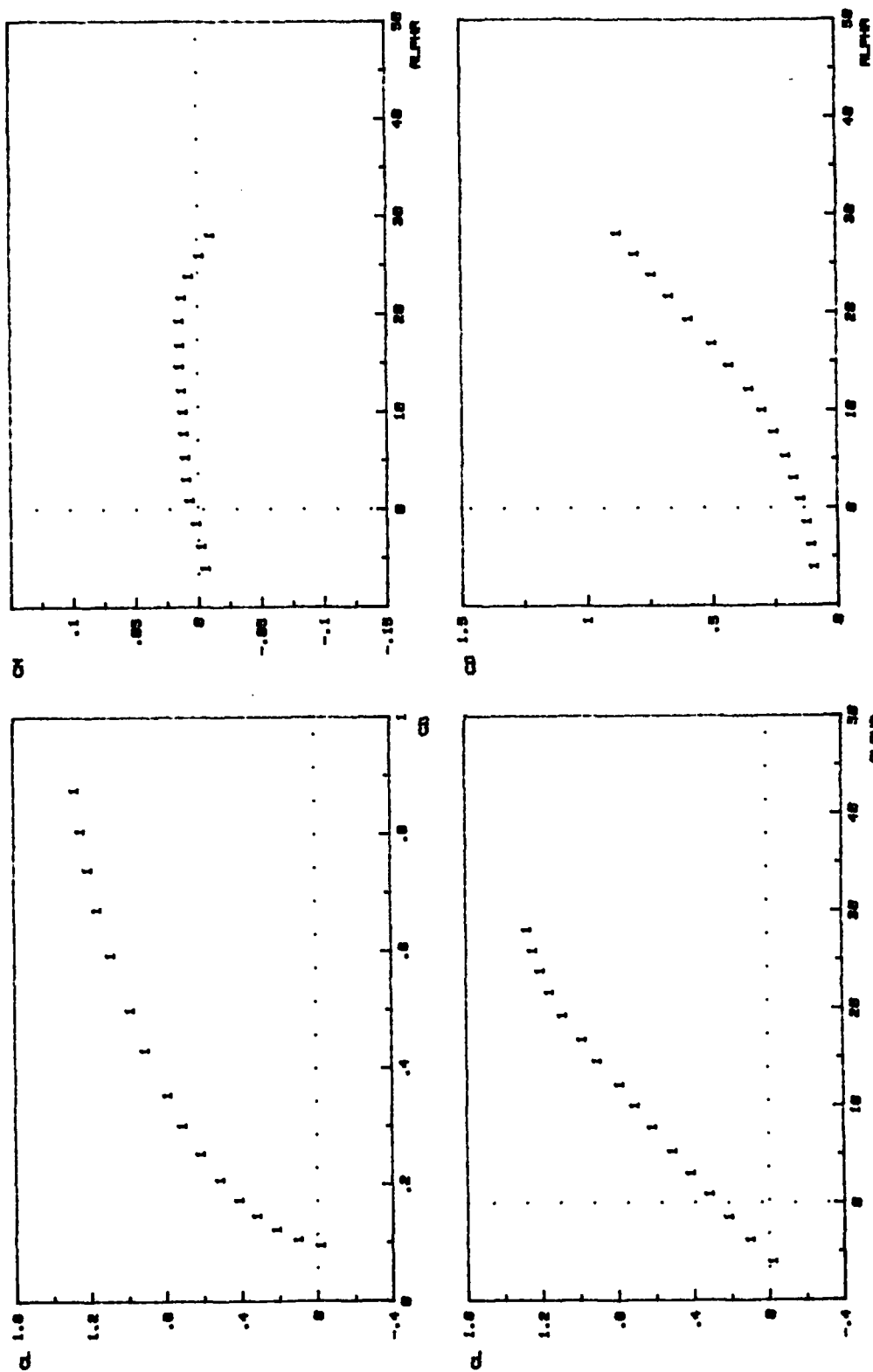
F1 (GOTHIC) @ 10 deg FLAP

FIG. C-21.



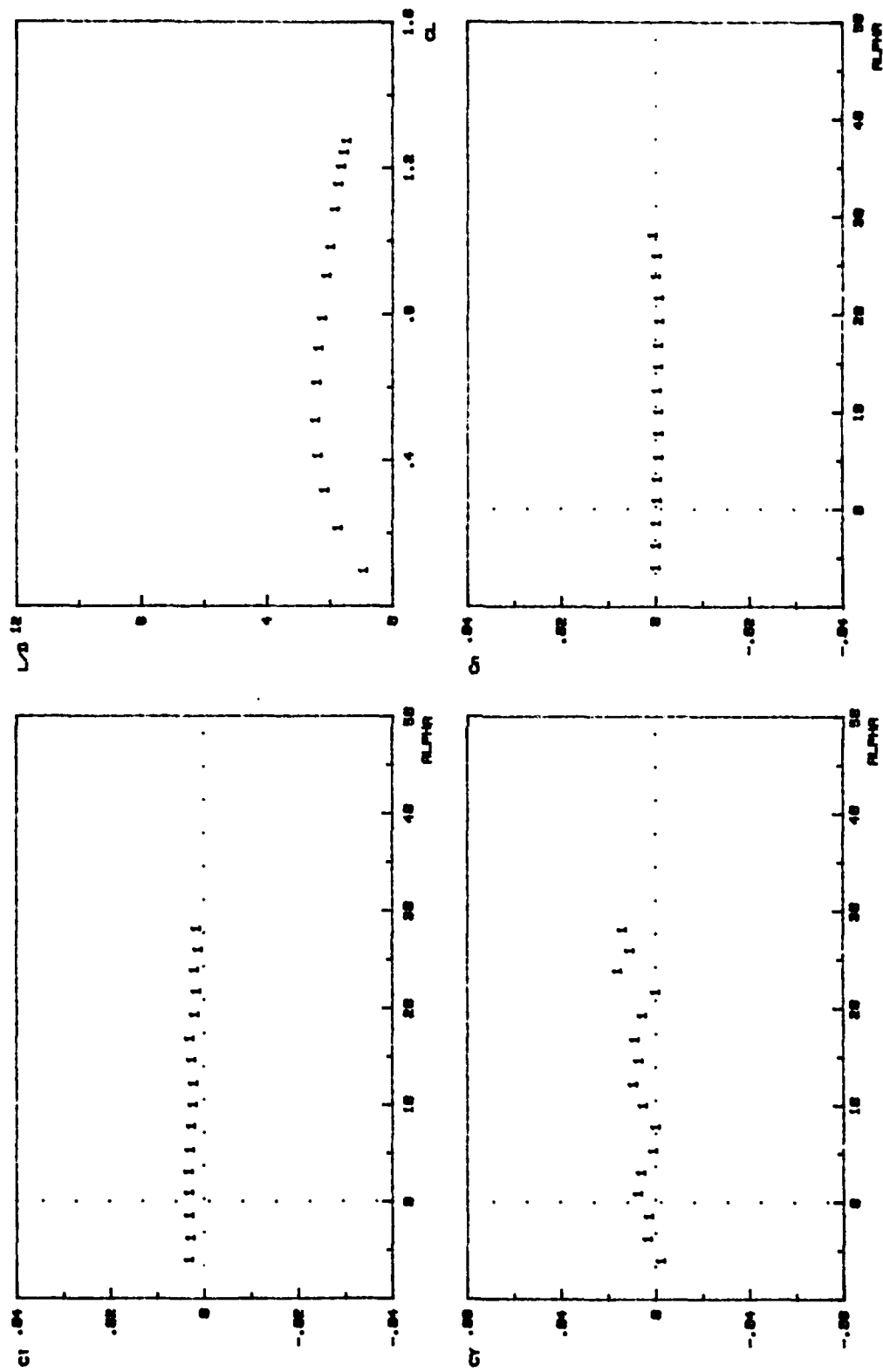
F1 (GOTHIC) @ 18 deg FLAP

FIG. C-21.



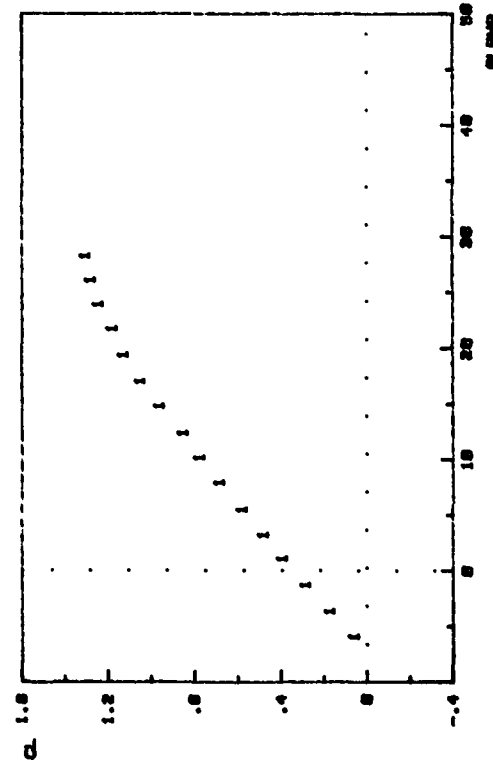
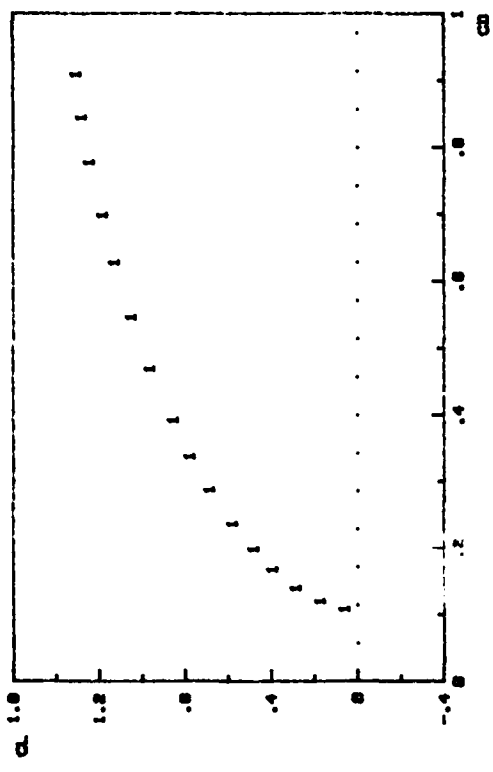
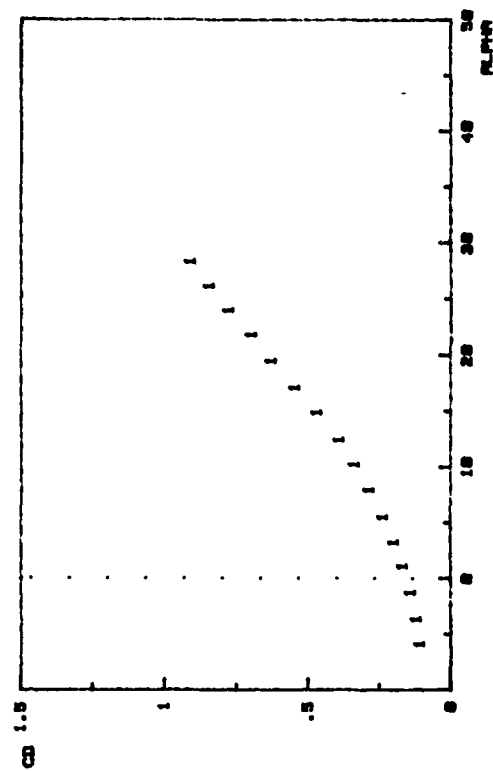
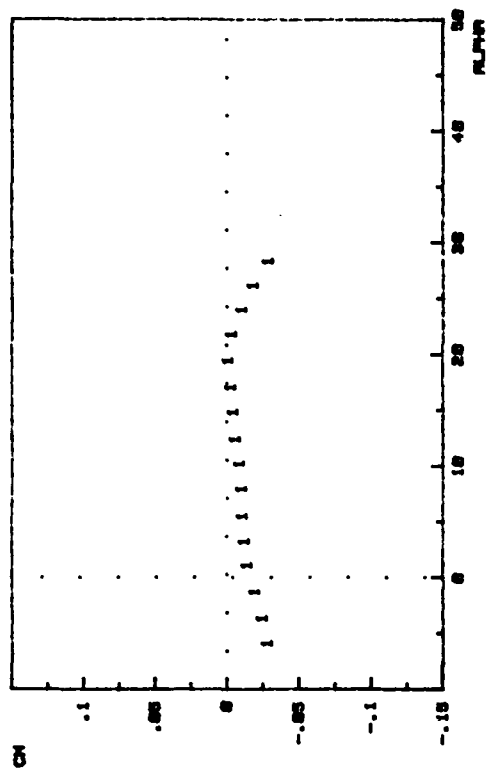
F1 (GOTHIC) @ 28 deg FLAP

FIG. C-22.



F1 (GOTHIC) @ 28 deg FLAP

FIG. C-22.



F1 (GOTHIC) @ 38 deg FLAP

FIG. C-23.



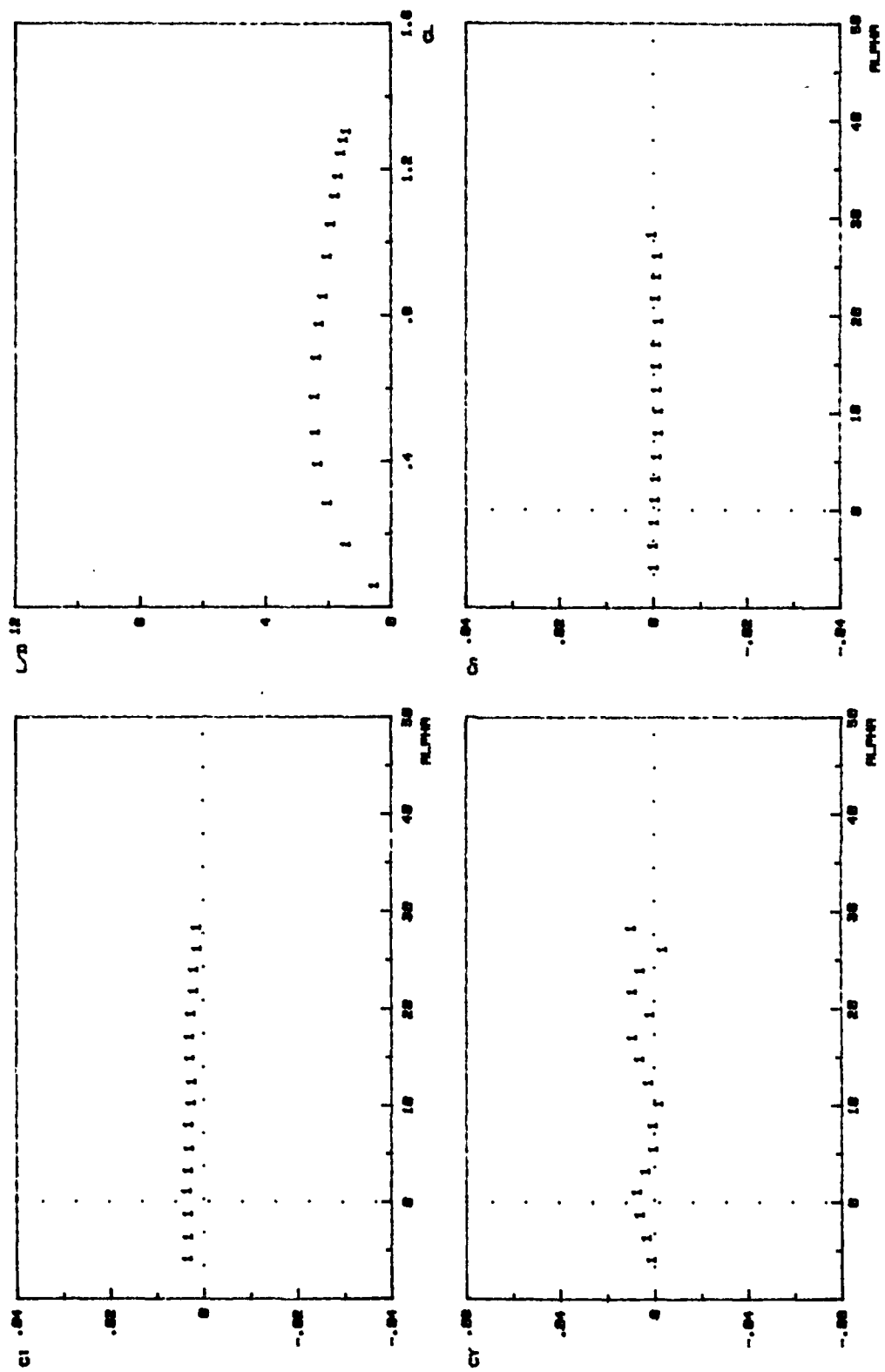
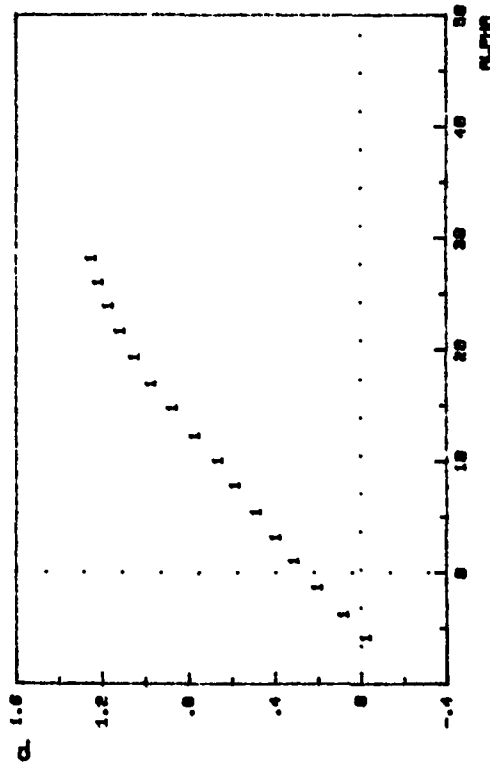
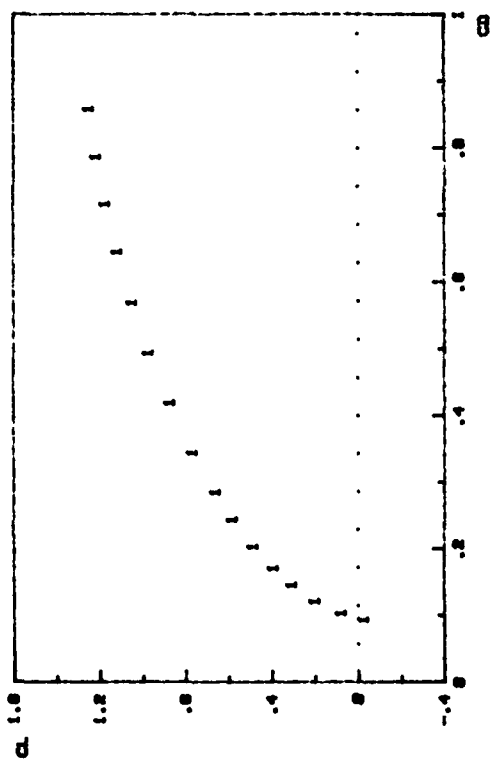
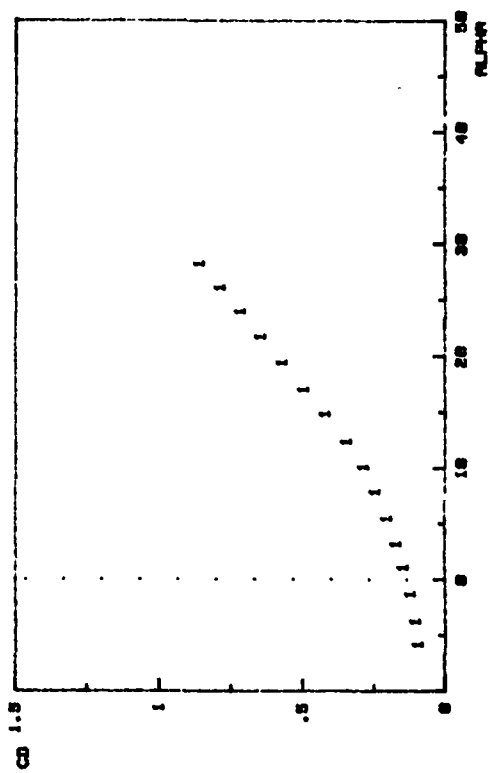
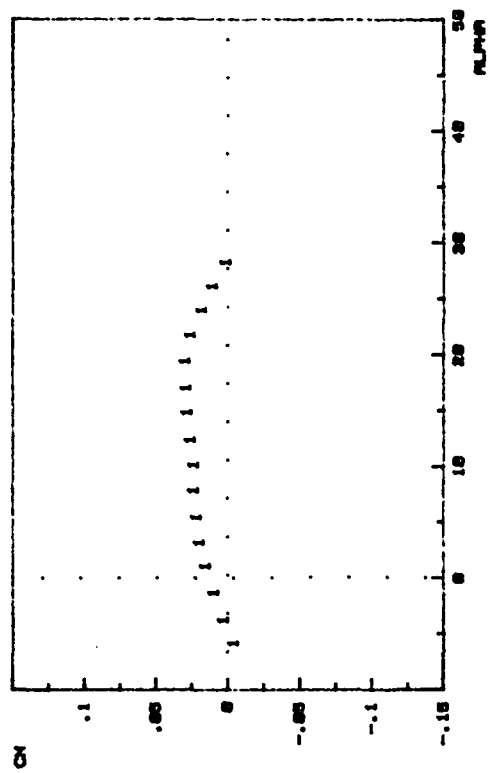
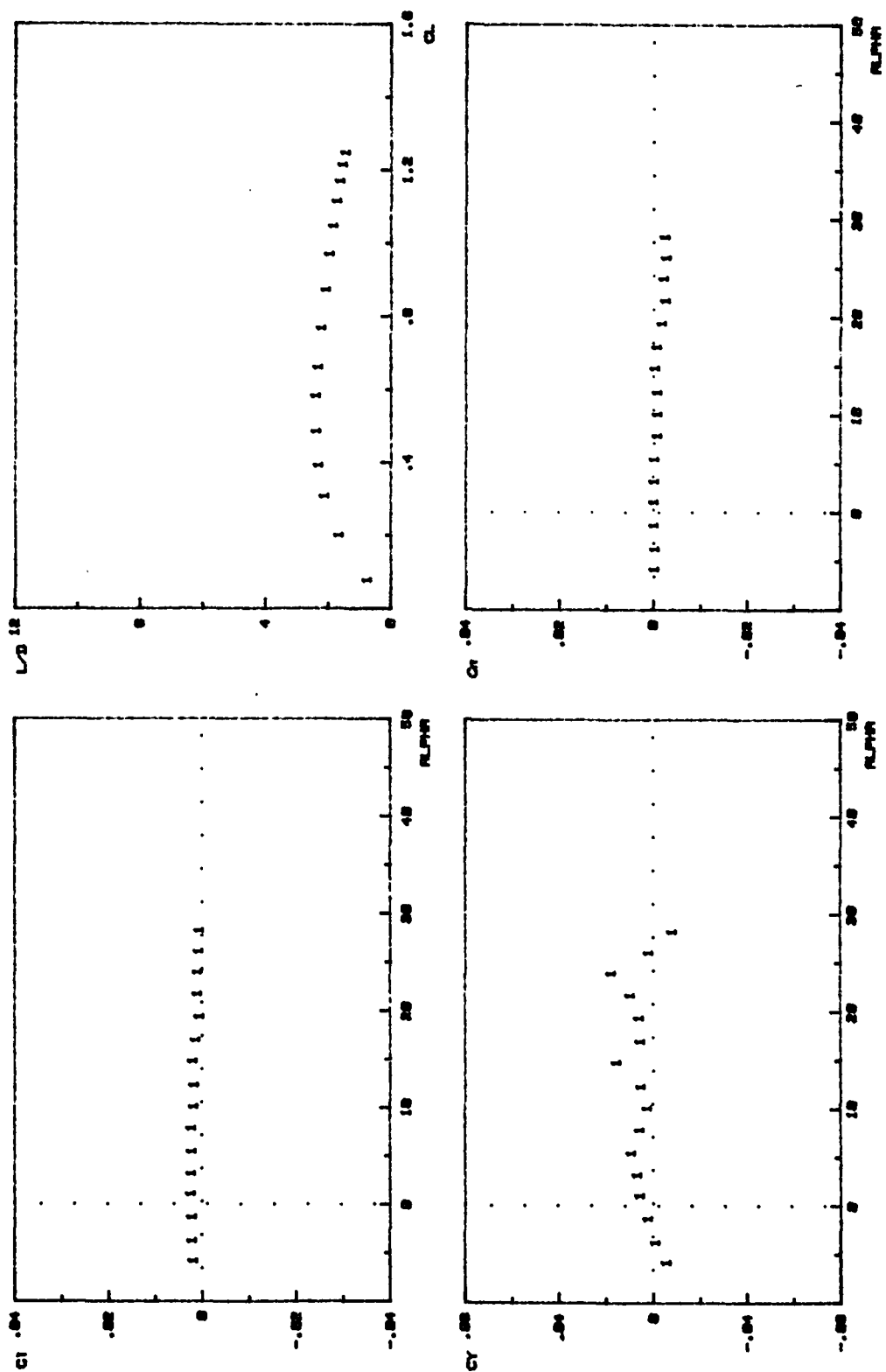


FIG. C-23.



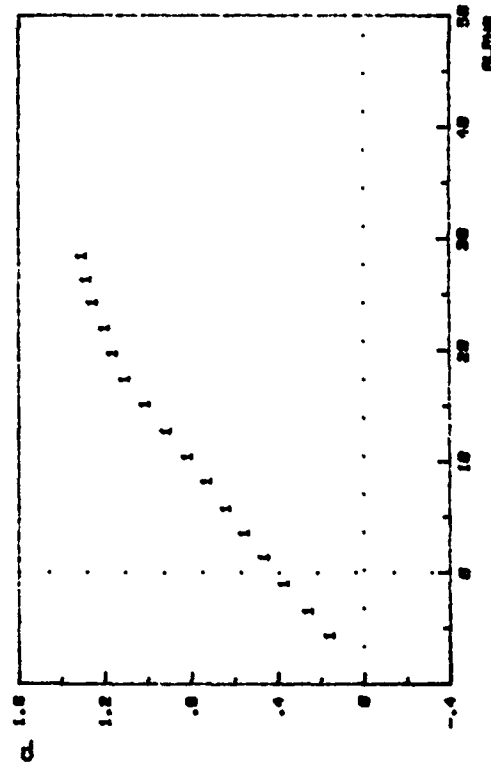
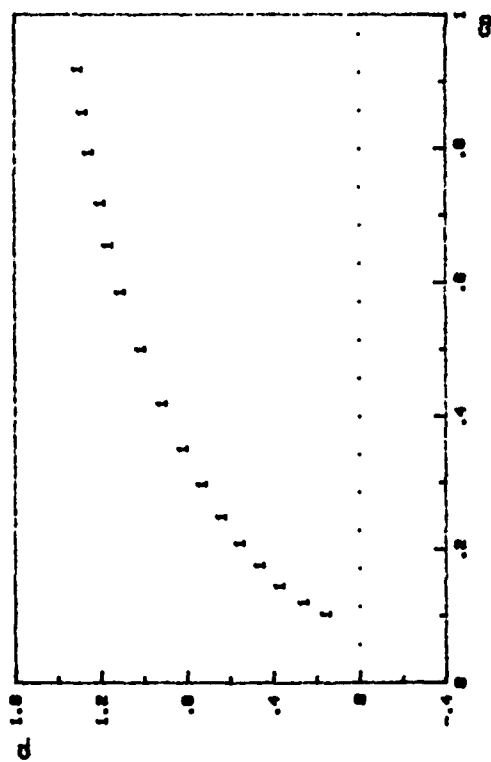
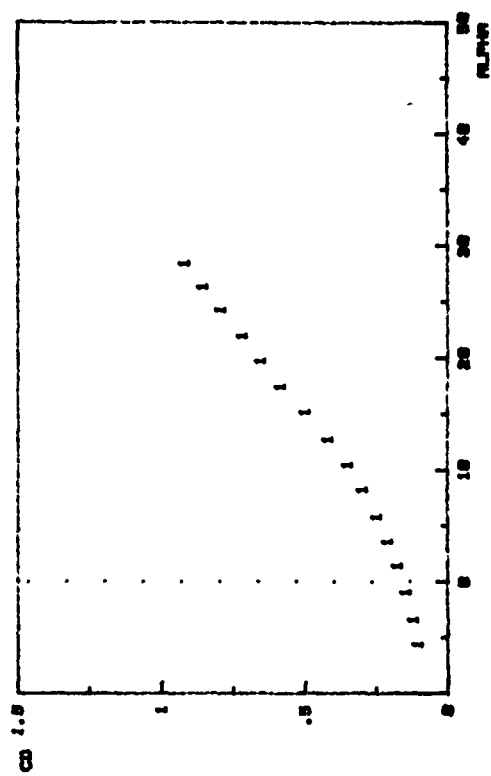
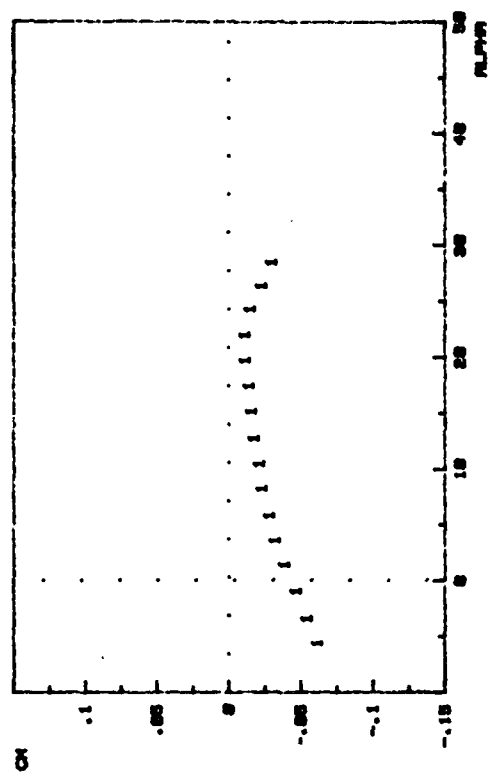
F1 (GOTHIC) • 10 deg TWIN FLAP

FIG. C-24.



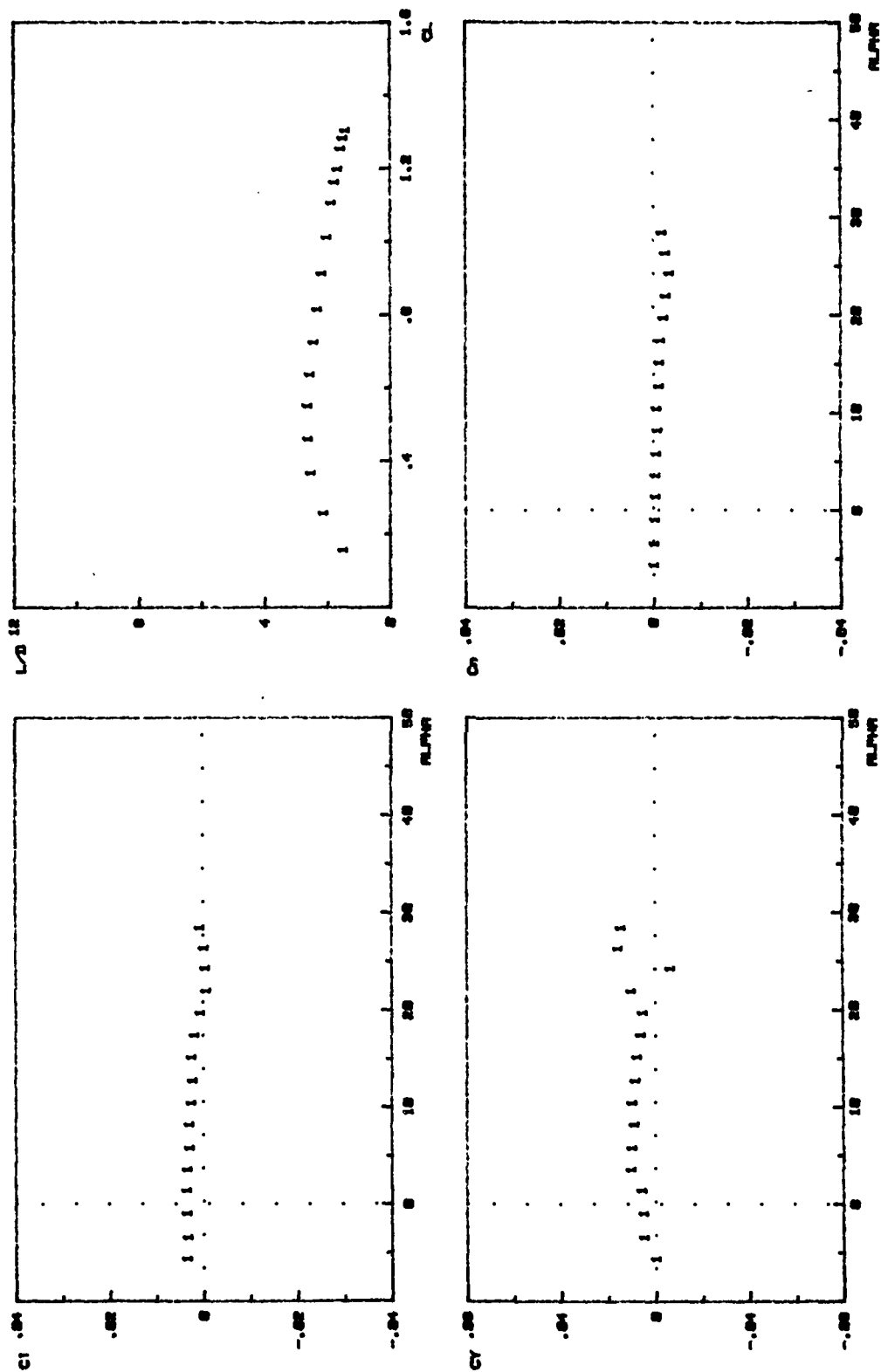
F1 (GOTHIC) @ 10 deg THIN FLAP

FIG. C-24.



F1 (GOTHIC) @ 20 deg TWIN FLAP

FIG. C-25.



F1 (GOTHIC) @ 20 deg TWIN FLAP

FIG. C-25.

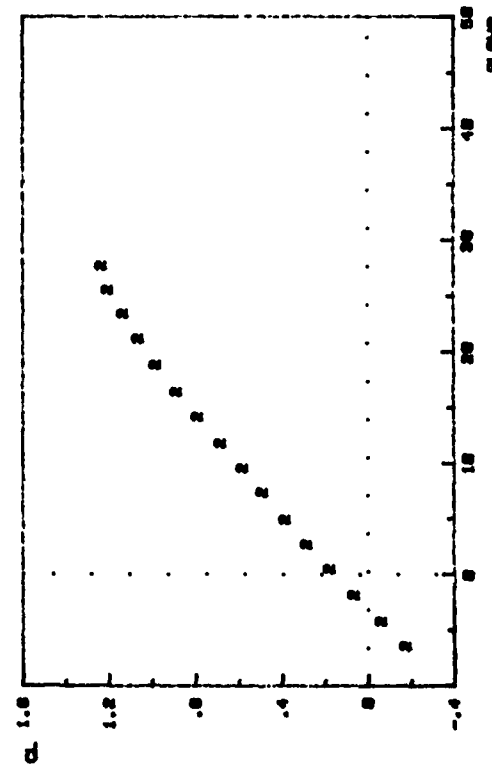
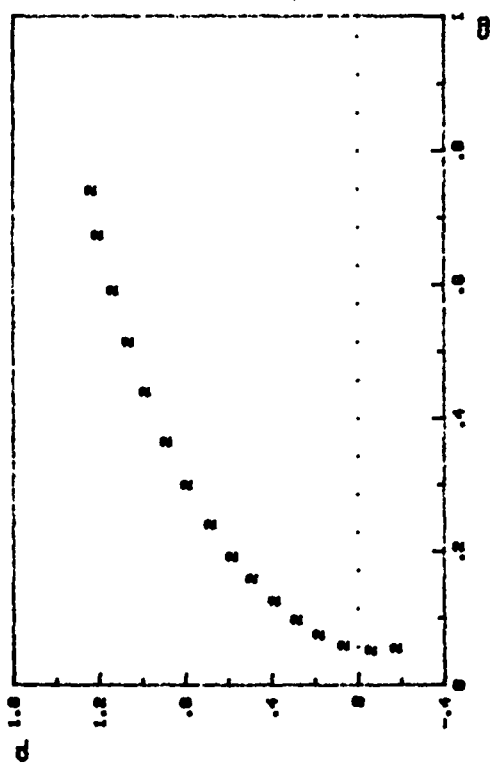
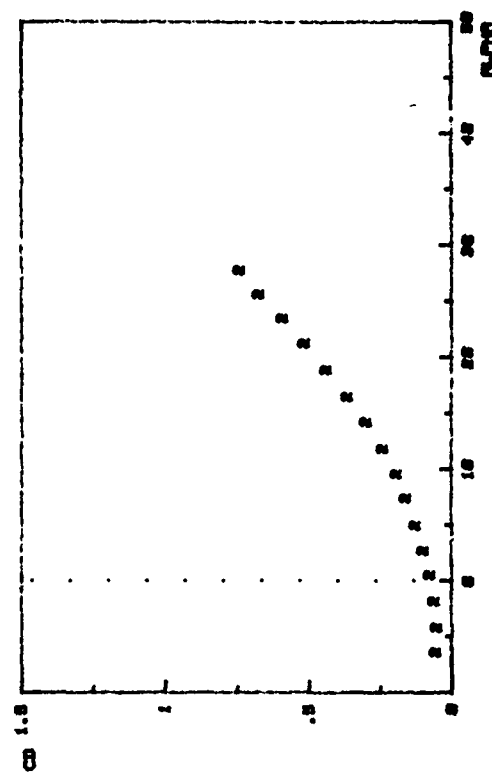
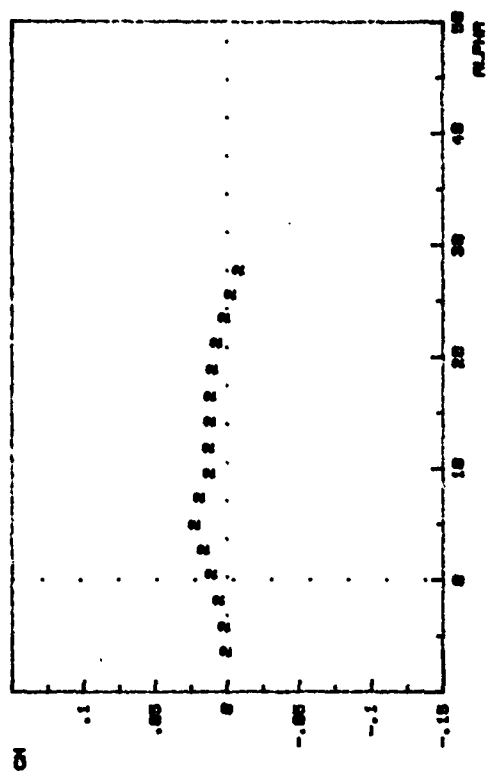


FIG. C-25.

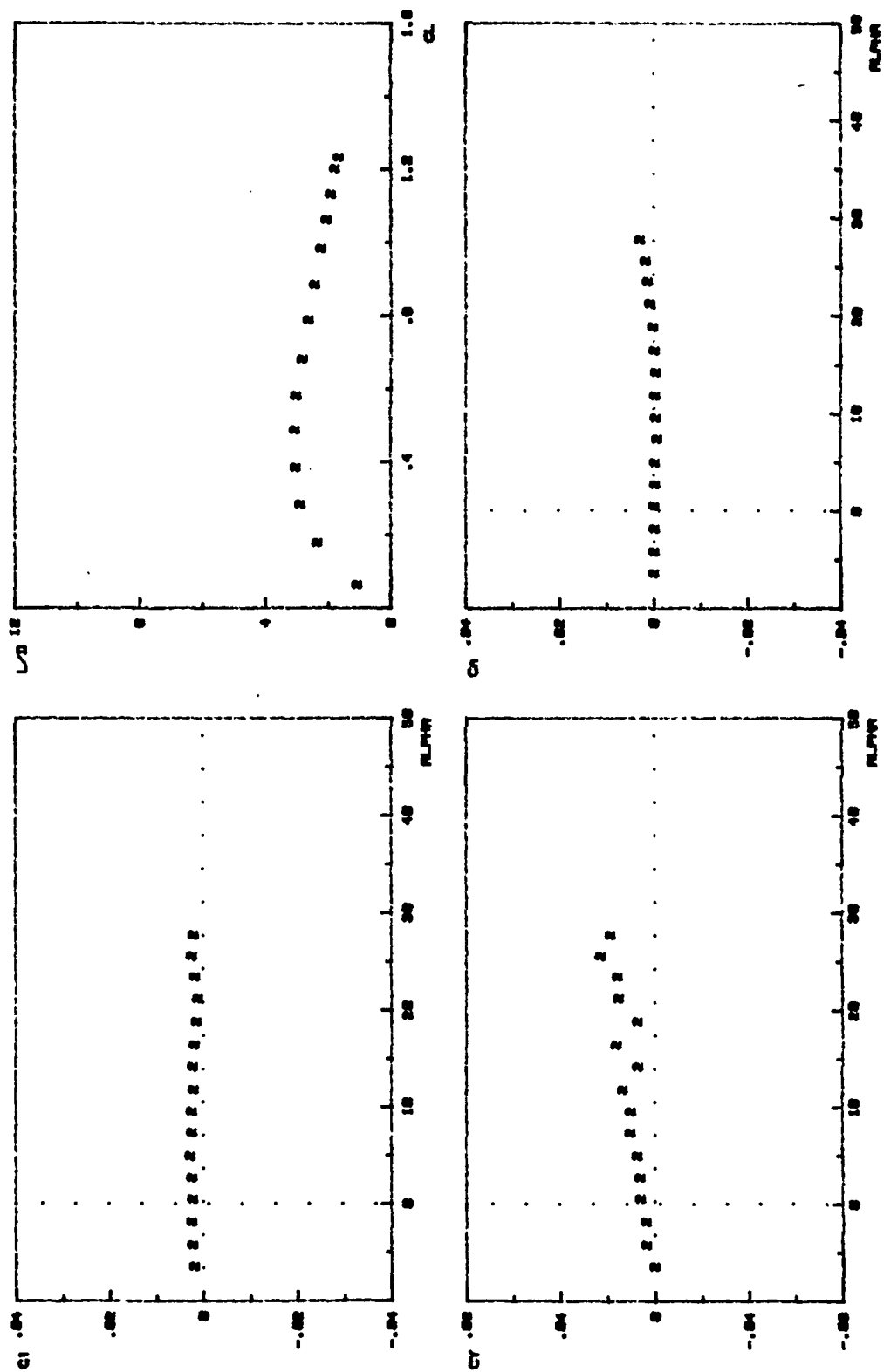


FIG. C-26.

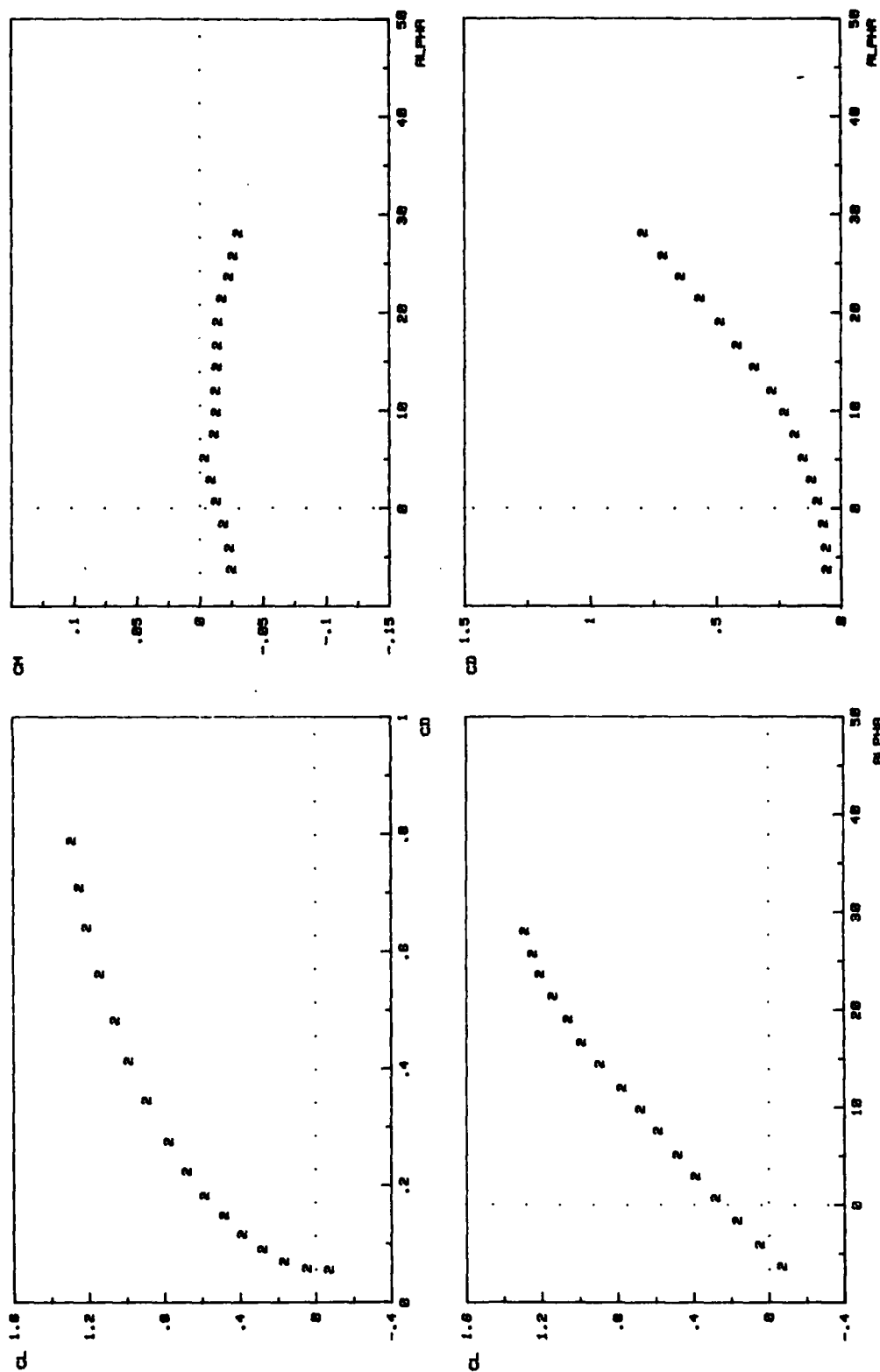
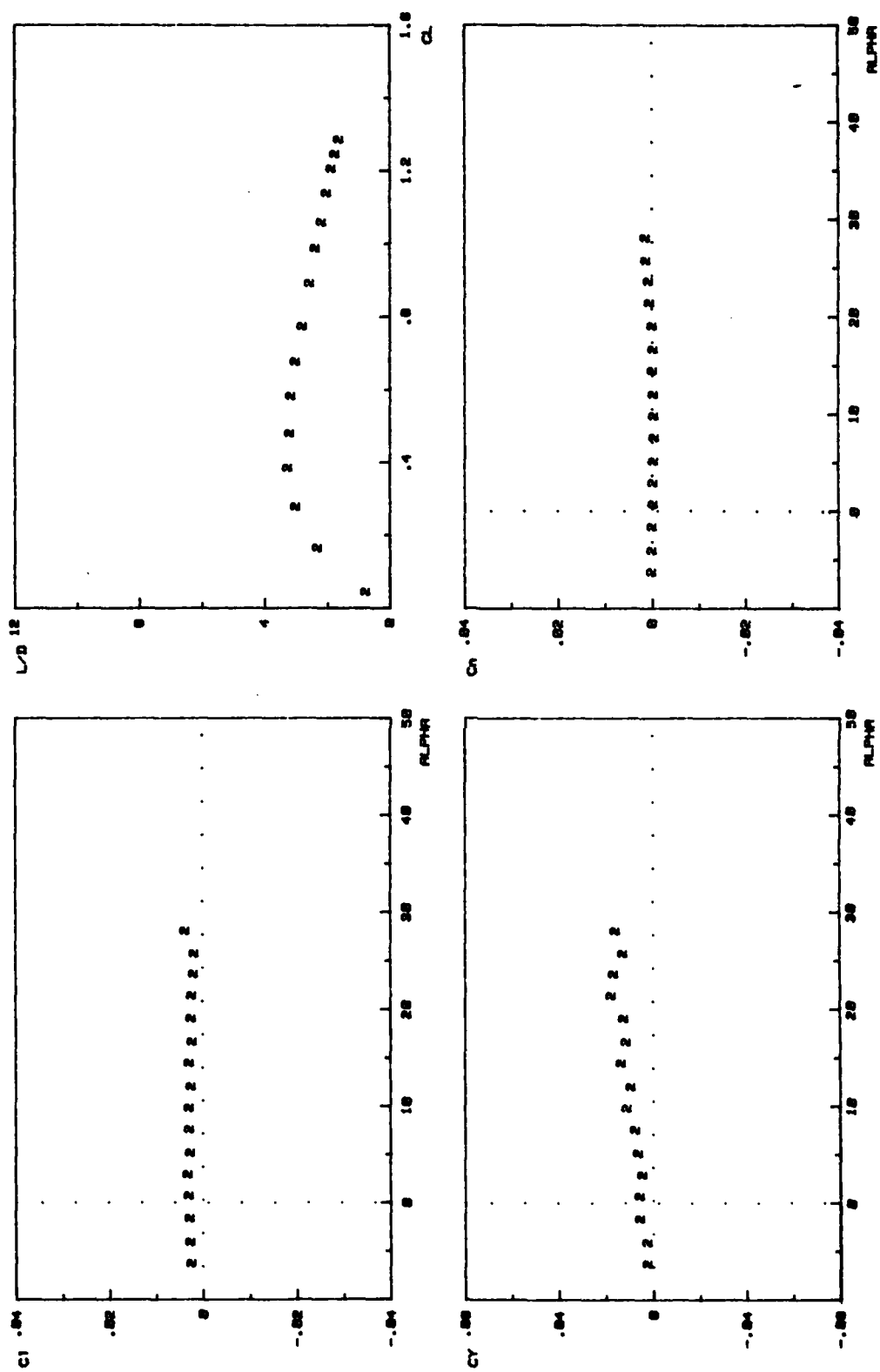


FIG. C-27. F2 (DELTA) @ 20 deg FLAP





F2 (DELTA) @ 20 deg FLAP

FIG. C-27.

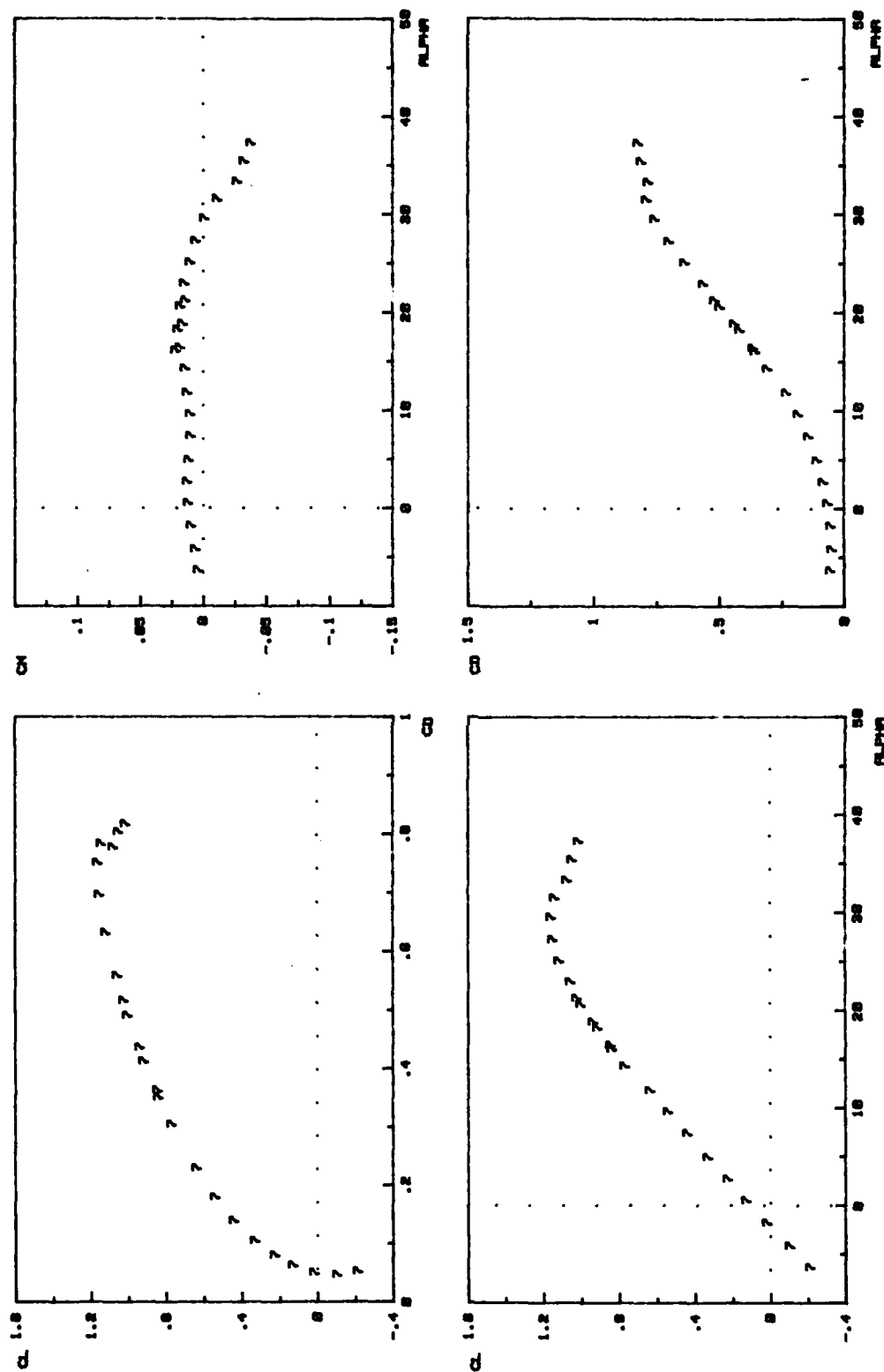
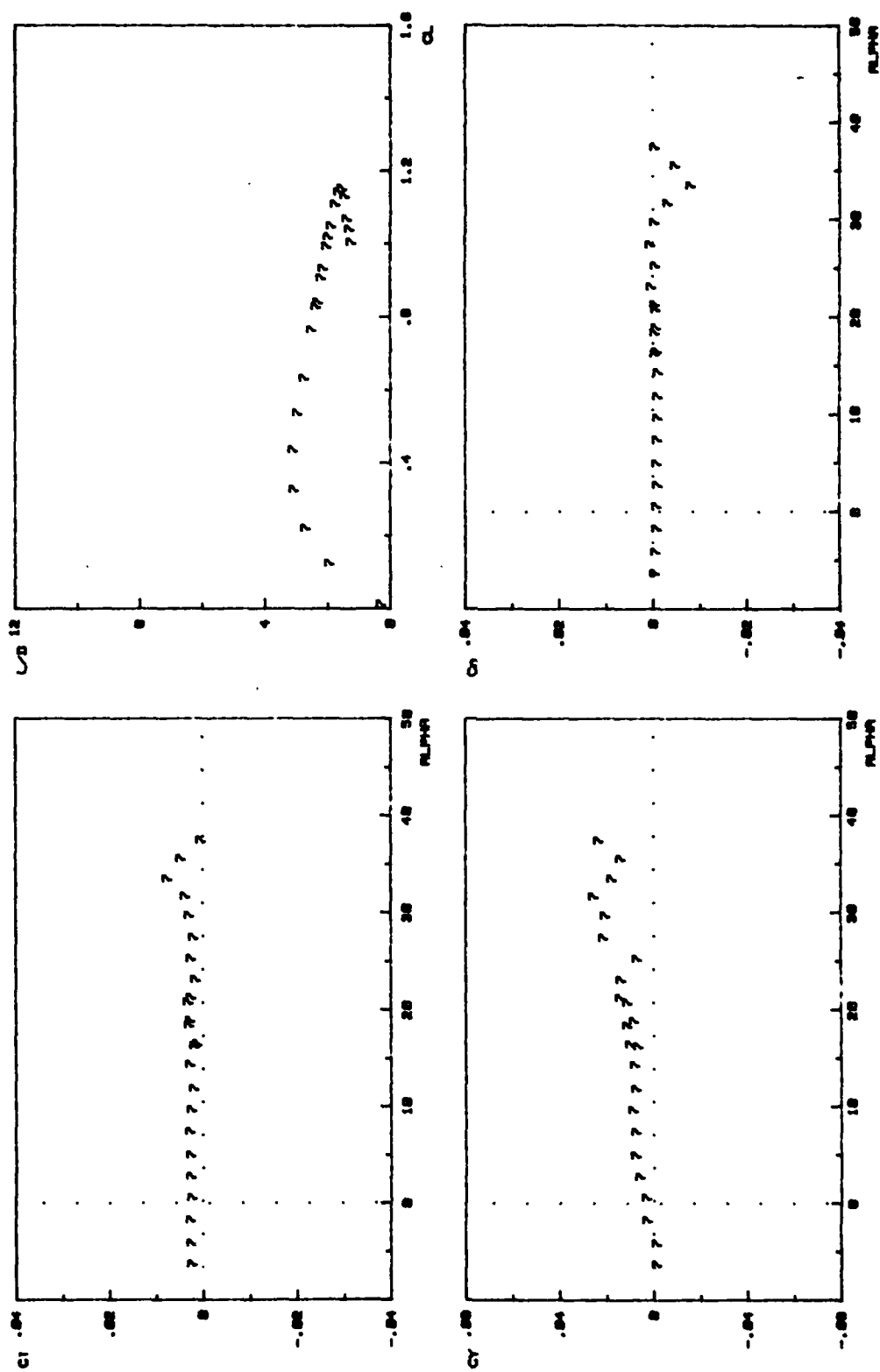
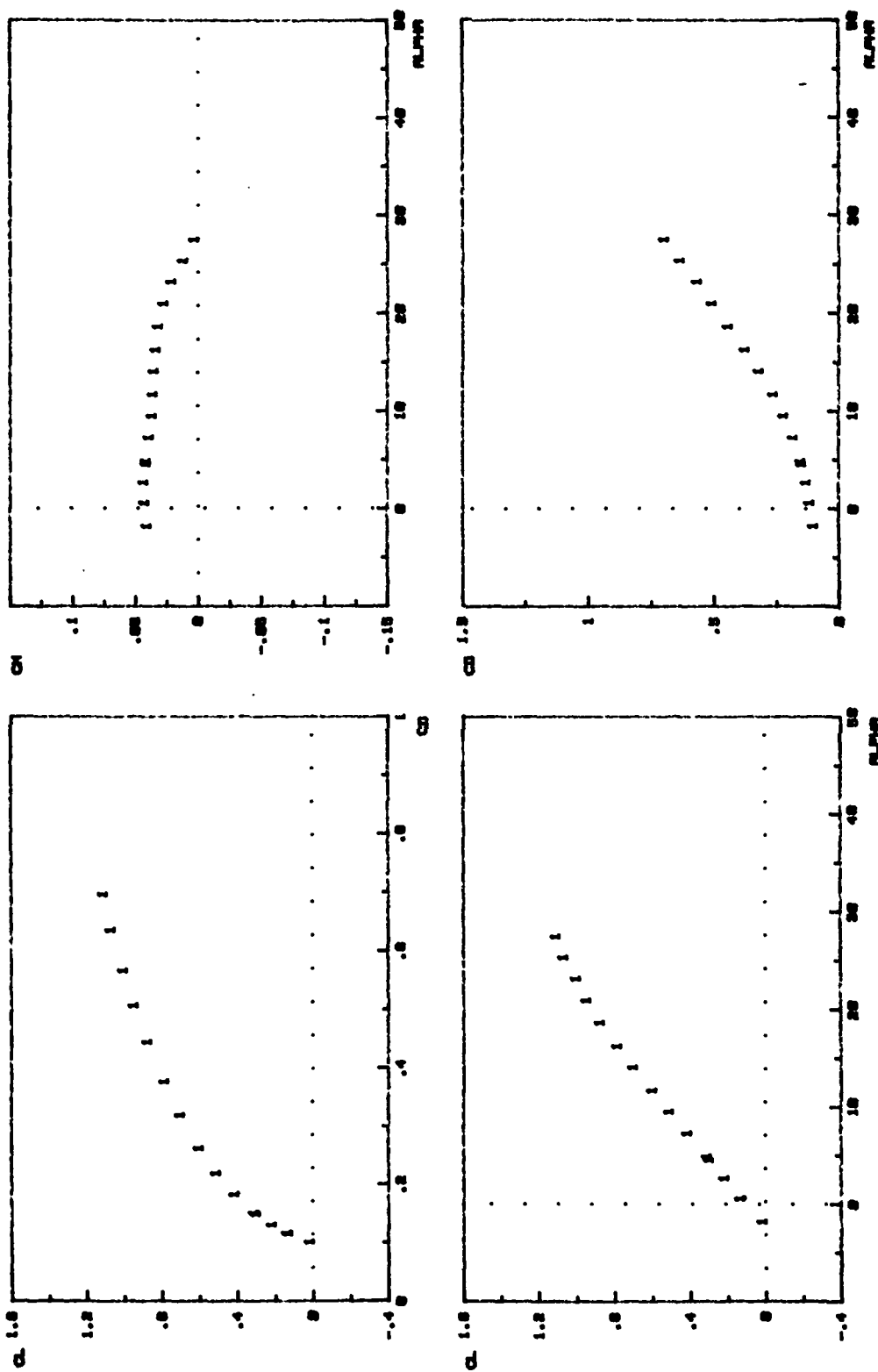


FIG. C-28. F7 (MOD. GOTHIC II) @ 10 deg FLAP



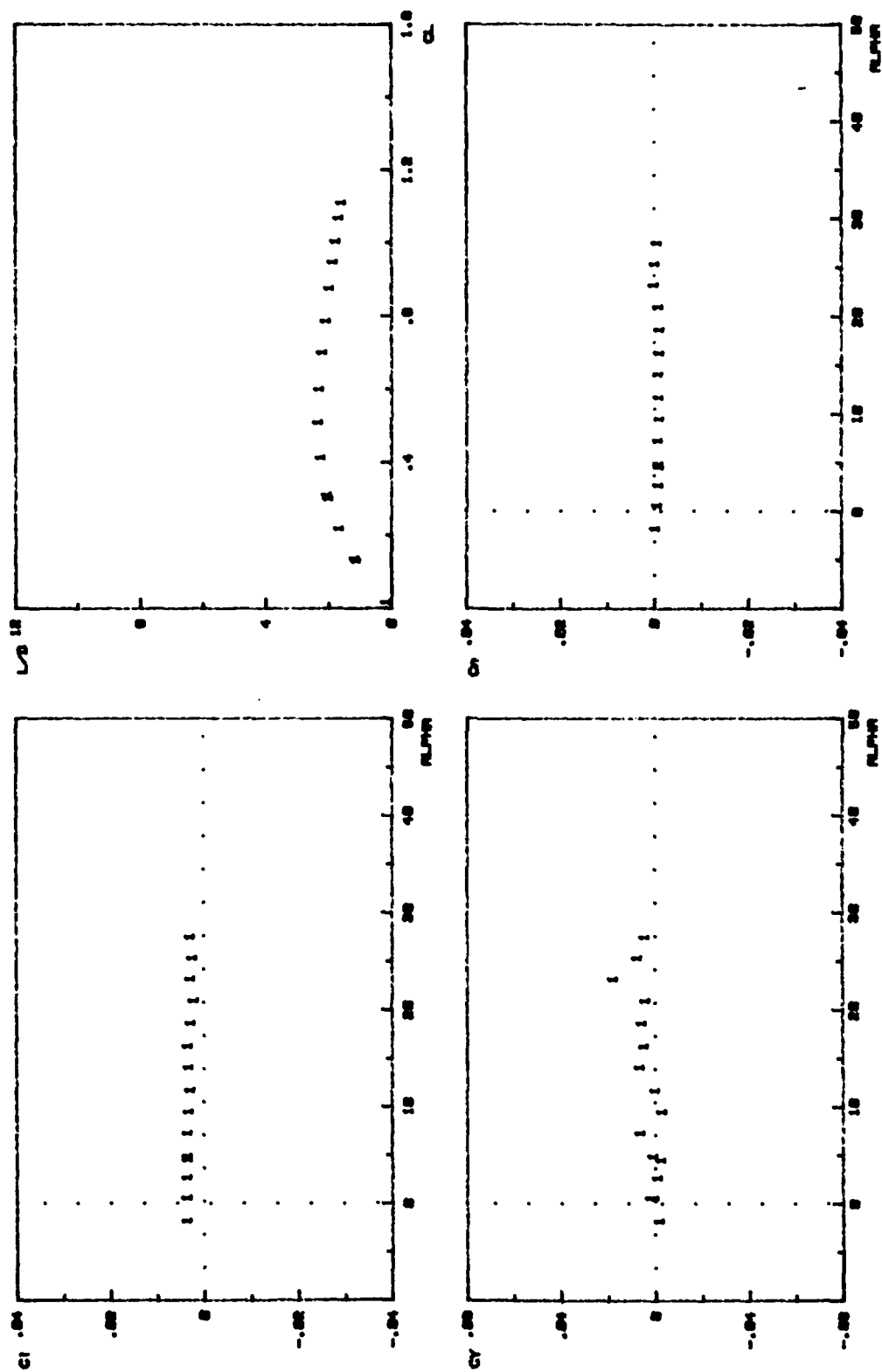
F7 (MOD. GOTHIC II) @ 18 deg FLAP

FIG. C-28.



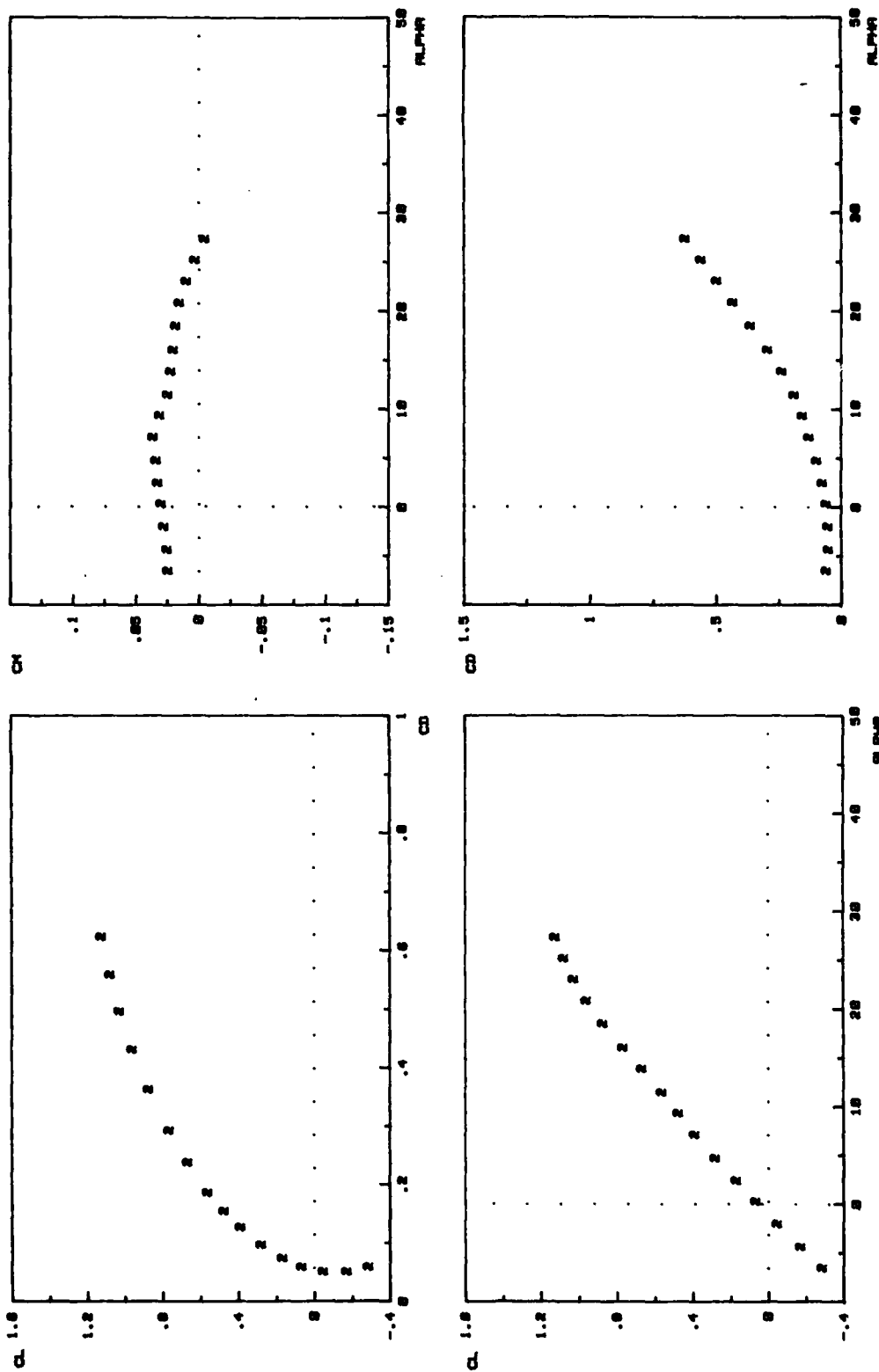
F1 (GOTHIC) @ -15 deg CRNT

FIG. C-29.



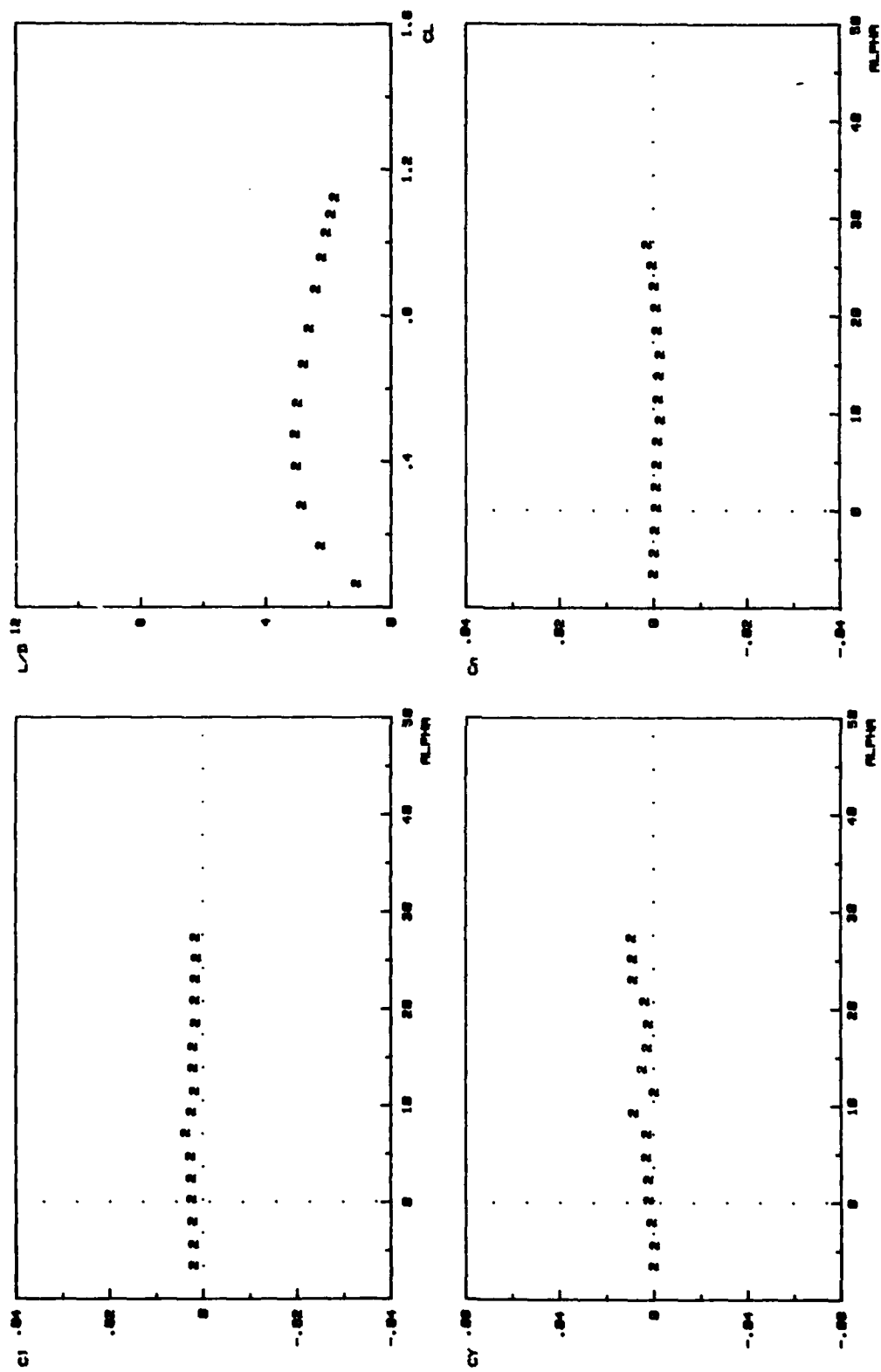
F1 (GOTHIC) @ -15 deg CRNT

FIG. C-29.



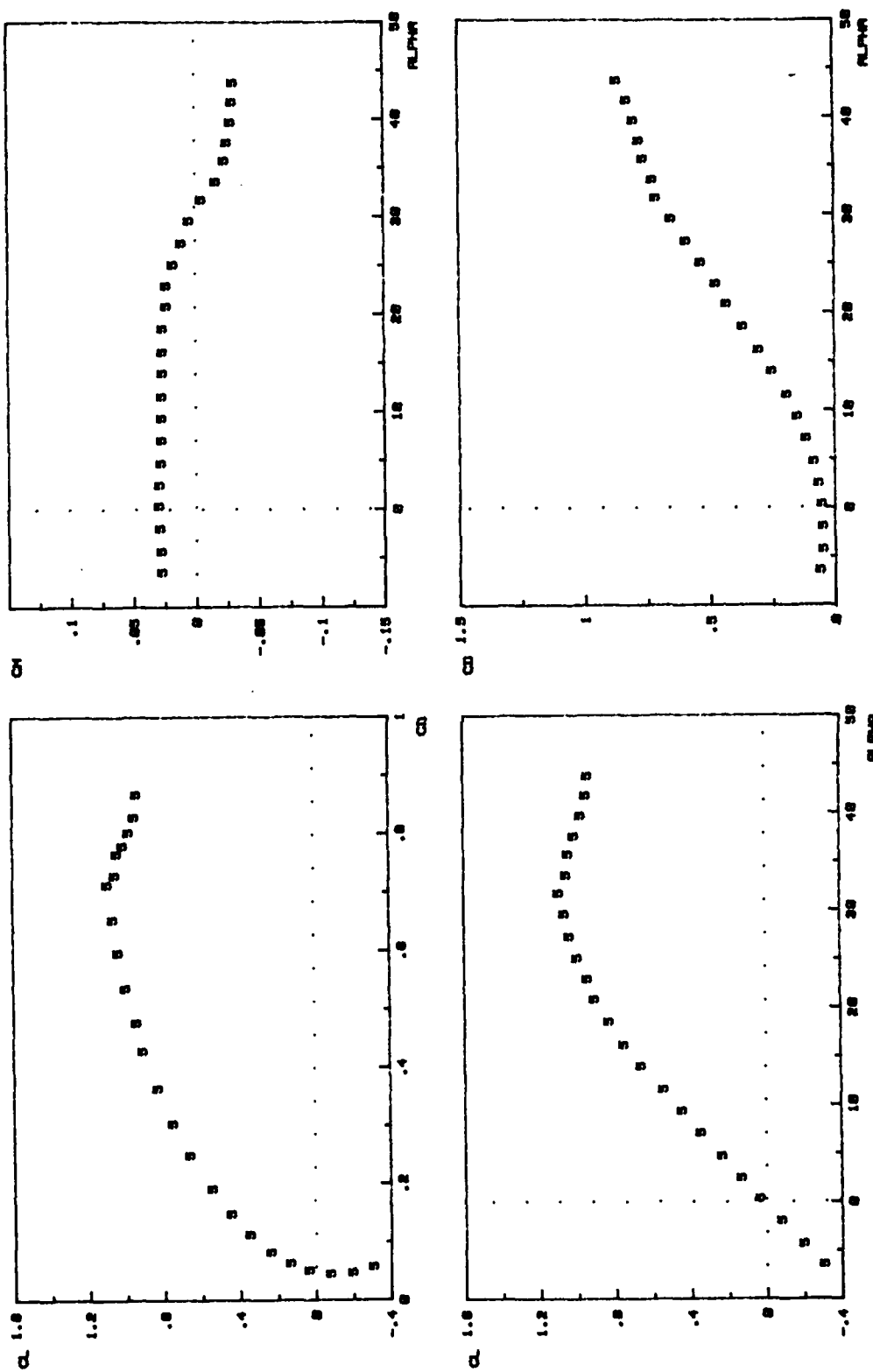
F2 (DELTA) @ -15 deg CANT

FIG. C-30.



F2 (DELTA) = -15 deg CANT

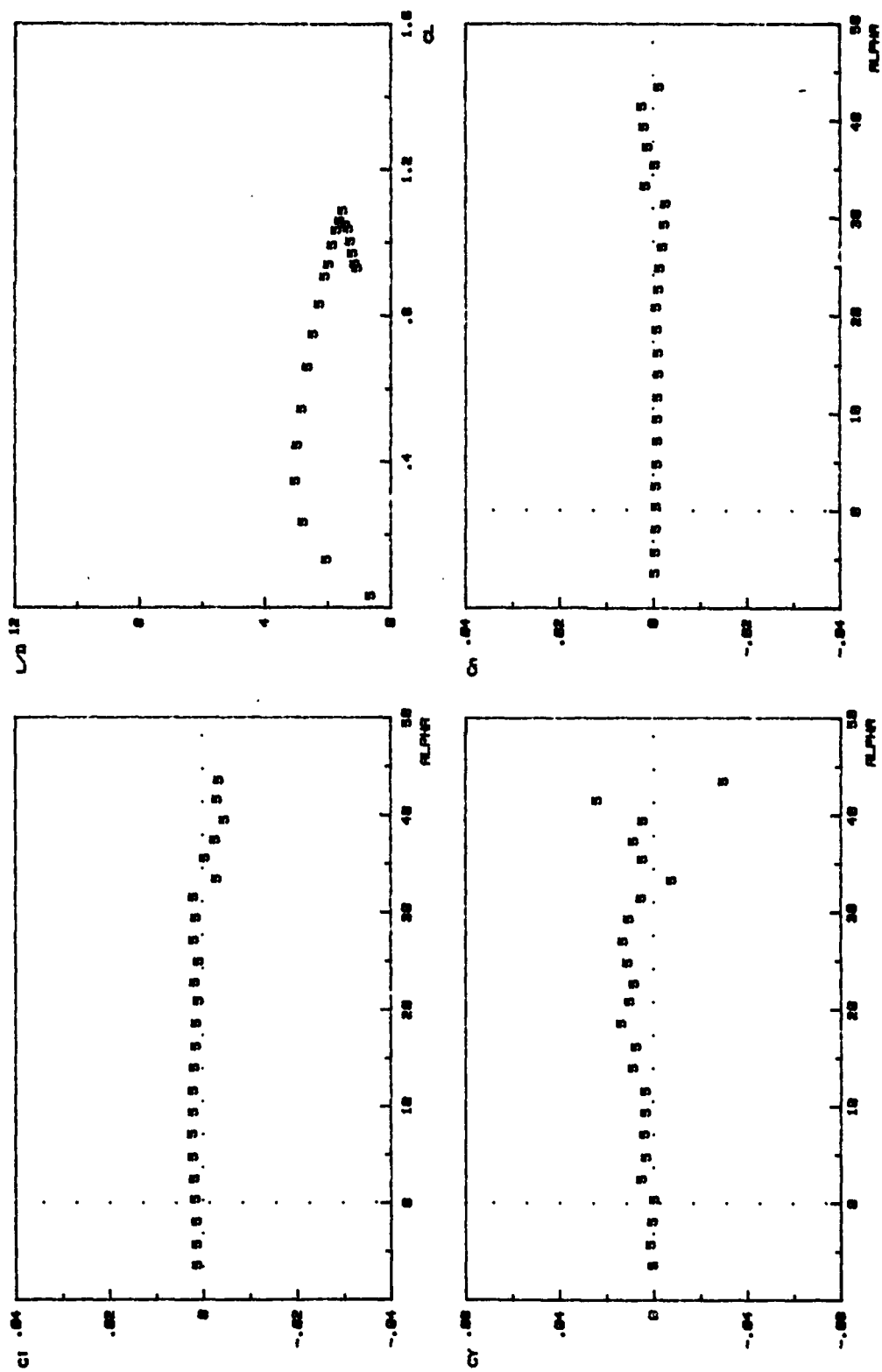
F2 (DELTA) = 0



F5 (DOUBLE GOTHIC) @ -15 deg CANT

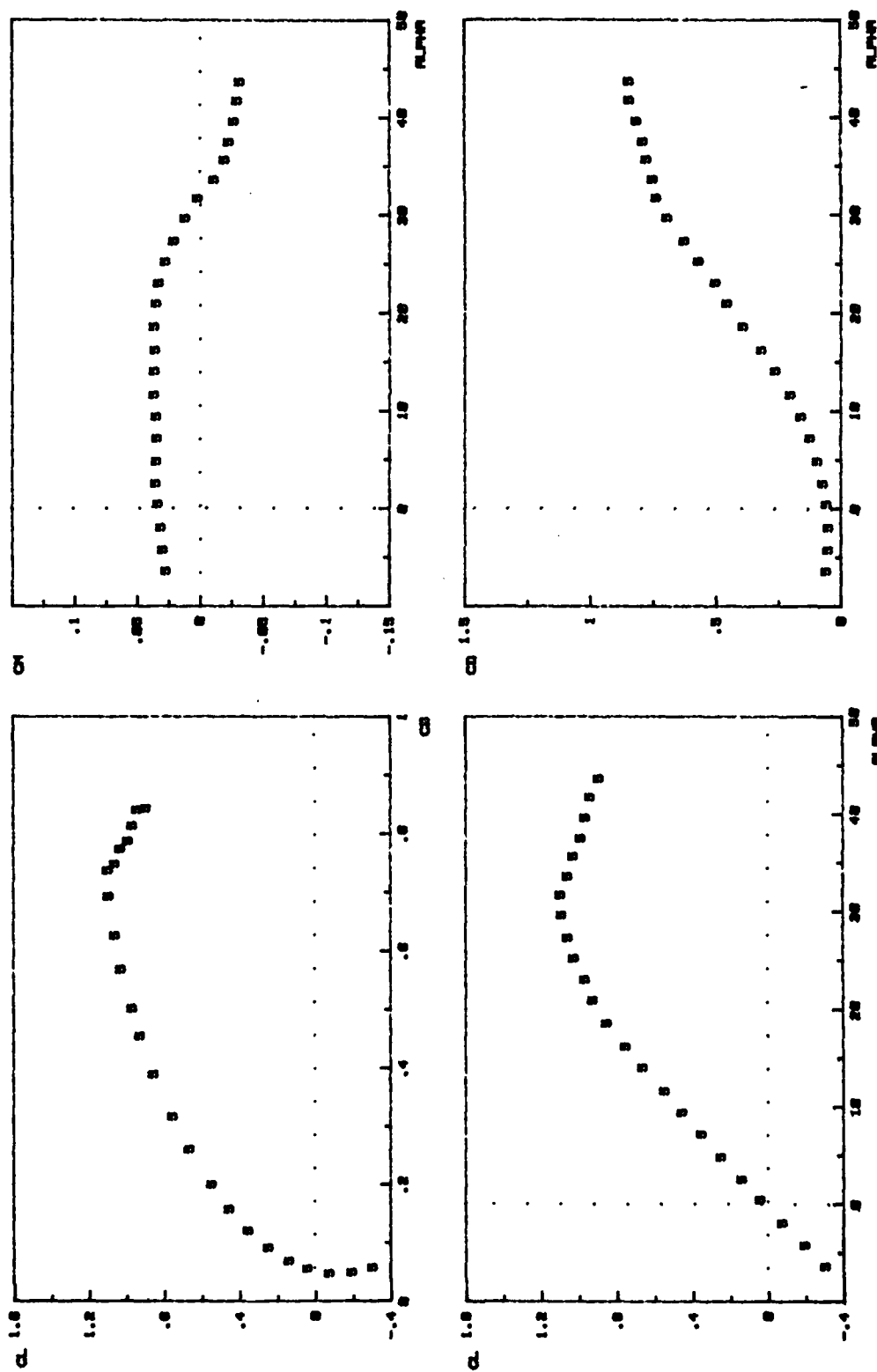
FIG. C-31.





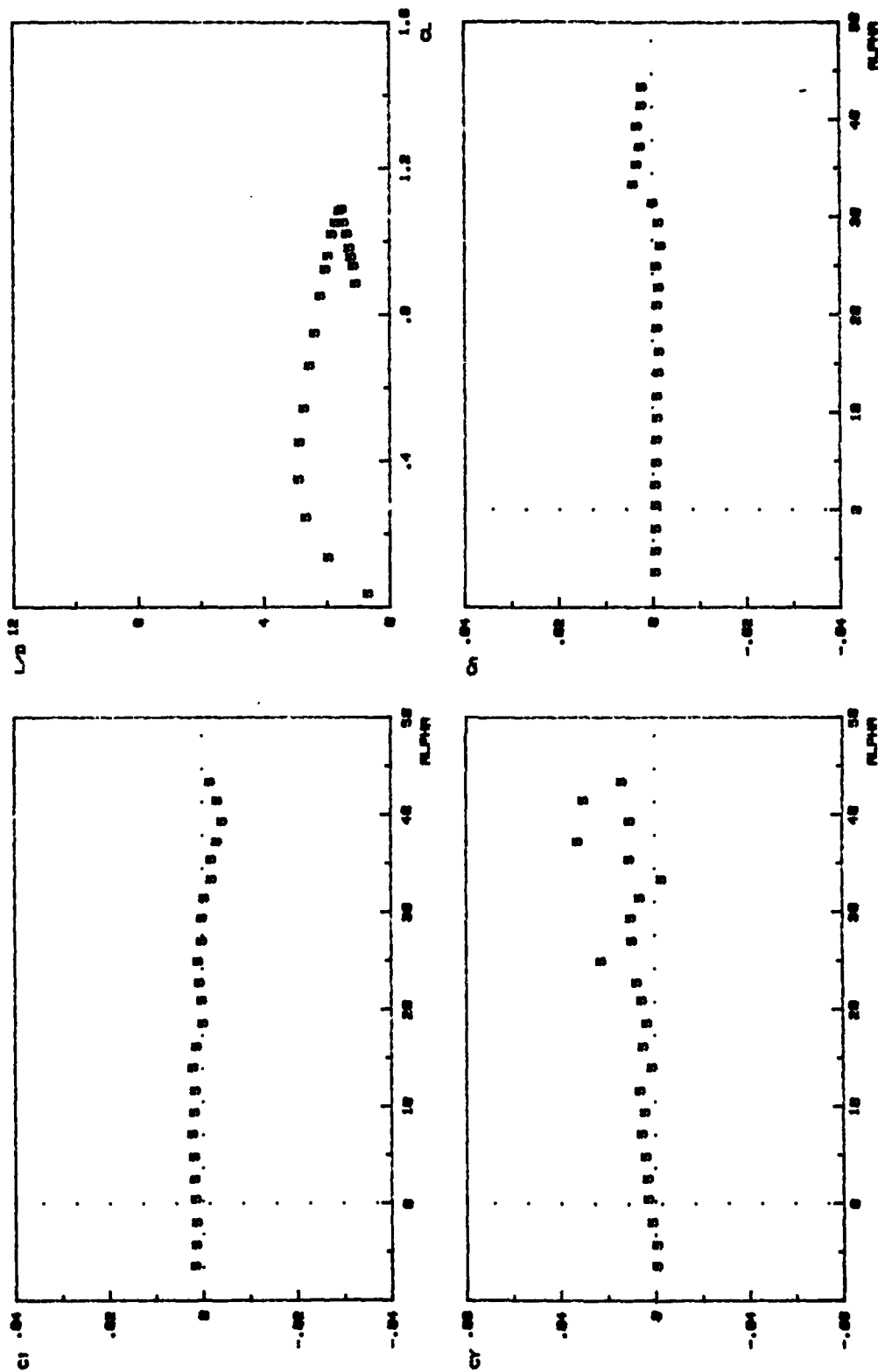
F5 (DOUBLE GOTHIC) @ -15 deg CANT

FIG. C-31,



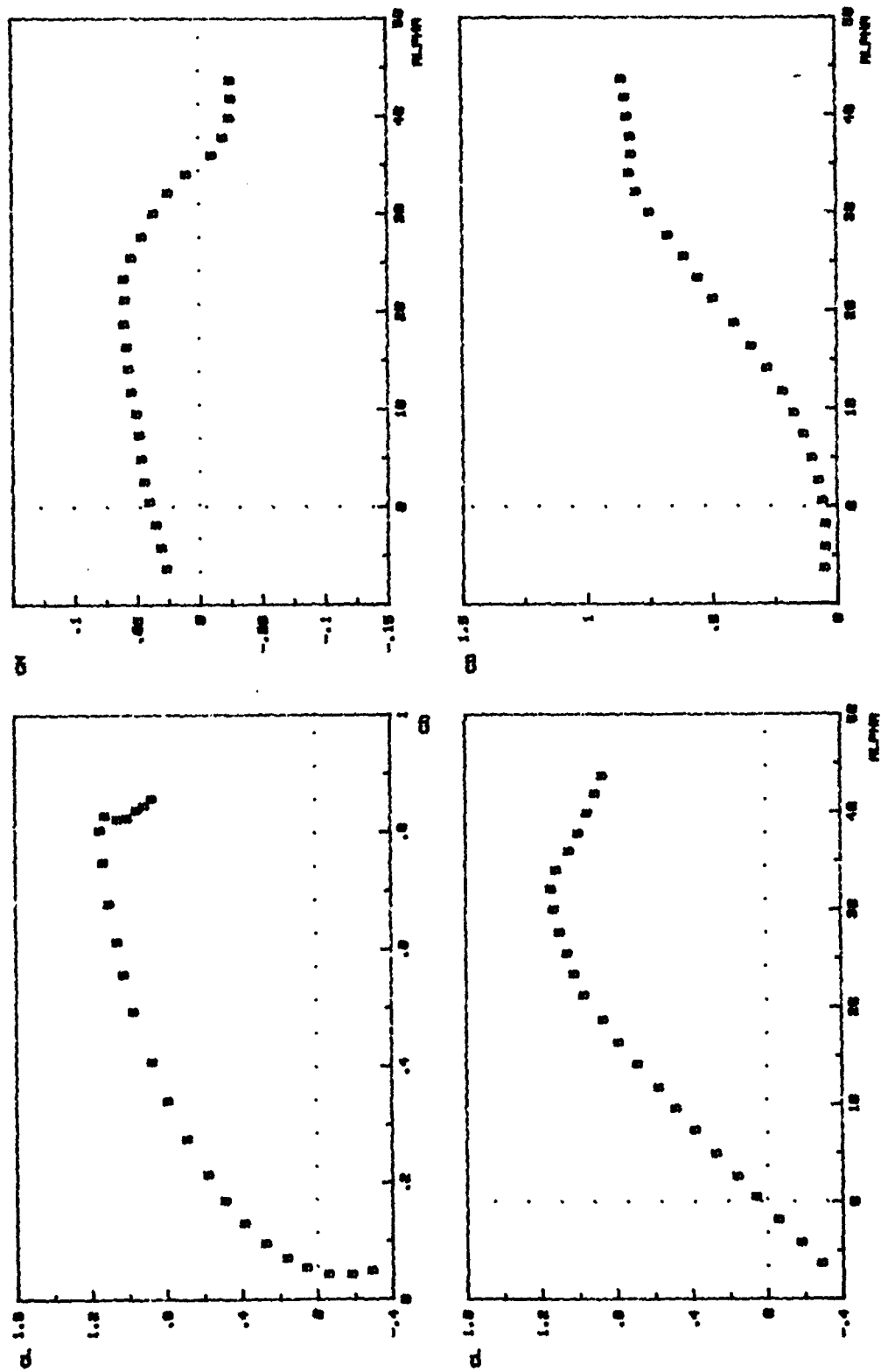
F5 (DOUBLE GOTHIC) @ -7.5 deg CANT

FIG. C-32.



F5 (DOUBLE GOTHIC) @ -7.5 deg CRNT

FIG. C-32.



F5 (DOUBLE GOTHIC) @ 7.5 deg CPNT

FIG. C-33.

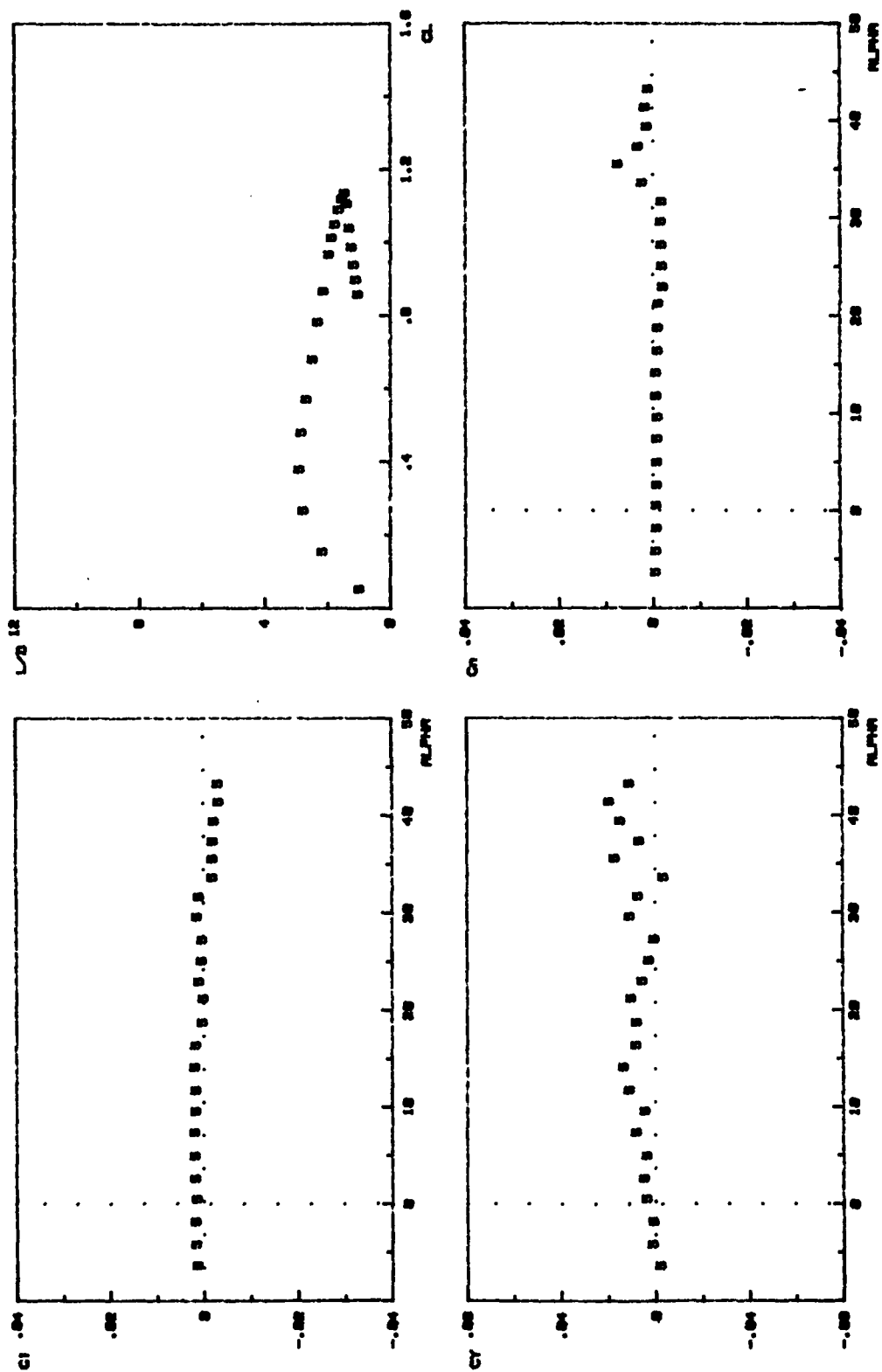


FIG. C-33. FS (DOUBLE GOTHIC) @ 7.5 deg CANT

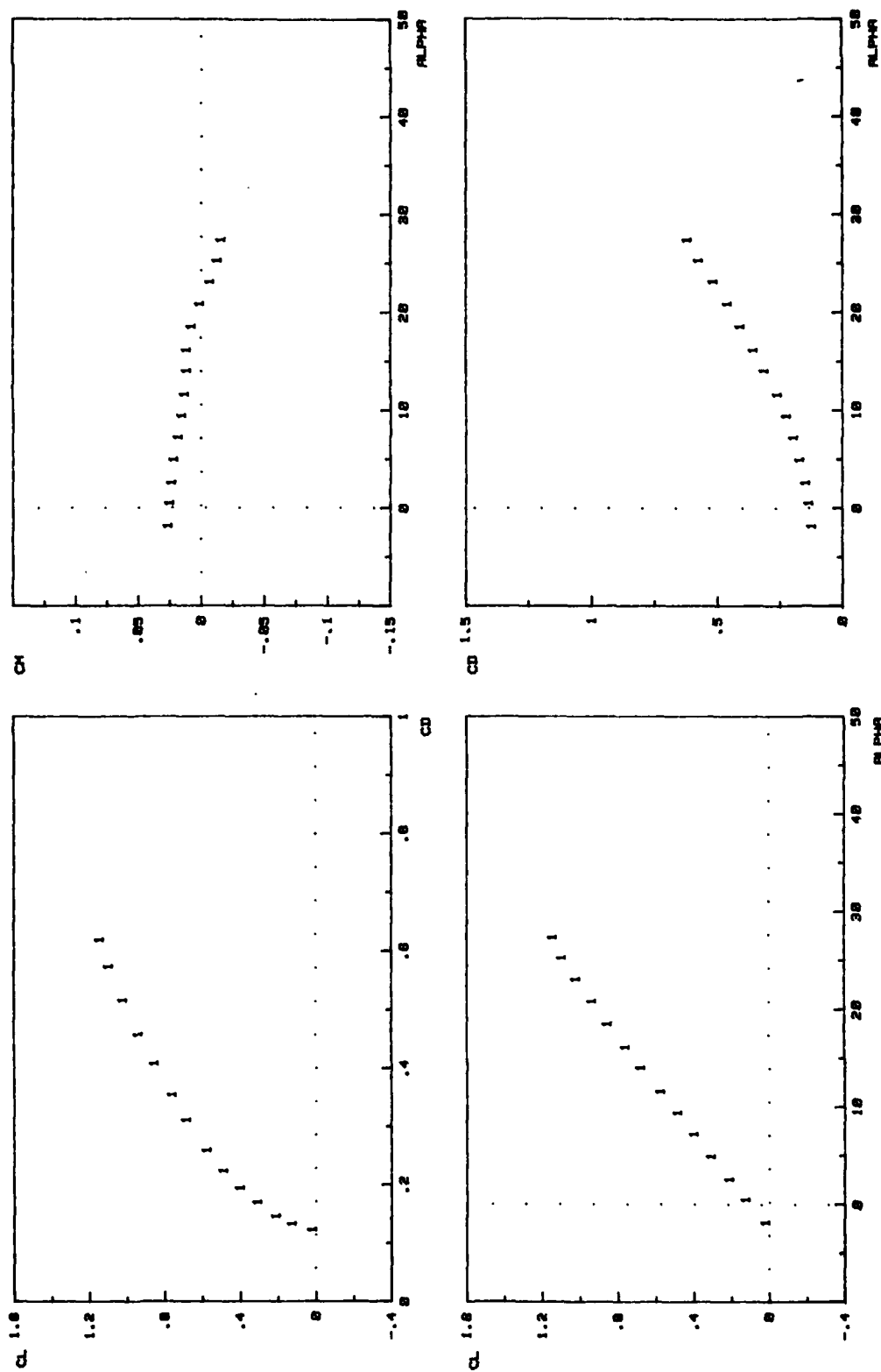
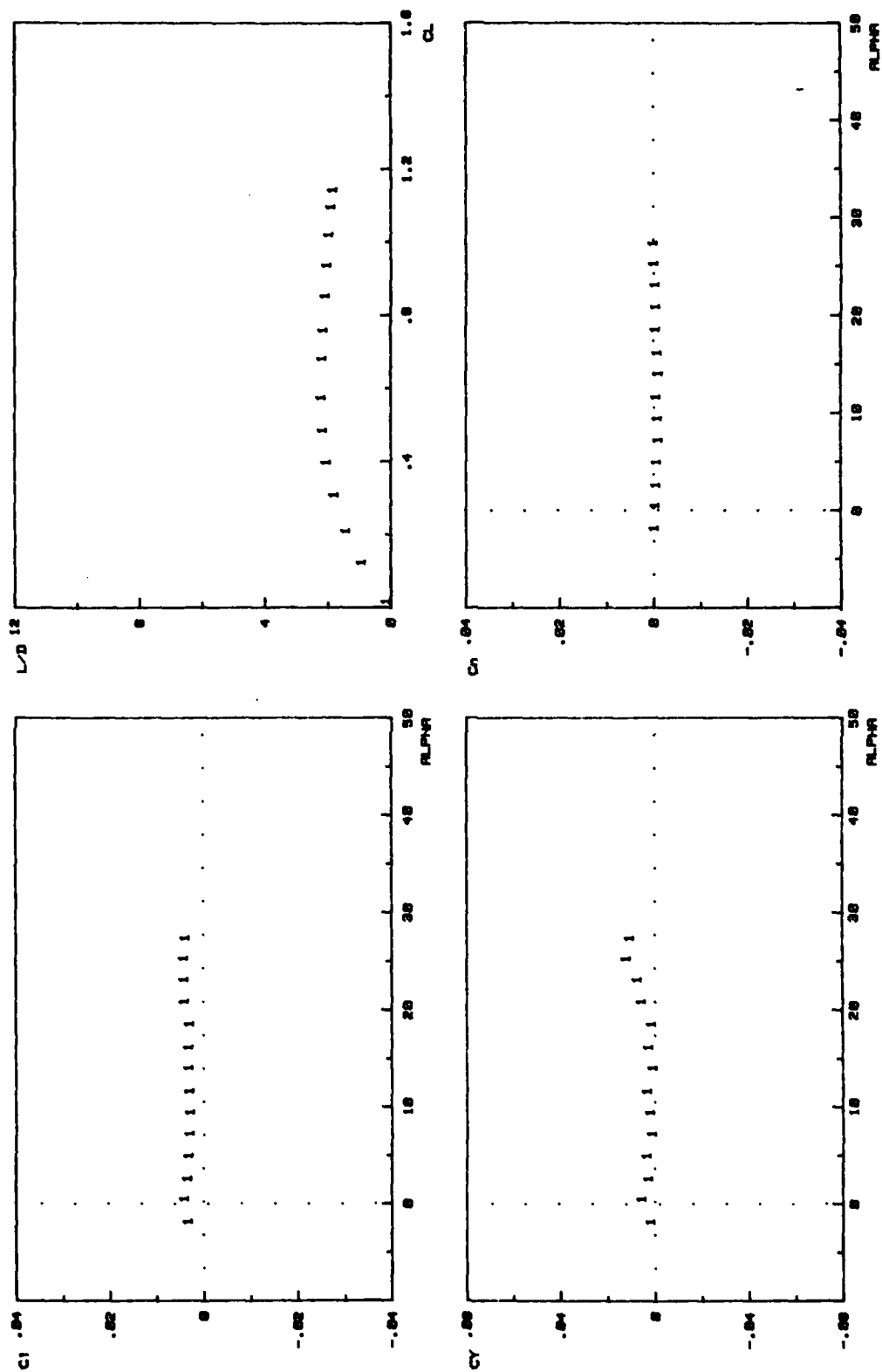
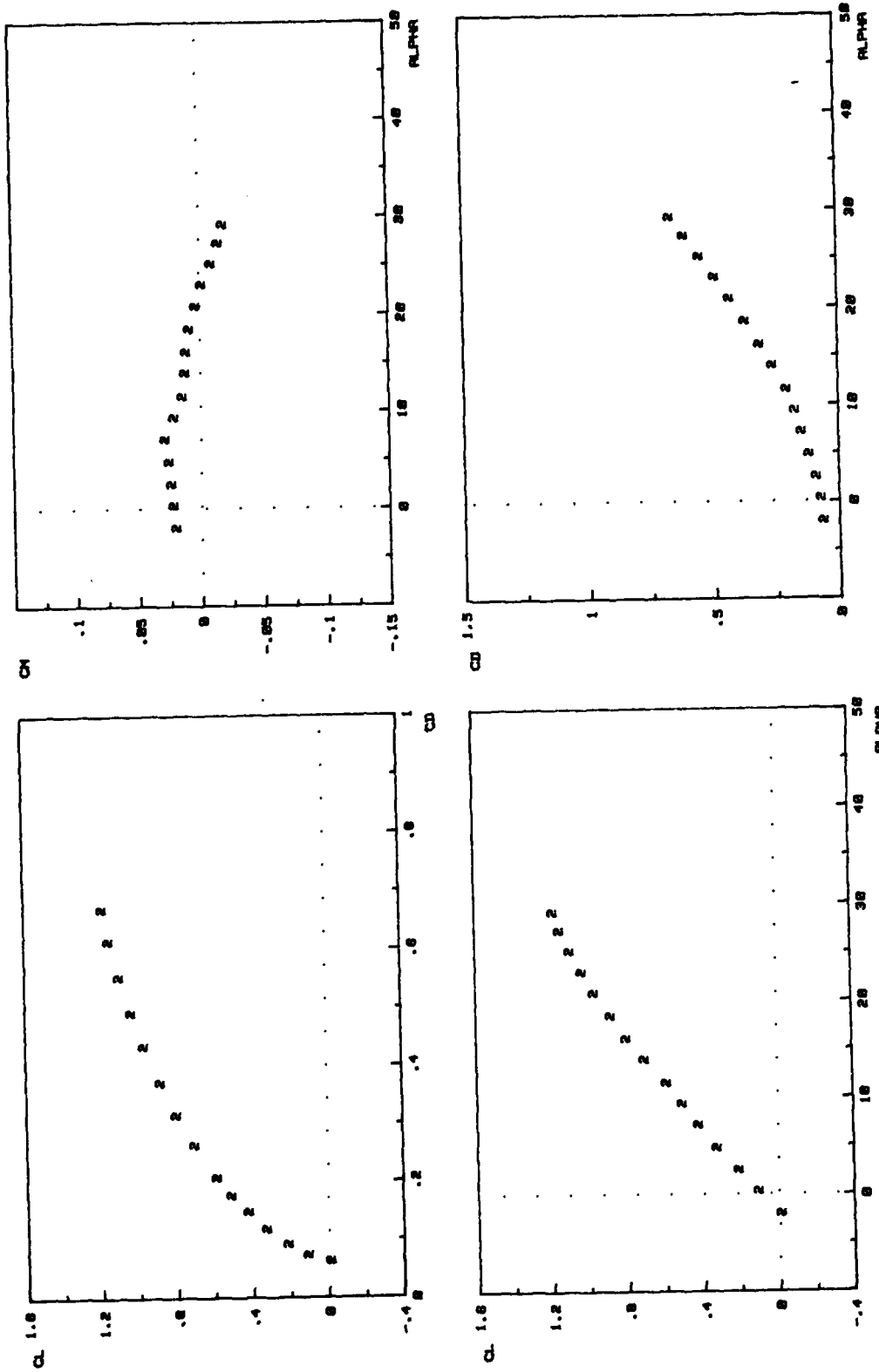


FIG. C-34. F1 (GOTHIC) INBOARD 1.5 inches



F1 (GOTHIC) INBOARD 1.5 inches

FIG. C-34.



F2 (DELTA) INBOARD 0.5 inches

FIG. C-35.



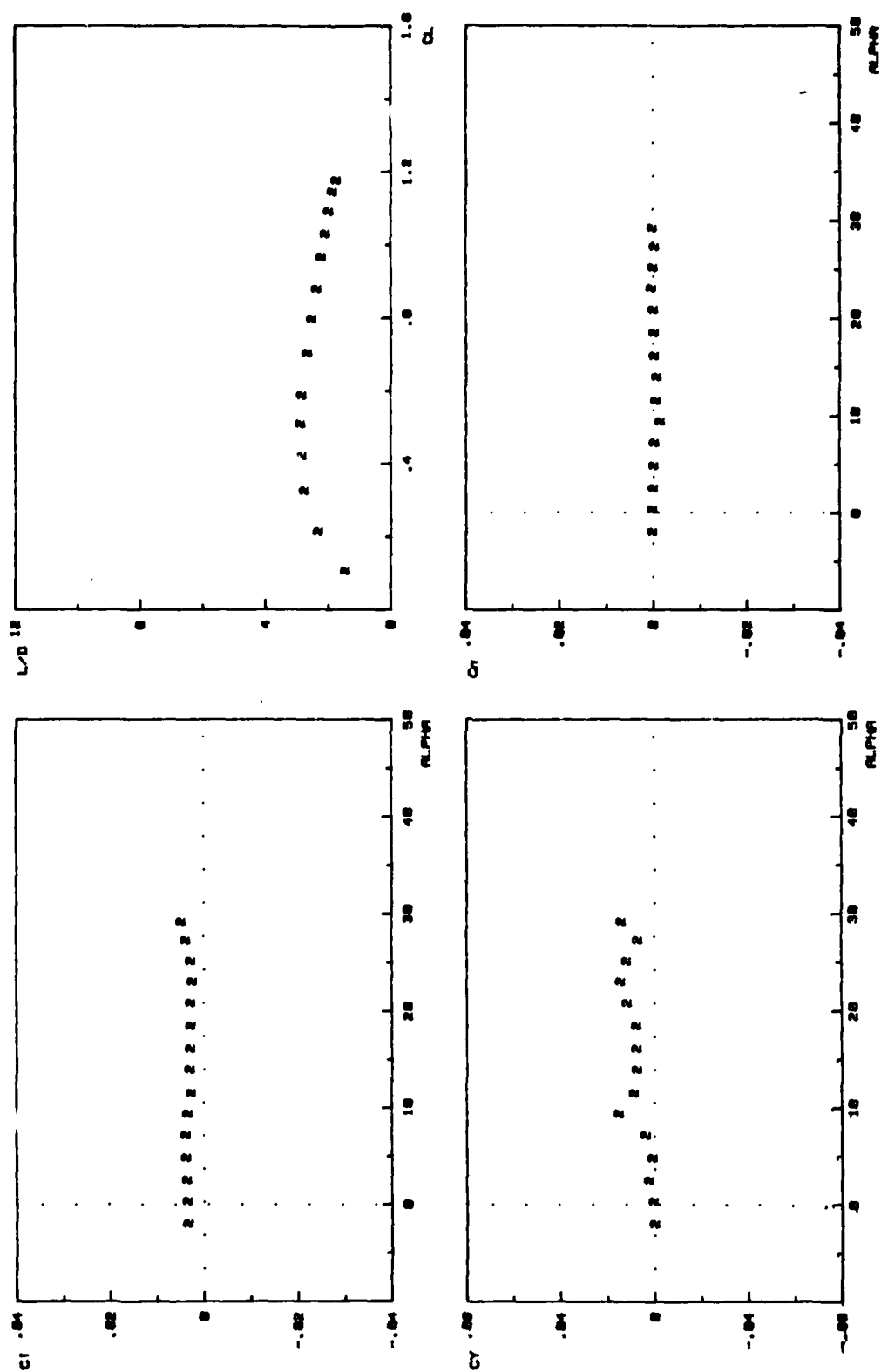
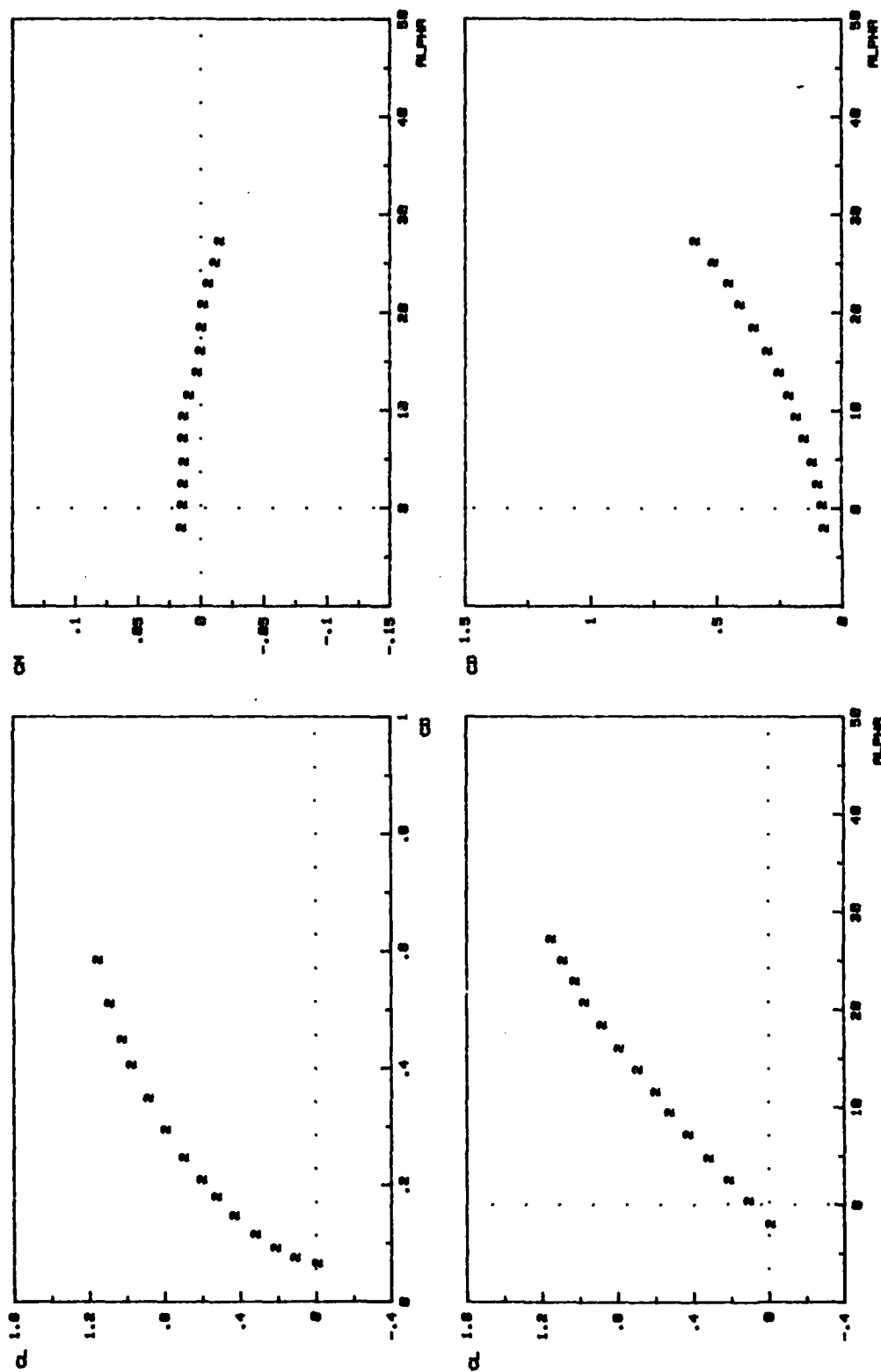
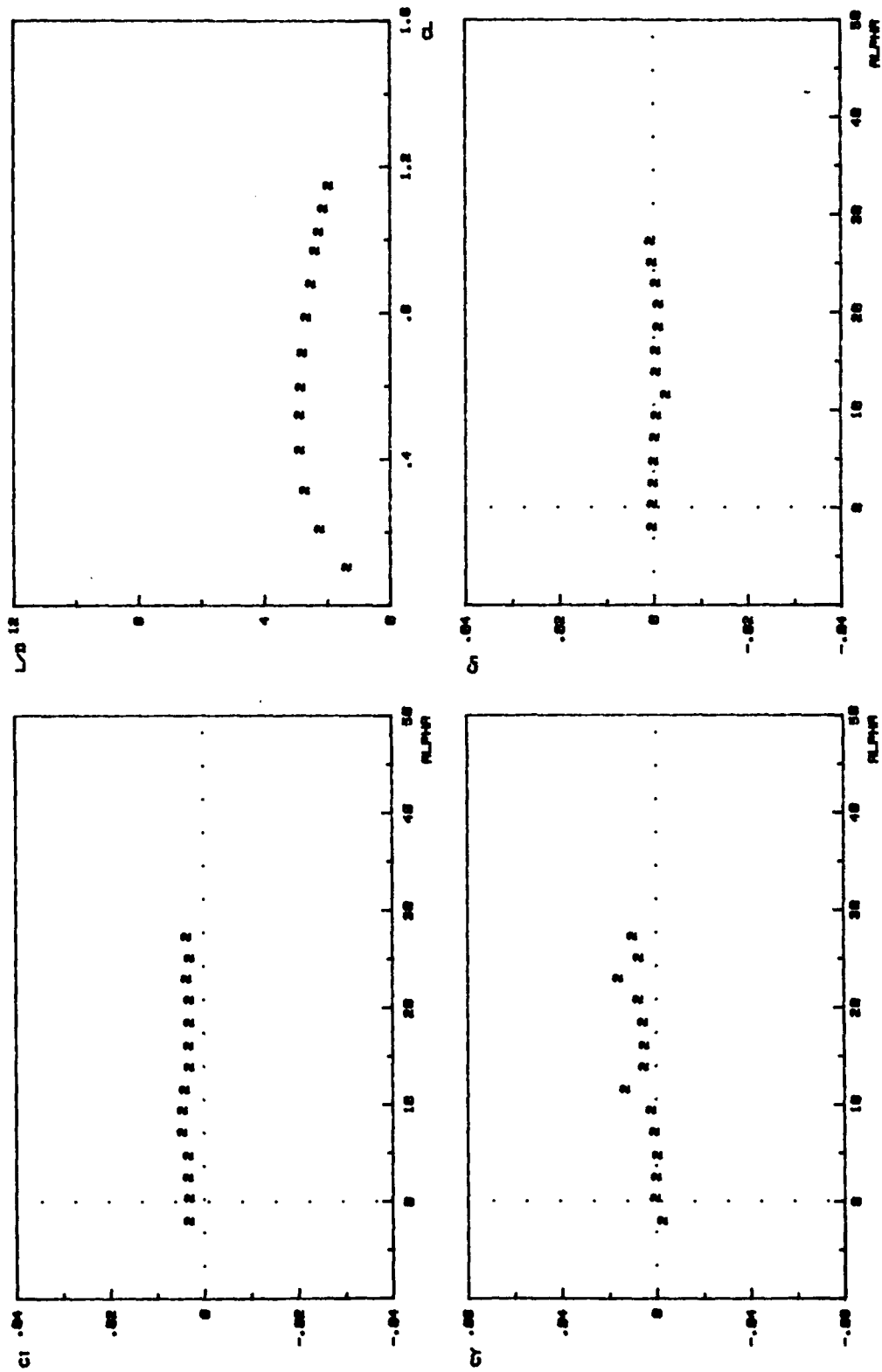


FIG. C-35.



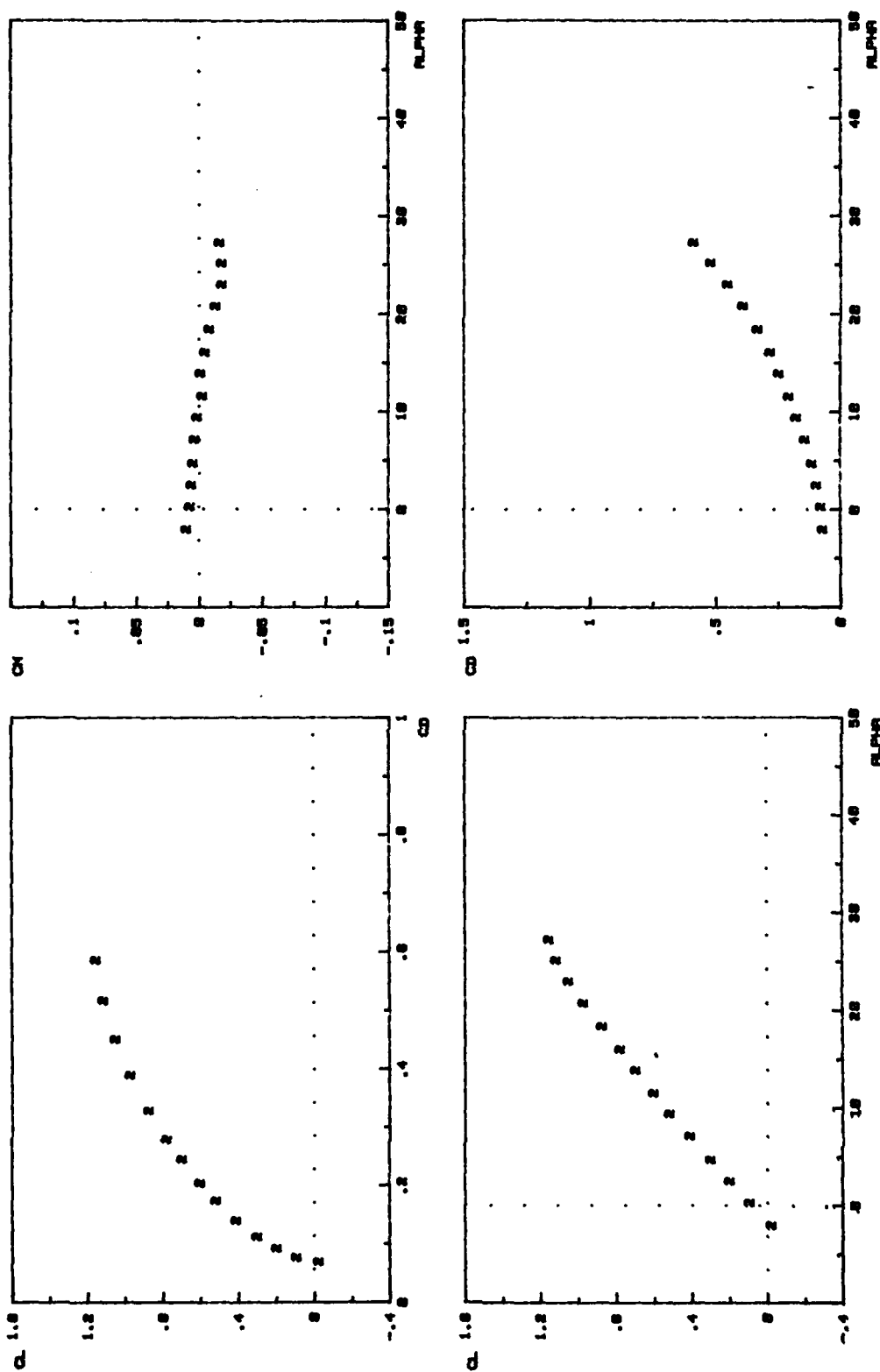
F2 (DELTA) INBOARD 1.0 inches

FIG. C-36.



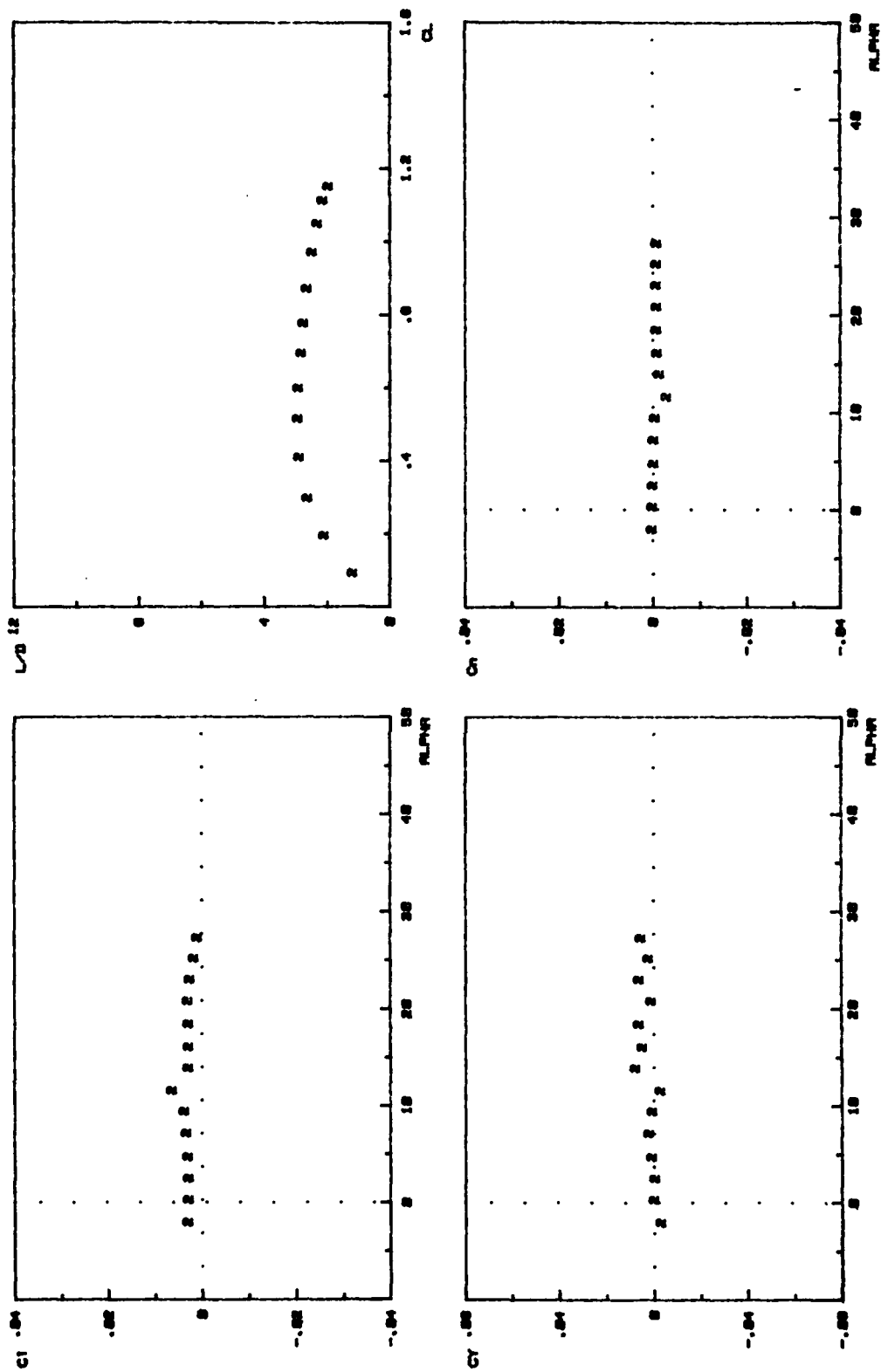
F2 (DELTA) INBOARD 1.0 inches

FIG. C-36.



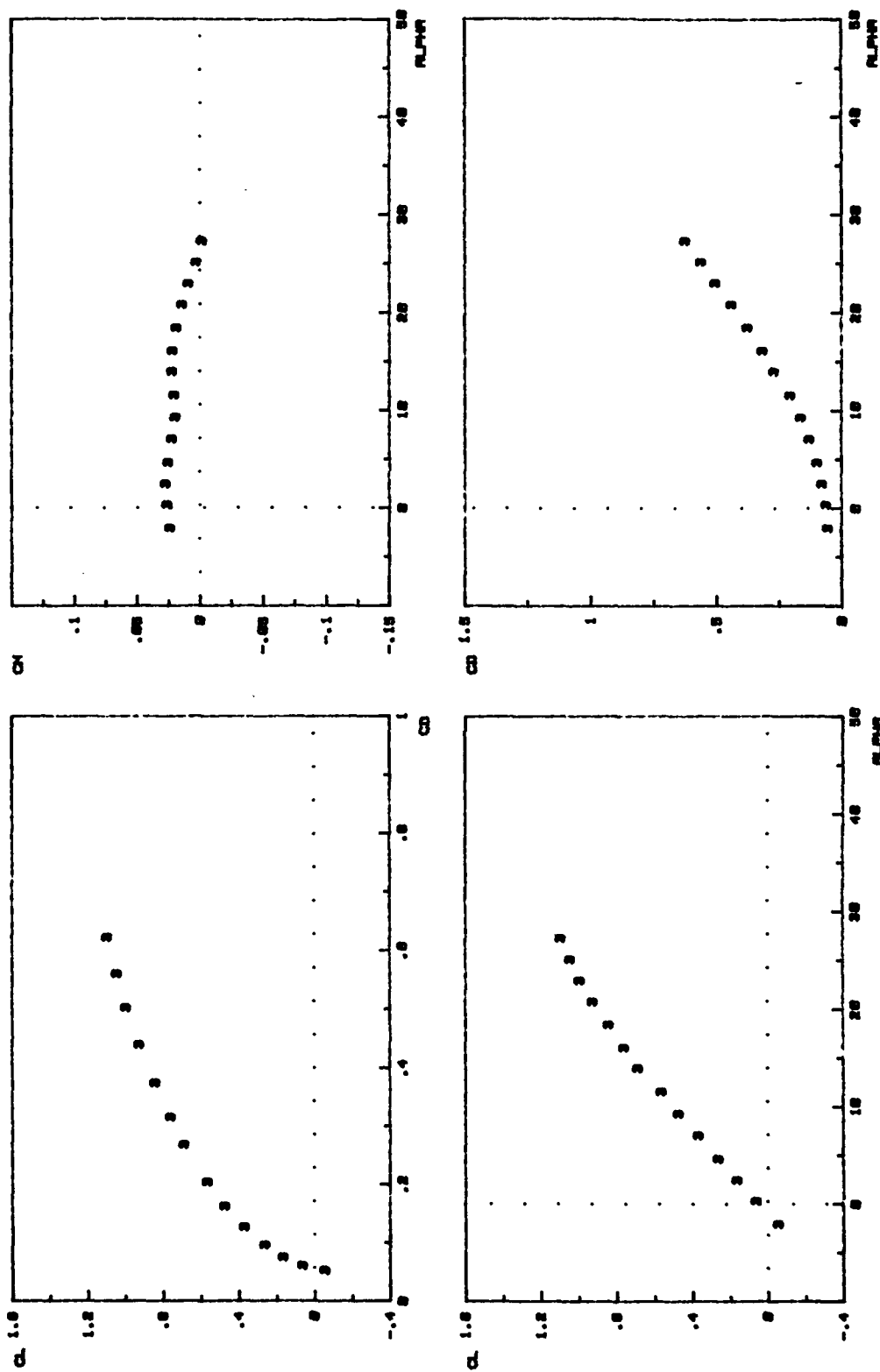
F2 (DELTA) INBOARD 1.5 inches

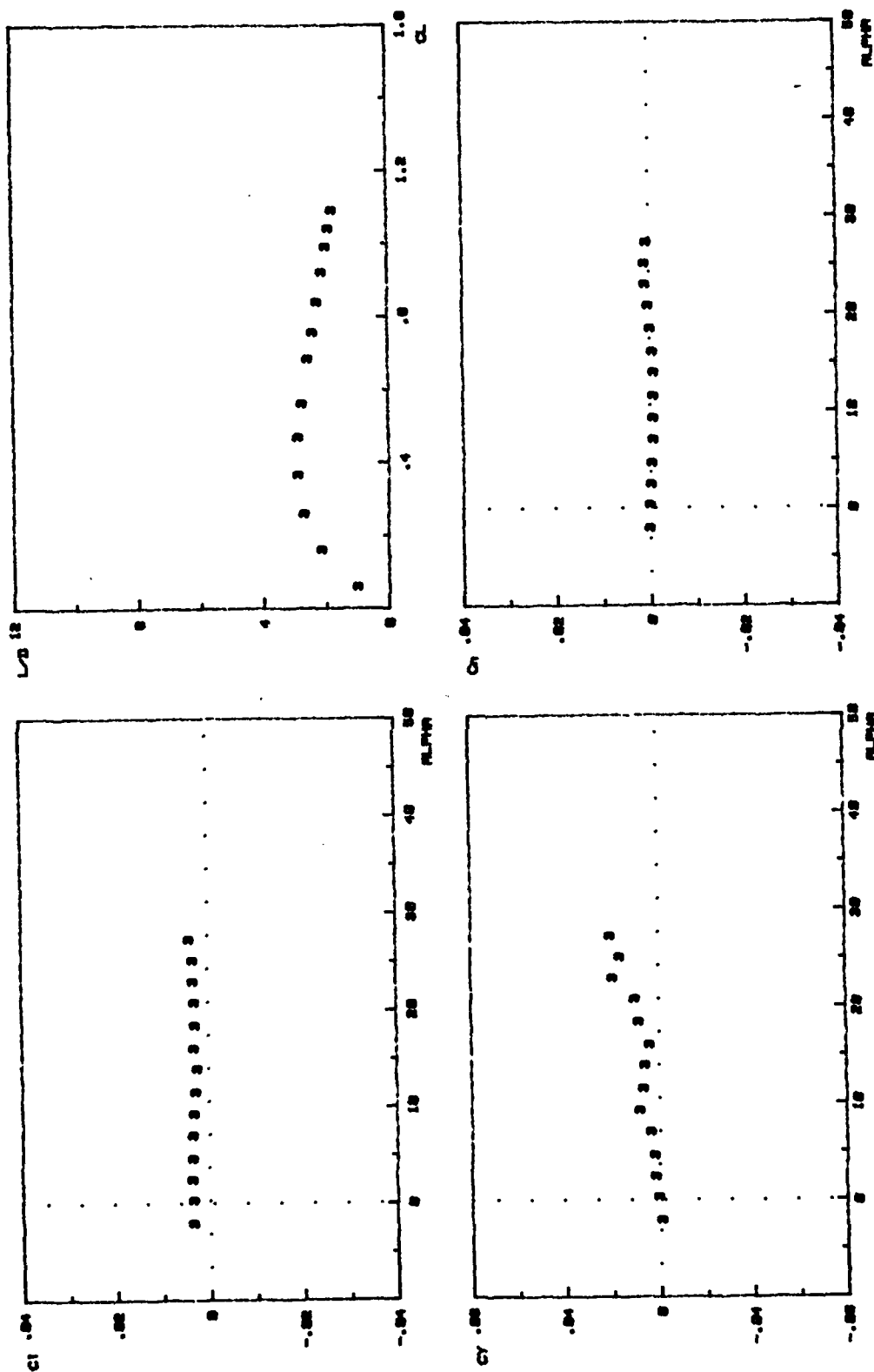
FIG. C-37.



F2 (DELTA) INBOARD 1.5 inches

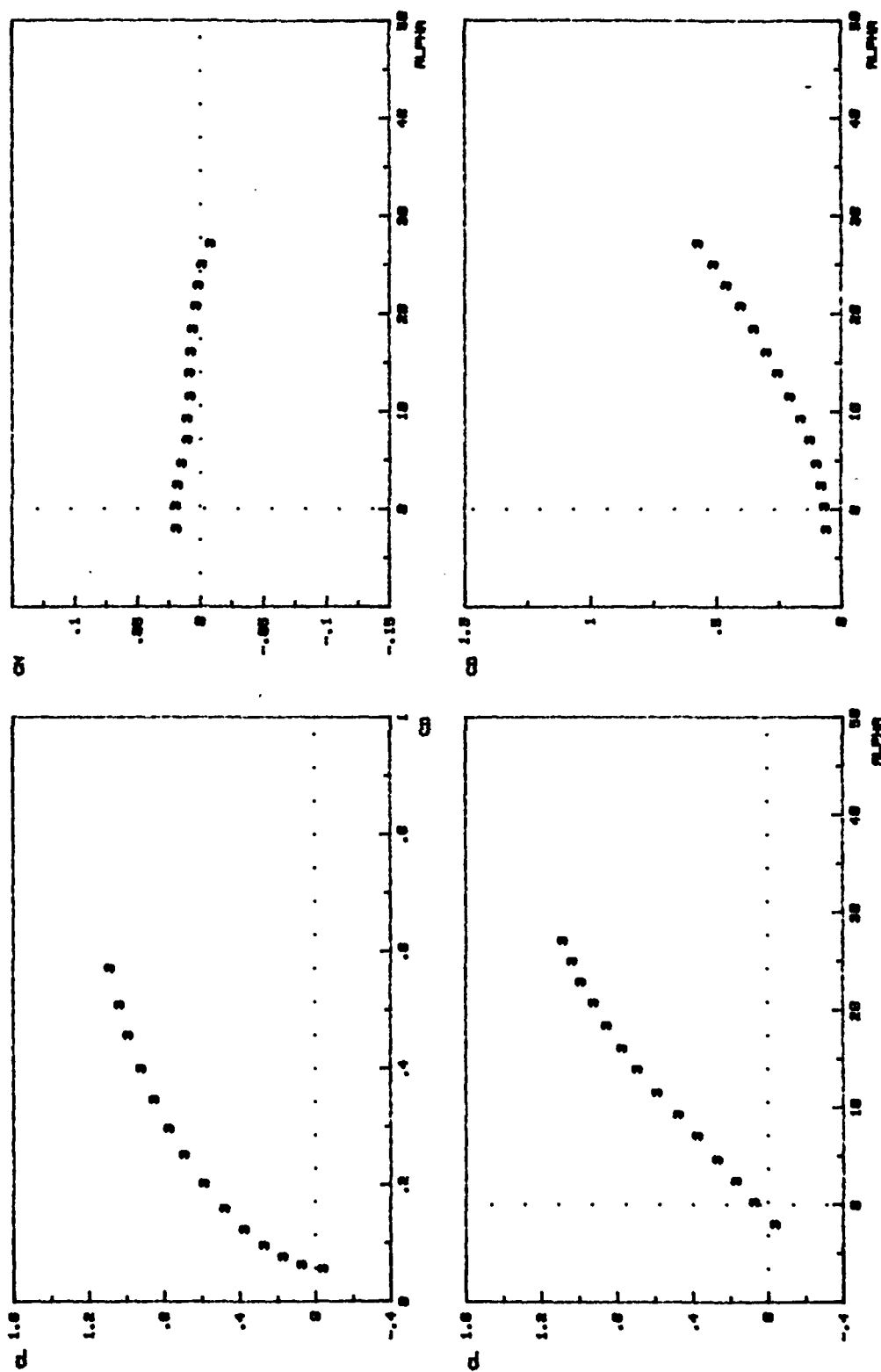
FIG. C-37.





F3 (CROPPED) INBOARD 0.5 inches

FIG. C-38.



F3 (CROPPED) INBOARD 1.8 inches

FIG. C-39.



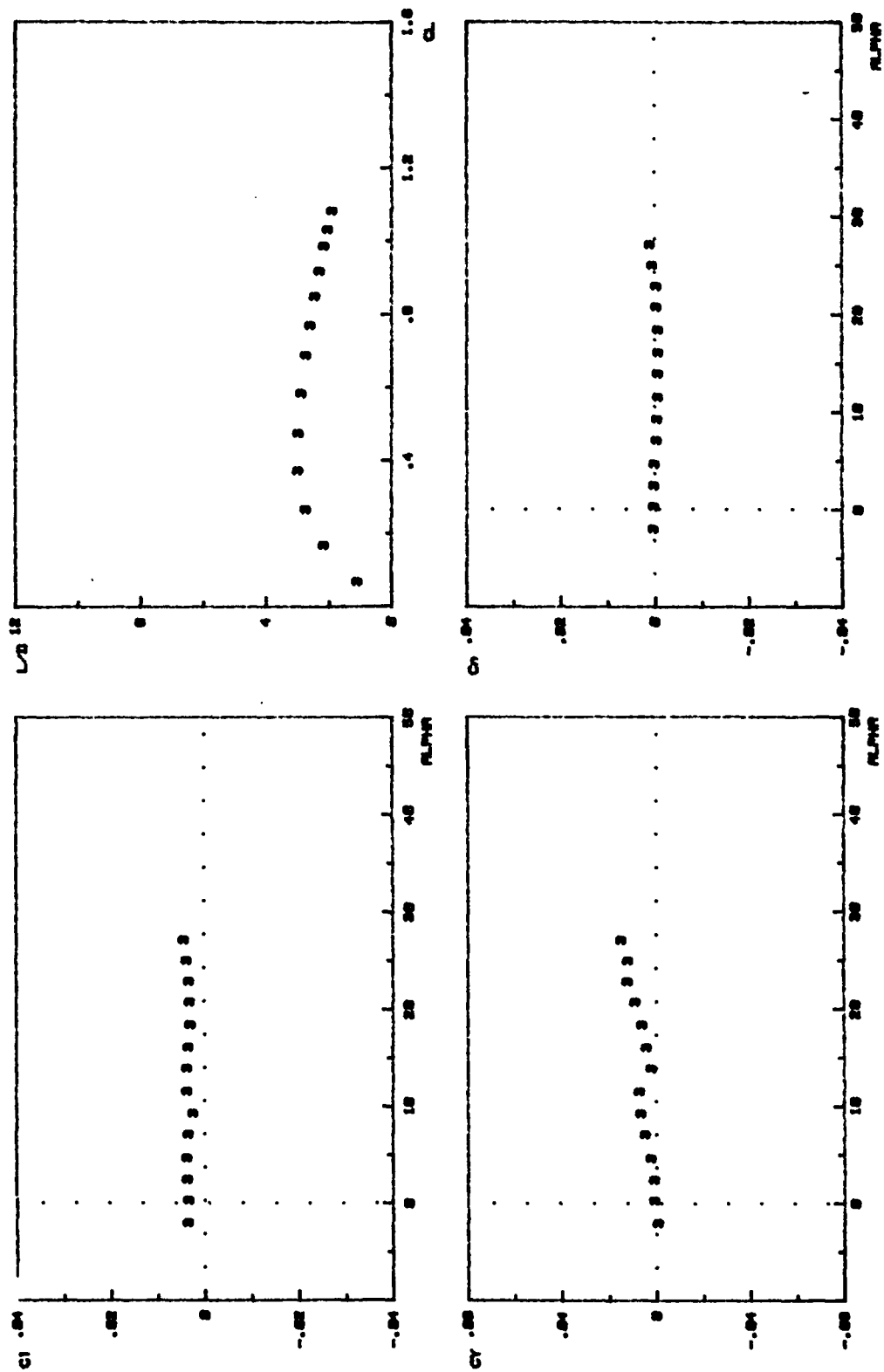
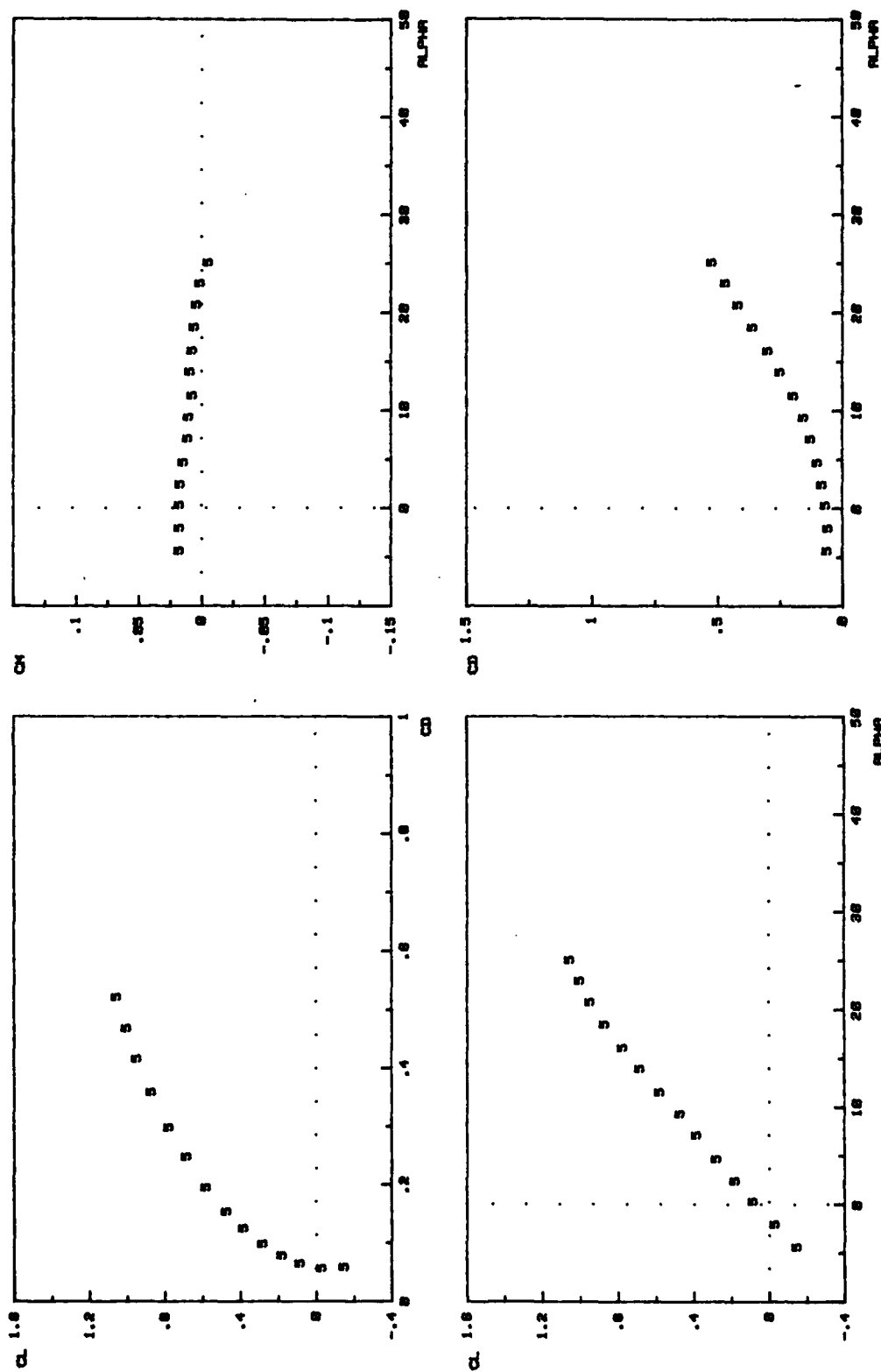


FIG. C-39.



F5 (DOUBLE GOTHIC) INBOARD 1.0 inches

FIG. C-48.

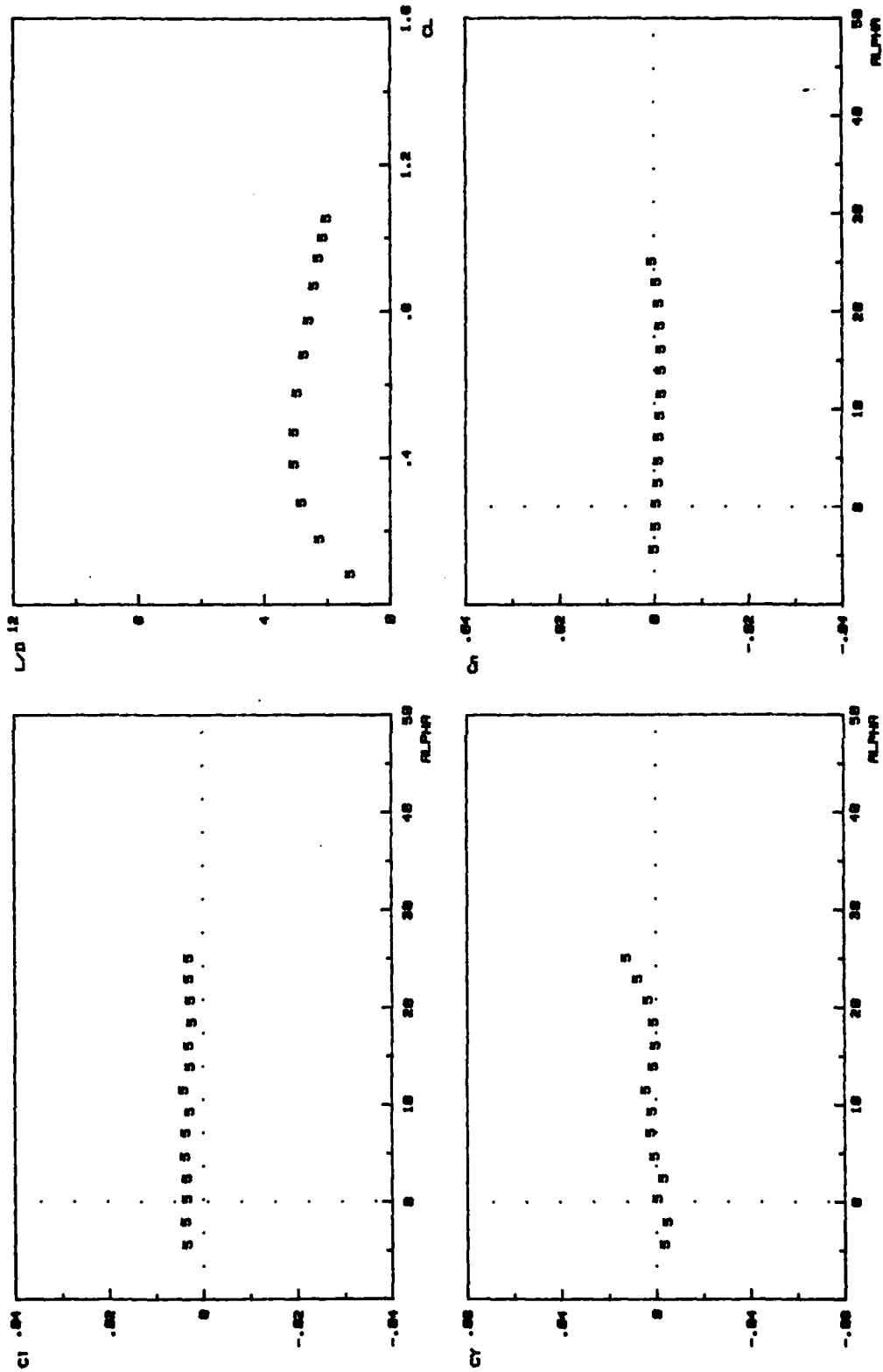


FIG. C-40. F5 (DOUBLE GOTHIC) INBOARD 1.0 inches

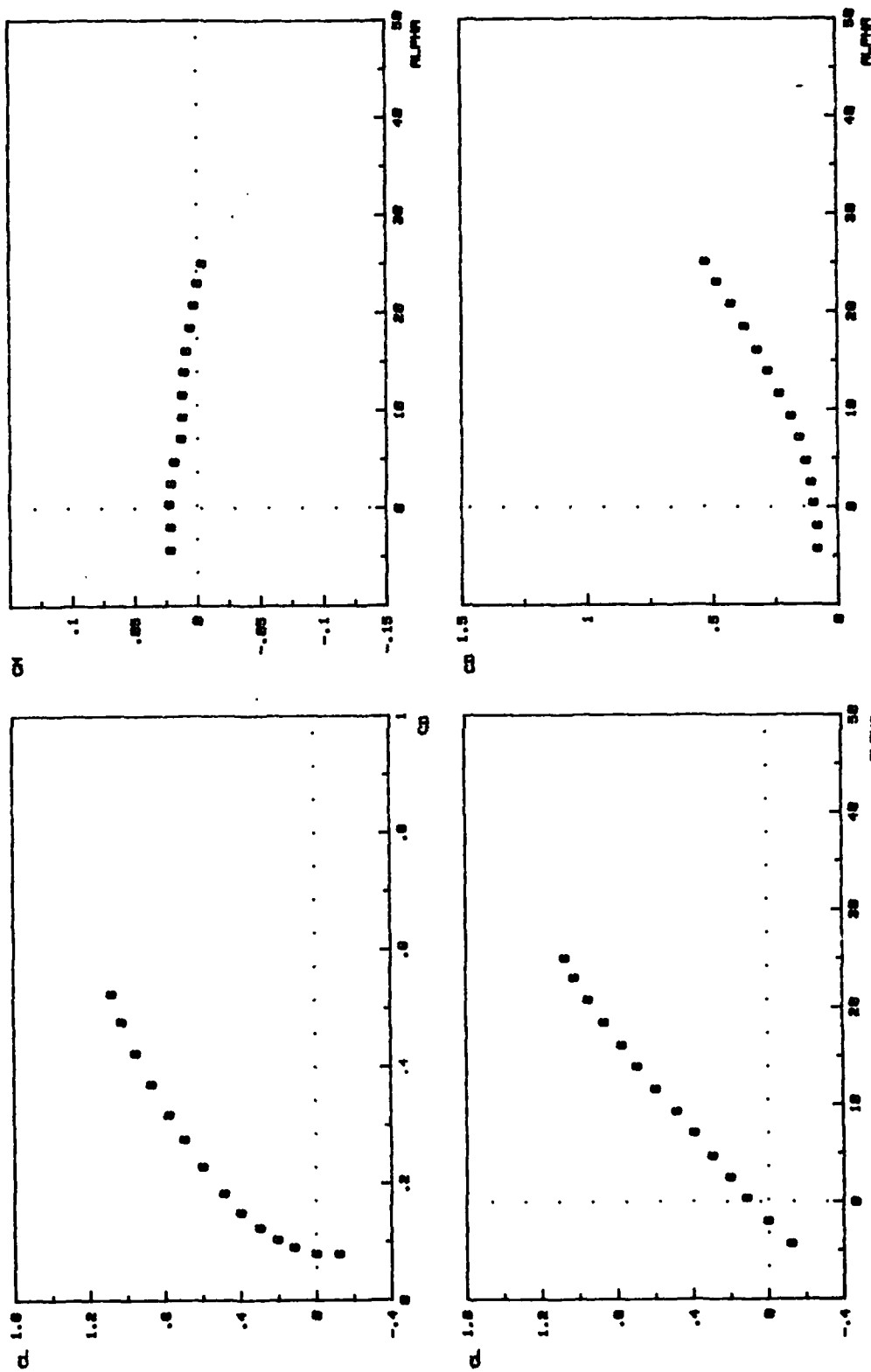
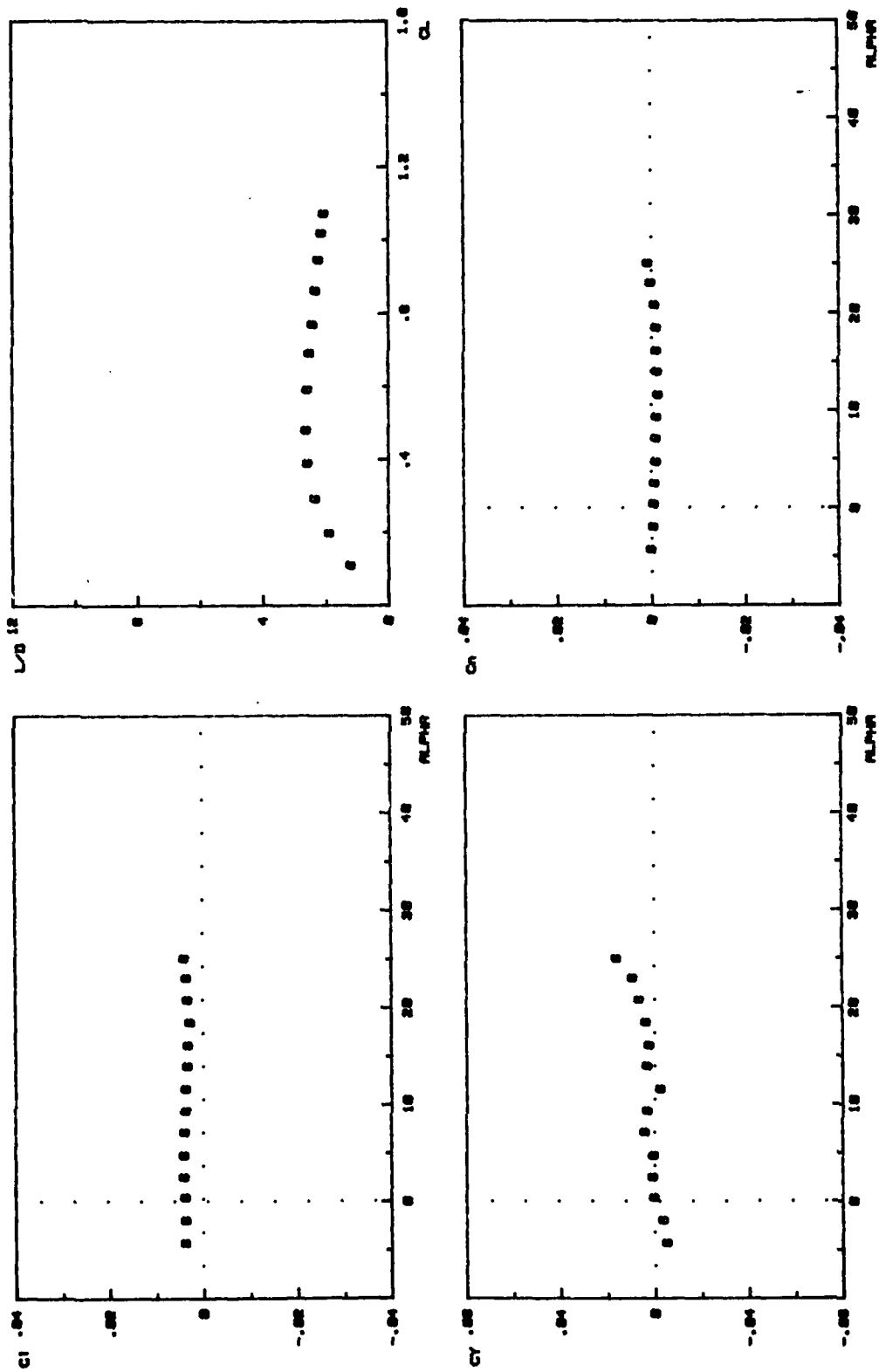
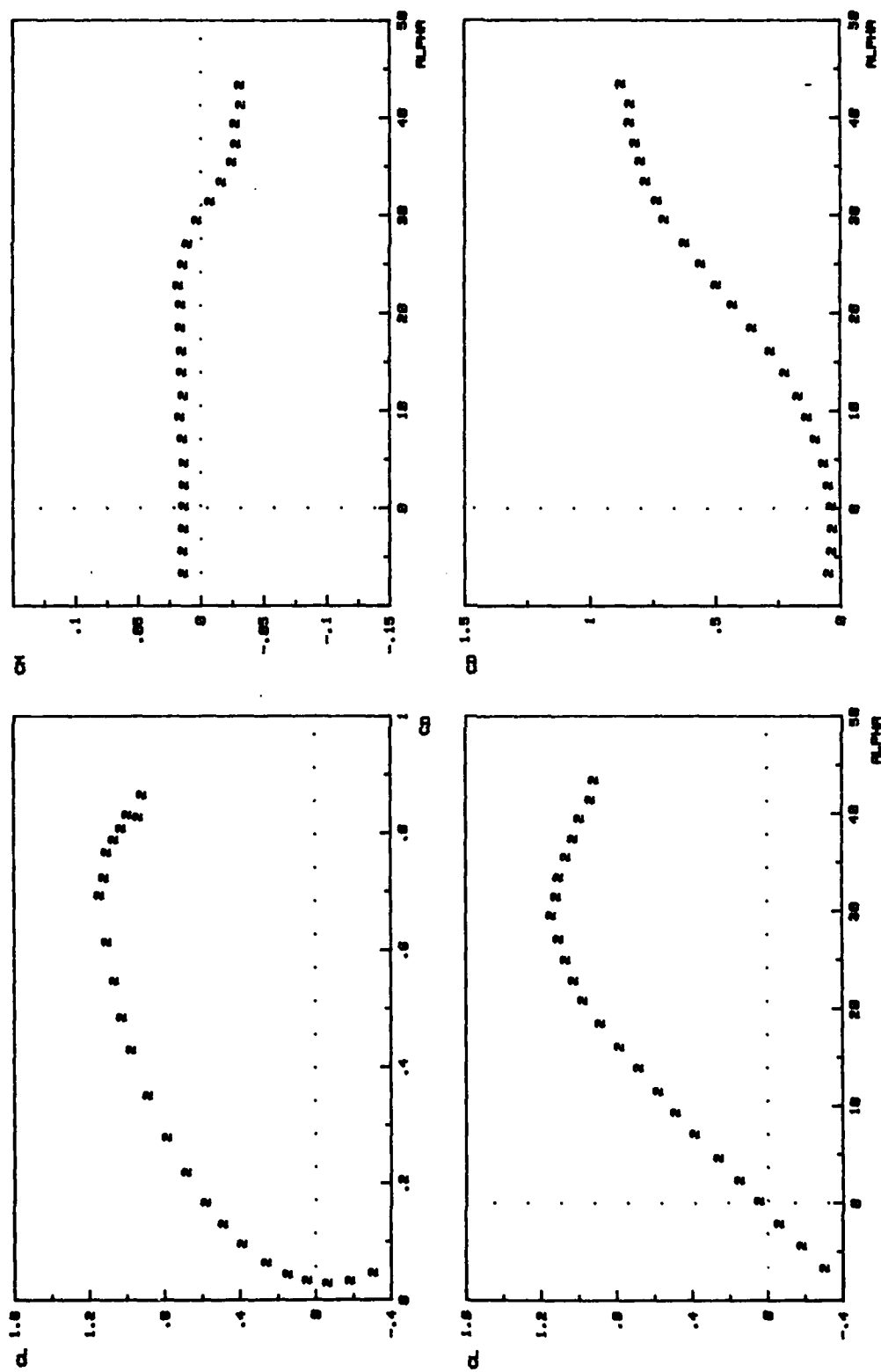


FIG. C-41.



FB (MOD. GOTHIC) INBOARD 1.0 inches

FIG. C-41.



F2 (DELTA) ON LEFT WING

FIG. C-42.

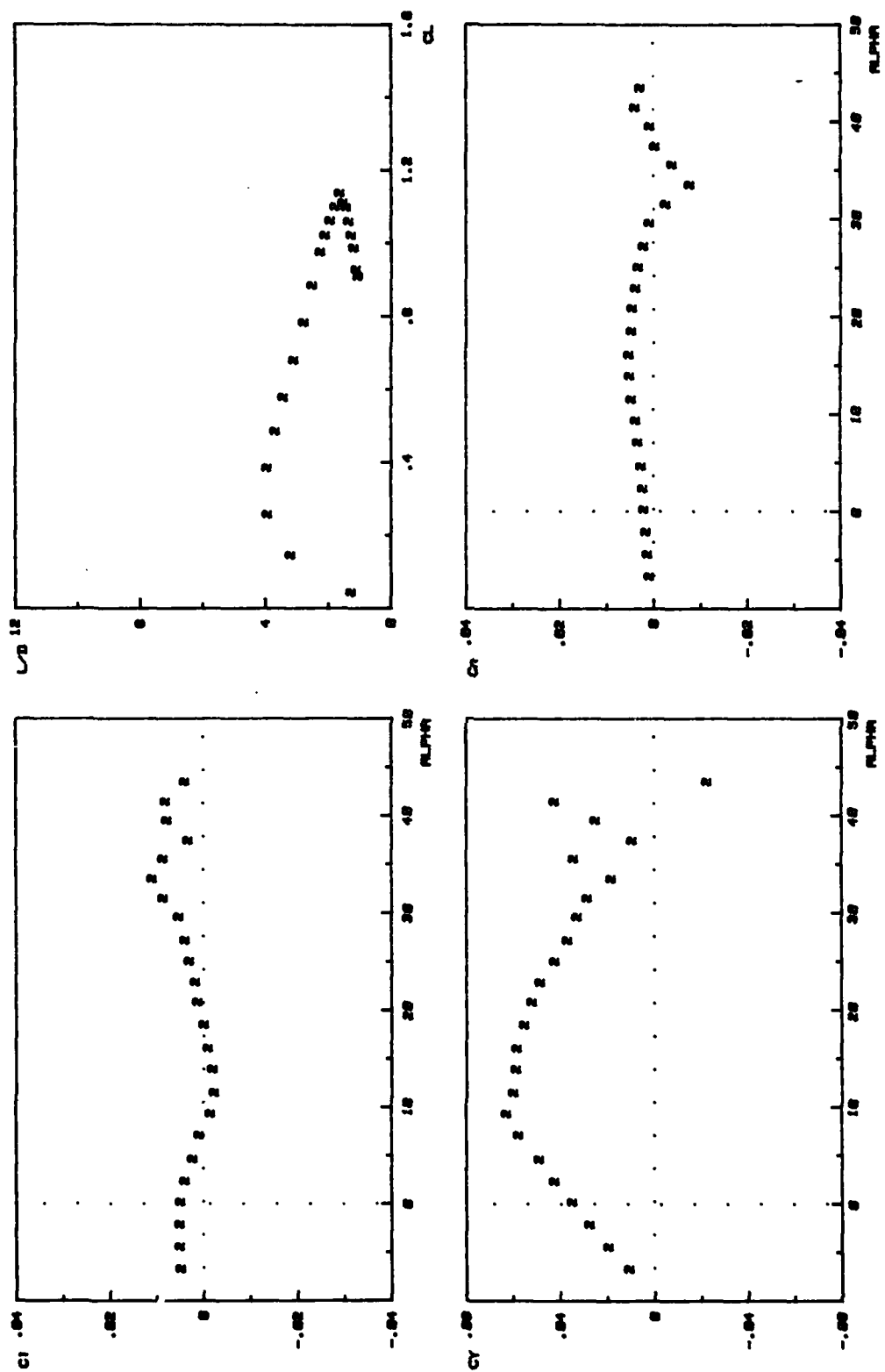
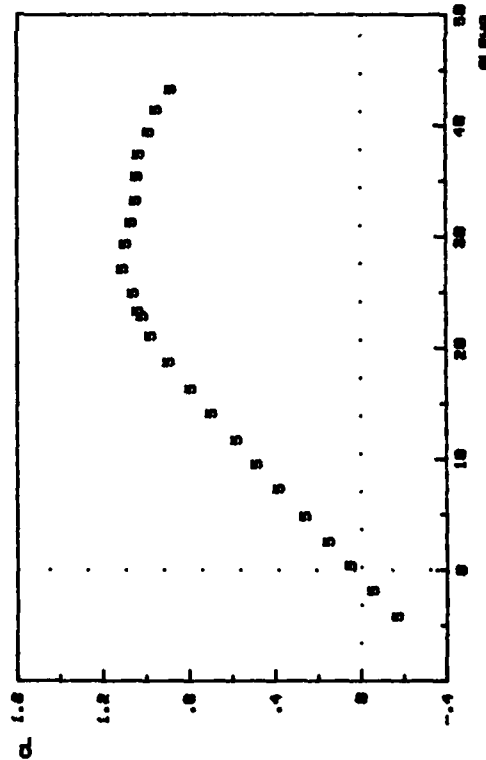
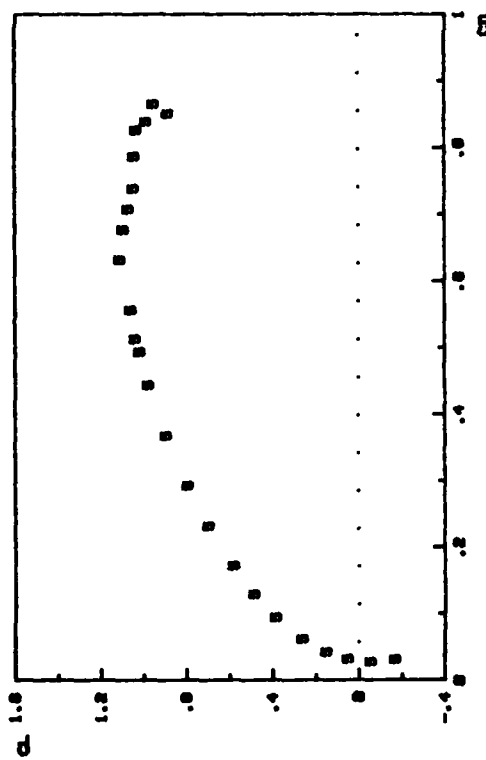
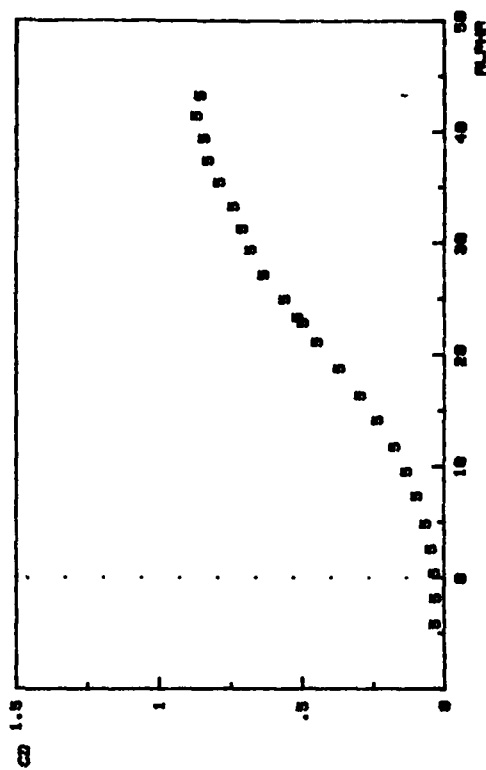
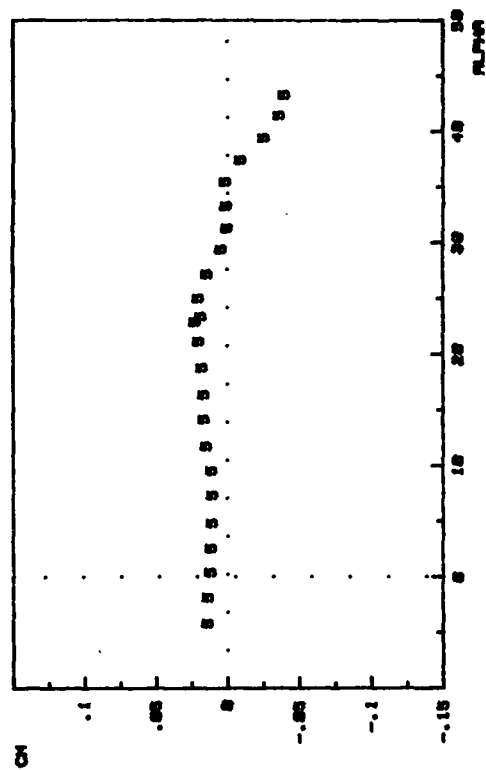


FIG. C-42.



F5 (DOUBLE GOTHIC) ON LEFT WING

FIG. C-43.



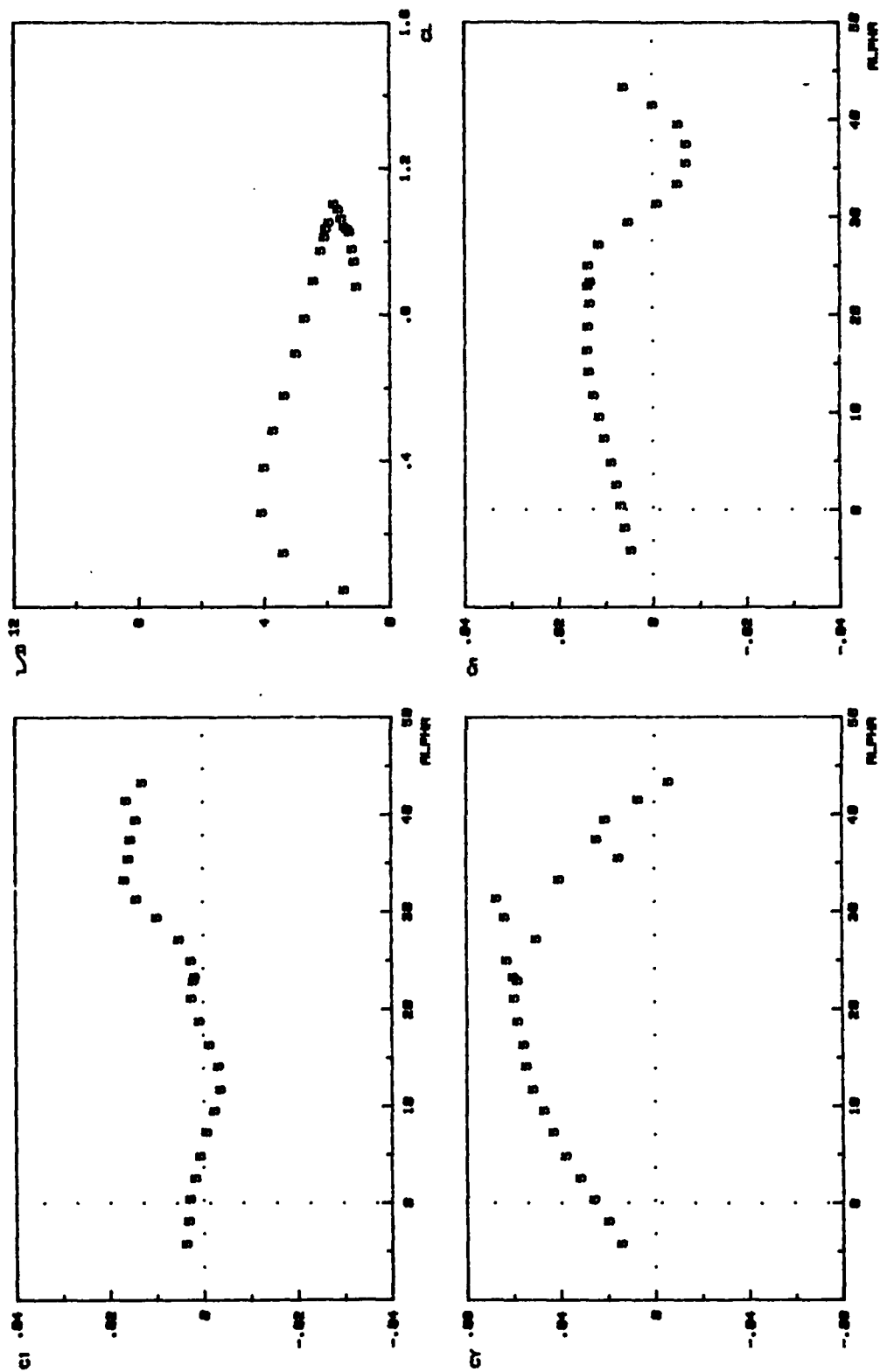
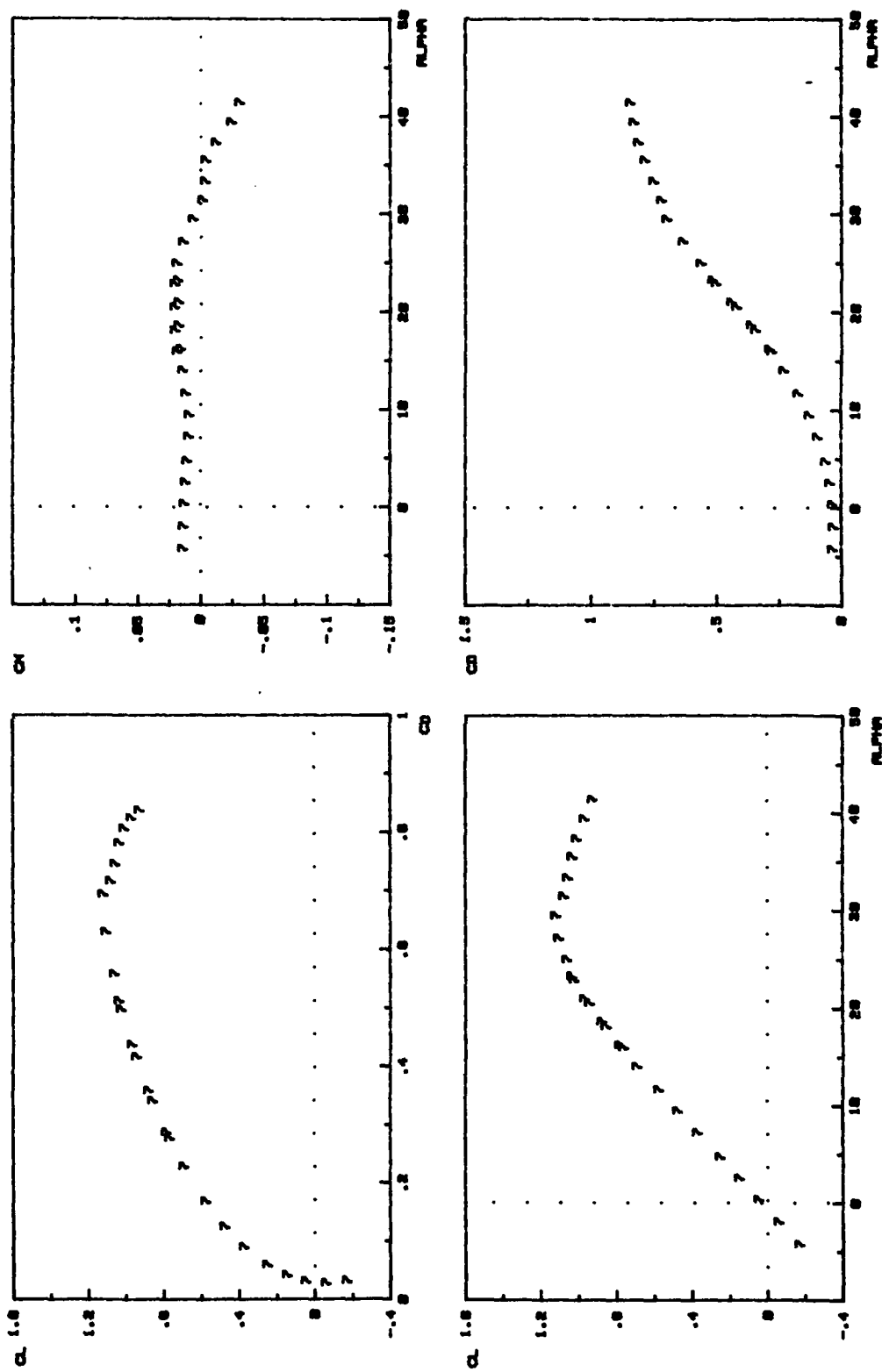
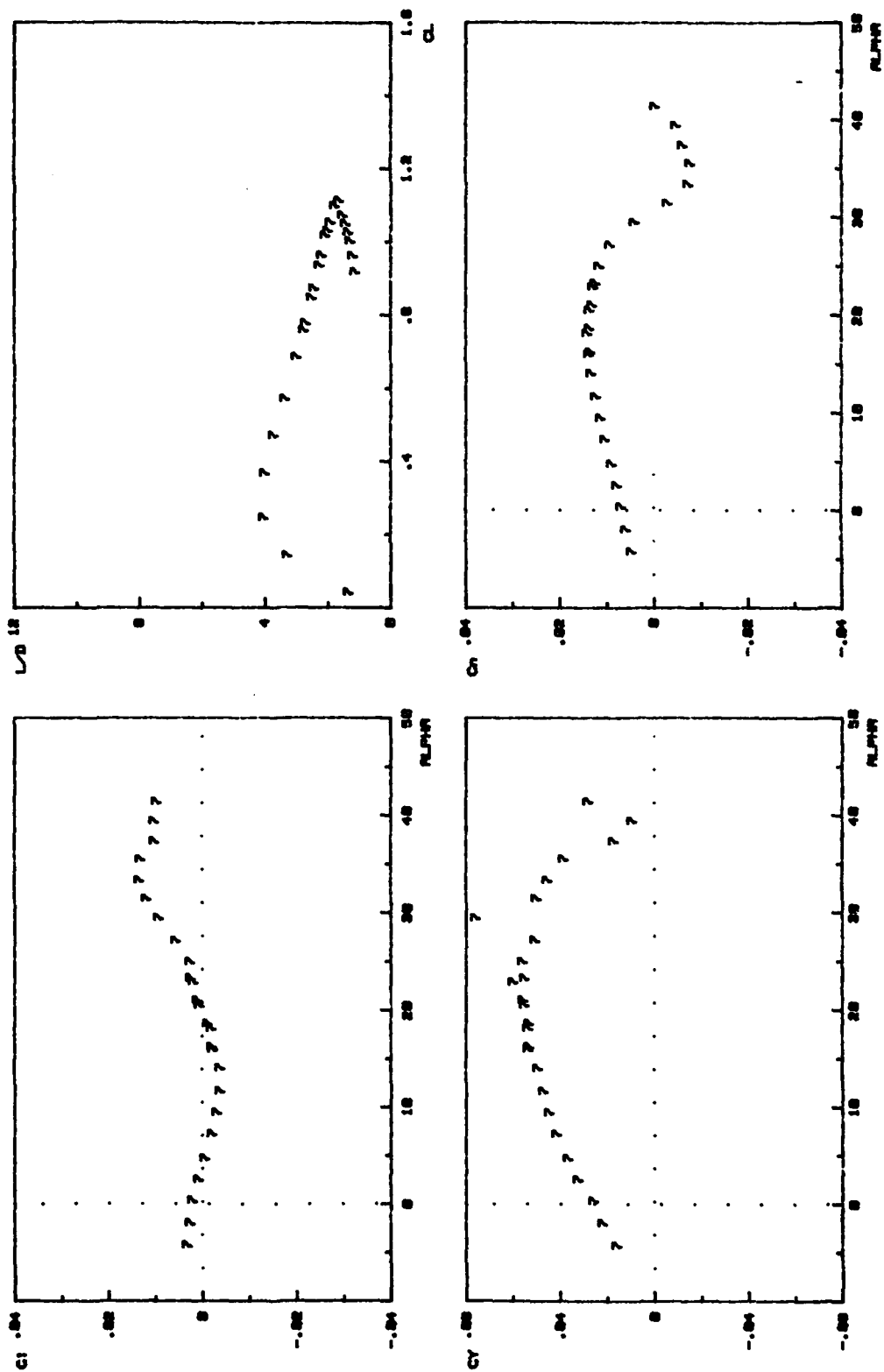


FIG. C-43.



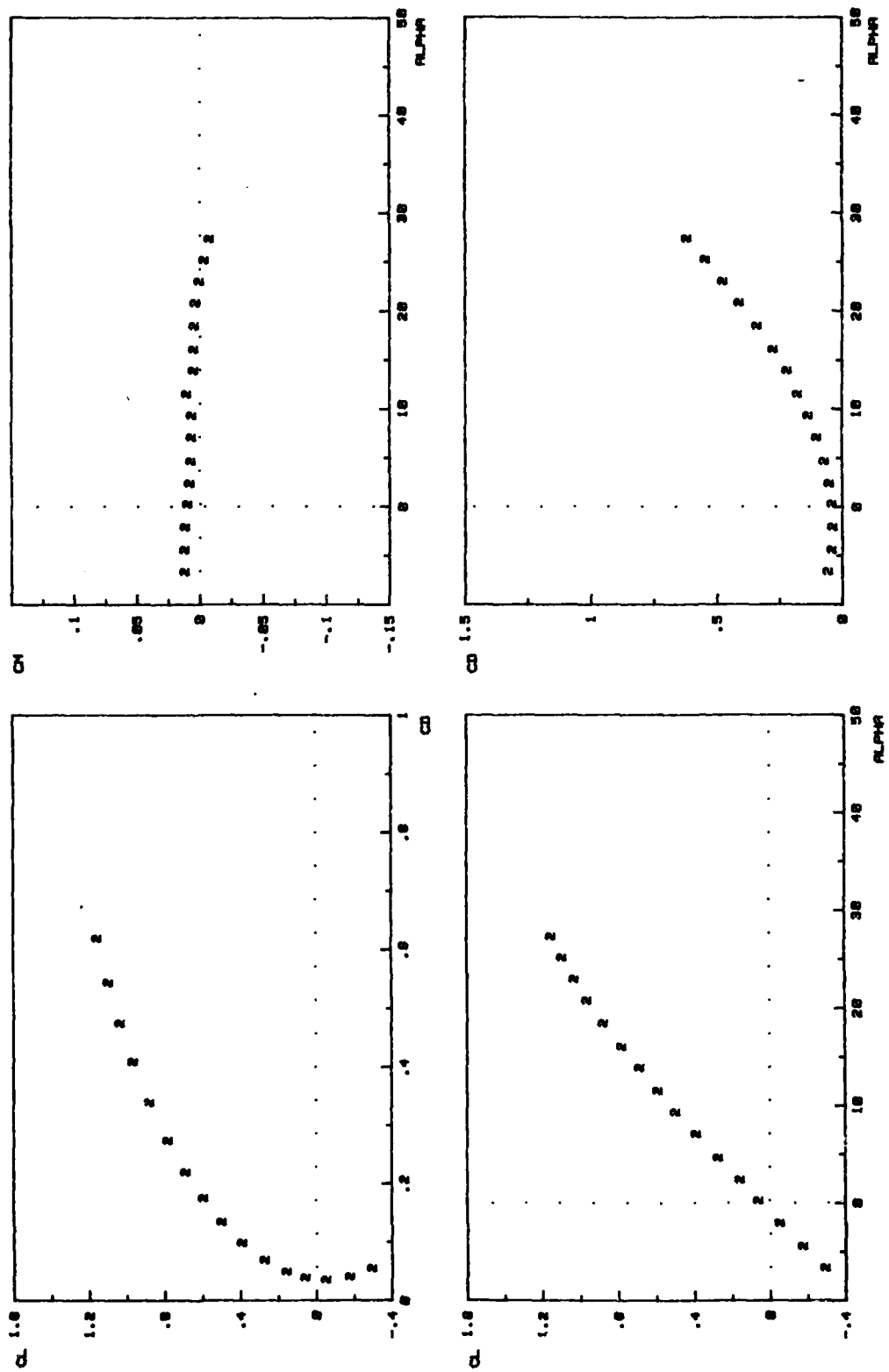
F7 (MOD. GOTHIC II) ON LEFT WING

FIG. C-44.



F7 (MOD. GOTHIC II) ON LEFT WING

FIG. C-44.



F2 (DELTA) INBOARD 0.5 in ON LEFT WING

FIG. C-45.

AD-A163 877

EXPERIMENTAL STUDY OF APEX FENCES FOR LIFT ENHANCEMENT  
ON A HIGHLY SWEPT. (U) AIR FORCE INST OF TECH  
WRIGHT-PATTERSON AFB OH SCHOOL OF ENGI.. M STUART

3/3

UNCLASSIFIED

DEC 85 AFIT/GAE/AA/85D-14

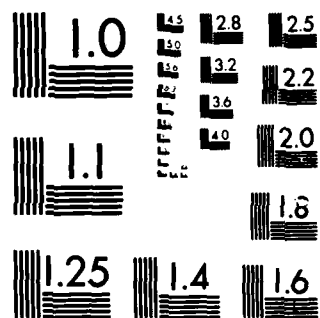
F/G 12/1

NL

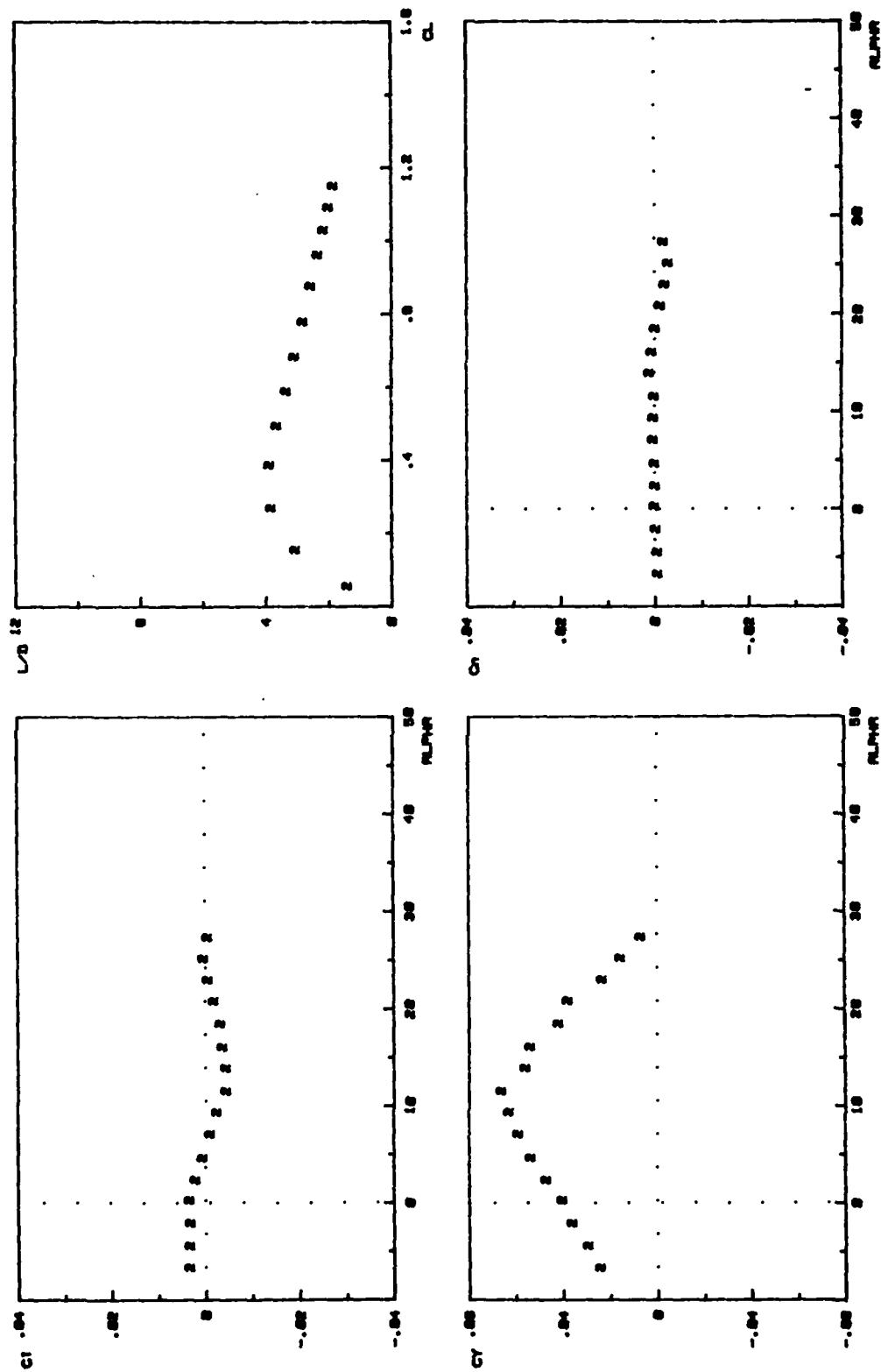
END

FILED

DTL



MICROCOPY RESOLUTION TEST CHART  
NATIONAL BUREAU OF STANDARDS 1963-A



F2 (DELTA) INBOARD 9.51m ON LEFT WING

FIG. C-45.

## BIBLIOGRAPHY

1. Sforza, P. M. and Smorto, M. J. "Streamwise Development of the Flow Over a Delta Wing", AIAA 18th Aerospace Sciences Meeting. Paper No 80-0200. American Institute of Aeronautics and Astronautics, New York, January 1980.
2. Marchman, J. F., III. "The Aerodynamics of Inverted Leading Edge Flaps on Delta Wings", AIAA 19th Aerospace Sciences Meeting. Paper No 81-0356. American Institute of Aeronautics and Astronautics, New York, January 1981.
3. Marchman, J. F., III. "Effectiveness of Leading-Edge Vortex Flaps on 60 and 75 Degree Delta Wings", Journal of Aircraft. AIAA Paper No 81-4101. American Institute of Aeronautics and Astronautics, New York, March 1980.
4. Marchman, J. F., III. "Trailing Edge Flap Influence on Leading Edge Vortex Flap Aerodynamics", AIAA 20th Aerospace Sciences Meeting. Paper No 82-0128. American Institute of Aeronautics and Astronautics, New York, January 1982.
5. Marchman, J. F., III and Hollins, Mark L. "Fuselage Effects In Leading Edge Vortex Flap Aerodynamics", AIAA Paper No 82-41006. American Institute of Aeronautics and Astronautics, New York, 1982.
6. Wahls, Richard A. and Vess, Robert J. "An Exploratory Study of Apex Fence Flaps on a 74 Degree Delta Wing", NASA Contractor Report. Cooperative Agreement NCC1-46. National Aeronautics and Space Administration, Washington, D. C., May 1985.
7. Rao, Dhanvada M. and Hoffler, Keith D. "Pressure and Flow Investigations of Vortex Fences on a 60 Degree Delta Wing", Research Report. Vigyan Research Associates, Incorporated, Hampton, Virginia, June 1985.
8. Spitler, Capt Charles R. A Wind Tunnel Investigation of Stability and Control Characteristics of the Fairchild T-46 at High Angles of Attack. MS Thesis GAE/AA/84D-27. School of Engineering, Air Force Institute of Technology (AU), Wright-Patterson AFB OH, December 1984.
9. McKernan, Capt Thomas J., Jr. A Wind Tunnel Investigation to Examine Stability and Control Characteristics of the T-46A at High Sideslip Angles. MS Thesis GAE/AA/84D-16. School of Engineering, Air Force Institute of Technology (AU), Wright-Patterson AFB OH, December 1984.



10. Mattick, A. A. and Stollery, J. L. "Increasing the Lift/Drag Ratio of a Flat Delta Wing", Aeronautical Journal, pp. 379-386. Research report. Cranfield Institute of Technology, October 1981.

## VITA

Lieutenant Michael Stuart was born on 29 May 1962 in Fairfax, Virginia. He graduated from high school in June 1980 and attended the University of Colorado at Boulder. While there, he enrolled in the Air Force Reserve Officers Training Corps program and subsequently completed the United States Army Infantry Airborne School and received his parachutist's wings in July 1983. Upon his graduation in 1984 he received the degree of Bachelor of Science in Aerospace Engineering with honors, and was commissioned in the United States Air Force. He remained on reserve status for four days before being called to active duty in the Air Force and entering the Air Force Institute of Technology Direct Accession program in May 1984.

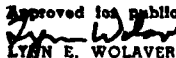
Permanent Address: 5406 Willcoxon Tavern Court  
Fairfax, Virginia 22032

UNCLASSIFIED

AD-A163877

SECURITY CLASSIFICATION OF THIS PAGE

## REPORT DOCUMENTATION PAGE

1a. REPORT SECURITY CLASSIFICATION <b>UNCLASSIFIED</b>			1b. RESTRICTIVE MARKINGS		
2a. SECURITY CLASSIFICATION AUTHORITY			3. DISTRIBUTION/AVAILABILITY OF REPORT  Approved for public release; distribution unlimited.		
2b. DECLASSIFICATION/DOWNGRADING SCHEDULE					
4. PERFORMING ORGANIZATION REPORT NUMBER(S)  AFIT/GAE/AA/85D-14			5. MONITORING ORGANIZATION REPORT NUMBER(S)		
6a. NAME OF PERFORMING ORGANIZATION  School of Engineering		6b. OFFICE SYMBOL (If applicable) AFIT/ENY		7a. NAME OF MONITORING ORGANIZATION	
6c. ADDRESS (City, State and ZIP Code)  Air Force Institute of Technology Wright Patterson AFB, Ohio 45433			7b. ADDRESS (City, State and ZIP Code)		
8a. NAME OF FUNDING/SPONSORING ORGANIZATION  AFWAL		8b. OFFICE SYMBOL (If applicable) FIRM		9. PROCUREMENT INSTRUMENT IDENTIFICATION NUMBER	
8c. ADDRESS (City, State and ZIP Code)  AFWAL/FIRM Wright Patterson AFB, Ohio 45433			10. SOURCE OF FUNDING NOS.		
11. TITLE (Include Security Classification) See box 19			PROGRAM ELEMENT NO.		PROJECT NO.
			TASK NO.		WORK UNIT NO.
12. PERSONAL AUTHOR(S) Michael Stuart, B.S., 2d Lt, USAF					
13a. TYPE OF REPORT MS Thesis		13b. TIME COVERED FROM _____ TO _____		14. DATE OF REPORT (Yr., Mo., Day) 1985 December	
15. PAGE COUNT 191					
16. SUPPLEMENTARY NOTATION					
17. COSATI CODES			18. SUBJECT TERMS (Continue on reverse if necessary and identify by block number)		
FIELD	GROUP	SUB. GR.	Apex Fences, Vortex Fences, Vortex Flaps, Delta Wings, Vortices, STOL		
01	03				
20	04				
19. ABSTRACT (Continue on reverse if necessary and identify by block number)					
Title: EXPERIMENTAL STUDY OF APEX FENCES FOR LIFT ENHANCEMENT ON A HIGHLY SWEEP DELTA WING CONFIGURATION					
Thesis Chairman: Wesley R. Cox, Captain, USAF Assistant Professor of Aeronautical Engineering					
<div style="text-align: right;"> <p>Approved for public release LAW AFR 100-17.    LYNN E. WOLAVER 16 JAN 86  Dean for Research and Professional Development  Air Force Institute of Technology (AFIT)  Wright-Patterson AFB OH 45433</p> </div>					
20. DISTRIBUTION/AVAILABILITY OF ABSTRACT  CLASSIFIED/UNLIMITED <input checked="" type="checkbox"/> SAME AS RPT. <input type="checkbox"/> DTIC USERS <input type="checkbox"/>			21. ABSTRACT SECURITY CLASSIFICATION  UNCLASSIFIED		
22a. NAME OF RESPONSIBLE INDIVIDUAL Wesley R. Cox, Captain, USAF			22b. TELEPHONE NUMBER (Include Area Code) 513-255-6998		22c. OFFICE SYMBOL AFIT/ENY

The longitudinal stability characteristics of a 60 degree delta wing/body model equipped with various types of apex fences were studied experimentally. The experimental effort utilized force balance instrumentation and oil flow visualization, and produced conclusive results. The locations of the fence-generated vortices and leading-edge vortices associated with highly swept wings were also determined. Five major fence parameters (shape, surface area, cant, length-to-height, movement) were studied and the results are given in a qualitative analysis.

The results indicate a favorable application of apex fences for STOL operations. The fences increase lift and positive pitching moment which dictates the use of trailing edge flaps, further increasing the available maximum lift for takeoff and landing. Accompanying this is a large increase in drag at low angles of attack and a marginal increase at moderate to high angles. The relative strength of nose-down pitching moments at high (above 35 degrees) angles of attack produced by apex fences is slight.

The assessment is made that apex fences are a technology whose time may have come. Further research of the lateral behavior of a "fenced" aircraft appears warranted.

from to be  
Apex Fences, Vortex Lifting,  
Vortex Dipping (Theory)

A

**END**

**FILMED**

3-86

**DTIC**